ASPECTOS CELULARES DA AÇÃO DOS METAIS CÁDMIO E MERCÚRIO EM CULTURA DE CÉLULAS E NOS ÓRGÃOS DO PEIXE TELEÓSTEO *Gymnotus carapo* (LINNAEUS 1758)

CRISTIANE DOS SANTOS VERGILIO

UNIVERSIDADE ESTADUAL DO NORTE FLUMINENSE

CAMPOS DOS GOYTACAZES

MAIO - 2013

ASPECTOS CELULARES DA AÇÃO DOS METAIS CÁDMIO E MERCÚRIO EM CULTURA DE CÉLULAS E NOS ÓRGÃOS DO PEIXE TELEÓSTEO *Gymnotus carapo* (LINNAEUS 1758)

CRISTIANE DOS SANTOS VERGILIO

Tese apresentada ao Centro de Biociências e Biotecnologia, da Universidade Estadual do Norte Fluminense, como parte das exigências para obtenção do título de Doutor em Biociências e Biotecnologia com ênfase em Biologia Celular.

Orientador: Professor Edésio José Tenório de Melo

UNIVERSIDADE ESTADUAL DO NORTE FLUMINENSE

CAMPOS DOS GOYTACAZES

MAIO - 2013

ASPECTOS CELULARES DA AÇÃO DOS METAIS CÁDMIO E MERCÚRIO EM CULTURA DE CÉLULAS E NOS ÓRGÃOS DO PEIXE TELEÓSTEO *Gymnotus carapo* (LINNAEUS 1758)

CRISTIANE DOS SANTOS VERGILIO

Tese apresentada ao Centro de Biociências e Biotecnologia, da Universidade Estadual do Norte Fluminense, como parte das exigências para obtenção do título de Doutor em Biociências e Biotecnologia com ênfase em Biologia Celular.

Tese aprovada em 23 de maio de 2013.

Comissão Examinadora:

Dr. Flávio Costa Miguens

(Professor, Universidade Estadual do Norte Fluminense)

Dr.(a) Olga Lima Tavares Machado

(Professora, Universidade Estadual do Norte Fluminense)

Dr. Olaf Malm

(Professor, Universidade Federal do Rio de Janeiro)

Dr. Edésio José Tenório de Melo (Orientador)

(Professor, Universidade Estadual do Norte Fluminense)

O presente estudo foi desenvolvido no Laboratório de Biologia Celular e Tecidual da Universidade Estadual do Norte Fluminense, sob a orientação do Dr. Edésio José Tenório de Melo, com auxílio financeiro da CAPES e FAPERJ (E-26/171.315/2004) (E-26/100.470/2007) (E-26/110.921/2008) E-26/110.600/2009).

Dedico essa tese à minha família que mesmo um pouquinho longe, sempre me apoiou em todos os momentos da minha vida.

"O mais alarmante de todos os ataques do ser humano ao meio ambiente é a contaminação do ar, do solo, dos rios e dos mares com materiais perigosos e até mesmo letais. Essa poluição é, na maior parte irrecuperável; a cadeia de males que ela desencadeia não apenas no mundo que deve sustentar a vida, mas como nos tecidos vivos, é, na maior parte, irreversível."

"Nesse meio ambiente de contaminação agora universal, os produtos químicos são os parceiros sinistros e raramente identificados, das radiações na alteração da própria natureza do mundo – a própria natureza da vida que nele habita."

Rachel Carson

Trechos do livro Primavera Silenciosa

AGRADECIMENTOS

É com muita felicidade que finalizo um trabalho de grande dedicação, que não poderia ser realizado sem a ajuda de várias pessoas que serão inesquecíveis nessa trajetória.

Durante a realização dos projetos de nossa vida não estamos totalmente sós, sendo as pessoas ao nosso redor indispensáveis para a conclusão de tais metas e de grande importância para o nosso crescimento pessoal e profissional. Com isso, primeiramente gostaria de agradecer e dedicar esse trabalho ao meu orientador Prof. Dr. Edésio José Tenório de Melo, por toda a orientação e críticas que serviram para meu aprimoramento. Pela amizade e incentivos que vou levar para toda minha vida. E por ter transmitido um pouco do seu conhecimento e experiência.

Ao Prof. Dr. Carlos Eduardo Veiga de Carvalho, por toda ajuda e palavras de incentivo em todos os momentos. Seus conselhos foram fundamentais para a minha vida acadêmica.

Agradeço a minha família que sempre esteve do meu lado e mesmo com a distância me deram o apoio necessário para a conclusão do meu curso. Em especial aos meus pais Mariana dos Santos Vergilio e Fernando Vergilio e a minha irmã Fernanda dos Santos Vergilio.

Ao Pedro Campeão Ferreira por me incentivar nos momentos em que meu cansaço e limitação de tempo me desanimavam. Sua presença e apoio foram fundamentais.

A Beatriz Ferreira Araújo, minha amiga de todas as horas, na verdade, a irmã que escolhi. Nem sei como começar a agradecer pela presença em todos os momentos.

A mestranda Laís Pessanha de Carvalho que mesmo sem gostar de peixes, sempre esteve presente com sua amizade. A aluna de iniciação científica Letícia de Souza Gomes pela participação direta em muitos experimentos e pela amizade em todos os momentos. Esse trabalho também é seu! A aluna de iniciação científica Amanda Braga de Menezes e a técnica Gabriela Carreira Muniz por toda a ajuda.

As amigas: Tatiana Wermelinger, Layra Passareli e Palloma Carvalho pela amizade e convivência durante tantos anos. Ao amigo Thiago Pessanha de Rangel por sempre me ajudar, mesmo nos momentos mais difíceis. Ao amigo Braulio Cherene pela amizade e por sempre estar disponível para me levar para as coletas. Aos amigos Renato Aguiar, Jomar Marques e Frederico Brito. E a todos os meus amigos e amigas da pós-graduação em Biociências e Biotecnologia, em especial a amiga Letícia Rocha.

A mestre Renata Vasconcellos Moreira pela participação direta nos experimentos e por toda a amizade.

Ao pescador Cesar por toda ajuda no fornecimento das amostras. Aprendi muito, mas ainda não sei pescar, sem você teria sido muito mais difícil.

A todos os professores do Laboratório de Biologia Celular e Tecidual, por todo conhecimento transmitido durante esses anos.

Ao professor Claudio Andres Rentamal pelos conselhos e ajuda durante esse trabalho. E ao técnico Arthur Rodrigues por todo o auxílio.

A professora Cristina Maria Magalhães de Souza pelos ensinamentos indispensáveis à minha formação. E aos demais professores do Laboratório de Ciências Ambientais. Em especial, ao professor Carlos Eduardo de Rezende por todo o apoio.

As técnicas do Laboratório de Biologia Celular e Tecidual pelo apoio na execução das atividades laboratoriais, pela amizade e disponibilidade, em especial a Giovana Alves de Moraes, Beatriz Ferreira Ribeiro, Adriana Alves Martins, Márcia Adriana de Carvalho, Darli Grativol Keller e Rosemay Cardoso Maciel. A secretária do LBCT Luciana Timóteo pela disponibilidade. E aos técnicos do Laboratório de Ciências Ambientais, em especial ao Marcelo Gomes de Almeida e Diogo Quitete pela ajuda fundamental.

Aos técnicos do setor de morfologia e anatomia patológica do Laboratório de Sanidade Animal (CCTA/UENF), por todo auxílio e disponibilidade. Em especial, a ajuda indispensável de Douglas Escocard, Elizabeth Gonçalves Pires e Luciana da Silva Lemos. E ao Prof. Eulógio Carlos Queiroz de Carvalho pela disponibilidade e por ter me passado um pouco da sua experiência na área da histologia.

A pós-graduação do CBB, em especial a Beatriz Almeida e Marlene dos Santos por toda ajuda. E as professoras Kátia Valevski Sales Fernandes e Olga Lima Tavares Machado pelo trabalho desenvolvido frente à coordenação.

Aos membros da banca examinadora: Prof. Olaf Malm, Prof.(a) Olga Machado e Prof. Flávio Miguens, pelos conhecimentos transmitidos para o aprimoramento desse trabalho.

Ao Setor de Toxicologia Celular do Laboratório de Biologia Celular e Tecidual e aos laboratórios LCA, LQFPP e LSA da Universidade Estadual do Norte Fluminense. A CAPES, FAPERJ e UENF pelo apoio logístico e financeiro.

SUMÁRIO

LISTA DE FIGURAS

LISTA DE TABELAS

RESUMO

A exposição aos metais como o cádmio e mercúrio desperta grande preocupação ambiental em função da potencialidade de induzir diversos efeitos tóxicos nos organismos. A avaliação das concentrações de metais nos peixes pode indicar o aumento da contaminação através dos níveis tróficos do ecossistema aquático até a exposição humana. Os peixes são organismos sensíveis à poluição química, capazes de sofrer alterações morfológicas, que podem ser avaliadas a fim de expressar os impactos endógenos do organismo e inferir o risco ao ambiente. O presente estudo visa avaliar os efeitos progressivos da exposição ao cádmio e mercúrio a nível celular e tecidual, através da caracterização da evolução dos danos nos principais órgãos relacionados com a acumulação desses metais e nos sítios intracelulares envolvidos na indução de morte celular, usando como modelos o peixe tropical *Gymnotus carapo* e a linhagem de hepatoma humano (células HuH-7). O tratamento com o cádmio e mercúrio induziu efeitos similares na cultura de células HuH-7, ocasionado decréscimo na viabilidade celular e danos estruturais e funcionais em diversas organelas e estruturas celulares. A diminuição da funcionalidade mitocondrial, acidificação citoplasmática, disfunções do citoesqueleto e do retículo endoplasmático foram os principais processos envolvidos na indução da morte celular por apoptose e autofagia. Os metais cádmio e mercúrio também foram eficientemente acumulados nos órgãos dos peixes *Gymnotus carapo* submetidos à exposição intraperitoneal, sendo o padrão de acumulação dos peixes tratados com cádmio (fígado > rim > brânquias > testículo > músculo) distinto do observado nos peixes tratados com mercúrio (testículo > fígado > brânquias > músculo). O padrão de acumulação entre os órgãos expressa o diferente aporte sanguíneo e funções exercidas por esses órgãos no metabolismo dos peixes. A maior tendência de retenção do mercúrio nos órgãos, mesmo após 96 h de exposição, em comparação com o cádmio é um indicativo que esses metais possuem toxicocinética distinta, influenciada por diferenças nas interações desses íons com moléculas endógenas, que estaria afetando a sua permanência no organismo. A exposição dos peixes com progressivas doses e tempos de exposição também possibilitou uma avaliação da evolução dos danos no testículo do peixe *Gymnotus carapo,* desde níveis sem efeitos adversos aparentes, até a indução de severas alterações capazes de induzir atrofia testicular. O presente estudo auxilia no entendimento da progressão dos efeitos tóxicos do cádmio e mercúrio a nível celular e tecidual, possibilitando a identificação dos principais alvos intracelulares e dos danos nos

distintos órgãos dos peixes expostos. As alterações observadas nos exemplares tratados de *Gymnotus carapo* aumentam o conhecimento sobre a histopatologia dos peixes tropicais e traz a perspectiva do uso das alterações morfológicas como ferramenta sensível a presença de agentes estressores, podendo ser empregada como um indicador adicional para avaliação da contaminação dos peixes no ambiente natural.

Palavras-chave: Cd, dano, efeito, histologia, Hg, peixe.

ABSTRACT

The metal exposure such as cadmium and mercury arouses great environmental concern, for their capability to induce various toxic effects on organisms. The assessment of metal concentrations in fish may indicate the increased contamination through the trophic levels of the aquatic ecosystem until human exposure. Fish are sensitive organisms to chemical pollution, able to undergo morphological changes that can be evaluated in order to express the endogenous impact of the organism and demonstrate the environmental risk. This study aims to evaluate the effects of progressive exposure to cadmium and mercury at cell and tissue levels, through characterization of damage evolution in the major organs involved in the accumulation of these metals and in the intracellular sites involved in the induction of cell death, using as models the tropical fish *Gymnotus carapo* and the human hepatoma line (HuH-7 cells). Cadmium and mercury treatments induced similar effects in the HuH-7 cell culture, leading to decrease in cell viability and structural and functional damage in several cellular organelles, being the decrease in mitochondrial functionality, cytoplasmic acidification, disorders of the endoplasmic reticulum and the cytoskeleton the main processes involved in the induction of cell death by apoptosis and autophagy. The metals cadmium and mercury were also efficiently accumulated in the organs of the *Gymnotus carapo* fishes submitted to intraperitoneal exposure, and the accumulation pattern of the fishes treated with cadmium (liver> kidney> gills> testis> muscle) differed from the fishes treated with mercury (testis> liver> gills> muscle). The accumulation pattern among the different organs expresses the blood supply and functions performed by these organs in the fish metabolism. The major trend of mercury retention in the organs even after 96 h of exposure, in comparison to cadmium is an indication that these metals have distinct toxicokinetics, due to differences in the interactions of these ions with endogenous molecules, which would affect their permanence in the organism. Fish exposure with progressive doses and times also allowed the assessment of the damage evolution in the testis of *Gymnotus carapo* fishes from levels without apparent adverse effects, until induction of severe changes that can induce testicular atrophy. This study contributes for the understanding of the progression of cadmium and mercury toxic effects in the cell and tissue levels, enabling the identification of the main intracellular targets and of the organ damages in the exposed fishes. Changes observed in the treated *Gymnotus carapo* specimens increase the knowledge of the histopathology of tropical fishes and brings the perspective of the use of morphological changes as a sensitive tool of the

presence of stressors agents; with possible use as an additional indicator for evaluation of fish contamination in the natural environment.

Key-words: Cd, damage, effect, fish, histology, Hg.

INTRODUÇÃO

Os ecossistemas aquáticos são o destino final de diversos poluentes provenientes de dejetos agroindustriais e urbanos. Áreas litorâneas e nas margens de rios, lagos, lagoas e estuários também abrigam grande parte da população humana mundial. Dessa forma, é crescente a degradação da qualidade dos ambientes, em função de aspectos diversos como o desmatamento das margens dos rios, poluição atmosférica e redução da qualidade da água de nascentes e mananciais. Dentre esses, a contaminação dos organismos aquáticos com substâncias tóxicas, como o cádmio e o mercúrio é de preocupação ecológica e de saúde humana.

Os metais como o mercúrio e cádmio despertam preocupação ambiental pela capacidade de induzir diversos efeitos tóxicos nos organismos **(Bucio *et al*., 1995)**. O consumo de peixes e frutos do mar se constitui um dos principais veículos de exposição humana aos metais **(WHO, 2007; Dang & Wang, 2012; Pastorelli *et al*., 2012)**. O acompanhamento dos níveis desses poluentes em peixes, juntamente com a elucidação dos seus efeitos tóxicos auxilia no entendimento da qualidade ambiental e no risco de exposição humana.

A exposição ao poluente tóxico normalmente desencadeia uma cascata de respostas biológicas **(Van der Oost *et al*., 2003)**. Acima de um determinado limiar (em certa dose e/ou tempo de exposição ao agente químico), respostas biológicas iniciais ao poluente são desenvolvidas e podem ser diferenciadas da faixa normal que ocorre em uma situação sem o agente estressor (Figura 1). Em exposição contínua ao poluente, as respostas biológicas iniciais podem evoluir, podendo levar a disfunções reprodutivas, afetando a susceptibilidade a doenças e sobrevivência dos organismos afetados, possibilitando a observação de múltiplos efeitos nos níveis hierárquicos mais elevados da organização biológica (Figura 1).

Na perspectiva de uma completa elucidação dos danos induzidos pelos metais pesados é necessário um entendimento dos efeitos toxicológicos que precedem a morte dos organismos **(Douhri & Sayah, 2009)**. A avaliação das respostas biológicas iniciais, a nível celular e tecidual permite a elucidação do estado de saúde dos organismos expostos a certos níveis de contaminação e com isso, torna possível um diagnóstico inicial e integrado da poluição ambiental, antes que efeitos mais severos ocorram a nível populacional.

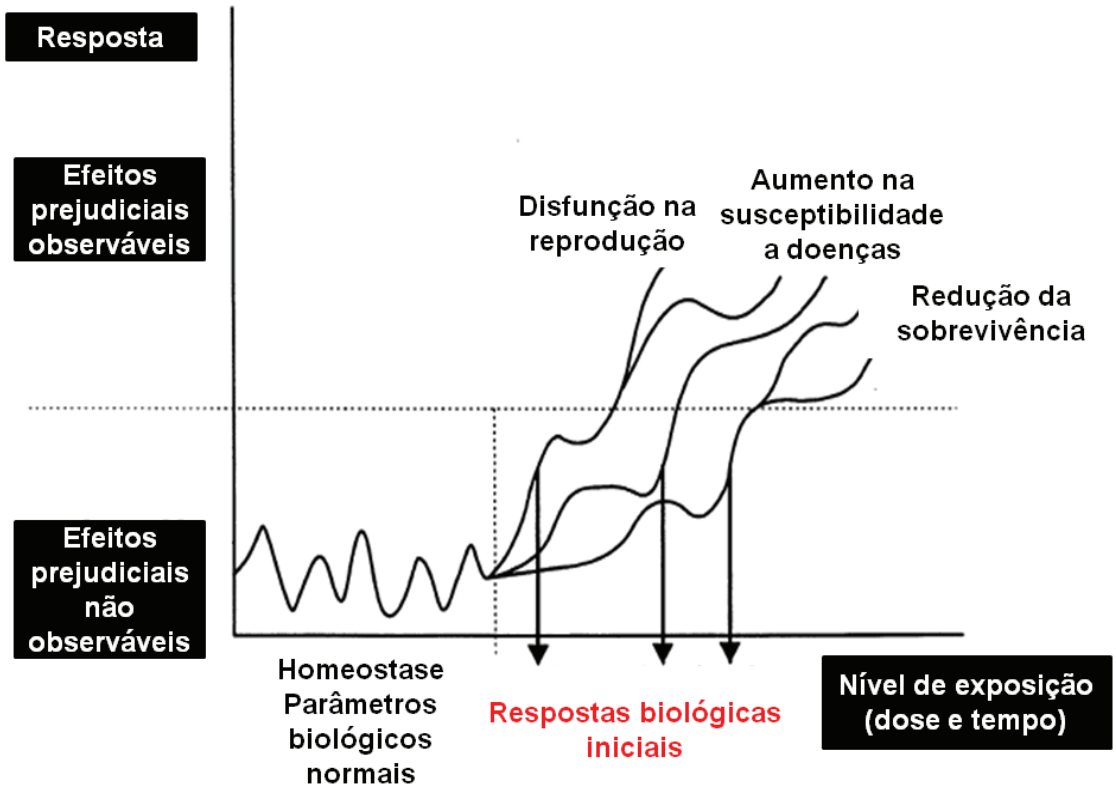

Figura 1. Esquema representando as respostas biológicas nos organismos após a exposição ao poluente. Adaptado de **Van der Oost *et al*., 2003.**

1. Os metais

Dos 114 elementos descritos, 90 ocorrem naturalmente na crosta terrestre, em sua maior parte (67) são constituídos por metais **(Cornelis & Nordberg, 2007)** (ver tabela periódica dos elementos, Figura 2). Dentre os metais, todos com exceção do mercúrio (Hg) são sólidos **(Morel *et al*., 1998).** Os metais são usualmente definidos com base nas suas propriedades físicas no estado sólido. As propriedades físicas de grande significância tecnológica são: (1) refletividade elevada, responsável pelo brilho metálico característico, (2) elevada condutividade elétrica, que diminui com o aumento da temperatura, (3) alta condutividade térmica, (4) propriedades mecânicas como força e maleabilidade **(Cornelis & Nordberg, 2007)**. Os metais ainda são caracterizados por sua estrutura cristalina, por suas ligações químicas específicas, em que os elétrons estão despareados e móveis; e por suas propriedades magnéticas **(Cornelis & Nordberg, 2007)**.

Os metais possuem algumas características que lhes conferem o caráter de poluentes ambientais. Os compostos metálicos orgânicos e inorgânicos possuem elevada reatividade, tendência de acumulação nos organismos e alta persistência no ambiente em função de sua estabilidade química **(Nriagu, 1988**; **Nordberg *et al*., 2007a**). Muitos compostos metálicos são solúveis e, portanto ambientalmente móveis **(van Dry *et al*., 2007)**. De acordo com a Organização Mundial de Saúde, os metais mercúrio, cádmio, chumbo e arsênio se encontram entre as dez substâncias químicas que despertam maior preocupação para saúde humana **(WHO, 2013)**. A associação com a contaminação ambiental e potencialidade de indução de efeitos tóxicos levou ao uso inapropriado do termo "metais pesados". Por anos, o termo "metal pesado" foi empregado para classificar os metais de acordo com a densidade, gravidade específica ou massa atômica. No entanto, tais classificações são imprecisas e podem levar a conclusões errôneas **(Nordberg *et al*., 2007a).**

Esses elementos ocorrem no ambiente em pequenas concentrações, na ordem de partes por bilhão (ppb) a partes por milhão (ppm). Dentre os metais, alguns se destacam por exercer funções essenciais nos organismos, por participar de processos fisiológicos, mesmo que em quantidades mínimas, como o zinco, ferro, manganês, cobalto e molibdênio. Outros metais como mercúrio e chumbo não têm função biológica conhecida e seus efeitos sobre os organismos vivos normalmente são deletérios **(Zagatto & Bertoletti, 2006)**. O uso dos metais em diversas atividades industriais, juntamente com o lançamento inapropriado de dejetos agroindustriais nos ecossistemas aquáticos estão aumentando as concentrações dos metais tanto essenciais como não essenciais. Os organismos aquáticos poderiam assim estar expostos a níveis não naturais desses elementos no ambiente **(van Dyk *et al*., 2007)**. Esse fato desperta grande preocupação ambiental, uma vez que mesmo os metais essenciais podem exercer efeitos tóxicos nos organismos.

Os metais podem ser acumulados pela biota e ser incorporados nos diversos níveis tróficos da cadeia alimentar. A elevada toxicidade dos metais para os organismos, mesmo em baixas concentrações, reforça a importância de estudos avaliando os efeitos induzidos por esses elementos **(Baatrup, 1991)**. Investigações sobre a absorção, acumulação, biotransformação e excreção desses poluentes, juntamente a observação dos danos nos diferentes órgãos de espécies-alvo são fundamentais para o entendimento da dinâmica dessas substâncias no ambiente e sua potencialidade de indução de efeitos tóxicos em certas faixas de concentração **(Liao *et al*., 2006)**.

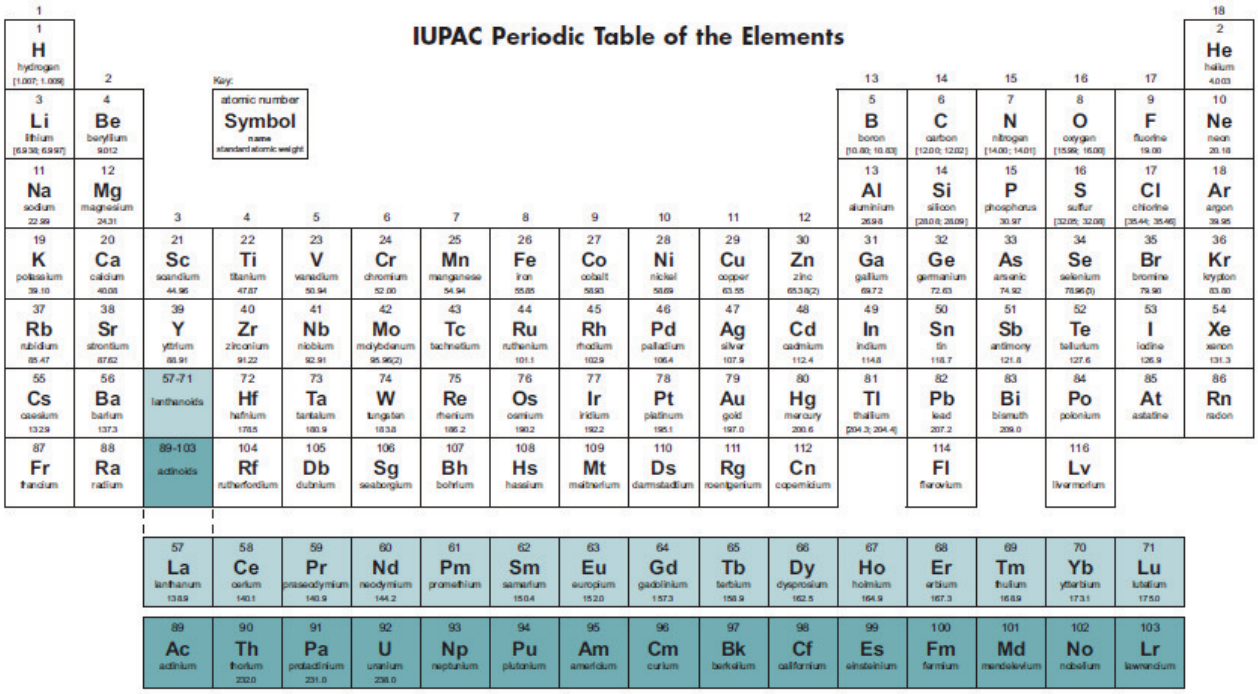

Figura 2. Tabela periódica dos elementos (disponível em: http://www.iupac.org/highlights/periodic-table-of-the-elements.htmlindex.html / acessada em 24/04/2013).

1.1. Cádmio

O cádmio (Cd) é membro do grupo 12 (II-B) da Tabela Periódica dos Elementos (Figura 2), possui massa atômica 112,4, número atômico 48, densidade de 8,6 g/cm^3, ponto de fusão de 320,9°C e ponto de ebulição de 765°C. É um metal maleável de coloração de cinza a branco e número de oxidação +2. Os isótopos de ocorrência natural são 106 (1.22%), 108 (0.88%), 110 (12.9%), 111 (12.75%), 112 (24.07%), 113 (12.6%), 114 (28.86%), e 116 (7.5%) **(Nordberg *et al.*, 2007b)**. No entanto, vários isótopos de artificiais são conhecidos como o cádmio 95, 96, 97, 98, 99, 100, 101, 102, 103, 104, 105, 107, 109, 115, 117, 118, 119, 120, 121, 122, 123, 124, 125, 126, 127, 128, 129, 130, 131, 132. Dentre os isótopos que não ocorrem naturalmente o cádmio 109 e 115 possuem a meia-vida mais longa de 462,6 dias e 53,46 horas, respectivamente. Os outros isótopos artificiais possui meia-vida curta, inferior a duas horas e meia, em função disso o cádmio 109, 111, e 115 são os mais utilizados em estudos experimentais **(Nordberg *et al.*, 2007b)**.

Dentre os compostos mais comuns estão o cádmio metálico (Cd), óxido de cádmio (CdO), cloreto de cádmio ($CdCl_2$), sulfeto de cádmio (CdS), sulfato de cádmio ($CdSO_4$) e carbonato de cádmio ($CdCO_3$) **(Cardoso e Chasin, 2001).** O cloreto e sulfato de cádmio apresentam maior solubilidade em água, enquanto que o óxido e sulfeto de cádmio são praticamente insolúveis **(Nordberg *et al*., 2007b).** O cádmio também tem a capacidade de se complexar com alguns compostos orgânicos. Em função disso, alguns compostos organometálicos sintéticos são conhecidos, no entanto, geralmente não são encontrados no ambiente por sofrerem rápida decomposição **(Nordberg *et al*., 2007b).**

O cádmio ocorre naturalmente no ambiente sendo encontrado na faixa de concentração de 0,1 a 5,0 µg/g na crosta terrestre e na atmosfera de 0,1 a 5,0 ng/m^3. **(Messner *et al*., 2012)**. É extraído a partir do refinamento de minério, juntamente com zinco, cobre e chumbo **(Järup, 2003; Nordberg *et al*., 2007b)**, mas pode ser liberado naturalmente a partir de atividades vulcânicas, erosão das rochas sedimentares, spray oceânico e incêndios florestais **(Burger, 2008).** Inúmeras atividades humanas atuam como fontes significativas para o incremento das concentrações de cádmio para o meio ambiente, dentre as tais destacam-se as atividades de mineração, uso e disposição pelas atividades industriais que utilizam o cádmio em seus processos, além de liberações indiretas durante o processamento de metais não-ferrosos, ligas de zinco, chumbo e cobre, emissões provenientes de indústrias de ferro e aço, cimento e queima de combustíveis fósseis (carvão, óleo, gás) **(WHO, 1992)**. A utilização do cádmio em pigmentos, na produção de baterias de níquel-cádmio, como estabilizadores de produtos de PVC, no recobrimento de produtos ferrosos e não-ferrosos, em ligas de cádmio e componentes eletrônicos representam suas principais aplicações industriais **(Messner *et al*., 2012).**

A contaminação por cádmio atinge os ecossistemas aquáticos através da liberação direta de dejetos agroindustriais e esgoto urbano nos corpos d'água, por processos de deposição seca ou úmida do cádmio atmosférico presente no material particulado **(Soriano *et al*., 2012)** ou através da lixiviação dos metais presentes no solo pela ação da chuva. No ambiente aquático, o cádmio pode ser incorporado no sedimento ou ser absorvido pelos organismos aquáticos. Isso ocorre uma vez que alguns sais e complexos de cádmio são solúveis e apresentam significativa mobilidade na água **(Nordberg *et al*., 2007b)**.

Dentro dessa dinâmica, a exposição humana pode ocorrer principalmente através da inalação do ar e ingestão de água e alimentos contaminados **(WHO, 1992)**. Certos alimentos como carnes, peixes, ovos e laticínios contêm pouco cádmio, apresentando níveis inferiores de 0,01 µg/g de peso úmido, porém órgãos internos, especialmente fígado e rins e produtos de origem vegetal, podem conter concentrações mais elevadas. A água e o consumo de peixes e frutos do mar também representam importantes fontes de exposição para as populações humanas **(Sirot *et al*., 2007; Pastorelli *et al*., 2012)**. A inalação de fumaça do cigarro também constitui uma fonte representativa de cádmio **(WHO, 1992)**. A planta do tabaco naturalmente acumula concentrações de cádmio relativamente altas nas suas folhas, com isso, representa uma importante fonte de exposição para fumantes (**Järup & Âkesson, 2009**; **Marano *et al*., 2012**). Um único cigarro pode conter cerca de 1-2 µg de cádmio, com algumas diferenças entre o tipo e marca, sendo parte do cádmio inalado durante o fumo é diretamente absorvido nos pulmões (cerca de 50%) **(WHO, 1992**; **Järup & Âkesson, 2009)**.

Apesar da baixa taxa de absorção intestinal (entre 5-10%), o cádmio possui efeito acumulativo, em função da longa meia vida biológica, estimada em cerca de 20 a 30 anos **(WHO, 1992)**. A exposição humana a esse metal induz efeitos severos, sendo o cádmio classificado na categoria 1 como carcinogênico pela Agência Internacional de Pesquisa sobre o Câncer (IARC: “International Agency for Research on Cancer”) **(IARC, 1993)**.

A exposição humana e de outros animais ao cádmio induz inúmeros efeitos tóxicos, sendo a função renal frequentemente afetada após exposição prolongada. Os efeitos nefrotóxicos são caracterizados pela degeneração dos túbulos proximais e proteinúria **(Järup *et al*., 1998; Järup & Åkesson, 2009)**. No homem, as alterações da função renal podem ser acompanhadas por danos nos ossos, osteomalácia e desmineralização **(WHO, 1992; Järup *et al*., 1998).** Efeitos adversos da exposição ao cádmio também podem ser observados em outros órgãos como o fígado, pulmão, pâncreas, testículo **(Thévenod, 2009).**

Um conhecido episódio de contaminação por cádmio ocorreu no Japão através da contaminação da água de irrigação de plantações de arroz, por efluentes de atividade mineradora instalada às margens do rio Jinzu. A exposição ao cádmio causou uma doença caracterizada por extrema dor, dano renal e fragilidade óssea, que afetou primeiramente as mulheres. A doença, conhecida como *Itai-Itai*, é uma combinação de

osteomalácia e osteoporose caracterizada por observação de múltiplas fraturas espontâneas nos ossos **(Nordberg *et al*., 2007b)**.

1.2. Mercúrio

O mercúrio (Hg) é membro do grupo 12 (II-B) da Tabela Periódica dos Elementos (Figura 2), possui massa atômica 200,6, número atômico 80, densidade de 13,6 g/cm^3, ponto de fusão de −38,9 °C e ponto de ebulição de 356,6°C. É um metal líquido a temperatura ambiente, possui coloração de cinza a branco e estados de oxidação 0, +1, +2 **(Morel *et al*., 1998; Berlin *et a*l., 2007)**.

O mercúrio encontra-se distribuído por toda a crosta terrestre, principalmente na forma de sulfetos, como o cinábrio (HgS), que é o principal minério de mercúrio **(Berlin *et a*l., 2007)**, podendo ser liberado naturalmente através do intemperismo das rochas e atividades vulcânicas. Diversas atividades humanas também atuam aumentando a liberação de mercúrio para o ambiente, como a queima de combustíveis fósseis, processos de produção de cimento, tratamento de minérios de enxofre, na incineração de lixo e na disposição de rejeitos de processos metalúrgicos **(Berlin *et al*., 2007)**. Além disso, o mercúrio é utilizado em diversas atividades industriais como na produção de cloro e soda cáustica (através de eletrólise em célula de amálgama de mercúrio), mineração, produção de compostos organomercuriais com ação bactericida e fungicida utilizados na agricultura, indústria de tintas e em amálgamas **(Li *et al*., 2009)**.

O mercúrio existe na forma metálica (Hg^0), mas também como compostos, adquirindo a forma monovalente, após a perda de um elétron e originando o mercúrio mercuroso (Hg^{+1}) ou na forma divalente, após a perda de dois elétrons originando o mercúrio mercúrico (Hg^{+2}). Essas duas últimas espécies formam diversos compostos químicos orgânicos e inorgânicos, sendo os compostos formados a partir do íon mercúrico (Hg^{+2}) mais abundantes que aqueles formados a partir do íon mercuroso (Hg^{+1}) **(Syversen & Kaur, 2012)**. O mercúrio ainda existe formando compostos organometálicos, onde o mercúrio é covalentemente ligado ao carbono.

Do ponto de vista toxicológico, os compostos de mercúrio podem ser divididos em compostos inorgânicos e compostos orgânicos. Dentre os compostos inorgânicos destaca-se o mercúrio elementar e o mercúrio divalente. O mercúrio elementar é volátil,

podendo se distribuir por longas distâncias a partir da fonte emissora, fazendo com que o mercúrio seja considerado um poluente global **(Boening, 2000)**. Os sais mercuriais como os cloretos, sulfatos e nitratos possuem solubilidade em água, podendo ser facilmente transportados nos ecossistemas aquáticos **(Morel *et al*., 1998)**. Dentre os compostos orgânicos destacam-se o metilmercúrio e o dimetilmercúrio que possuem elevada toxicidade. As formas orgânicas do mercúrio, em especial o metilmercúrio despertam grande preocupação em função da sua lipossolubilidade, rápida absorção nos organismo e indução de severos efeitos adversos em baixas concentrações **(Berlin *et al*., 2007; Syversen & Kaur, 2012).** No entanto, todas as formas químicas do mercúrio induzem efeitos tóxicos em diferentes espécies de mamíferos, incluindo o homem. A extensão dos danos induzidos pelo mercúrio vai depender da forma química, duração da exposição e via de exposição **(Berlin *et al*., 2007; Caranza-Rozales *et al*., 2005)**.

As formas mercuriais também podem se interconverter no ambiente, assumindo diferentes trajetórias, através de diversas reações que constituem o ciclo biogeoquímico do mercúrio (Figura 3). O mercúrio é liberado no ambiente através de emissões de fontes naturais ou antrópicas, na forma de mercúrio elementar (Hg^o) ou nas suas formas iônicas. Após processos de deposição, o mercúrio é carreado para o ambiente aquático, onde pode ser incorporado pela biota ou imobilizado no sedimento **(Bisinoti & Jardim, 2004)**. A formação do metilmercúrio no ambiente aquático ocorre em grande parte pela ação de bactérias sulfato-redutoras. Esta formação pode ocorrer em condições aeróbias e anaeróbias, sendo mais intensa em condições anaeróbias, que ocorrem na superfície do sedimento. Condições ácidas, com baixos valores de potencial redox e concentração de matéria orgânica elevada são favoráveis à formação do metilmercúrio **(Bisinoti & Jardim, 2004)**.

Os peixes podem entrar em contato com as diversas formas de mercúrio existentes no meio aquático (Figura 3) e após a absorção pela alimentação ou respiração branquial, esse metal se distribuirá pelo organismo através da circulação sanguínea. Além da capacidade de acumulação nos organismos, ainda existe um incremento das concentrações de mercúrio entre os diferentes níveis tróficos, referido como capacidade de biomagnificação. Essa capacidade faz com que concentrações de mercúrio possam atingir níveis mais elevados em peixes predadores **(Holmes *et al*., 2009)**. Em função disso, o consumo de peixes e frutos do mar é considerado um dos principais responsáveis pela exposição humana ao mercúrio **(Dang & Wang, 2012)**. Dentre as outras fontes destacam-se a água, cereais, vegetais e carne que contribuem em menor extensão para a

exposição de mercúrio para as populações humanas **(WHO, 1991; WHO, 2004; WHO 2007)**.

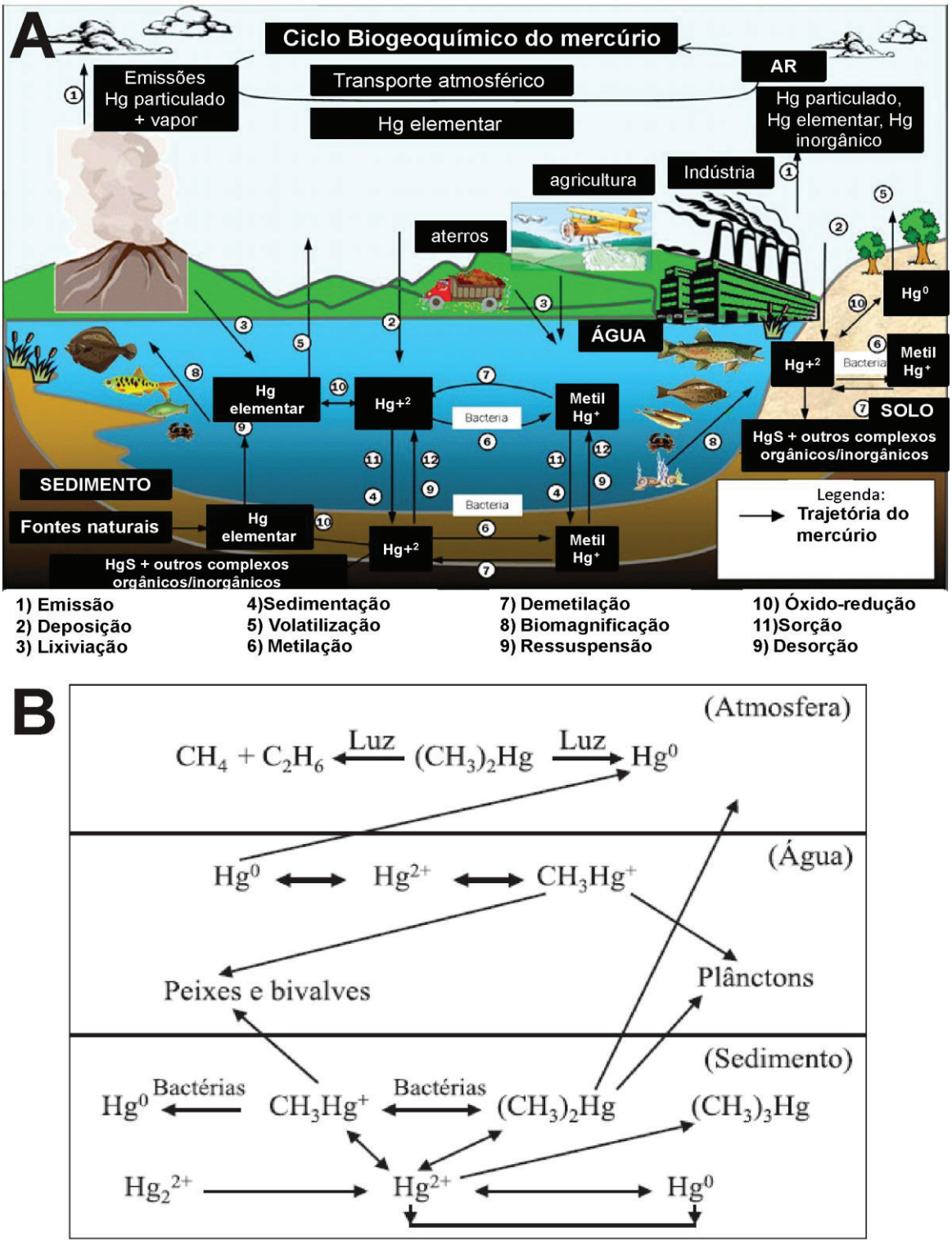

Figura 3. Representações do ciclo biogeoquímico de mercúrio. (a) Transporte do mercúrio entre os diferentes compartimentos ambientais. (b) Diferentes formas químicas assumidas pelo mercúrio durante o seu transporte no ambiente. Adaptado de **Bisinoti & Jardim (2004).**

A afinidade com o enxofre e grupamentos sulfidrila (SH) é um fator importante para a toxicidade dos compostos mercuriais. O mercúrio se liga aos grupamentos sulfidrilas presentes nas membranas e enzimas, interferindo com a estrutura de membrana e atividade enzimática **(Syversen & Kaur, 2012)**. Essa capacidade dos íons mercúrico e mercuroso em se ligar com os grupamentos sulfidrila e outros nucleófilos também diminui a probabilidade desses íons existirem na forma livre nos compartimentos nos organismos **(Berlin *et al*., 2007)**. Pelo contrário, as espécies iônicas possuem a tendência de se ligar aos grupamentos sulfidrila presentes na glutationa (SH), cisteína (Cys), homocisteína (Hcy), N-acetilcisteína (NAC), metalotioneína (MT) e albumina. Em presença dessas moléculas de baixo peso molecular que contém o grupamento tiol, os íons de mercúrio irão se ligar formando compostos lineares coordenados I ou II, dependendo da espécie iônica do mercúrio **(Bridges & Zalups, 2010)**. A formação constante de ligações Hg-SH ocorre em uma ordem de magnitude de pelo menos 10 vezes maior o que as ligações formadas entre os íons de mercúrio e outros nucleófilos presentes no mesmo ambiente **(Zalups, 2000)**.

Os complexos Hg-SH formados podem mimetizar moléculas endógenas, como proteínas intracelulares e enzimas. Um exemplo disso, é que Cys-*S*-Hg-*S*-Cys atua como um mimético do aminoácido cisteína, no sítio de ligação de enzimas intracelulares (Figura 4). No entanto, o conjugado mercurial atua como um mimético estrutural, mas não funcional da cisteína, uma vez que induz inativação da atividade enzimática. Essa habilidade mimética pode levar a sérios efeitos deletérios nos processos intracelulares **(Bridges & Zalups, 2005)**.

Em função dessas diversas interações, efeitos tóxicos do mercúrio foram demonstrados no sistema cardiovascular, no sistema gastrointestinal, fígado, rins e sistema nervoso **(WHO, 1991; WHO, 2004; Berlin *et al*., 2007)**.

O maior caso de exposição humana ao mercúrio ocorreu em 1953 na Baía de Minamata, no Japão. Resíduos da indústria Chisso Fertilizer Co. Ltda foram despejados nas águas da baía, juntamente com o metilmercúrio que era produzido como um subproduto do processo de produção do acetaldeído. A exposição da população, que se alimentava dos peixes provenientes da baía, levou ao óbito mais de mil pessoas, além de manifestações de severos efeitos locomotores e no sistema nervoso que ficaram conhecidos como “doença de Minamata” **(Tsuda *et al*., 2009)**.

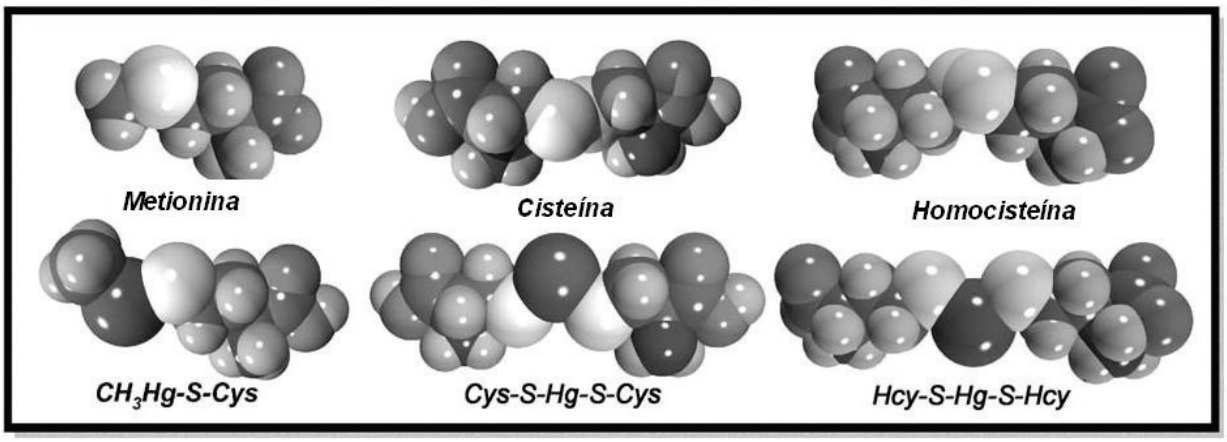

Figura 4. Representação da estrutura dos aminoácidos metionina, cisteína e homocisteína e dos respectivos conjugados mercuriais, evidenciando as semelhanças estruturais. Adaptado de **Bridges & Zalups (2005).**

1.3. Transporte e distribuição diferencial do cádmio e mercúrio entre os órgãos

Após a absorção por inalação ou através da dieta, os íons de cádmio e mercúrio são transportados dos pulmões ou do intestino para a circulação sistêmica, atingindo outros órgãos do organismo **(Zalups & Ahmad, 2003)**. Grande parte dos íons absorvidos pelo intestino são inicialmente carreados até o fígado através da circulação porta, onde são absorvidos pelos hepatócitos por meio da microcirculação hepática (sinusóides). Nesse processo, íons de cádmio e mercúrio estão em grande parte ligados a moléculas de baixo peso molecular que possuem o grupamento sulfidrila, como a metalotioneína (MT) e glutationa (GSH). Ligado a essas moléculas, os íons de cádmio e mercúrio podem ser transportados, armazenados e eliminados dos organismos **(Nordberg & Nordberg, 2000)**. Íons de cádmio e mercúrio ainda podem se ligar a outras moléculas como a cisteína **(Zalups and Ahmad, 2003)** e a albumina, que é a uma das proteínas mais abundantes no plasma e que também possui um grupo SH livre **(Brown e Shockley, 1982, Zalups, 2000)**.

Metalotioneínas (MT) são proteínas com baixo peso molecular, resistente ao calor e ricas em resíduos de cisteína, o que confere alta afinidade com ligantes metálicos, através de ligação direta com os seus grupamentos sulfidrila **(Klaassen *et al.*, 1999; Bertin & Averbeck, 2006)**. O aumento da expressão da MT e do subsequente teor de proteína observado após a exposição ao cádmio e mercúrio, principalmente no fígado e

nos rins, demonstra o seu papel importante na homeostase dos metais **(Klaassen *et al*., 1999)**. GSH é outra importante molécula envolvida na proteção contra o estresse oxidativo e na manutenção do estado de tiol de muitas proteínas na sua forma reduzida, sendo esse um requisito para a sua função normal **(Pastore *et al*., 2003)**. GSH exibe uma elevada afinidade para os íons metálicos em função da presença do grupamento sulfidrila, formando conjugados de GSH-metal para serem excretados **(Jozefczak *et al*., 2012)**.

Um mecanismo adicional de transporte de cádmio para as células envolve a presença de canais de cálcio **(Bridges & Zalups, 2005).** O cádmio possui um raio iônico (0,95 angstroms) similar ao cálcio (1,00 angstroms) **(Nordberg *et al*., 2007b)**, com isso os íons de cádmio poderiam mimetizar o cálcio no nível dos seus transportadores, facilitando a sua transloção para dentro das células (Figura 5). Estudos *in vitro* utilizando linhagens de hepatócitos (**Blazka & Shaikh, 1991; Souza *et al*., 1997)** indicaram que os íons de cádmio podem ser transportados através dos canais de cálcio, uma vez que o uso de bloqueadores de tais canais (diltiazem e verapamil) inibiu significativamente o transporte de cádmio para os hepatócitos.

O transportador DMT-1 (transportador de metais divalentes 1, do termo inglês *divalent metal transporter 1*) que representa um importante meio para o influxo de íons de ferro para as células, também está envolvido na absorção do cádmio e mercúrio **(Bridges & Zalups, 2005)** (Figura 5). Íons de cádmio e mercúrio podem substituir o ferro no nível dos transportadores DMT-1 e em outras moléculas com afinidade ao ferro, como a ferritina. De acordo com **Zalups & Ahmad (2003)**, a ligação dos íons de cádmio com a molécula de ferritina possibilitaria a entrada de complexos Cd-ferritina nas células por mecanismos similares aos caracterizados para a Fe-ferritina. O zinco possui baixa afinidade ao transportador DMT-1, sendo sua entrada nas células viabilizada por transportadores de zinco **(Zalups & Ahmad, 2003)**. Íons de cádmio e mercúrio também podem utilizar esse transportador para a sua entrada nas células. De acordo com **Wang *et al*. (2010)** os íons de cádmio competem com o zinco para ganhar acesso nos sítios de translocação de um ou mais transportadores de zinco.

No fígado, os metais complexados podem ser excretados através da bile (Figura 6), ou então, os complexos Cd/HgMT e Cd/HgGSH podem ser desfeitos, liberando íons que induzem efeitos tóxicos nas células hepáticas (Figura 6). Uma parte do metal complexado é ainda liberada para o sangue, sendo carreados até os rins, que em função do seu tamanho reduzido, são filtradas através da membrana glomerular, sendo absorvido pelas

células tubulares renais. Após a entrada nas células tubulares, a MT é catabolizada nos lisossomos, liberando íons de cádmio ou mercúrio **(Nordberg *et al*., 2007b)**, que vão induzir inúmeros danos teciduais (**Caranza-Rozales *et al*., 2005)** (Figura 6).

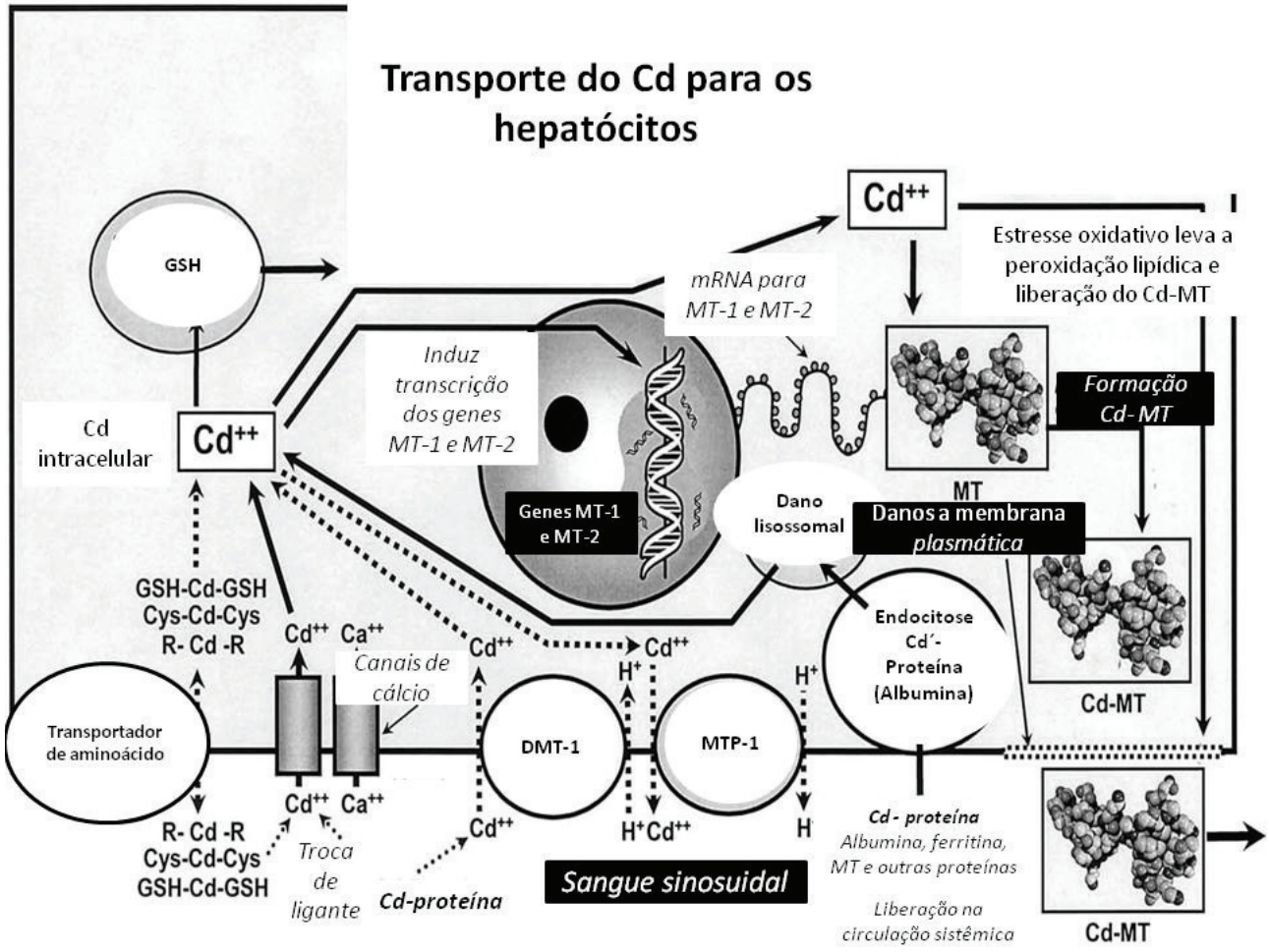

Figura 5. Esquema representando os mecanismos de transporte do cádmio dos sinusóides para os hepatócitos. Após a exposição ao cádmio, os íons presentes no sangue se ligam a proteínas como a albumina e ferritina. O cádmio também pode formar conjugados com a cisteína (Cys) ou se ligar a GSH e outras moléculas de baixo peso molecular que possuem o grupamento tiol (R-Cd-R). O cádmio pode ser absorvido pelos hepatócitos por meio de endocitose ou por transportadores de metais divalentes (DMT-1) e de proteínas metálicas (MTP-1) localizados na membrana plasmática dos hepatócitos. Outro mecanismo para cádmio atingir o ambiente intracelular dos hepatócitos é através de canais de cálcio. O cádmio atuaria como um mimético iônico do cálcio nos seus transportadores presentes na membrana dos hepatócitos. Em função dos íons de cádmio não existirem de forma livre, algumas reações de troca de ligantes ocorrem no nível dos canais de cálcio para permitir a entrada do cádmio através desse sistema de transporte. Transportadores de aminoácidos também estão envolvidos no transporte de compostos

miméticos de cádmio do sangue para os hepatócitos. No interior dos hepatócitos, o cádmio pode induzir a expressão dos genes da MT-1 e MT-2, o que faz com que grande parte do cádmio esteja ligada com a MT e com a GSH como mecanismo de proteção celular. No entanto, quando o aumento do cádmio intracelular ultrapassa a capacidade de defesa celular ocorre a indução de estresse oxidativo, que pode levar a peroxidação da membrana plasmática e morte celular. Parte do complexo Cd-MT é liberado para o sangue podendo atingir outros órgãos. Modificado de **Zalups & Ahmad (2003).**

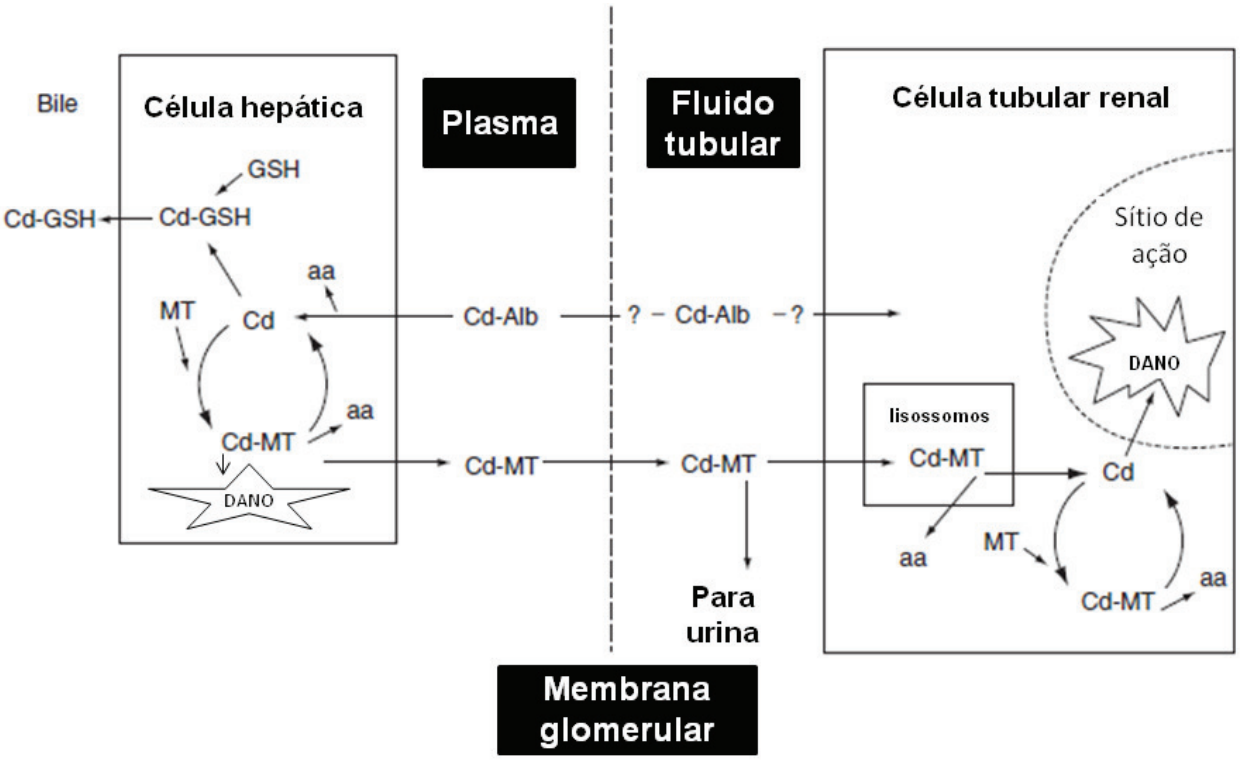

Figura 6. Fluxograma básico demonstrando a importância da glutationa (GSH), albumina (Alb) e metalotioneína (MT) no transporte do cádmio no organismo e a síntese e degradação de metalotioneína. aa: aminoácidos. Modificado de **Nordberg *et al*. (2007).**

A formação de compostos miméticos, como Cys-*S*-Hg-*S*-Cys e Cys-S-Cd-S-Cys também está envolvida no transporte de mercúrio e cádmio para as células tubulares renais através de transportadores de aminoácidos **(Zalups & Barfuss, 1993; Wang *et al*., 2010)**. Por apresentar semelhanças estruturais (Figura 4), os compostos Cys-*S*-Hg-*S*-Cys e Cys-S-Cd-S-Cys estariam mimetizando a cisteína no nível de um ou mais transportadores de membrana plasmática luminal das células tubulares renais **(Bridges &**

Zalups, 2010). A capacidade transporte de compostos miméticos de mercúrio foi demonstrada através do sistema $b^{0,+}$, um transportador heterodímero formado por duas sub-unidades $b^{0,+}$ e BAT **(Palacin *et al.*, 2001)**, que possui alta afinidade por cisteína e aminoácidos básicos, sendo um excelente alvo para a absorção do Cys-*S*-Hg-*S*-Cys **(Bridges & Zalups, 2010)** (Figura 7). Estudos *in vitro* em células MDCK tipo II (linhagem celular proveniente de rim canino) transfectadas com o sistema $b^{0,+}$ indicaram que a Cys-*S*-Hg-*S*-Cys é um substrato transportado por esse carreador **(Bridges *et al.*, 2004)**.

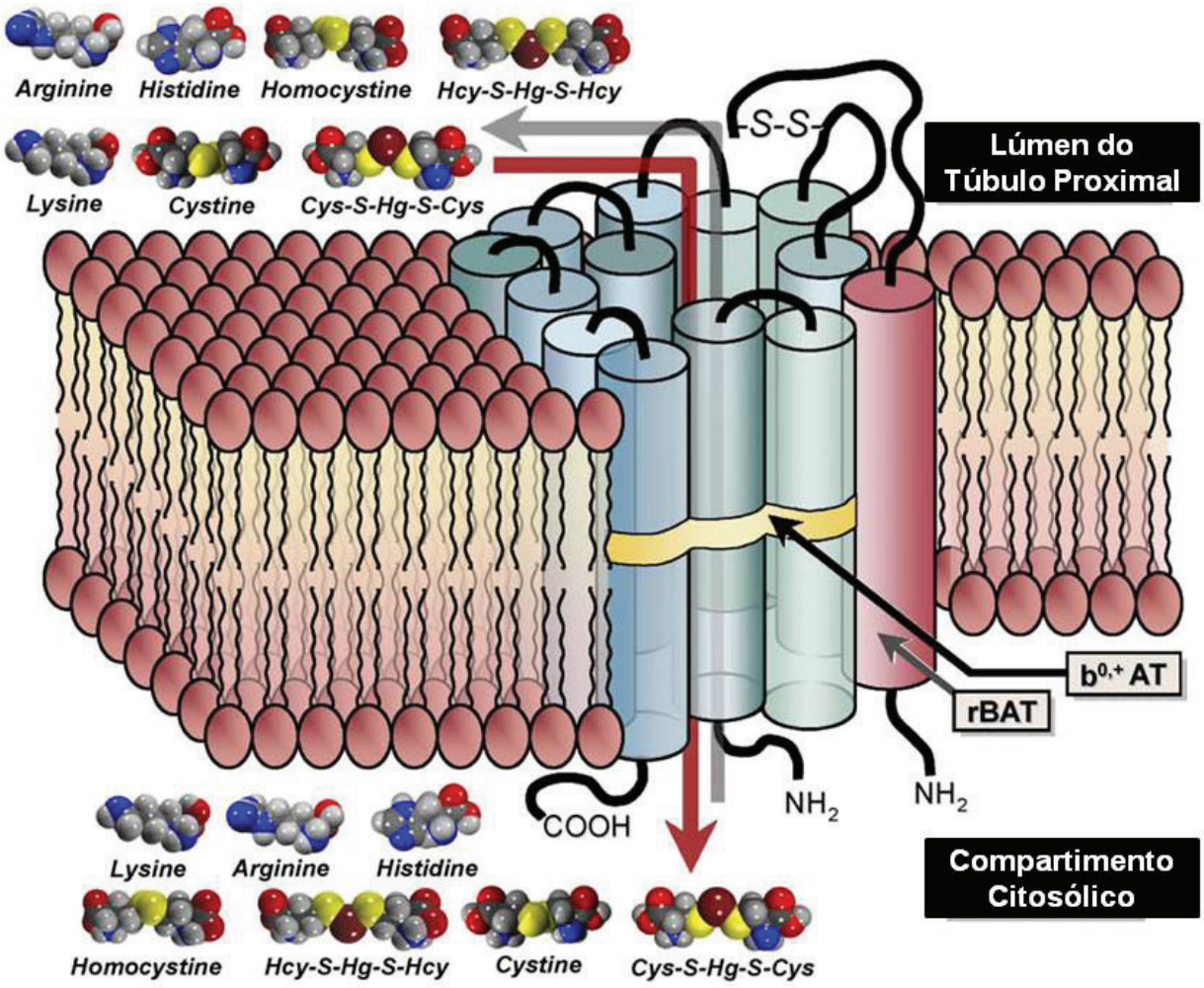

Figura 7. Esquema do transporte de aminoácidos e conjugados mercuriais pelo transportador de aminoácidos, sistema $b^{0,+}$. O sistema $b^{0,+}$ é um transportador formado por uma cadeia leve e outra pesada ligadas por pontes dissulfeto (S-S). A cadeia leve $b^{0,+}$AT (cilindros azuis) possui 12 domínios transmembrana, enquanto que a cadeia pesada rBAT (cilindro vermelho) atravessa a membrana plasmática apenas uma vez. Esse carreador é localizado na membrana plasmática das células epiteliais do túbulo proximal renal e atua como transportador de aminoácidos, bem como dos miméticos

estruturais como a Cys-S-Hg-S-Cys e Hcy-S-S-Hg-Hcy. Adaptado de **Bridges & Zalups (2005).**

Além do rim e do fígado, parte dos íons de cádmio e mercúrio complexados do sangue podem ainda atingir outros tecidos periféricos, sendo a acumulação diferencial nos tecidos influenciada por (1) características físico-químicas do composto (por exemplo, o pKa, a solubilidade lipídica, o volume molecular, (2) gradiente de concentração entre o sangue e os tecidos, (3) razão de fluxo sanguíneo para a massa de tecido, (4) afinidade relativa da química do sangue e dos constituintes de tecidos, e (5) atividade com proteínas transportadoras de membrana específicas **(Kleinow *et al.*, 2008)**.

1.4. Aspectos celulares e moleculares envolvidos na acumulação intracelular do cádmio e mercúrio

No meio intracelular, os íons cádmio e mercúrio permanecem acoplados com ligantes solúveis do citoplasma (principalmente GSH e MT), que sequestram esses íons metálicos no citosol, inicialmente como uma estratégia de redução do montante disponível para outras organelas e estruturas celulares críticas. Após a acumulação no citosol parte dos íons pode alcançar organelas celulares, como a mitocôndria e o núcleo que parecem ser os principais sítios intracelulares de acumulação de cádmio e mercúrio. Estudos *in vitro* realizados em linhagem de hepatócitos humano (células WRL-68) exposta ao mercúrio (5 μM for 1 h) demonstraram que a mitocôndria e o núcleo são importantes (48% e 38%, respectivamente) na acumulação de mercúrio **(Bucio *et al.*, 1995)**.

A acumulação de cádmio e mercúrio na mitocôndria induz alterações tanto na sua estrutura como na sua função. Decréscimo do potencial de membrana mitocondrial **(Lasfer *et al.*, 2008; Ye *et al.*, 2007)**, aumento de volume mitocondrial e desorganização das cristas mitocondriais foram descritos após eventos de contaminação por cádmio e mercúrio **(Bucio *et al.*, 1995**; **Giari *et al.*, 2007; Wang *et al.*, 2013)**. Os íons de cádmio e mercúrio também podem inibir atividade de complexos da cadeia transportadora de elétrons **(Wang *et al.*, 2004; Bertin & Averbeck, 2006)**. Essa disfunção pode levar a um acréscimo na produção de espécies reativas de oxigênio (EROs) em níveis superiores do que a capacidade de neutralização dos antioxidantes celulares, alguns deles já afetados

pela alta afinidade dos íons de cádmio e mercúrio aos grupamentos sulfidrila, levando a situação de estresse oxidativo **(Gobe & Crane, 2010)**.

O núcleo concentra grande quantidade de macromoléculas incluindo proteínas nucleares e ácidos nucleicos, sendo assim um importante sítio de acumulação de íons de cádmio e mercúrio **(Bose *et al*., 1993)**. A acumulação nuclear induz efeitos nas células expostas, inicialmente diagnosticada como alterações na condensação de cromatina, incidência de núcleos picnóticos (núcleos onde a cromatina se encontra altamente condensada) e dilatação do envelope nuclear **(Bucio *et al*., 1995; Mela *et al*., 2007; Giari *et al*., 2007; Ye *et al*., 2007; Giari *et al*., 2008; Wang *et al*., 2013).** Alterações severas como quebras no DNA foram observadas 3 h após o tratamento com o cloreto de mercúrio ($HgCl_2$) (0,5 µM) em linhagem de hepatócito humana (células WRL-68) **(Bucio *et al*., 1999)** e após 8 h de exposição com altas concentrações de cloreto de cádmio ($CdCl_2$) (200, 500 e 1000 µM) **(Fotakis *et al*., 2005)**. Quebras de DNA podem ocorrer após aumento intracelular de EROs ou através da inibição de várias enzimas envolvidas no sistema de reparo do DNA após exposição com cádmio ou mercúrio **(Bertin & Averbeck, 2006)**. Outra possibilidade de dano ao DNA é proveniente da liberação das enzimas lisossomais para o citosol, devido à desestabilização da membrana lisossomal induzida pela exposição aos metais **(Messner, 2012; Marchi *et al*., 2004)**. Alterações no DNA podem alterar diversos processos celulares como a expressão genética, transdução de sinal, parada do ciclo celular, proliferação e diferenciação celular e finalmente induzir morte celular **(Hartwig, 2010; Bertin e Averbeck, 2006)**.

Os lisossomos também parecem ser sítios de acumulação de cádmio e mercúrio, mesmo em menor proporção comparado com o citoplasma, mitocôndrias e núcleo **(Bose *et al*., 1993)**. A exposição aos metais induz a desestabilização da membrana lisossomal levando à liberação de enzimas lisossomais para o citoplasma, que podem atingir compartimentos celulares distintos e induzir quebras de DNA **(Fotakis *et al*., 2005)**. Perda de integridade lisossomal foi observada tão cedo quanto 5 h após o tratamento com cloreto de cádmio em células de hepatoma de rato (células HTC) (20 µM) **(Fotakis *et al*., 2005)**.

O retículo endoplasmático é parte integrante do sistema de endomembranar envolvido no tráfego e metabolismo de lípidos e proteínas **(Voeltz *et al*., 2002)**. Esta organela exerce também função importante na desintoxicação de substâncias hidrofóbicas exógenas **(Voeltz *et al*., 2002)**. Alterações como hipertrofia dos elementos do

retículo endoplasmático documentadas após eventos de exposição por mercúrio e cádmio **(Giari *et al*., 2007)** indicam a ocorrência de resposta ao estresse celular. A disfunção do retículo endoplasmático também pode contribuir para a produção de proteínas desenoveladas. Em resposta celular a exposição ao cádmio e mercúrio, as "proteínas de estresse" hsp70 são ativadas como parte do sistema de chaperonas para a reparação de proteínas deformadas ou eliminação pelo sistema ubiquitina-proteassoma **(Bertin e Averbeck, 2006)**.

Alterações na organização do citoesqueleto também foram documentadas após a exposição ao cádmio e mercúrio **(Mela *et al*., 2007)**. Esse efeito ocorre devido ao dano em diversas proteínas envolvidas no arranjo do citoesqueleto pela situação de estresse oxidativo induzida após a exposição aos metais **(Wang *et al*., 2011)**. Disfunções do citoesqueleto podem afetar não somente o posicionamento e movimento das organelas, como observado na desorganização citoplasmática das células tratadas com mercúrio e cádmio **(Giari *et al*., 2007; Mela *et al*., 2007; Giari *et al*., 2008)**, mas também interfere no tráfego de vesículas e secreção levando a vacuolização citoplasmática.

Dessa forma, a exposição aos metais cádmio e mercúrio induz a disfunção mitocondrial, danos à estrutura do DNA, alterações lisossomais e disfunção nos elementos do retículo endoplasmático e do citoesqueleto. Todos esses fatores atuam em conjunto para induzir a morte celular observada como efeito terminal da exposição ao mercúrio e cádmio **(Faverney *et al*., 2004; Ye *et al*., 2007; Lasfer *et al*., 2008**; **Ceccatelli *et al*., 2010; Cuello *et al*., 2010)**.

2. Avaliação do efeito dos metais pesados nos diversos níveis de organização biológica

A exposição aos poluentes induz inúmeros efeitos adversos nos organismos expostos, levando a ocorrência de alterações moleculares, celulares e fisiológicas nas espécies em reposta à contaminação **(Bernet *et al*., 1999)**. Essas alterações podem ser consideradas como indicadoras da exposição aos poluentes ou podem indicar um comprometimento da integridade fisiológica **(Costa *et al*., 2013).** Nesse sentido, um conjunto de ferramentas e índices é capaz expressar alterações no estado de saúde dos organismos expostos **(Moore *et al*., 2006).**

Dados que avaliam os níveis de poluentes nos organismos e os impactos da sua exposição são fragmentados tanto espacialmente como temporalmente **(Moore *et al*., 2006)**. Isso traz a necessidade de abordagens interdisciplinares para identificar tal ligação, uma vez que a avaliação do estado de saúde de espécies representativas pode ser usada no monitoramento das condições ambientais **(van der Oost *et al*., 2003)**.

Os efeitos tóxicos da contaminação podem ser visualizados em diversos níveis de organização biológica (Figura 8). Para uma completa avaliação dos impactos causados pelos poluentes é necessária a elucidação dos efeitos toxicológicos, desde os níveis molecular e celular, até investigações em níveis superiores de organismo e ecossistema **(Moore, 2002)**. No entanto, os efeitos deletérios da exposição aos metais podem não se tornar aparentes até que mudanças ocorram no nível de população ou ecossistema. Já sendo muito tarde para que medidas preventivas sejam tomadas, restando a remediação do dano ambiental.

O conceito da ecotoxicologia afirma que os efeitos deletérios dos metais são sempre precedidos de alterações sub-letais em níveis molecular e celular **(Migliarini *et al*., 2005)**. De acordo com **Moore (2002)**, em sistemas biológicos as reações tóxicas ocorrem em ordem sequencial de resposta ao poluente estressante (Figura 8). Efeitos a níveis hierárquicos superiores (população, organismo) são sempre precedidos por mudanças em processos biológicos anteriores (teciduais, celulares, moleculares) **(Boudou & Ribeyre, 1997)**. Assim, se faz necessário o uso de ferramentas que possibilitem a avaliação da contaminação, antes da ocorrência de efeitos críticos que ocasionam a morte dos organismos susceptíveis, já que o monitoramento ambiental, realizado por análises químicas tradicionais dos poluentes nos ecossistemas, não fornece uma evidência das consequências toxicológicas diretas e progressivas nas células e tecidos nos diferentes organismos (**Shea *et al.,* 2008)**.

A avaliação das alterações teciduais, celulares e moleculares pode ser utilizada como um indicador inicial da biodisponibilidade do contaminante e do seu impacto, fornecendo assim, informação valiosa sobre a extensão e possíveis consequências da exposição prolongada ou contínua **(Migliarini *et al*., 2005).** Tais respostas devem ser monitoradas, uma vez que podem indicar redução no desempenho dos organismos expostos, sendo um prognóstico para uma patologia emergente e de severos danos para a saúde dos animais **(Moore, 2002).**

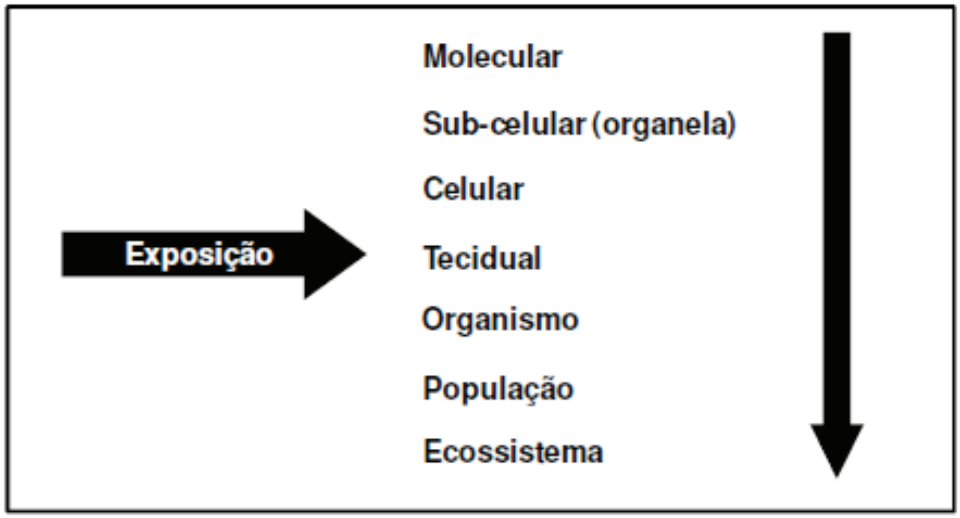

Figura 8. Ordem da resposta aos poluentes dentro do sistema biológico. Adaptado de **Van der Oost *et al.*, 2003.**

3. Avaliação do efeito dos metais pesados através de cultura de células

A pesquisa toxicológica é baseada na maior parte em estudos *in vivo*, principalmente no campo do monitoramento ambiental através da avaliação dos níveis de poluentes nos tecidos dos peixes. No entanto, diversas abordagens vêm sendo usadas para identificar os efeitos e entender os processos básicos que ocorrem nos sistemas biológicos **(Filipak Neto *et al.*, 2006)**.

As culturas de células têm sido amplamente exploradas como uma ferramenta para avaliação da toxicidade de metais **(Tan *et al.*, 2008)**, por oferecer uma alternativa para a utilização de animais *in vivo*, assegurando um ambiente bem definido para estudos toxicológicos **(Shea *et al.*, 2008; Romero *et al.*, 2004; Duncan-Achanzar *et al.*, 1996)**.

Estudos em cultura de células possibilitam o controle rigoroso das condições experimentais, a facilidade de aumentar o número de réplicas e na interpretação dos resultados, a baixa variabilidade experimental, o menor número de espécimes requeridos para os estudos, além dos ensaios serem geralmente mais rápidos e de menor custo **(Tan *et al.*, 2008**; **Guillouzo *et al.*, 1997)**.

Dentre os diversos modelos celulares para o estudo dos efeitos dos metais, os hepatócitos são interessantes em função da complexidade das funções hepática no

metabolismo dos organismos e na participação nos processos de toxicidade **(Guillouzo *et al*., 1997)**.

As células HuH-7, utilizadas no presente estudo, são hepatócitos bem diferenciados derivados de um carcinoma celular hepático humano **(Nakabayshi *et al.*, 1982)**. Essa linhagem está depositada originalmente no banco de células JCBR na Universidade de Okayama, nos Estados Unidos.

As células HuH-7 demonstram a capacidade de replicação contínua em meio definido, sem a adição de hormônios e fatores de crescimento, produzindo várias proteínas do plasma **(Nakabayshi *et al.*, 1982).** Depois de cultivadas, essas células ainda possuíam funções diferenciadas das células hepáticas *in vivo*, uma vez que foi observada a expressão de proteínas do plasma, de enzimas hepáticas como a glicose-6-fosfatase e frutose-1,6-difosfatase **(Nakabayshi *et al.*, 1982)** e também a capacidade de secreção de ácidos biliares, como o ácido cólico e quenodesoxicólico **(Amuro *et al*., 1994)**.

4. Uso dos peixes como indicadores biológicos de contaminação

Os peixes são considerados indicadores sensíveis de poluição aquática, uma vez que possuem um elevado potencial de acumulação **(Hinton *et al*., 2008)**. A avaliação das concentrações de metais nos tecidos dos peixes pode indicar o aumento da contaminação através dos níveis tróficos do ecossistema aquático até a exposição humana, expressando assim os riscos para o homem e para o meio ambiente. Isso ocorre porque os peixes apresentam ampla distribuição geográfica, desempenhando um importante papel ecológico nas cadeias alimentares aquáticas, com função de transportar energia para níveis tróficos superiores **(van der Oost *et al*., 2003)**. O consumo de peixe e frutos do mar também constitui uma das principais fontes de exposição ao cádmio e mercúrio para as populações humanas **(Malm *et al*., 1995; Ceccatelli *et al*., 2010; Ju *et al*., 2012).**

Por essas razões, os peixes têm atraído considerável interesse em estudos biológicos para avaliação da exposição aos contaminantes ambientais. No entanto, as espécies de monitoramento devem ser selecionadas considerando seu papel ecológico e sua relação com a matriz ambiental a ser avaliada **(van der Oost *et al*., 2003)**. Para avaliação de toxicidade, alguns fatores não podem ser negligenciados como o tamanho, idade, ecologia do animal e hábitos alimentares, uma vez que influenciam na acumulação dos metais entre esses organismos **(Dang & Wang, 2012).**

4.1. Avaliação das alterações morfológicas em diversos órgãos dos peixes como indicador do efeito tóxico dos metais.

A exposição dos peixes a poluição química presente no ambiente aquático é capaz de induzir alterações morfológicas **(Bernet *et al*., 1999)**. A histopatologia tem sido reconhecida como uma importante ferramenta para a avaliação do impacto ambiental **(Teh *et al*., 1997)**. Características histopatológicas de diversos órgãos dos peixes como fígado, rins e brânquias, podem ser avaliadas, sendo um parâmetro integrativo que pode expressar os impactos endógenos no organismo **(Teh *et al.,* 1997)**. Uma das principais vantagens do uso da histopatologia em programas de biomonitoramento das condições ambientais se refere à sua capacidade de fornecer informações sobre o estado de saúde e aptidão dos organismos expostos **(Costa *et al*., 2013).**

A aplicação de índices histopatológicos permite uma avaliação objetiva da integridade dos órgãos dos peixes, expressando as alterações entre a morfologia normal e as condições patológicas de forma quantitativa, sendo uma ferramenta importante para vincular o grau de poluição com a gravidade das alterações induzidas **(Bernet *et al*., 1999).**

- Histopatologia do fígado

Devido a sua estrutura e função, o fígado é um órgão central no metabolismo e homeostase dos peixes e tem sido descrito com alto potencial de acumulação tanto para o cádmio **(Klaassen *et al*., 2009)**, como para o mercúrio **(Liao *et al*., 2006; Mela *et al*., 2007**; **Chyb *et al*., 2001)**. Os íons de cádmio e mercúrio atingem o fígado independente da via de exposição (branquial ou alimentar) **(Chyb *et al*., 2001)**, o que reduz a disponibilidade do metal para outros órgãos como o rim e testículo, e aumenta a susceptibilidade desse órgão para seus efeitos tóxicos **(Souza *et al*., 1997).**

O fígado dos peixes é um órgão que apresenta usualmente um único lóbulo onde os hepatócitos estão organizados em túbulos. No parênquima hepático estão distribuídas células endoteliais que delimitam os sinusóides e células fagocíticas (Figura 9). O fígado ainda apresenta duplo aporte sanguíneo, sendo a maior parte proveniente da veia porta,

que drena o trato gastrointestinal, e uma contribuição adicional é realizada pela artéria hepática. Independente da fonte arterial ou venosa, o sangue entra nos sinusóides hepáticos. Os sinusóides são a base para o fígado ser um compartimento altamente irrigado, o que possibilita uma rápida absorção das substâncias **(Hinton *et al*., 2008)**.

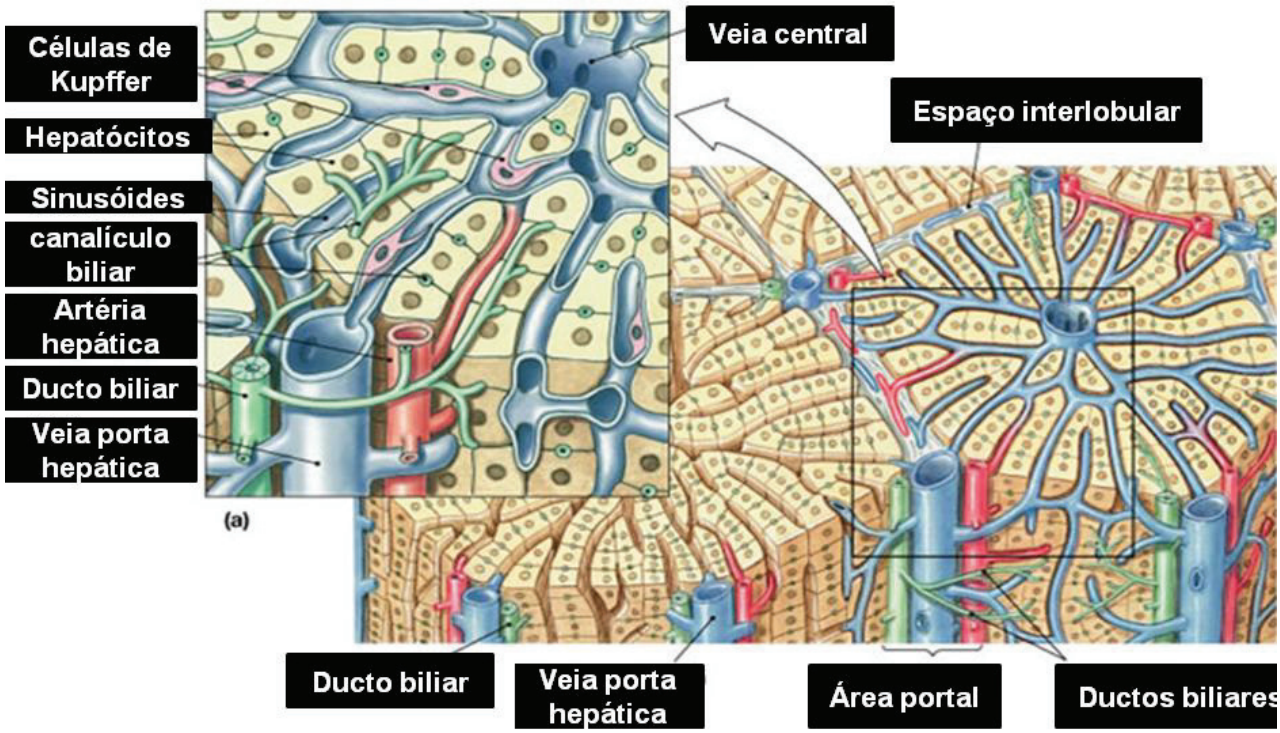

Figura 9. Esquema demonstrando a organização estrutural do fígado. Disponível em: http://www.as.miami.edu/chemistry/2086/Chap%2024/Chapter%2024-ewPART2.htm. Acesso: 29/04/2013.

O alto fornecimento de sangue é vital para as funções fundamentais do fígado no metabolismo básico dos peixes. No fígado, os nutrientes absorvidos são processados, armazenados e redistribuídos para a utilização pelos outros órgãos. No fígado também ocorrem importantes reações de biotransformação, que facilitam a eliminação de compostos exógenos. Esta função de desintoxicação é importante por fazer que substâncias com pouca solubilidade em água, se tornem metabólitos mais hidrofílicos, podendo ser mais facilmente excretados (**Hinton *et al*., 2008)**.

Vários estudos descreveram os danos no tecido hepático em peixes submetidos à contaminação natural **(Teh *et al*., 1997; Schwaiger *et al*., 1997; Rabitto *et al*., 2011)** e exposição laboratorial por cádmio **(Wangsongsak *et al*., 2007; Costa *et al*., 2010)** ou mercúrio **(Oliveira Ribeiro *et al*., 2002; Liao *et al*., 2006; Mela *et al*., 2007; Vergilio *et***

***al*., 2012a)** (Tabela 1). Alterações como perda das reservas lipídicas dentro dos hepatócitos, necrose, aumento da incidência de agregados de macrófagos e proliferação de tecido conjuntivo foram documentadas em peixes expostos a diferentes concentrações de cádmio ou mercúrio (Tabela 1). Nos hepatócitos também foram observadas alterações mitocondriais, ocorrência de núcleos picnóticos (núcleos com alta condensação de cromatina), hipertrofia do retículo endoplasmático, vacuolização, entre outros. A incidência de tais alterações demonstra a vulnerabilidade hepática à ação deletéria desses metais e desperta para a importância do seu monitoramento em peixes submetidos à contaminação ambiental.

Tabela 1. Principais alterações observadas no fígado de diferentes espécies de peixes após a exposição ao cádmio e mercúrio.

Alteração Hepática	Peixe	Fonte de contaminação	Referência
Degeneração das reservas lipídicas dos hepatócitos	*Lepomis auritus*	Fontes distintas incluindo PCBs e Hg	Teh *et al.*, 1997
	Salmo trutta f. fario	Fontes distintas incluindo metais, pesticidas e HPAs	Schwaiger *et al.*, 1997
	Salvelinus alpinus	Metil Hg e Hg inorgânico	Oliveira Ribeiro *et al.*, 2002
	Pontius gonionotus	Cloreto de Cd	Wangsongsak *et al.*, 2007
Ocorrência de áreas de necrose	*Channa punctatus*	Fungicida organo-mercurial (Emisan - MeEHgCl)	Ram & Sathyanesan, 1987
	Lepomis auritus	Fontes distintas incluindo PCBs e Hg	Teh *et al.*, 1997
	Salvelinus alpinus	Metil Hg	Oliveira Ribeiro *et al.*, 2002
	Oryzias latipes	Cloreto de Metil Hg	Liao *et al.*, 2006
	Hoplias malabaricus	Metil Hg	Mela *et al.*, 2007
	Hoplias malabaricus	Exposição ambiental incluindo Hg	Rabitto *et al.*, 2011
	Solea senegalensis	Cloreto de Cd	Costa *et al.*, 2010
Degradação do parênquima hepático	*Channa punctatus*	Fungicida organo-mercurial (Emisan - MeEHgCl)	Ram & Sathyanesan, 1987
	Gymnotus carapo	Cloreto de Hg	Vergilio *et al.*, 2012a
Processo inflamatório	*Salmo trutta f. fario*	Fontes distintas incluindo metais, pesticidas e HPAs	Schwaiger *et al.*, 1997
	Hoplias malabaricus	Exposição ambiental incluindo Hg	Rabitto *et al.*, 2011

Alteração Hepática	Peixe	Fonte de contaminação	Referência
Aumento nos centros de melano-macrófagos	*Lepomis auritus*	Fontes distintas incluindo PCBs e Hg	Teh *et al.*, 1997
	Hoplias malabaricus	Metil Hg	Mela *et al.*, 2007
	Hoplias malabaricus	Exposição ambiental incluindo Hg	Rabitto *et al.*, 2011
Proliferação do tecido conectivo	*Salvelinus alpinus*	Metil Hg	Oliveira Ribeiro *et al.*, 2002

- Histopatologia do rim

O papel multifuncional do rim dos peixes é refletido por sua complexa estrutura que envolve vários tipos de células diferentes e um intrincado sistema vascular **(Bonga & Lock, 2008)** (Figura 10). O rim dos teleósteos é um órgão misto compreendendo elementos do tecido hematopoiético, retículo-endotelial, endócrino e excretor **(Mumford *et al.*, 2007)**. O rim dos peixes é normalmente localizado numa posição retroperitoneal contra a coluna vertebral. É um órgão de coloração normalmente escura, estendido pela cavidade do corpo **(Bonga & Lock, 2008)**.

A principal função do rim dos peixes é a regulação osmótica de água e sais, ao invés da excreção de resíduos nitrogenados como nos mamíferos. No peixe, a maioria dos resíduos nitrogenados são excretados pelas brânquias. Em peixes de água doce, o rim deve conservar sal e eliminar o excesso de água. Isto é conseguido por uma alta taxa de filtração glomerular, reabsorção de sais nos túbulos proximais, e a diluição da urina no túbulo contorcido distal **(Mumford *et al.*, 2007)**. Nos peixes marinhos, a excreção de água tem de ser reduzida tanto quanto possível, em função do ambiente hiperosmótico, através da redução da taxa de filtração glomerular **(Beyenbach, 1995)**. Além das funções osmóticas, o rim também está envolvido na detoxificação de metais **(Mela *et al.*, 2007; Mieiro *et al.*, 2011)**.

Estudos toxicológicos revelaram extensas alterações histopatológicas no rim, como resultado de exposição ao cádmio e mercúrio. Os túbulos proximais parecem ser os primeiros afetados, mas os danos progridem para os segmentos posteriores e glomérulos, após exposição por um período mais longo ou uma maior concentração do agente tóxico.

Dentre as alterações renais descritas em peixes submetidos ao mercúrio e cádmio destaca-se a ocorrência de total degeneração dos túbulos renais, vacuolização e hiperplasia das células tubulares epiteliais, dentre outras **(Schwaiger *et al.*, 1997; Giari *et al.*, 2007; Wangsongsak *et al.*, 2007).**

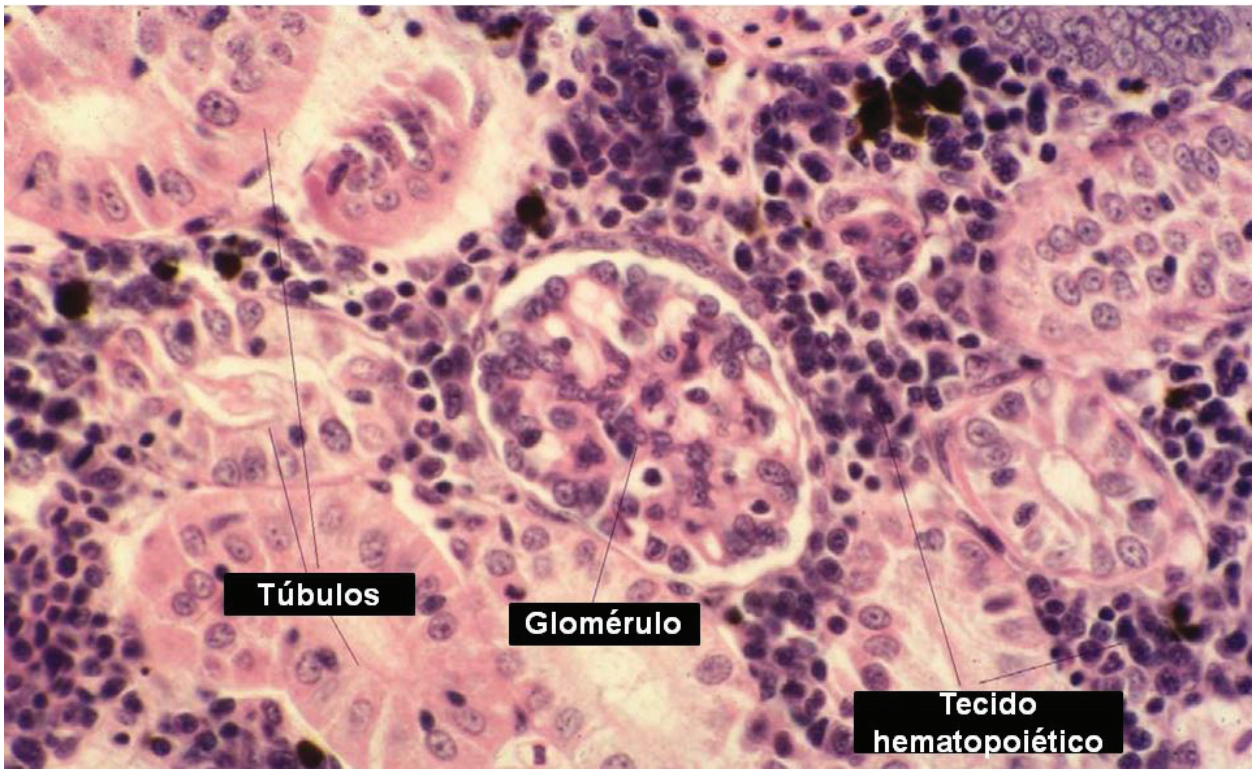

Figura 10. Corte histológico do rim demonstrando sua organização tecidual nos peixes. Presença dos túbulos proximais, glomérulo e tecido hematopoiético. Adaptado de **Mumford *et al.*, 2007**.

- Histopatologia das brânquias

As brânquias são responsáveis por funções relevantes, como a troca gasosa, regulação osmótica, equilíbrio ácido-base e excreção de resíduos nitrogenados **(Wilson & Laurent, 2002; Evans *et al.*, 2005)**. O epitélio branquial dos peixes é intensamente vascularizado com uma elevada área superficial, proporcionando uma fina barreira entre o sangue e o ambiente aquático **(Evans *et al.*, 2005).**

Por estarem em contato permanente com a água (Figura 11), as brânquias dos peixes estão diretamente envolvidas na absorção de poluentes, e assim, em geral,

refletem as exposições recentes **(Mieiro *et al.*, 2011)**, sendo um órgão importante para avaliações toxicológicas. Alternativamente, as brânquias dos peixes também são capazes de acumular substâncias químicas absorvidas por outras vias de exposição, devido à sua posição entre a circulação venosa e arterial, recebendo assim, quase todo o aporte cardíaco **(Pereira *et al.*, 2010)**. As brânquias têm sido amplamente utilizadas para investigar os efeitos da exposição do metal em peixes, devido à capacidade imediata de bioacumulação de metal, concomitante com a indução de resposta morfológica.

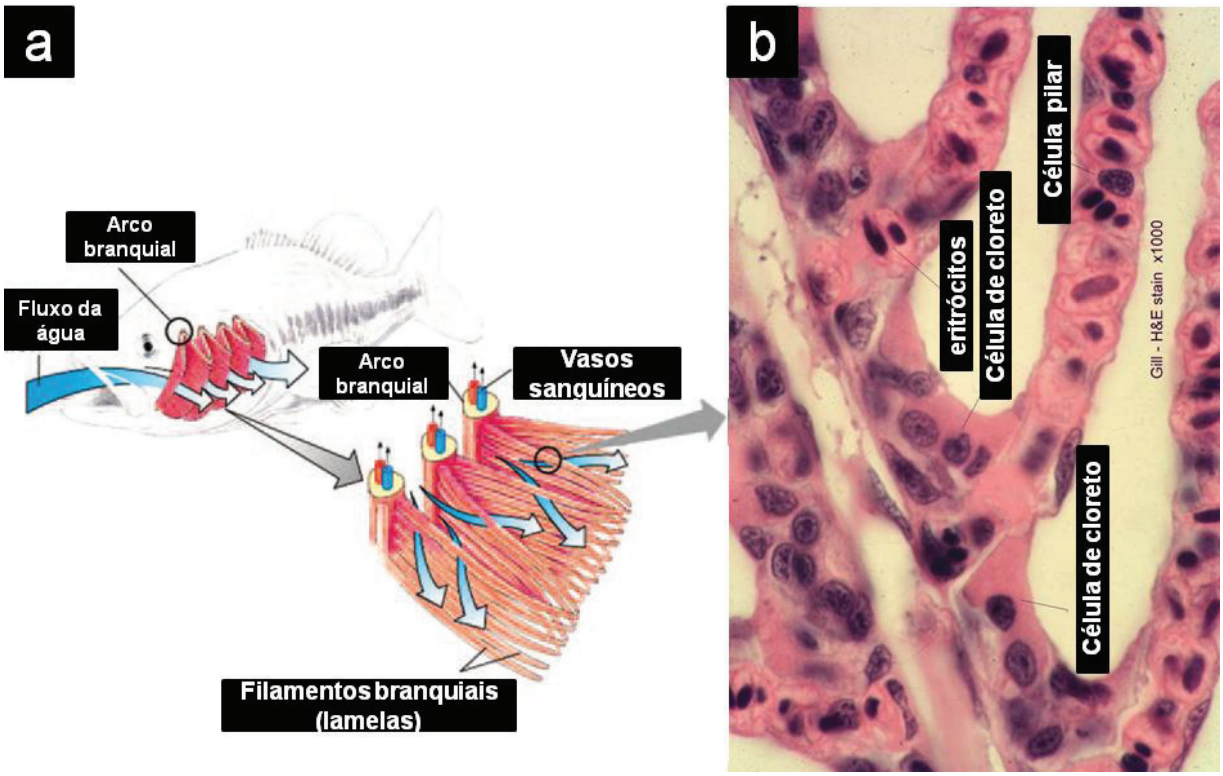

Figura 11. Esquema demonstrando a organização estrutural das brânquias. (a) Fluxo de água nas pelos filamentos branquiais. Adaptado de **Evans *et al.* (2005)** (b) Corte histológico da lamela secundária mostrando os diferentes tipos celulares presentes. Adaptado de **Mumford *et al.*, 2007**.

As brânquias são órgãos bilaterais compostos por uma série de estruturas em forma de arco **(Wilson & Laurent 2002)** (Figura 11). Os arcos branquiais são estruturas curvas que fornecem o suporte físico para os filamentos branquiais ou lamelas primárias. Alinhado ao longo de ambos os lados das lamelas primárias estão distribuídas as lamelas secundárias. Estes filamentos são considerados a unidade funcional básica das

brânquias, com uma grande área de superfície para a troca gasosa **(Wilson & Laurent, 2002)**. O epitélio branquial é normalmente composto por três ou mais camadas de células, incluindo a presença de células epiteliais de suporte, separadas por células pilares (Figura 11). As células pilares têm essencialmente uma função de suporte, mas também são encontradas no revestimento dos vasos sanguíneos lamelares. Células de cloreto e células mucosas aparecem espalhadas principalmente na base das lamelas secundárias.

Os íons de cádmio e mercúrio afetam inicialmente o epitélio branquial responsável pela cobertura lamelar externa. Alterações na superfície lamelar, como esfoliação das células epiteliais, desprendimento do epitélio lamelar, hiperplasia, edema e necrose foram descritas após eventos de contaminação por cádmio ou mercúrio. Efeitos nas células pilares também foram documentados após a exposição ao mercúrio e podem levar a expansão do lúmen dos vasos sanguíneos, resultando na congestão do sangue e telangiectasia (dilatações dos capilares ou aneurismas lamelares), sugerindo alterações adicionais na circulação das brânquias **(Teh *et al*., 1997; Oliveira Ribeiro *et al*., 2002; Liao *et al*., 2006; Giari *et al*., 2007; Giari *et al*., 2008)**. A exposição ao cádmio e mercúrio também induziu alterações nas células de cloreto **(Pratap & Bonga, 1993; Jagoe *et al*., 1996; Giari *et al*., 2007; Giari *et al*., 2008).** Essas células são responsáveis pelo transporte de íons pelas brânquias, exercendo importante função de regulação osmótica e excreção **(Wilson & Laurent, 2002).** O aumento no número de células de cloreto após o tratamento é um indicativo da necessidade de excreção dos íons de cádmio e mercúrio **(Laurent & Perry, 1991)**. Os danos aos diferentes tipos celulares branquiais leva a um efeito global, com a fusão completa das lamelas secundárias, o que foi demonstrado em vários estudos **(Oliveira Ribeiro *et al*., 2000; Liao *et al*., 2006; Giari *et al*., 2007; Giari *et al*., 2008; Rabitto *et al*., 2011)**. Esta mudança pode afetar diretamente a função branquial através da redução de área de superfície disponível para trocas gasosas.

Tabela 2. Principais alterações observadas nas brânquias de diferentes espécies de peixes após a exposição ao cádmio e mercúrio.

Alteração branquial	Peixe	Fonte de contaminação	Referência
Esfoliação das células epiteliais	*Salvelinus alpinus*	Hg inorgânico	Oliveira Ribeiro *et al.*, 2002
	Oryzias latipes	Cloreto de Metil Hg	Liao *et al.*, 2006
	Dicentrarchus labrax	Cd	Giari *et al.*, 2007
	Dicentrarchus labrax	Hg	Giari *et al.*, 2008
	Gymotus carapo	Cloreto de Hg	Vergilio *et al.*, 2012a
Alterações na superfície lamelar	*Oreochromis mossambicus*	Cd	Pratap & Bonga, 1993
	Gambusiu holbrooki	Cloreto de Hg	Jagoe *et al.*, 1996
	Trichomycterus zonatus	Hg inorgânico	Oliveira Ribeiro *et al.*, 2000
	Synechogobius hasta	Cloreto de Cd	Liu *et al.*, 2011
Necrose das células epiteliais	*Oreochromis mossambicus*	Cd	Pratap & Bonga, 1993
	Dicentrarchus labrax	Cd	Giari *et al.*, 2007
	Dicentrarchus labrax	Hg	Giari *et al.*, 2008
Necrose de células pilares e mucosas	*Oryzias latipes*	Cloreto de Metil Hg	Liao *et al.*, 2006
Aumento do número de células de cloreto	*Gambusiu holbrooki*	Cloreto de Hg	Jagoe *et al.*, 1996
	Oreochromis mossambicus	Cd	Pratap & Bonga, 1993
	Dicentrarchus labrax	Cd	Giari *et al.*, 2007
	Dicentrarchus labrax	Hg	Giari *et al.*, 2008
Telangiectasia (aneurismas nas lamelas secundárias)	*Lepomis auritus*	Fontes distintas incluindo PCBs e Hg	Teh *et al.*, 1997
	Salvelinus alpinus	Hg inorgânico	Oliveira Ribeiro *et al.*, 2002
	Oryzias latipes	Cloreto de Metil Hg	Liao *et al.*, 2006
	Dicentrarchus labrax	Cd	Giari *et al.*, 2007
	Dicentrarchus labrax	Hg	Giari *et al.*, 2008
	Synechogobius hasta	Cloreto de Cd	Liu *et al.*, 2011
Fusão de lamelas secundárias	*Gambusiu holbrooki*	Cloreto de Hg	Jagoe *et al.*, 1996
	Lepomis auritus	Fontes distintas incluindo PCBs e Hg	Teh *et al.*, 1997
	Salmo trutta f. fario	Fontes distintas incluindo metais, pesticidas e HPAs	Schwaiger *et al.*, 1997
	Trichomycterus zonatus	Hg inorgânico	Oliveira Ribeiro *et al.*, 2000
	Dicentrarchus labrax	Cd	Giari *et al.*, 2007
	Dicentrarchus labrax	Hg	Giari *et al.*, 2008
	Gymotus carapo	Cloreto de Hg	Vergilio *et al.*, 2012a

- Histopatologia do testículo

O testículo dos peixes segue a organização observada em todos os vertebrados, onde o parênquima é organizado em dois compartimentos: intersticial e tubular **(Schulz *et al.*, 2010)**. O testículo é coberto pela túnica albugínea, um tecido fibroso que circunda o órgão **(Rupik *et al.*, 2011)** que é contínuo com o compartimento intersticial.

O compartimento tubular é delimitado pela membrana basal e por células peritubulares e abriga o epitélio germinal, o qual é composto por células de Sertoli e por células germinativas **(Schulz *et al.*, 2010)**. Células germinativas estão organizadas em cistos onde ocorre a espermatogênese (Figura 12).

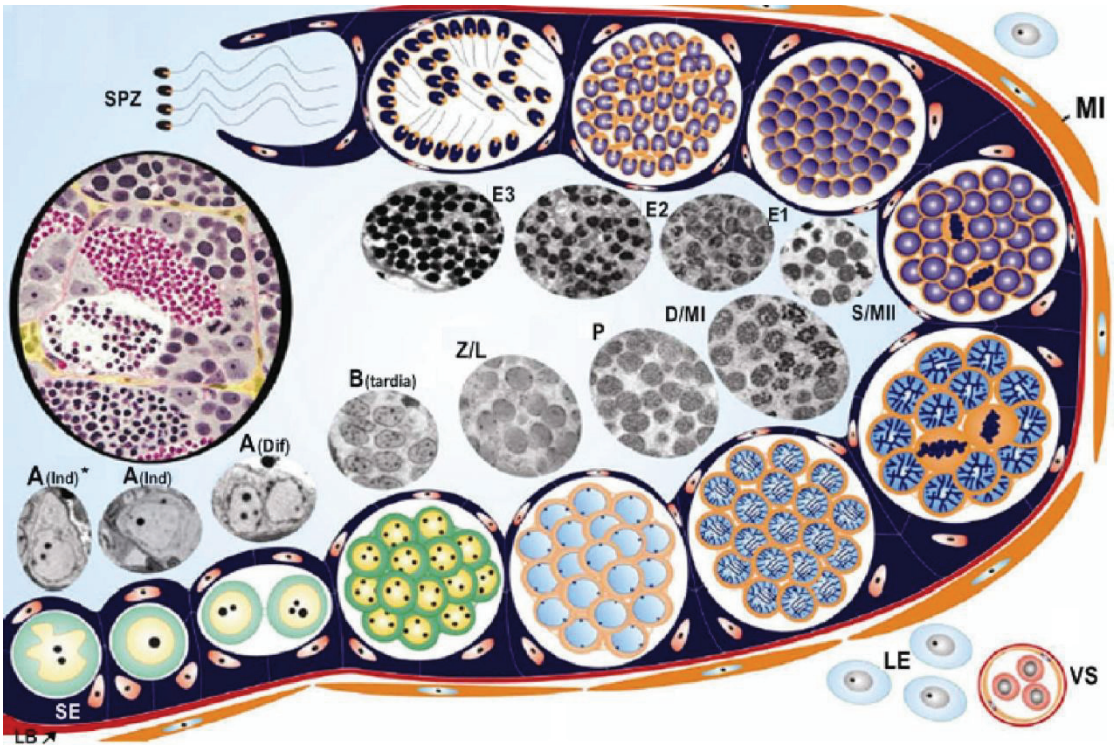

Figura 12. Esquema da espermatogênese nos peixes. O epitélio germinal contém células de Sertoli (SE), células germinativas envolvidas por uma lâmina basal (LB) e células mióides peritubulares (MI). No espaço intersticial são encontradas células de Leydig (L) e vasos sanguíneos (VS). A(Ind*): Espermatogônia tipo A (I) indiferenciada (célula-tronco); A(Ind): Espermatogônia tipo A (I) indiferenciada; B (tardia): Espermatogônia B (II) tardia; Z/L: Espermatócitos primários em leptóteno e zigóteno; P: Espermatócito primário em paquíteno; D/MI: Espermatócito primário em diplóteno / metáfase I; S/MII: Espermatócito secundário/ metáfase secundária II; E1: Espermátide inicial; E2: Espermátide intermediária; E3: Espermátide final. Adaptado de **Schulz, *et al,* 2010.**

No interior dos cistos, as células germinativas, em diferentes estágios de diferenciação são distribuídas como: espermatogônias primárias (SPGI) e secundárias (SPGII), espermatócitos primários (SPCI) e secundários (SPCII) e espermátides (SPD) (Figura 12). Essas células passam por várias divisões celulares, até a formação do espermatozóides ser completada dentro dos cistos **(Vergilio *et al*., 2012b)**.

As células germinativas são altamente especializadas, responsáveis pela propagação genética **(Celino *et al*., 2011)** e sua integridade é essencial para o desenvolvimento de futuras gerações e sobrevivência da prole **(Friedmann *et al*., 1996)**. No entanto, o sistema reprodutivo masculino é vulnerável a exposição a substâncias tóxicas, durante as sucessivas divisões celulares realizadas pelas células germinativas, antes da liberação do espermatozóide maduro **(Bonde, 2010)**. Apesar desta importância conhecida, ainda há pouca informação disponível sobre os mecanismos na patogênese induzida após exposição a metais no sistema reprodutor masculino em peixes **(Boujbiha *et al*., 2009)**.

Alterações testiculares descritas após exposição ao cádmio e mercúrio em diferentes espécies de peixes incluem rompimento da arquitetura normal do parênquima testicular, desorganização completa dos lóbulos seminíferos, degeneração lobular e decréscimo do número de células germinativas (dentre outras, ver referências, Tabela 3) ilustram a vulnerabilidade dos testículos para a toxicidade de metais.

Tabela 3. Alterações observadas no testículo de diferentes espécies de peixes após a exposição ao cádmio e mercúrio.

Alteração testicular	Peixe	Fonte de contaminação	Referência
Alteração da morfologia normal do parênquima testicular	*Stizostedion vitreum*	Metil Hg	Friedmann *et al*., 1996
	Puntius sarana	Cd	Kumari & Dutt, 1991
	Gymotus carapo	Cloreto de Hg	Vergilio *et al*., 2012a
Degeneração lobular	*Salvelinus fontinalis*	Cd	Sangalang & O' Halloran, 1973
	Puntius sarana	Cd	Kumari & Dutt, 1991
	Gymotus carapo	Cloreto de Hg	Vergilio *et al*., 2012a
Decréscimo no número de espematogônia, espermatócitos e espermátides	*Puntius sarana*	Cd	Kumari & Dutt, 1991
Ocorrência de espematozóides mortos no interior dos cistos	*Poecilia reticulata*	Cloreto de Metil Hg	Wester & Canton, 1992
	Oryzias latipes	Cloreto de Metil Hg	Liao *et al*., 2006
	Gymotus carapo	Cloreto de Hg	Vergilio *et al*., 2012a

4.2. Espécie de peixe Gymnotus carapo como modelo de estudo dos efeitos dos metais

Muitas das informações em relação a distribuição dos metais nos organismos e seus efeitos está baseada em espécies de peixe de água doce e de clima temperado. Ainda é limitada a poucas espécies tropicais a investigação da acumulação diferencial dos metais e dos efeitos tóxicos em diferentes tecidos e órgãos **(Mela *et al*., 2007; Oliveira Ribeiro *et al*., 1996)**. A absorção dos metais e os efeitos sobre a fisiologia dos peixes podem mudar devido as interações complexas com fatores ambientais entre os ecossistemas, fazendo necessários estudos para examinar os efeitos toxicológicos diretos dos metais sobre os tecidos e órgãos em espécies de peixes tropicais **(Oliveira Ribeiro *et al*., 2000)**.

A tuvira (*Gymnotus carapo*) **(Linnaeus, 1758)** é um peixe teleósteo (possuem esqueleto ósseo) da classe dos Actinopterígios de água doce e pertence à ordem dos Gymnotiformes, família dos Gymnotidae. Essa espécie é também conhecida como sarapoá, peixe espada, sarapó, carapó e ituí, sendo muito utilizada como isca viva na pesca esportiva por ser a mais preferida de espécies consideradas nobres, como os piscívoros de grande porte **(Vergilio *et al*., 2012b**). Os Gymnotiformes apresentam corpo anguiformes, abertura branquial muito estreita e são desprovidos das nadadeiras dorsal e ventral; possuem nadadeira anal muito longa, estendendo-se por quase toda a face ventral.

Essa espécie se encontra amplamente distribuída entre as Américas do Sul e Central, sendo facilmente encontrada em grande parte dos rios e lagos **(FISHBASE, 2013; Alberts *et al*., 2004)** (Figura 13). Os ambientes de ocorrência das tuviras são geralmente locais rasos, com profundidades inferiores a um metro, como áreas marginais de baías e vazantes, com bastante vegetação aquática **(Lovejoy *et al*., 2010; Crampton, 1996)**. Estudos feitos por **Resende & Pereira (2000)** sobre os aspectos biológicos e ecológicos da tuvira demonstram que esses peixes vivem em ambientes lênticos, com plantas aquáticas, onde se abrigam e encontram alimento. Caracterizam-se também por respiração aérea facultativa, sendo uma adaptação comum em peixes que vivem em ambientes hipóxicos e pela bexiga natatória altamente vascularizada **(Moraes *et al.,* 2002)**. A alta ocorrência da espécie em ambiente com baixo teor de oxigênio **(Crampton,**

1996), também possibilita a utilização dessa espécie no monitoramento das condições ambientais com possíveis fontes contaminantes.

Possuem hábito noturno, saindo durante esse período para águas mais abertas **(Menin, 1989; Barbieri & Barbieri, 1984)**. Essa espécie ainda apresenta órgãos elétricos que podem emitir uma pequena descarga elétrica, exercendo papel na eletrolocalização e eletrocomunicação **(Westby, 1975).** O campo elétrico é utilizado para a orientação da tuvira, compensando assim, a sua falta de visão na hora de predar espécies menores e também auxilia nas interações sociais, principalmente na época reprodutiva **(Corrêa & Hoffmann, 1999).**

A espécie *Gymnotus carapo* possui comportamento agressivo e territorial **(Westby, 1975; Alberts *et al*., 2004)**, sendo considerada uma das espécies mais agressivas, dentre os peixes elétricos que emitem fracas descargas. A hierárquica no comportamento é notável, uma vez que o comportamento territorial torna-se evidente quando mais de três peixes convivem no mesmo aquário **(Capurro *et al*., 1997).**

Em relação aos hábitos alimentares, a tuvira está adaptada a uma dieta predominantemente carnívora. Nesta espécie, a presença do estômago químico desenvolvido sugere uma adaptação à digestão de uma dieta rica em proteínas, porém não adaptada para a digestão de presas vivas de grande porte, pois poderiam perfurar a superfície desse órgão **(Silva & Oliveira, 1997)**. No ambiente natural, essa espécie se alimenta de forma seletiva, ingerindo organismos disponíveis no ambiente, preferencialmente insetos (odonatas) e microcrustáceos (cladóceros) encontrados usualmente nas margens dos corpos d'água **(Resende & Pereira, 2000; Silva & Oliveira, 1997)**.

A tuvira apresenta crescimento rápido em comprimento no seu primeiro ano de vida, antes de alcançar a maturidade sexual, quando os indivíduos atingem, em média, cerca de 20 cm de comprimento. Quanto ao peso, o comportamento é o inverso, uma vez que esses peixes começam a ganhar mais peso após o segundo ano de vida **(Barbieri & Barbieri, 1984)**. Segundo **Westby (1975)** não é possível reconhecer macroscopicamente diferenças sexuais na tuvira. Os machos, diferentemente das fêmeas, não apresentam alterações morfológicas perceptíveis nos testículos que possibilitem identificar diferentes estádios de maturação **(Resende & Pereira, 2000)**. A atividade espermatogênica da espécie *Gymnotus carapo* ocorre durante todo o ano, com diferentes intensidades, sendo maior entre novembro e janeiro, atingindo um pico entre outubro e dezembro **(Barbieri &**

Barbieri, 1984). O ciclo reprodutivo entre novembro e março também foi observado por **Cognato & Fialho (2006).**

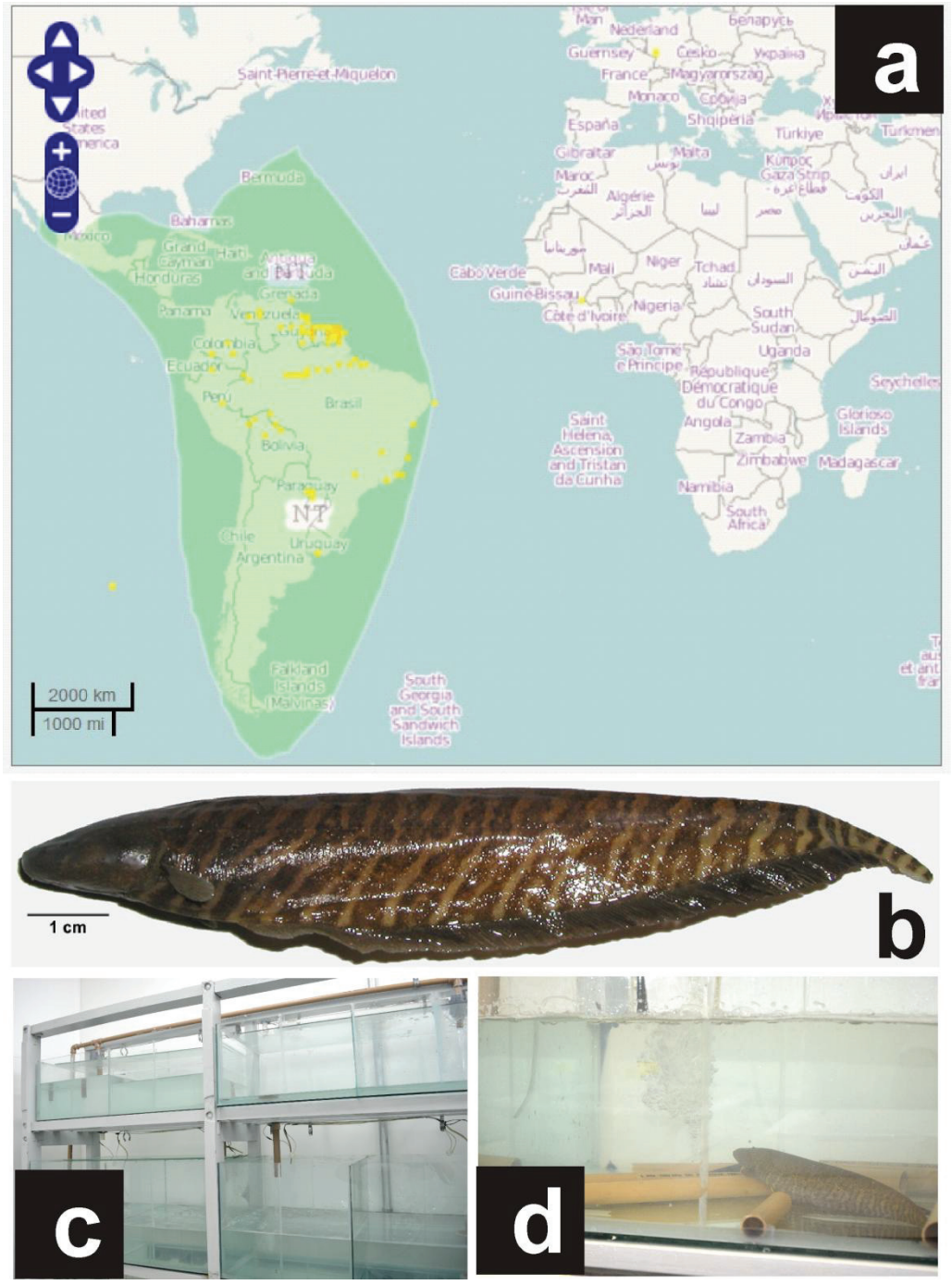

Figura 13. Mapa da distribuição da espécie *Gymnotus carapo* em regiões das Américas do Sul e Central. Os pontos amarelos indicam os locais de maior incidência. Disponível em: **GEIF, 2013**. (b) Foto do exemplar de *Gymnotus carapo*. Barra de escala = 1 cm. (c) Sistema de aquários utilizado no presente estudo. (d) Exemplar de *Gymnotus carapo* acondicionado no aquário durante a execução dos experimentos. Fonte: arquivo pessoal Cristiane Vergilio.

OBJETIVOS

OBJETIVO GERAL:

Avaliar os efeitos progressivos da exposição ao cádmio e mercúrio a nível celular e tecidual, caracterizando a evolução dos danos nos principais órgãos relacionados com a acumulação desses metais e nos sítios intracelulares envolvidos na indução de morte celular, usando como modelos o peixe tropical *Gymnotus carapo* e a linhagem hepatoma humano (células HuH-7).

OBJETIVOS ESPECÍFICOS:

- Analisar os efeitos da exposição aos metais mercúrio e cádmio em cultura de células, avaliando os danos em diferentes organelas celulares que estão envolvidas na indução de morte celular.

- Avaliar a acumulação diferencial e os potenciais danos morfológicos induzidos após a exposição aos metais mercúrio e cádmio em diferentes órgãos do peixe teleósteo *Gymnotus carapo*.

- Caracterizar a morfologia do testículo e espermatozóides do peixe teleósteo *Gymnotus carapo*

- Avaliar os danos na morfologia do testículo e espermatozóides do peixe teleósteo *Gymnotus carapo* induzidos após a exposição aos metais mercúrio e cádmio

MATERIAL E MÉTODOS

Os efeitos progressivos da exposição ao cádmio e mercúrio foram avaliados utilizando dois modelos: **1)** Linhagem de hepatócito humano (células HuH-7) e **2)** Peixe tropical *Gymnotus carapo*.

1. Efeitos da exposição ao cádmio e mercúrio em cultura de células HuH-7

Para observação dos efeitos da exposição ao cádmio e mercúrio, as culturas foram mantidas em meio de cultivo e plaqueadas fins experimentais. A exposição aos metais ocorreu com a incubação de solução de cádmio ou mercúrio em meio de cultura nas concentrações finais de 1 µM, 5 µM, 10 µM, 15 µM e 20 µM, durante os tempos de exposição de 2 h, 6 h, 12 h e 24 horas para observação dos efeitos tóxicos.

Os procedimentos experimentais realizados foram descritos detalhadamente como parte integrante dos artigos científicos listados:

- Autophagy, apoptosis and organelle features during cell exposure to cadmium
Vergilio, C.S & Melo, E. J. T. (manuscrito submetido para revista Biocell)

- Mercury effects in multiple organelles lead to cell death for both apoptotic and autophagic events
Vergilio, C.S & Melo, E. J. T. (manuscrito em preparação).

Um esquema dos procedimentos realizados na cultura de células HuH-7 após a exposição ao cádmio e mercúrio está demonstrado na Figura 14:

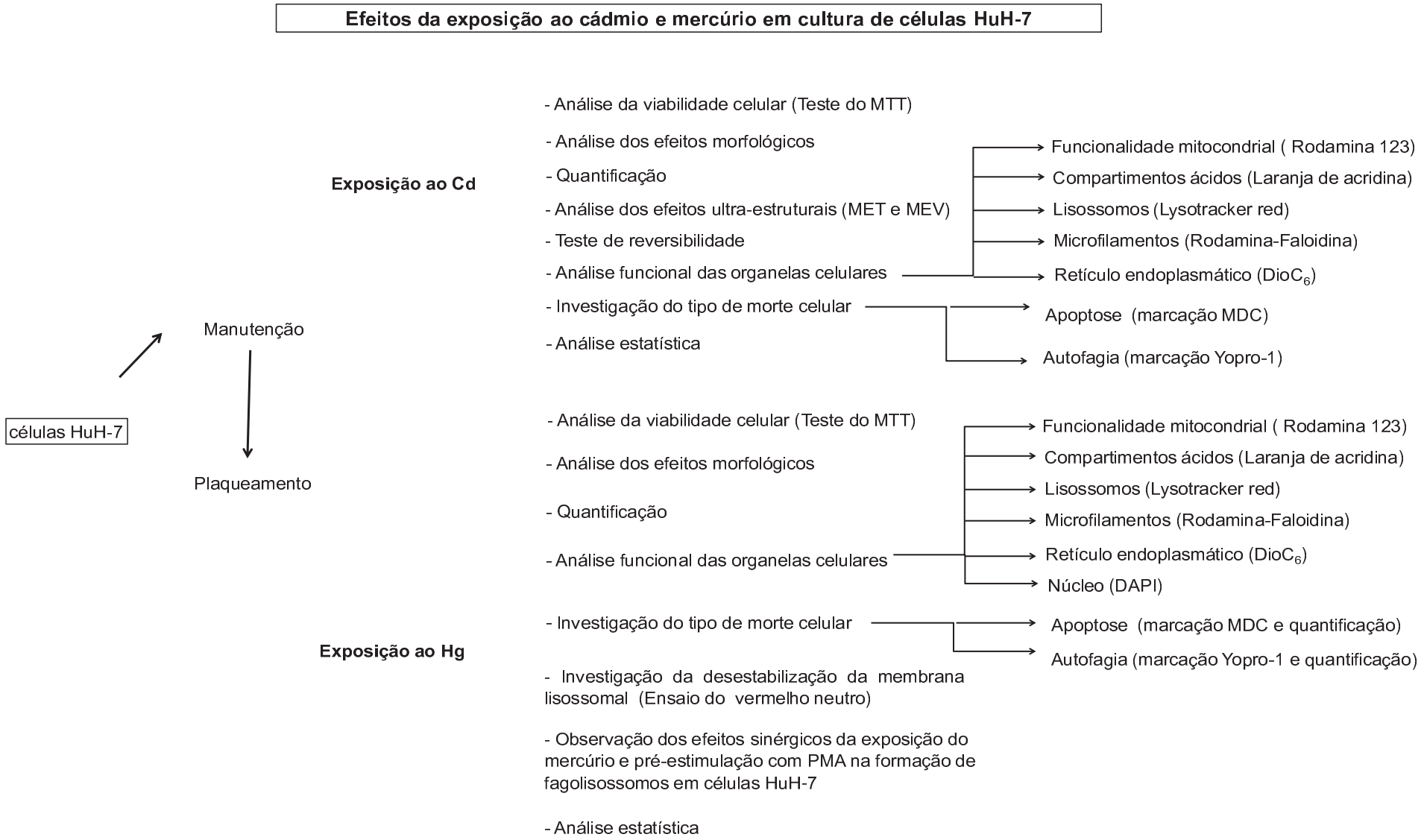

Figura 14. Esquema demonstrando os experimentos realizados na cultura de células HuH-7 após exposição ao cádmio e mercúrio.

2. Efeitos da exposição ao cádmio e mercúrio nos órgãos do peixe tropical *Gymnotus carapo*

Os exemplares utilizados neste trabalho foram coletados na Lagoa de Cima (Figura 15), localizada na região norte do Estado do Rio de Janeiro (21º 46' S e 41º 31' W), sendo compradas diretamente de pescadores locais que trabalham na lagoa. As amostras foram coletadas durante o período de março de 2009 a novembro de 2012. No presente estudo foram coletados 320 exemplares de *Gymnotus carapo.*

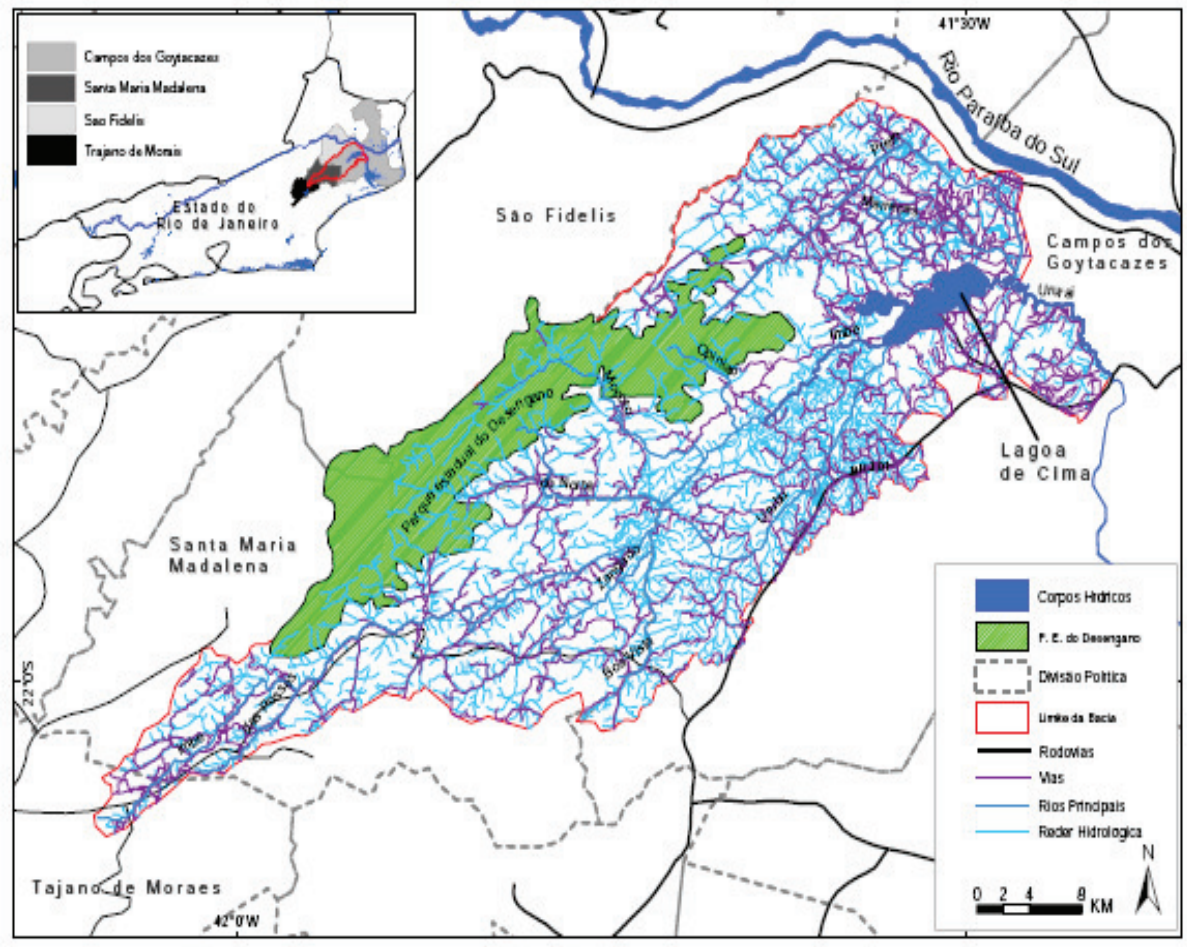

Figura 15. Localização da Lagoa de Cima no município de Campos dos Goytacazes, no estado do Rio de Janeiro.

Estudos prévios realizados na região indicam que a Lagoa de Cima apresenta baixos níveis de mercúrio, justificando a sua utilização como área para a coleta dos exemplares para os experimentos. De acordo com o estudo de **Sousa (2000)** que

determinou a concentração de Hg nos sedimentos e solos de lagoas do norte do Estado do Rio de Janeiro, encontrou uma média de 158,4 $\mu g.Kg^{-1}$ de mercúrio para o sedimento da lagoa de Cima, valor esse considerado inferior em comparação com as médias encontradas nas outras áreas estudadas. Posteriormente, **Ferreira *et al.* (2003)** e **Gomes (2004)** também adotaram a lagoa de Cima como área controle ao encontrar baixas concentrações de mercúrio nos tecidos muscular e hepático de *Hoplias malabaricus*.

Os peixes coletados foram transportados vivos em caixas de isopor com água obtida de seu habitat natural, sendo encaminhados para o Laboratório de Ciências Ambientais (LCA), na UENF. Os peixes permaneceram acondicionados num sistema de aquários de fluxo contínuo (livre de cloro, por evaporação), com circulação constante da água por um sistema de bombas com filtros internos. A qualidade da água foi monitorada, medindo-se amônia tóxica, nitrito, pH através de kits colorimétricos (Labcon Teste – Alcon). Os valores de pH estão de acordo com o banco de dados publicados pelo FISHBASE para a espécie **(FISHBASE, 2013)**. Durante este período, os peixes foram mantidos sob fotoperíodo natural a uma temperatura média de 25ºC.

Os peixes coletados foram utilizados visando o cumprimento das seguintes metas:

- *Avaliação da acumulação diferencial e dos efeitos histopatológicos nos órgãos de Gymnotus carapo após a exposição ao cádmio e mercúrio*

- *Caracterização do testículo maduro de morfologia do espermatozóide de Gymnotus carapo*

- *Efeitos da exposição ao cádmio e mercúrio na estrutura do testículo e espermatozoide de Gymnotus carapo*

2.1. Avaliação da acumulação diferencial e dos efeitos histopatológicos nos órgãos de *Gymnotus carapo* após a exposição ao cádmio e mercúrio

Para avaliação da acumulação diferencial de cádmio ou mercúrio nos órgãos do peixe *Gymnotus carapo*, os exemplares coletados (n= 40 para os experimentos com cádmio e n= 48 para os experimentos com mercúrio) foram expostos a uma única

concentração de cada um dos metais (30 µM, equivalente a 0,6 $\mu g.g^{-1}$, considerando o peso do exemplar tratado) e os efeitos observados após 24 h, 48 h, 72 h e 96 h de exposição. Os peixes foram expostos através de injeção intra-peritoneal, sendo injetado o volume de 0,1 mL da solução de cádmio ou mercúrio em cada espécime. O grupo controle, por sua vez, foi injetado com solução de PBS (do termo em inglês "Phosphate Buffer Saline"). Após cada tempo de exposição, os indivíduos foram medidos, pesados e necropsiados para retirada do rim, fígado, testículo, brânquias e músculo para as análises histológicas e determinação de metais. No caso do rim, as análises só foram realizadas após o tratamento com cádmio.

Os procedimentos experimentais realizados foram descritos detalhadamente como parte integrante dos artigos científicos listados:

- Differential accumulation and histopathological effects of cadmium exposure in the tropical fish *Gymnotus carapo*

Vergilio, C. S., Moreira, R. V., Gomes, L. S., Carvalho, C. E.V. & Melo, E. J. T. (manuscrito em preparação)

- Accumulation and histopathological effects of mercury chloride after acute exposure in tropical fish *Gymnotus carapo*

Vergilio, C. S., Carvalho, C. E.V. & Melo, E. J. T. (2012). *Journal of Chemical Health Risks 2(4): 01-08, 2012.*

Um esquema dos procedimentos realizados para avaliação da acumulação diferencial e dos efeitos histopatológicos nos órgãos de *Gymnotus carapo* após a exposição ao cádmio e mercúrio está demonstrado na Figura 16:

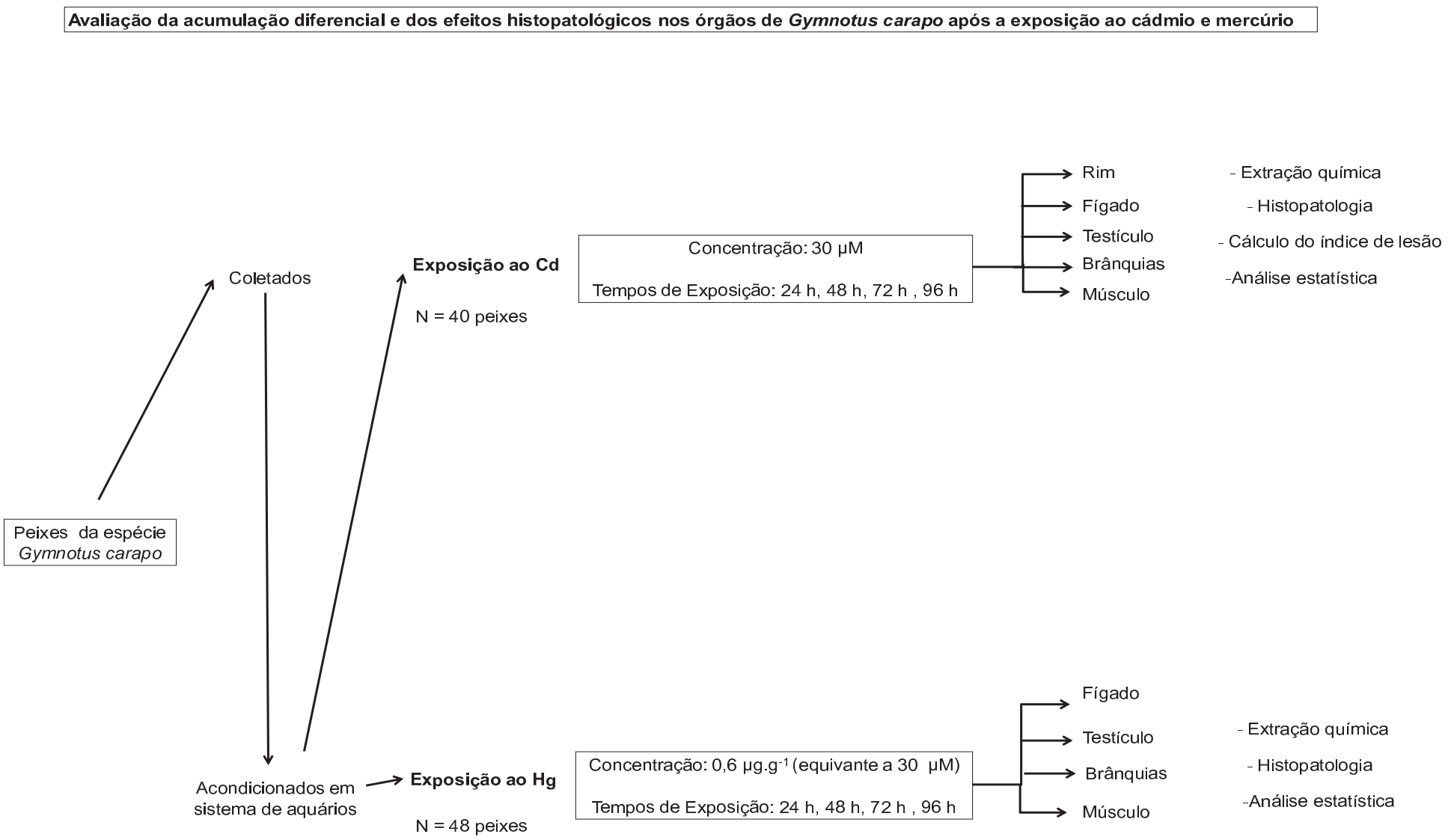

Figura 16. Esquema demonstrando os experimentos realizados para avaliação da acumulação diferencial e dos efeitos histopatológicos nos órgãos de *Gymnotus carapo* após a exposição ao cádmio e mercúrio.

2.2. Caracterização do testículo maduro de morfologia do espermatozóide de *Gymnotus carapo*

Aspectos da dinâmica reprodutiva e histologia gonadal da espécie Gymnotus sp. estão descritos na literatura, no entanto, uma caracterização detalhada da estrutura do testículo e da morfologia do espermatozoide dessa espécie ainda são necessários. Com isso, o presente estudo examinou a estrutura testicular e morfologia dos espermatozóides da espécie de peixe tropical *Gymnotus carapo*. Os exemplares (n = 36) utilizados eram machos em mesmo estágio de maturação sexual. Os peixes foram medidos, pesados e necropsiados para retirada do testículo para as análises morfológicas. Os testículos também foram preparados para análise dos espermatozóides e pesados para determinação do índice gonadossomático.

Os procedimentos experimentais realizados foram descritos detalhadamente como parte integrante do artigo científico listado:

- Characterization of mature testis and sperm morphology of Gymnotus carapo (Gymnotidae, Teleostei) from the southeast of Brazil

Vergilio, C. S., Moreira, R. V., Carvalho, C. E.V. & Melo, E. J. T. (2013). *Acta Zoologica*, 94: 364–370. doi: 10.1111/j.1463-6395.2012.00569.x

Um esquema dos procedimentos realizados para a caracterização morfológica do testículo e espermatozóide do peixe teleósteo *Gymnotus carapo* estão demonstrados na Figura 17:

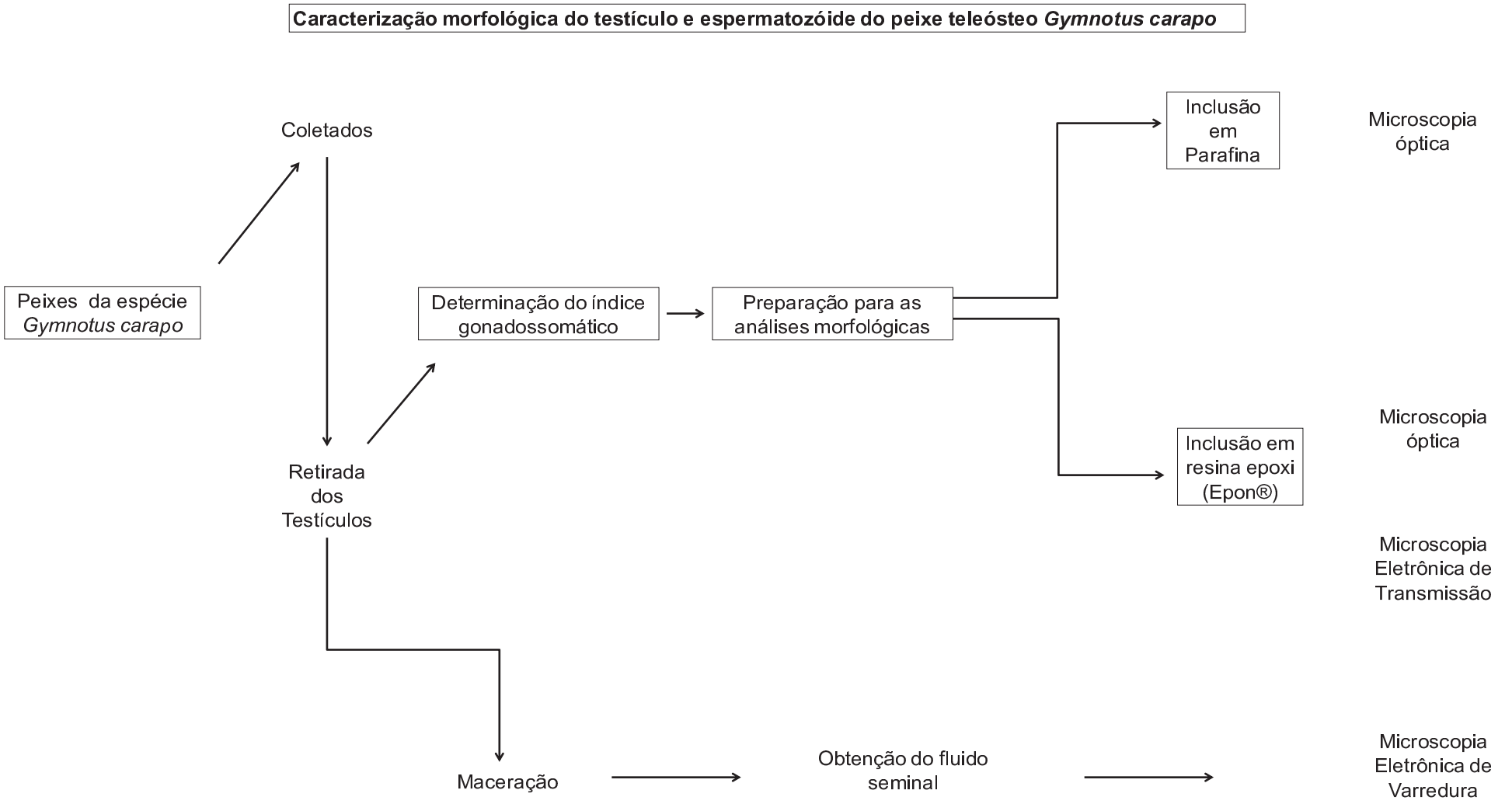

Figura 17. Esquema demonstrando os experimentos realizados para a caracterização do testículo e espermatozoide do peixe teleósteo *Gymnotus carapo*.

2.3. Efeitos da exposição ao cádmio e mercúrio na estrutura do testículo e espermatozóide de *Gymnotus carapo*

Após a caracterização do testículo e espermatozóide da espécie *Gymnotus carapo*, os efeitos progressivos da exposição ao cádmio e mercúrio foram avaliados. Os exemplares coletados (n= 40 nos experimentos de cádmio e n= 116 nos experimentos de mercúrio) foram expostos a concentrações crescentes de cádmio e mercúrio nas concentrações de 5 µM, 10 µM, 20 µM, 30 µM (a concentração de 40 µM foi utilizada para apenas o tratamento com cádmio). Os peixes expostos a cada uma das concentrações foram dissecados após 96 h para os experimentos com cádmio e após 24 h, 48 h, 72 h e 96 h nos tratamentos com mercúrio. Seis peixes foram utilizados para avaliação dos efeitos em cada concentração/tempo de exposição, desses três eram para as análises morfológicas e três para determinação química dos metais. Os peixes foram expostos através de injeção intra-peritoneal, sendo injetado o volume de 0,1 mL da solução de cádmio ou mercúrio em cada espécime. O grupo controle, por sua vez, foi injetado com solução de PBS (do termo em inglês "Phosphate Buffer Saline"). Após cada tempo de exposição, os indivíduos foram medidos, pesados e necropsiados para retirada testículo para as análises histológicas e determinação de metais. Preparações também foram realizadas para avaliação do efeito da exposição ao cádmio e mercúrio no número e morfologia dos espermatozóides.

Os procedimentos experimentais realizados foram descritos detalhadamente como parte integrante dos artigos científicos listados:

- ***Effects of cadmium exposure in male gonads and sperm structure of the tropical fish Gymnotus carapo***

Vergilio, C. S., Moreira, R. V., Gomes, L. S., Carvalho, C. E.V. & Melo, E. J. T. (manuscrito submetido para o *Bulletin of Environmental Contamination and Toxicology*)

- Effects of in vitro exposure to mercury on male gonads and sperm structure of the tropical fish tuvira Gymnotus carapo (L.)

Vergilio, C. S., Moreira, R. V., Carvalho, C. E.V. & Melo, E. J. T. (2013). *Journal of Fish Diseases*. n/a-n/a. doi:10.1111/jfd.12148

Um esquema dos procedimentos realizados para avaliação dos efeitos da exposição ao cádmio e mercúrio na estrutura do testículo e espermatozóide de *Gymnotus carapo* estão demonstrados na Figura 18:

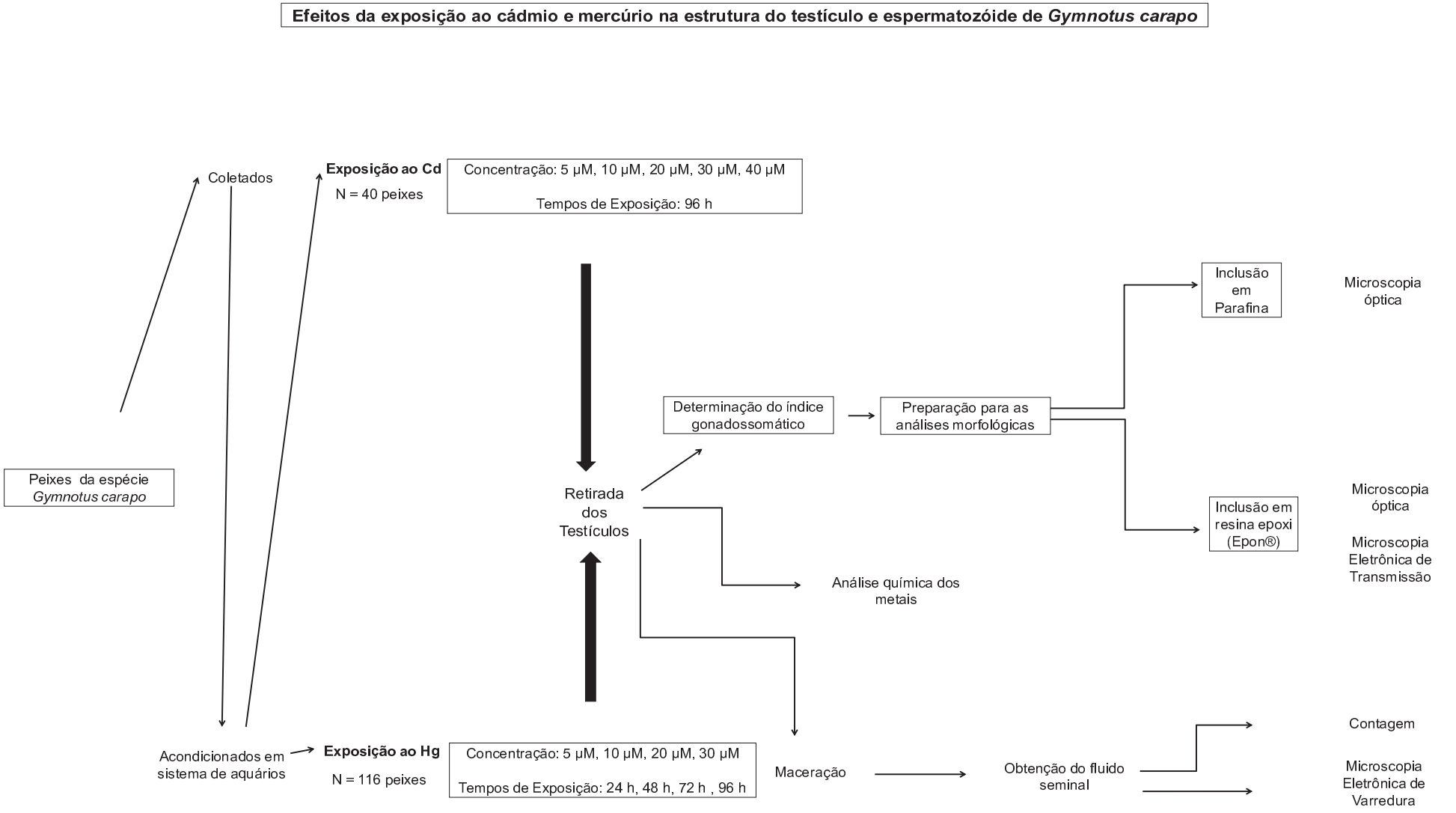

Figura 18. Esquema demonstrando os experimentos realizados para avaliação dos efeitos da exposição ao cádmio e mercúrio na estrutura do testículo e espermatozóide de *Gymnotus carapo.*

RESULTADOS

Os resultados dessa tese serão apresentados na forma de artigos científicos como listados a seguir:

1. Autophagy, apoptosis and organelle features during cell exposure to cadmium

Vergilio, C.S & Melo, E. J. T. (manuscrito submetido para revista Biocell).

2. Mercury effects in multiple organelles lead to cell death for both apoptotic and autophagic events

Vergilio, C.S & Melo, E. J. T. (manuscrito em preparação).

3. Differential accumulation and histopathological effects of cadmium exposure in the tropical fish Gymnotus carapo

Vergilio, C. S., Moreira, R. V., Gomes, L. S., Carvalho, C. E.V. & Melo, E. J. T. (manuscrito em preparação)

4. Accumulation and histopathological effects of mercury chloride after acute exposure in tropical fish Gymnotus carapo

Vergilio, C. S., Carvalho, C. E.V. & Melo, E. J. T. (2012). *Journal of Chemical Health Risks 2(4): 01-08, 2012.*

5. Characterization of mature testis and sperm morphology of Gymnotus carapo (Gymnotidae, Teleostei) from the southeast of Brazil

Vergilio, C. S., Moreira, R. V., Carvalho, C. E.V. & Melo, E. J. T. (2012). *Acta Zoologica*, 94: 364–370. doi: 10.1111/j.1463-6395.2012.00569.x

6. Effects of cadmium exposure in male gonads and sperm structure of the tropical fish Gymnotus carapo

Vergilio, C. S., Moreira, R. V., Gomes, L. S., Carvalho, C. E.V. & Melo, E. J. T. (manuscrito submetido para o *Bulletin of Environmental Contamination and Toxicology*)

7. Effects of mercury in vitro exposure in male gonads and sperm structure of the tropical fish Gymnotus carapo (L.)

Vergilio, C. S., Moreira, R. V., Carvalho, C. E.V. & Melo, E. J. T. (2013). *Journal of Fish Diseases*. n/a-n/a. doi:10.1111/jfd.12148

Autophagy, apoptosis and organelle features during cell exposure to cadmium

Cristiane dos Santos VERGILIO[1] and Edésio José Tenório de MELO[1]

1. Universidade Estadual do Norte Fluminense, Centro de Biociências e Biotecnologia, Laboratório de Biologia Celular e Tecidual, Campos dos Goytacazes, RJ, Brasil, 28013-602;

ABSTRACT

Cadmium (Cd) induces several effects in different tissues, but little is known about the relationship between toxic metal effects and organelle functions. To observe the progression of Cd effects on cellular organelle structure and function, HuH-7 cells (human hepatic carcinoma cell line) were exposed to Cd in increasing concentrations (1 μM – 20 μM) and exposure times (2 h – 24 h). During Cd treatment, the cells exhibited a progressive decrease in viability that was both time- and dose-dependent. Cd-treated cells displayed progressive morphological changes that included cytoplasm retraction and nuclear condensation preceding a total loss of cell adhesion. Treatment with 10 μM for 12 h led to irreversible damages. Before these drastic and irreparable damages, treated cells (5 μM for 12 h) presented a progressive loss of mitochondrial functionality and cytoplasm acidification as well as the dysfunction and disorganization in microfilaments and endoplasmic reticulum. These damages lead to the induction of apoptotic events and an increase in autophagic bodies in the cytoplasm. The results revealed that Cd affects multiple intra-cellular targets for inducing alterations in the mitochondria, cytoskeleton, endoplasmic reticulum and acidic compartments, ultimately culminating in cell death (toxic effect) via apoptotic and autophagic pathways.

Key words: Cd ; cell death; hepatocyte; HuH-7 cells; mitochondria

INTRODUCTION

Cadmium (Cd) is a highly toxic metal that exerts multiple effects on organisms (Filipič, 2012; Waisberg *et al*., 2003; Bertin and Averbeck, 2006). However, the complexity and diversity of events associated with cell-Cd interactions have resulted in fragmented data mainly related with organelle structure and function (Cannino *et al*., 2009).

Biochemical studies have demonstrated the involvement of organelles in Cd toxicity including mitochondria, lysosomes and the cytoskeleton in various cell lines (Cannino *et al*., 2009, Fotakis *et al*., 2005; Faverney *et al*., 2004; L'Azou *et al*., 2002). However, the wide-ranging effects of the metal on organelles and their involvement in induced cell death remain to be fully understood (Fabbri *et al*., 2012). Therefore, the observation of cytotoxic effects on different intra-cellular targets is necessary especially using vital fluorescent probes and microscopy for the overall understanding of Cd-induced cell damage and toxicity.

Cd exposure in organisms can induce pathological and physiological injuries in the liver, testes, lungs, kidneys and bones (Ye *et al*., 2007; Joseph, 2009; Nordberg, 2009; Siu *et al*., 2009). Cd uptake by hepatocytes in the liver reduces its availability to other organs (Souza *et al*., 1997), making the liver one of the major sites of Cd accumulation (Fabbri *et al*., 2012). Therefore, studies observing hepatocyte organelles may add to understanding the progression from the direct effects of Cd to its ultimate toxicity.

To address this, we assessed the structure and function of mitochondria, acidic organelles and vesicles, endoplasmic reticulum elements and microfilaments in HuH-7 cells to observe the progressive toxicity of Cd chloride. The relationship between the metal damage in structure and functions of different cellular organelles was demonstrated to understand the sequence and cooperative events associated with Cd toxicity progression.

MATERIALS AND METHODS

Cell Culture and Treatments

HuH-7 cells (human hepatic carcinoma cell line) were maintained in 25 cm^2 cell culture flasks with Dulbecco's Modified Eagle's Medium (DMEM-1152, Sigma- Aldrich, St. Louis, MO, USA) supplemented with 10% foetal bovine serum (FBS) (Gibco, Grand Island, NY, USA) in a

humidified atmosphere containing 5% CO_2 at 37 °C. For experimental purposes, the cells were seeded onto 24-well plastic plates. The optimum cell concentration determined from cell line growth profiles was 10^5 cells/mL. Cells were allowed to attach for 24 h before Cd treatments.

For Cd toxicity assays, stock solutions (0.1 M) were prepared using ultra-pure quality water, and dilutions were made with medium (DMEM) to 1 µM, 5 µM, 10 µM, 15 µM and 20 µM final concentrations. To observe the progression of Cd-mediated toxicity, these concentrations were added to cell cultures for 2, 6, 12 and 24 h.

Quantification and morphological analysis of Cd-mediated toxicity effects

The control cells and cells exposed to $CdCl_2$ were fixed in Bouin's solution and stained with Giemsa (10%) for observation by light microscopy. All preparations were examined using a Zeiss Axioplan photomicroscope equipped with 20x and 40x objectives. HuH-7 cell survival was determined by counting the number of living cells in a given area. The cell spread on the substrate and nuclear condensation were considered for discrimination between live and dead cells. For each sample, 6 randomly chosen fields were scored at a magnification of 400x, and results were expressed as the mean ± standard deviation. HuH-7 control cell numbers counted at each time point were considered to be 100%. Digital images were obtained using an Axioplan microscope equipped with a Canon Power Shot camera A610/620 employing 20x and 40x objectives.

Cell viability analysis with MTT assay

Following exposure to Cd, the cells were incubated with an MTT (3-(4,5-dimethylthiazol-2-yl)-2,5-diphenyltetrazolium bromide) solution (6 mg/mL) in medium for 4 h at 37 °C (Mosmann, 1983). After the removal of MTT-containing medium, 200 µL of DMSO (dimethyl sulfoxide) was added, and the absorbance at 540 nm was measured after 5 min in a microplate reader (Thermoplate TP reader). The results were expressed as the mean ± standard deviation of triplicate experiments.

Scanning and Transmission electron microscopy (SEM and TEM)

HuH-7 cells treated with 5 µM of $CdCl_2$ for 12 h were fixed in 2.5% (v/v) glutaraldehyde 4% (v/v) formaldehyde in 0.1 M cacodylate buffer (pH 7.2). For SEM preparations, the samples were washed, dehydrated with a graded series of ethanol, immediately critical-point dried in CO_2, positioned on a specimen support and sputtered with gold. All micrographs were recorded using a Zeiss Evo 40 microscope employing secondary electrons. For TEM, the fixed samples were post-fixed with (1:1) 1% osmium tetraoxide and 0.8% potassium ferricyanide, dehydrated with acetone and embedded in Epon. Ultra-thin slices (70 nm) were obtained with a Reichercuts Leica

Ultramicrotome, contrasted with uranyl acetate (5%) and lead citrate and observed using a Zeiss 900 transmission electron microscope.

Reversibility of Cd toxicity effects

For reversibility testing, HuH-7 cells were incubated for 6 h with 10 µM and 20 µM $CdCl_2$ or for 12 h with 5 µM and 10 µM of $CdCl_2$. After exposure, the cells were washed and the medium was replaced with Cd-free medium. After a 24 h recovery period in Cd-free media, cells were analysed by light microscopy and quantified as described above.

Fluorescence analyses

For assessment of mitochondrial function, control and Cd-exposed HuH-7 cells were incubated with rhodamine 123 (10 µg/mL) (Sigma- Aldrich, St. Louis, MO, USA) for 30 minutes in 5% CO_2 at 37 °C (Johnson *et al*., 1980). To observe acidic organelles and compartments, control and Cd-treated cultures were incubated with acridine orange (5 µg/mL) (Sigma- Aldrich, St. Louis, MO, USA) for 40 minutes in a 5% CO_2 incubator at 37 °C (Kielian and Cohn, 1980). Lysosomes were stained with LysoTracker Red (Molecular Probes, Eugene, OR) (50 nM) added to the HuH-7 cultures in cell medium without FBS for 30 minutes at 37°C. Rhodamine phalloidin (Molecular Probes, Eugene, OR) and $DiOC_6$ (Sigma- Aldrich, St. Louis, MO, USA) were used to observe F-actin (a major component of the cytoskeleton) and the endoplasmic reticulum, respectively, and were added to formaldehyde-fixed control and Cd-exposed HuH-7 cells. Rhodamine phalloidin (200 units/mL) was added to cell cultures for 40 minutes (Barak *et al*., 1980), and $DiOC_6$ (2.5 µg/mL) was incubated with cells for 10 minutes (Terasaki *et al*., 1984).

Given that only apoptotic cells will take up YO-PRO-1 and viable cells exclude the dye, YO-PRO-1 dye was used (Molecular Probes, Eugene, OR) for detection of apoptosis (Idziorek *et al*., 1995; Plantin-Carrenard *et al*., 2003). YO-PRO-1 (1 µM) was added to HuH-7 cell cultures for 30 minutes in an incubator with 5% CO_2 at 37 °C. For autophagic vacuole detection, a selective marker monodansylcadaverine (MDC) (Sigma- Aldrich, St. Louis, MO, USA) was used as described by Biederbick *et al*. (1995). The cell culture was incubated with 0.05 mM MDC in PBS at 37°C for 10 minutes. All the stained cells were observed under a Zeiss Confocal Laser Scan Microscope (CLSM) using a 543 nm argon laser and a 40x objective.

Statistical analysis

All data are expressed as the means and standard errors. The statistical significance was determined using GraphPad Prism v.4 software (GraphPad Software, Inc. CA, USA). The two-way

analysis of variance followed by the Bonferroni test was performed for cell viability data and reversibility test data. Differences were considered significant when $p < 0.05$.

RESULTS

To determine the threshold of metal damage and its relationship to metal toxicity (induction of cell death), the present study investigated the effects of cadmium chloride over the HuH-7 cell machinery after treatments with increasing concentrations and exposure times.

The dose and duration of treatment were critical factors in the induction of cell death (Fig 1a). These toxic effects were evaluated after each Cd treatment following the observation of reduced cell numbers demonstrated by the attached cell count (Fig 1a). The cell viability was assessed through the MTT assay, verifying the decrease of cell viability indicated by the failure of mitochondrial function (Fig 1b). The results obtained by counting the surviving cells or through assessment of mitochondrial functionality by MTT assay corroborate the Cd toxicity in the culture.

The observation of the Cd-induced toxic effects indicated that healthy cells at semi-confluence, evidenced by adherence and spread cytoplasm on the substrate with prominent nuclei and nucleoli, changed during Cd treatment (Fig 2a, 2b). Cells experienced different degrees of cytoplasm shrinkage and nuclear condensation (Fig 2b). This morphological process of cytoplasmic retraction was more evident at higher doses (20 µM), but occurred asynchronously among the culture (Fig 2c, inset) and lead to the gradual loss of cell viability and subsequent release from the substrate.

The ultra-structural analysis of cell culture indicated that cell morphology (Fig 3a) changed in the presence of metal (5 µM for 12 h) as evidenced by cytoplasm retraction (Fig 3b), severe vacuolization (Fig 3c, arrows) and alterations in mitochondrial structure (Fig 3c, arrows). The presence of blebs on the membrane cell surface (Fig 3d, arrows) also indicated apoptosis.

The occurrence of this apoptotic process was confirmed through YO-PRO-1 nuclear staining (Fig 4a - d). No indicative probe (Fig 4b, arrowhead) was observed in the adherent control cells (Fig 4a). However, following Cd exposure (5 µM for 12 h), the staining was evident in cells with cytoplasmic retraction and nuclear disorganisation (Fig 4c, d, arrowheads). The cells displayed different stages of cellular retraction (Fig 4c) with distinct apoptotic staining (Fig 4d), suggesting that the process occurred asynchronously in culture.

To analyse the reversibility of Cd damage, the cells were treated with 5 and 10 µM $CdCl_2$ for 12 h or with 10 and 20 µM $CdCl_2$ for 6 h, and then maintained in the absence of the metal for 24 h. After Cd removal, both treatments (10 and 20 µM) for the short period (6 h) and the lower concentration (5 µM) with long-term exposure (12 h) allowed the culture to recuperate (Fig 5 a – h). However, the treatment with 10 µM for 12 h promoted severe deleterious changes (Fig 5i, j) that compromised cellular recovery (Fig 5b). This discovery is important in understanding the kinetics of metal action on the cellular machinery.

To investigate the organelle structures and clarify the consequent damages induced by Cd, the treatment with 5 µM for 12 h was chosen. In this treatment, the cells showed severe damages that compromised cell survival.

Initially, the organelle functionality was analysed using the mitochondrial fluorescent stain rhodamine 123 (Fig 6 a - d). The intense and spread filaments indicative of functional mitochondria (Fig 6b, arrowheads) present in control cells changed to punctate staining (Fig 6d, arrowheads), suggesting the loss of mitochondrial function in Cd-treated cells. These results agree with the evidence from the MTT assay (Fig 1b) and occurred in cells that remain attached following Cd treatment (5 µM/12 h), indicating that the mitochondrion is an initial target in Cd toxicity.

While the mitochondrial function was impaired after Cd exposure in cells, the acidic compartments increased in frequency and size (Fig 7 a - d). This improvement of acidic vesicle presence is related with increased abundance of lysosomes in the cytoplasm (Fig 8 a - d). Therefore, the cells changed from a punctate regular fluorescent staining (Fig 7b, 8b) to an intense fluorescence pattern corresponding to acid structures in the cytoplasm (Fig 7d, 8d arrowheads).

The presence of fluorescent-positive acidic compartments or lysosomal vacuoles further suggests the possibility of intracellular autophagic digestion. To analyse the presence of autophagosomes during Cd treatment, the cells were incubated with MDC (Fig 9). Untreated cells (Fig 9a) exhibited no fluorescence indicative of autophagic vacuoles (Fig 9b), while treated cells (Fig 9c) demonstrated high frequency of fluorescent-positive compartments even with formation of larger vacuoles (Fig 9d). Therefore, the obtained results strongly suggest that the apoptotic pathway and autophagy processes are involved in Cd-mediated cell death.

The major organelle involved in detoxification, the endoplasmic reticulum, was analysed with the fluorescent dye $DiOC_6$ (Fig 10). The dispersion of endoplasmic reticulum elements observed in untreated cells (Fig 10a, b) changed after Cd treatment (Fig 10 c, d) even with the cell remaining adherent and spread (Fig 10c).

Cytoskeleton microfilaments were analysed to understand the changes in cell structure after Cd treatment (Fig 11). The extended cytoplasmic network of microfilaments (Fig 11b, arrowheads) changed after Cd treatment, given that the cells lost their microfilament projections in the cytoplasm (Fig 11d, arrowheads) and their adhesion points on the substrates (Fig 11d, arrowheads), leading to an alteration in cell morphology (Fig 11c, d, arrow).

Interestingly, the multiple Cd-induced damages in organelles were observed in treated cells that remained attached, indicating that the severity of the effect in different targets is important in inducing cell death. Therefore, the Cd reached several targets at the same time leading to loss of mitochondrial function, endoplasmic reticulum dysfunction, cytoplasmic acidification and microfilament disorganisation. These processes are all occurring together in treated cells, and if the exposure is not halted, might lead to cell death by apoptotic and autophagic pathways (Fig 12).

DISCUSSION

The results obtained clearly show that Cd induces a decrease in cell viability and progressive damage to cell morphology in HuH-7 cells through simultaneous effects in multiple intracellular targets, including the mitochondria, cytoskeleton, endoplasmic reticulum and acidic compartments, leading to cell death through the apoptotic and autophagic pathways (Fig 12).

Apoptosis is considered a normal housekeeping event, but it is also necessary to arrest abnormal cell proliferation in development. Apoptosis can also be induced by a variety of chemicals, including many toxic metals (Rana, 2008), and is a known pathway of Cd-mediated cell death (Wang *et al*., 2009; Lasfer *et al*., 2008; Ye *et al*., 2007; Mao *et al*., 2007; Pulido and Parrish, 2003; Faverney *et al*., 2004). However, the present study indicates that apoptosis is not the only process observed in Cd treated cells, given that the autophagic pathway was also observed after sustained Cd exposure.

The autophagic pathway allows the digestion of dysfunctional organelles with resulting recirculation and reuse of their molecular constituents (Templeton and Liu, 2010). This pathway was also observed in organelles in the presence of cadmium. Furthermore, when the cell damage induced by Cd exceeds its capacity of repair, the death occurred. Dying cells generate increasing amounts of autophagic vacuoles and clear large proportions of their cytoplasm, before their death (Bursch *et al*., 2008).

The induction of Cd toxicity (cell death) in culture was asynchronous, indicating preferential interference in some stages of the cell cycle. In fact, Cd can lead to cell cycle arrest, which may affect several cellular processes including cell proliferation and differentiation (Hartwig, 2010; Bertin and Averbeck, 2006). G2/M phase arrest was demonstrated after Cd exposure (Bork *et al*., 2010), preventing damaged cells from entering into mitosis, until DNA damage is repaired. Therefore, some stages of the cell cycle might be more susceptible to Cd damage as demonstrated by the differential effect along the culture in the present study.

Other authors have shown the isolated involvement of mitochondria (Caninno et al., 2009), cytoskeleton (L'Azou *et al*., 2002), endoplasmic reticulum (Wang *et al*., 2009) and lysosomes (Lekube *et al*., 2000) demonstrating the role of separate organelles and structures in Cd-induced cell death. The present study shows that these intra-cellular targets are all being affected simultaneously and are all contributing to cell dysfunction leading to cell death (Fig 12). Moreover, the present study shows that the extent of damages induced by Cd treatment is eventually so severe that cells do not reverse the toxic effects as demonstrated by the 10 μM treatment for 12 h in the reversibility test.

The present study demonstrated the stages of Cd-induced cell damage, where mitochondria, lysosomes, acidic compartments, the cytoskeleton and the endoplasmic reticulum were all targets of $CdCl_2$ toxicity in HuH-7 cells. Therefore, further investigation of Cd toxicity is necessary to show the effects of this metal on each organelle. This study will increase the understanding of Cd effects and the cellular mechanisms leading to Cd-induced cell death.

ACKNOWLEDGMENTS

This work was supported by Fundação Carlos Chagas Filho de Amparo à Pesquisa do Estado do Rio de Janeiro (E-26/171.315/2004) (E-26/ 100.470/2007) (E-26/110.921/2008).

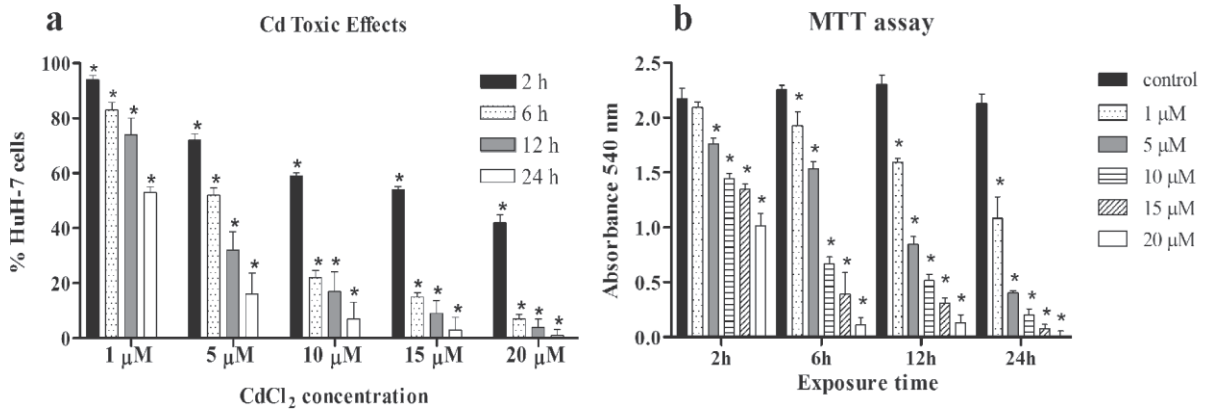

Fig 1. $CdCl_2$ toxic effects in viability of HuH-7 cells. (a) Quantification of giemsa stained HuH-7 cells after $CdCl_2$ treatment. All concentrations tested were compared to a control group that was defined as 100%. (b) Decrease in cell viability by MTT assay in a dose/time dependent manner. * Significantly different from control ($p < 0.001$).

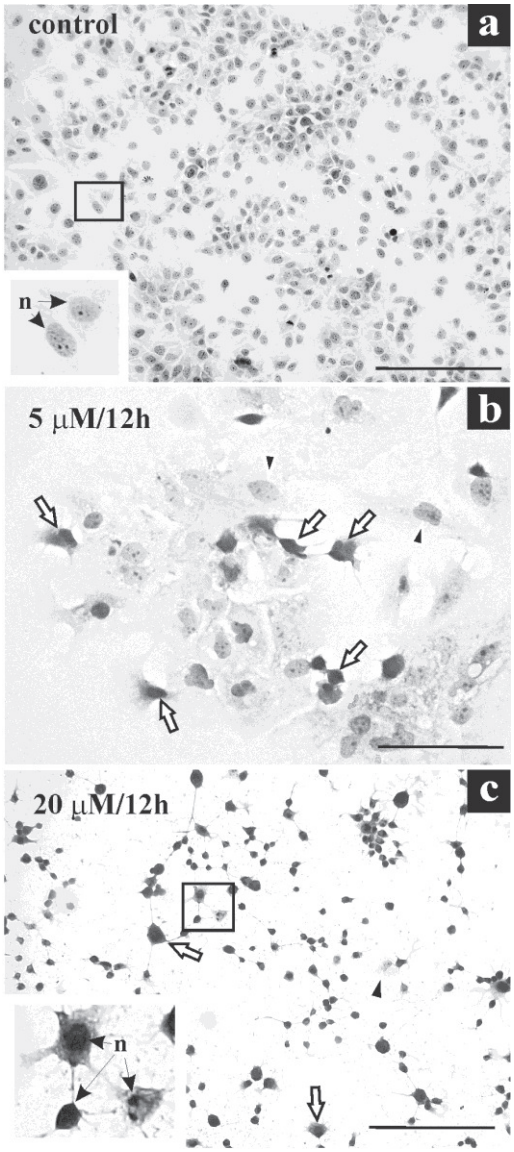

Fig 2. Light microscopy of HuH-7 cells showing morphological alterations induced by $CdCl_2$. (a) Control cell in monolayer aspect. (b) Changes in the cell monolayer following incubation with 5 μM for 12 h. (c) Complete loss of cell monolayer after incubation with 20 μM for 12 h. (b) and (c) also shows treated cells with retraction and nuclear condensation (arrows). Cells displaying normal morphology is also demonstrated (arrowheads), indicating that Cd-mediated toxicity effect was not homogeneous. n = nucleus. Scale bar: A and C: 200μm; B: 100μm.

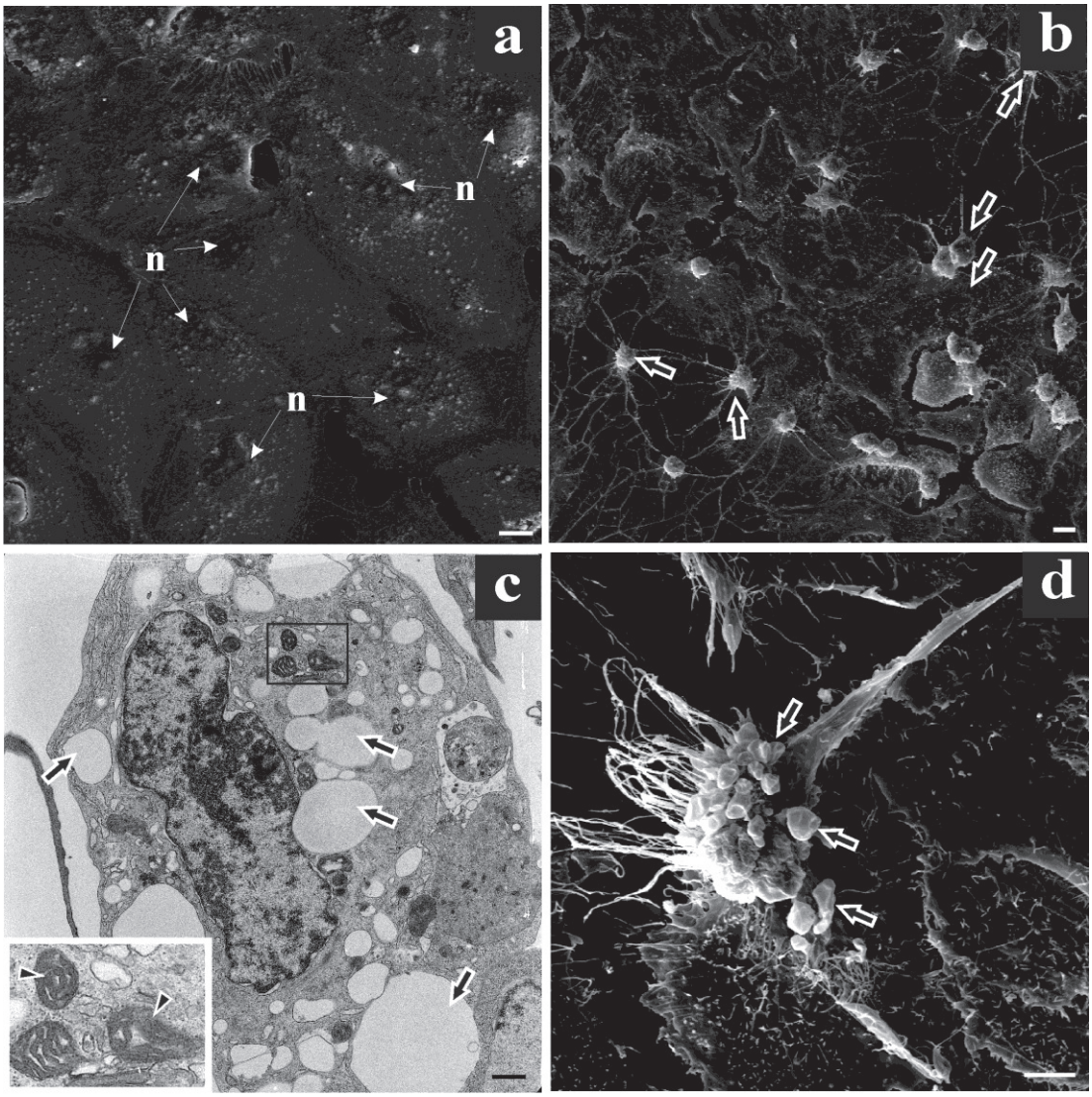

Fig 3. Scanning (a, b, d) and transmission (c) electron microscopy evidencing HuH-7 cells before (a) and after Cd treatment (b - d) (5 µM for 12 h). (a) Characteristic monolayer aspect of control culture. (b) Loss of the monolayer aspect with the presence of many rounded cells (arrows). (c) The ultra-structural appearance of Cd treated cells with many vacuoles in the cytoplasm (arrows) and the collapse of some mitochondrial cristae (inset, arrowheads). (d) Cells with membrane blebs (arrows) following Cd treatment. n = nucleus. Scale bar: A: 20 µm, B: 20 µm, C: 1.1 µm, D: 10 µm.

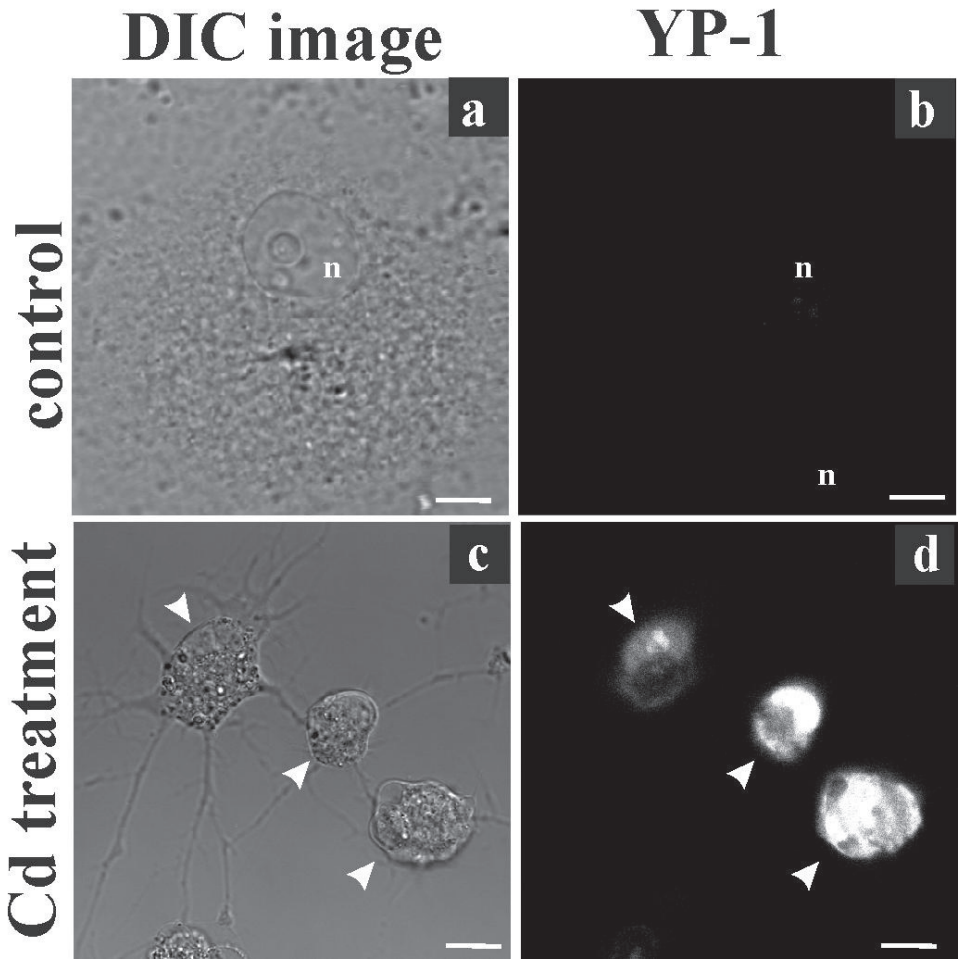

Fig 4. Differential interference contrast microscopy (DIC) (a and c) and confocal laser scanning microscopy of HuH-7 cells stained with Yopro-1 (YP-1) (1 µM) (b an d) before (a and b) and after Cd treatment with 5 µM for 12 h (c and d). (a) Control cells. (b) No fluorescence signal in untreated cell. (c) Differential levels of cytoplasm retraction and nuclear disorganisation, both characteristics of apoptotic processes observed in Cd treated cell. (d) Cellular staining indicative of cell death via apoptotic processes following $CdCl_2$ exposure. n= nucleus. Scale bar: 10µm.

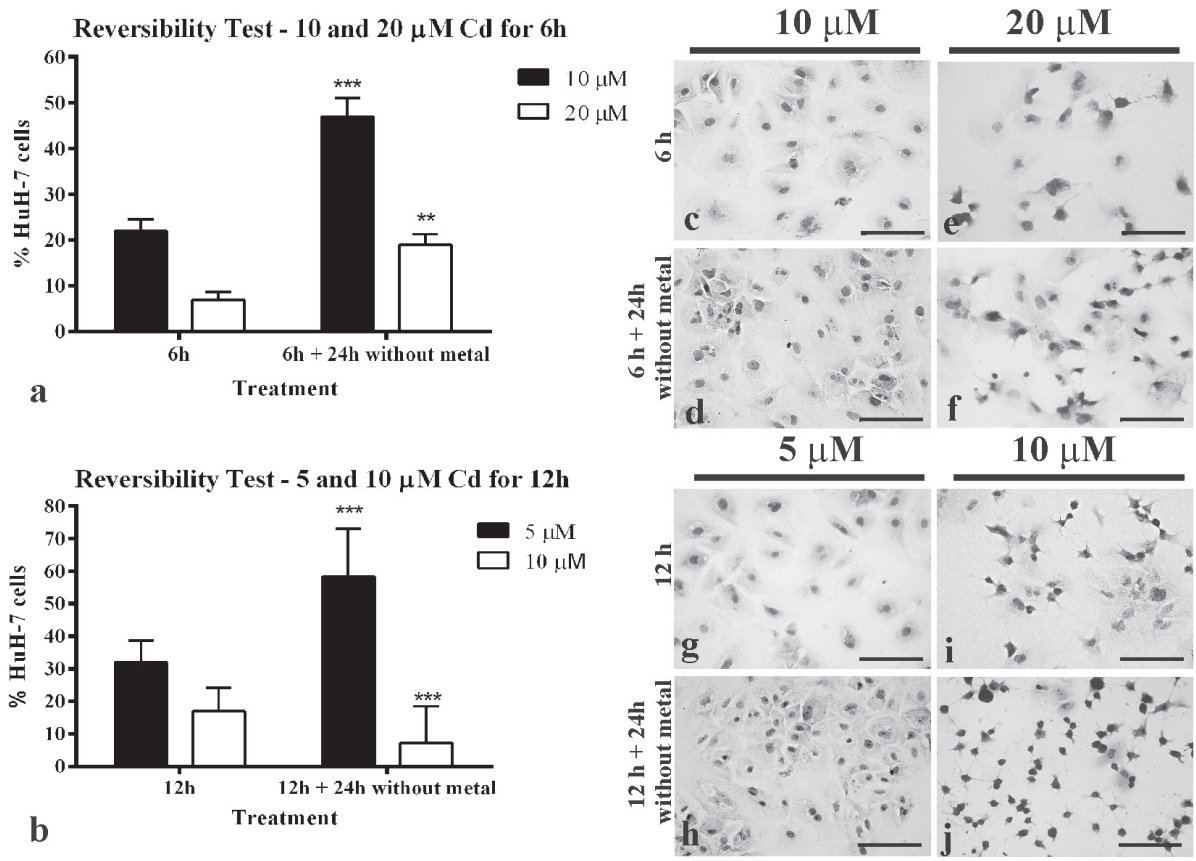

Fig 5. Reversibility of Cd effects on HuH-7 cells. (a) Recovery in culture after 24 h of Cd removal following the treatments with higher concentrations and short exposure time (10 µM and 20 µM for 6 h). (b) Recovery of culture following long-term exposure (12 h) with 5 µM with subsequent 24 h of Cd removal. However, the same capacity to reverse Cd toxicity was not observed after 12 h incubation with 10 µM; where the toxic effects last even with Cd removal. (c - j) Morphological aspects of the culture following each Cd treatment: (c) 10 µM for 6 h, (d) 10 µM for 6 h + 24 h without metal, (e) 20 µM for 6 h, (f) 20 µM for 6 h + 24 h without metal, (g) 5 µM for 12 h, (h) 5 µM for 12 h + 24 h without metal, (i) 10 µM for 12 h, (j) 10 µM for 12 h + 24 h without metal. The concentrations tested were compared with a control group that was considered 100%. ***$p<0.001$.

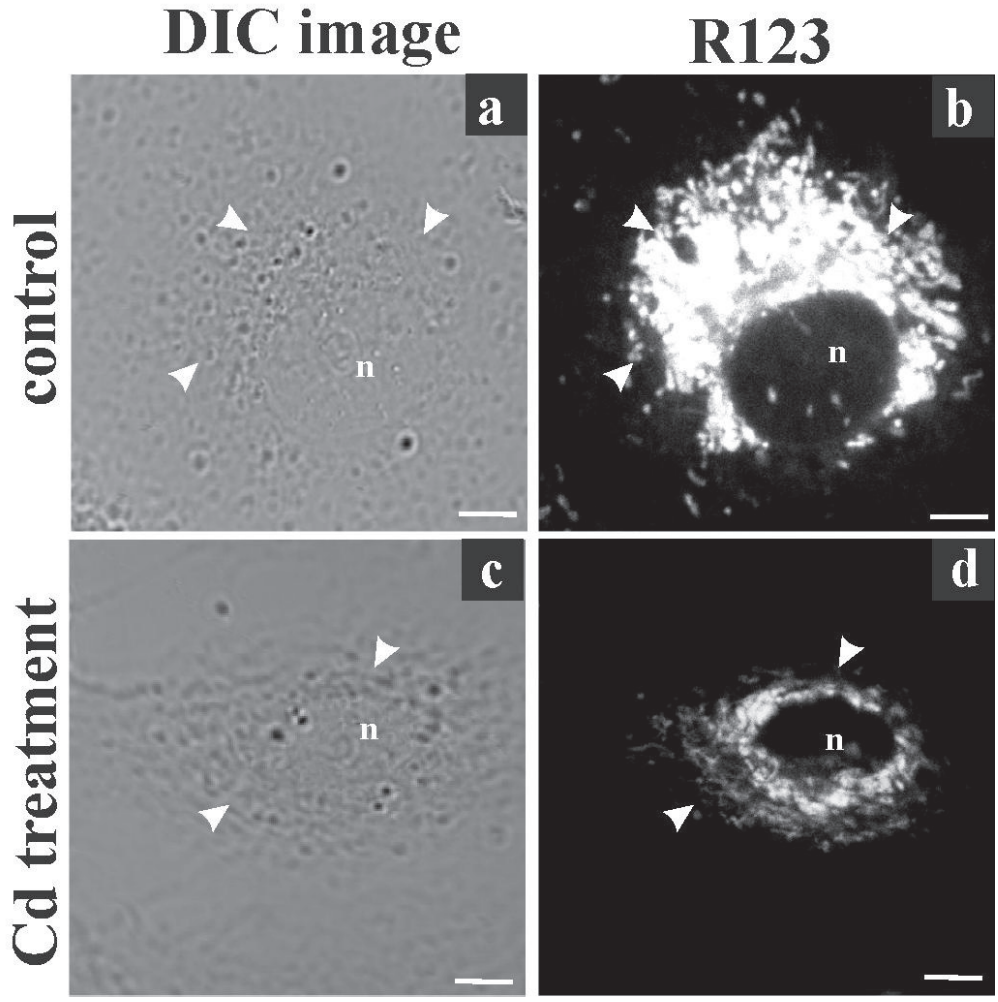

Fig 6. Differential interference contrast microscopy (DIC) (a, c) and confocal laser scanning microscopy of HuH-7 cells stained with rhodamine 123 (R123) (10 µg/mL) (b, d). (a) Normal aspect of untreated cell. (b) Control cell with filamentous fluorescence spread in the cytoplasm, indicating the functional area of the mitochondria (arrowheads). (c) Cd treated cell (5 µM for 12 h). (d) Cd treated cell (5 µM for 12 h) with punctate fluorescence, suggesting loss of mitochondrial functionality (arrowheads). n = nucleus. Scale bar: 10µm.

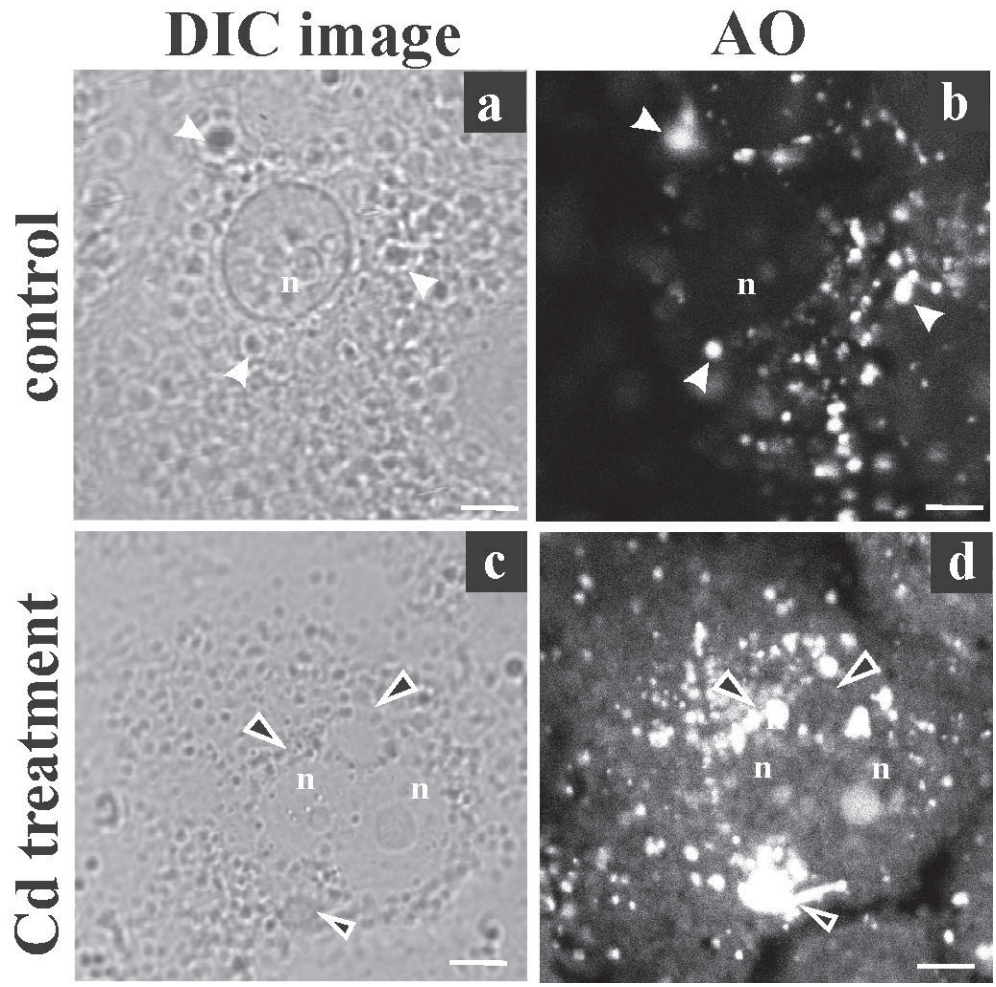

Fig 7. Differential interference contrast microscopy (DIC) (a, c) and confocal laser scanning microscopy of HuH-7 cells stained with acridine orange (AO) (5 µg/mL) (b, d). (a) Control cell. (b) Untreated cell with punctate fluorescence staining in the cytoplasm corresponding to acidic organelles, such as endosome and lysosome (arrowheads). (c) Vacuolisation in Cd treated cells (5 µM for 12 h) (arrow). (d) Intense dispersed fluorescence observed in the cytoplasm (arrowheads) of treated cells (5 µM for 12 h). n = nucleus. Scale bar: 10µm.

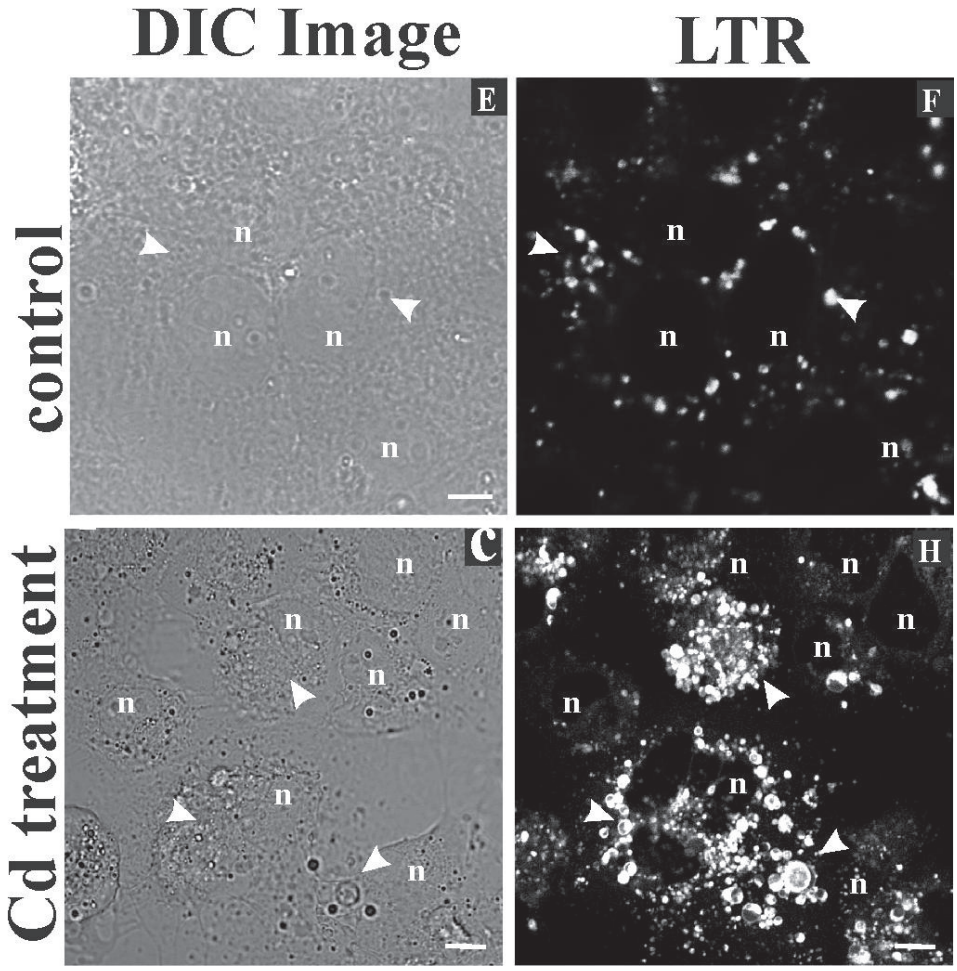

Fig 8. Differential interference contrast microscopy (DIC) (a and c) and confocal laser scanning microscopy of HuH-7 cells stained with LysoTracker Red (50 nM) (b and d). (a) Control cells. (b) Punctate fluorescence pattern observed in untreated culture (arrowheads). (c) Cd treated cell (5 μM for 12 h). (d) Intense and dispersed fluorescence pattern indicate increased lysosomes throughout the cytoplasm (arrowheads). n = nucleus. Scale bar: 10μm (x400).

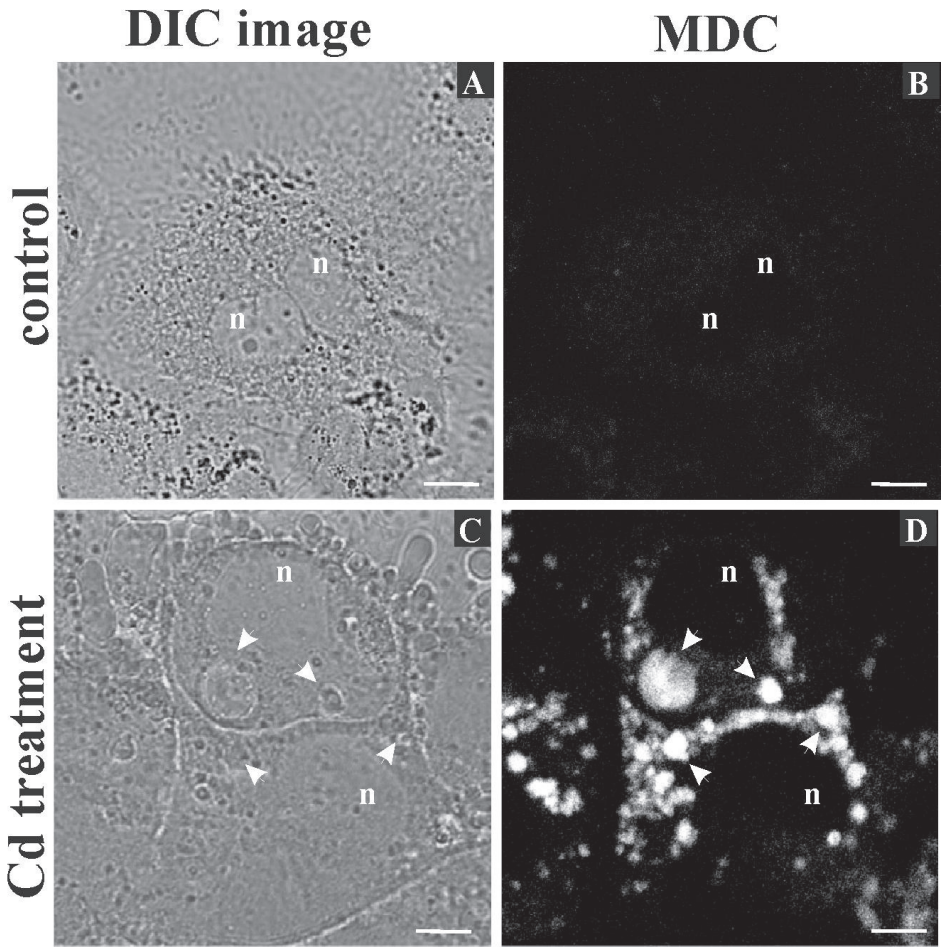

Fig 9. Differential interference contrast microscopy (DIC) (a and c) and confocal laser scanning microscopy of HuH-7 cells stained with monodansylcadaverine (MDC) (0.05 mM) (b and d) after Cd treatment (5 µM for 12 h). (a) Control cells. (b) No fluorescence signal in untreated cells. (c) Cd treated cells with vacuoles in cytoplasm (arrowheads). (d) Autophagic vacuoles (arrowheads) staining in Cd treated cell indicating Cd-mediated cell death through autophagic processes. n= nucleus. Scale bar: 10µm.

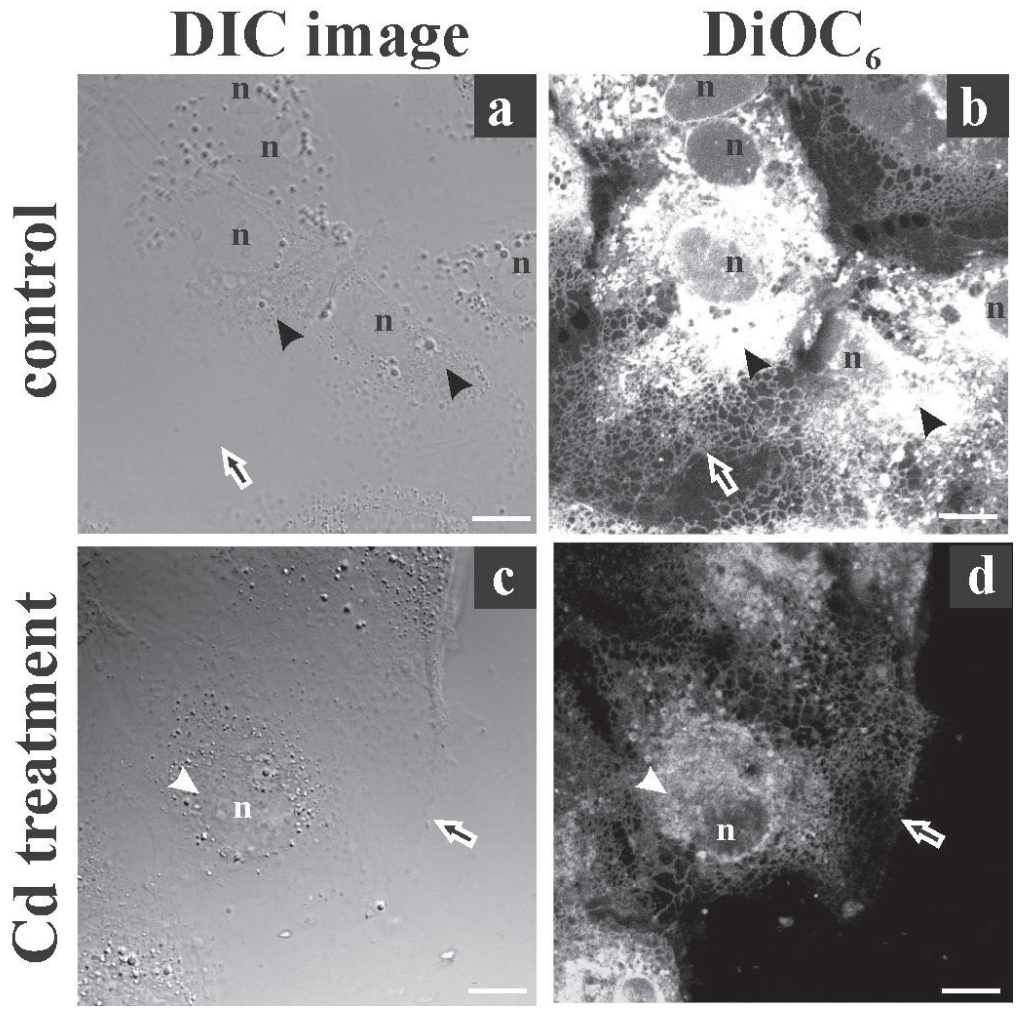

Fig 10. Differential interference contrast microscopy (DIC) (a, c) and confocal laser scanning microscopy of HuH-7 cells stained with $DiOC_6$ (2.5 µg/mL) (b, d). (a) Control cells. (b) Morphological aspect of the reticular network of control cells with thinner peripheral regions (arrow) and regions with high fluorescence close to the nucleus, mainly because of the concentration of reticulum and other membranes, such as mitochondria (arrowheads) (c) Cd treated cells (5 µM for 12 h). (d) Weaker fluorescence signal in treated cells (5 µM for 12 h); with evidence of the disorganisation in reticular arrangement close to nucleus (arrowheads) and in cell periphery (arrow). n = nucleus. Scale bar: 10µm.

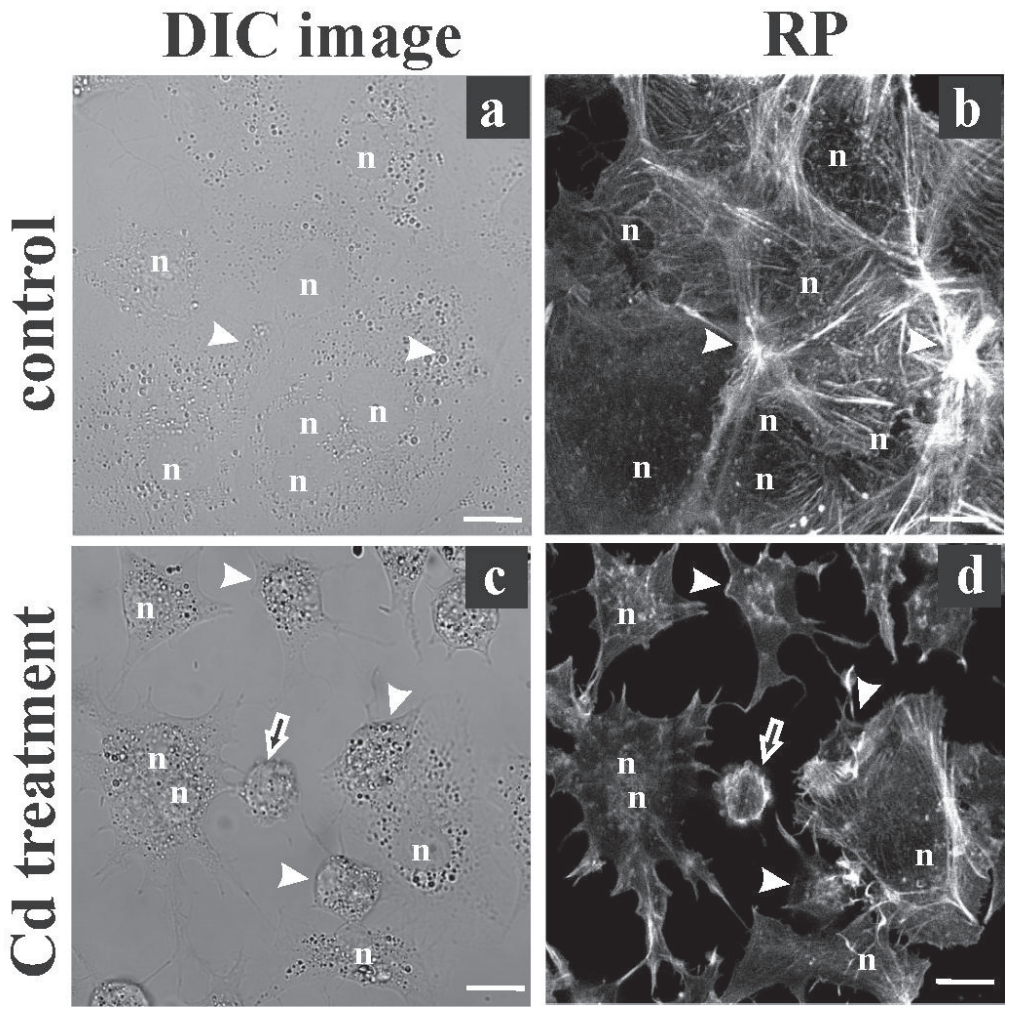

Fig 11. Differential interference contrast microscopy (DIC) (a, c) and confocal laser scanning microscopy of HuH-7 cells stained with rhodamine phalloidin (RP) (b, d). (a) The monolayer aspect of untreated cells. (b) Extended cytoplasmic network of microfilaments and adhesion points (arrowheads) in control cells. (c) Cd treated cells (5 µM for 12 h) displaying rounded morphology (arrow). (d) Loss of microfilament projections in the cytoplasm and of the adhesion points (arrowheads) in Cd treated cells (5 µM for 12 h). n = nucleus. Scale bar: 10µm.

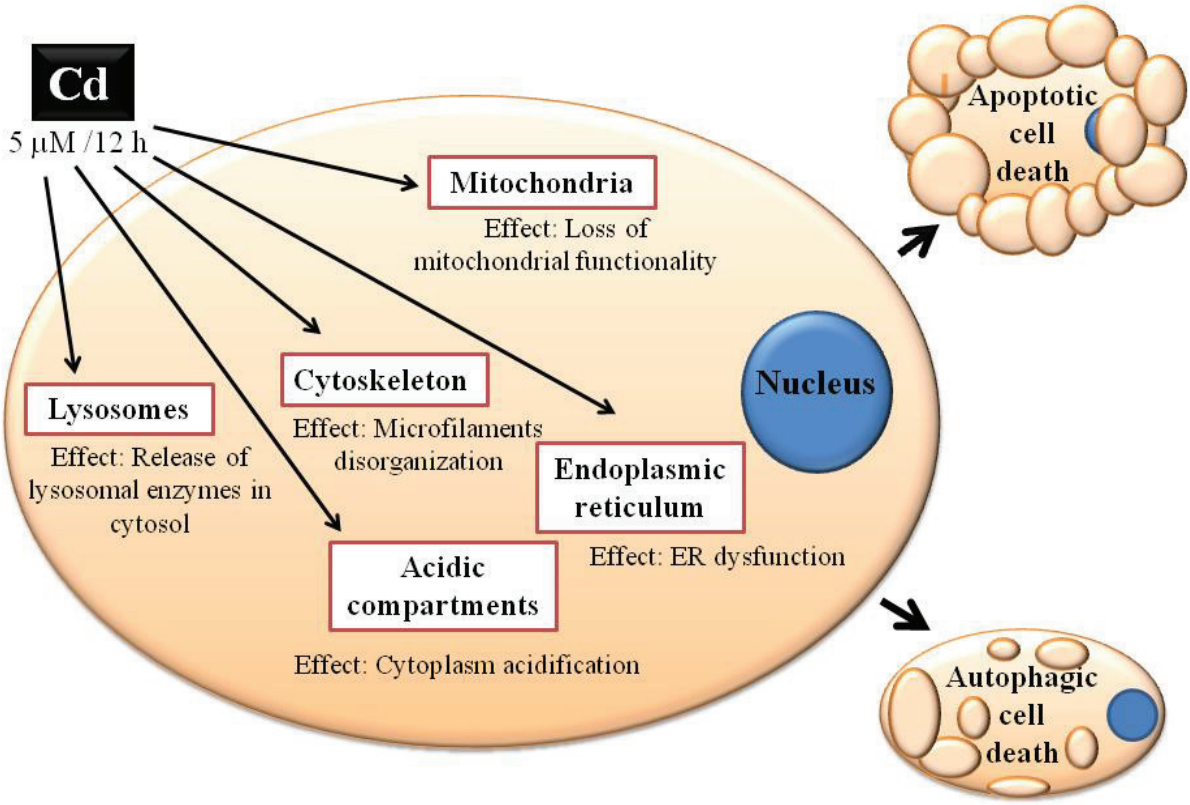

Fig 12. Cd induces effects in multiple intracellular targets at same time, as mitochondria, cytoskeleton, endoplasmic reticulum and acidic compartments leading to cell death through the apoptotic and autophagic pathways. Each intracellular target is contributing to overall Cd induced toxicity.

REFERENCES

Barak LS, Yocum RR, Nothnagel EA, Webb WW (1980). Fluorescence staining of the actin cytoskeleton in living cells with 7-nitrobenz-2-oxa-1,3-diazole-phallacidin. *Proceedings of the National Academy of Sciences (USA)* **77**: 980-984.

Bertin G, Averbeck D (2006). Cadmium: cellular effects, modifications of biomolecules, modulation of DNA repair and genotoxic consequences (a review). *Biochimie* **88**: 1549-1559.

Biederbick A, Kern HF, Elsasser HP (1995). Monodansylcadaverine (MDC) is a specific *in vivo* marker for autophagic vacuoles. *European Journal of Cell Biology* **66**: 3-14.

Bork U, Lee WK, Kuchler A, Dittmar T, Thévenod F (2010). Cadmium-induced DNA damage triggers G2/M arrest via chk1/2 and cdc2 in p53-deficient kidney proximal tubule cells. *American Journal of Physiology - Renal Physiology* **298**: 255–265.

Bursch W, Karwan A, Mayer M, Dornetshuber J, Fröhwein U, Schulte-Hermann R, Fazi B, Sano FD, Piredda L, Piacentini M, Petrovski G, Fésüs L, Gerner C (2008). Cell death and autophagy: Cytokines, drugs, and nutritional factors. *Toxicology* **254**: 147-157.

Cannino G, Ferruggia E, Luparello C, Rinaldi AM (2009). Cadmium and mitochondria. *Mitochodrion* **9**: 377-384.

Fabbri M, Urani C, Sacco MG, Procaccianti C, Gribaldo L (2012). Whole genome analysis and microRNAs regulation in HepG2 cells exposed to cadmium. *Altex* **29**: 2-12.

Faverney CR, Orsini N, Sousa G, Rahmani R (2004). Cadmium-induced apoptosis through the mitochondrial pathway in rainbow trout hepatocytes: involvement of oxidative stress. *Aquatic Toxicology* **69**: 247-258.

Filipič M (2012). Mechanisms of cadmium induced genomic instability. *Mutation Research* **733**: 69-77.

Fotakis G, Cemeli E, Anderson D, Timbrell J (2005). Cadmium chloride-induced DNA and lysosomes damage in hepatoma cell line. *Toxicology in Vitro* **19**: 481-489.

Hartwig A (2010). Mechanisms in cadmium-induced carcinogenicity: recent insights. *Biometals* **23**: 951–960.

Idziorek T, Estaquier J, De Bells F, Ameisen JC (1995). YO-PRO-1 permits cytofluorometric analysis of programmed cell death (apoptosis) without interfering with cell viability. *Journal of Immunological Methods* **185**: 249-258.

Joseph P (2009). Mechanisms of cadmium carcinogenesis. *Toxicology and Applied Pharmacology* **238**: 272-279.

Johnson LV, Walsh ML, Chen LB (1980). Localization of mitochondria in living cells with rhodamine 123. *Proceedings of the National Academy of Sciences (USA)* **77**: 990-994.

Kielian MC, Cohn ZA (1980). Phagosome-lysosome fusion. *Journal of Cell Biology* **85**: 54–765.

Lasfer M, Vadrot N, Aoudjehane L, Conti F, Bringuier AF, Feldmann G, Reyl-Desmars F (2008). Cadmium induces mitochondria-dependent apoptosis of normal human hepatocytes. *Cell Biology and Toxicology* **24**: 55-62.

L'Azou B, Dubus I, Courtès CO, Labouyrie JP, Perez L, Pouvreau C, Juvet L, Cambar J (2002). Cadmium induces direct morphological changes in mesangial cell culture. *Toxicology* **179**: 233-245.

Lekube X, Cajaraville PM, Marigomez I (2000). Use of polyclonal antibodies for the detection of changes by cadmium in lysosomes of aquatic organisms. *The Science of Total Environment* **247**: 201-212.

Mao WP, Ye JL, Guan ZB, Zhao JM, Zhang C, Zhang NN, Jiang P, Tian T (2007). Cadmium induces apoptosis in human embryonic kidney (HEK) 293 cells by caspase-dependent and independent pathways acting on mitochondria. *Toxicology in Vitro* **21**: 343–354

Mosmann T (1983). Rapid colorimetric assay for cellular growth and survival: application to proliferation and cytotoxicity assays. *Journal of Immunological Methods* **65**: 55–63.

Nordberg G (2009). Historical perspectives on cadmium toxicology. *Toxicology and Applied Pharmacology* **238**: 192-200.

Plantin-Carrenard E, Bringuier A, Derappe C, Pichon J, Guillot R, Bernard M, Foglietti MJ, Feldmann G, Aubery M, Braut-Boucher F (2003). A fluorescence microplate assay using yopro-1 to measure apoptosis: Application to HL60 cells subjected to oxidative stress. *Cell Biology and Toxicology* **19**: 121-133.

Pulido MD, Parish AR (2003). Metal-induced apoptosis: Mechanisms. *Mutation Research* **533**: 227-241.

Rana SVS (2008). Metals and apoptosis: Recent developments. *Journal of Trace Elements in Medicine and Biology* **22**: 262-284.

Siu ER, Mruk DD, Porto CS, Cheng CY (2009). Cadmium-induced testicular injury. *Toxicology and Applied Pharmacology* **238**: 240-249.

Souza V, Bucio L, Ruiz MCG (1997). Cadmium uptake by a human hepatic cell line (WRL-68 cells). *Toxicology* **120**: 215-220.

Templeton DM, Liu Y (2010). Multiple roles of cadmium in cell death and survival. *Chemical Biological Interactions* **188**: 267-275.

Terasaki M, Song J, Wong JR, Weiss MJ, Chen LB (1984). Localization of endoplasmic reticulum in living and glutaraldehyde-fixed cells with fluorescent dyes. *Cell* **38**: 101-108.

Waisberg M, Joseph P, Hale B, Beyersmann D (2003). Molecular and cellular mechanisms of cadmium carcinogenesis. *Toxicology* **192**: 95-117.

Wang SH, Shih YL, Lee CC, Chen WL, Lin CJ, Lin YS, Wu KH, Shih CM (2009). The role of endoplasmic reticulum in cadmium-induced mesangial cell apoptosis. *Chemical Biological Interactions* **181**: 45-51.

Ye JL, Mao WP, Wu AL, Zhang NN, Zhang C, Yu YJ, Zhou L, Wei CJ (2007). Cadmium-induced apoptosis in human normal liver L-02 cells by acting on mitochondria and regulating Ca^{2+} signals. *Environmental Toxicology and Pharmacology* **24**: 45-54.

Mercury effects in multiple organelles lead to cell death for both apoptotic and autophagic events

Cristiane dos Santos Vergilio[1] and Edésio José Tenório de Melo[1]

1. Universidade Estadual do Norte Fluminense, Centro de Biociências e Biotecnologia, Laboratório de Biologia Celular e Tecidual, Campos dos Goytacazes, RJ, Brasil, 28013-602;

Abstract

Mercury (Hg) is a high toxic metal that can exert multiple adverse effects ultimately leading to cell death. In fact, the occurrence of apoptosis was demonstrated in diverse cell types following Hg treatments, mainly with mitochondrial involvement. Only a few reports demonstrated the incidence of autophagy following Hg exposure. In addition, the role of others cellular organelles in Hg toxicity process was neglected. Therefore, the present study aimed to investigate the structure and function of several cellular organelles, as mitochondria, acidic compartments and vesicles, endoplasmic reticulum elements and microfilaments following Hg exposure in human hepatic cell line (HuH-7 cells) to demonstrate the sequence and cooperative events associated with Hg- induced cell death. Hg exposure leaded to progressive decrease in cell viability inducing alterations in cell morphology as cytoplasm shrinkage and nuclear fragmentation. Hg treatment (10 μM for 12 h) affected multiple intra-cellular targets simultaneously, inducing loss of mitochondrial functionality, pronounced cytoplasmic acidification and dysfunctions in the cytoskeleton and endoplasmic reticulum. This overall damage lead to autophagic death together with apoptosis as part of Hg toxicity in human hepatocytes cell line (HUH-7 cells).

Keywords: apoptosis; autophagy; cell death; hepatocytes; HuH-7 cells; mercury

Abbreviations

DAPI:4',6-diamidino-2-phenylindole; $DiOC_6$: 3,3′-dihexyloxacarbocyanine iodide); DMSO: dimethyl sulfoxide; MTT: 3-(4,5-dimethylthiazol-2-yl)-2,5-diphenyltetrazolium bromide; NR: Neutral red; ROS: reactive oxygen species

Introduction

Mercury (Hg) is a high toxic metal that can induce severe adverse effects on both organisms and humans under certain exposure concentrations (Liao *et al*., 2006). Among the organs, the liver is the main site of metal toxicity for its central role in physiological metabolism and for being involved in several detoxification reactions (Hinton *et al*., 2008). Hepatocytes are the main cellular type present in liver and exert important functions in liver injury response (Malhi *et al*., 2010).

Hg effects come from its high affinity to thiol intra-cellular groups, present in important biomolecules as constituent of proteins, transcription factors, and nucleic acids (Fabbri *et al*., 2012; Syversen and Kaur, 2012). This elevated reactivity with distinct molecules reflects the capacity of Hg in disturbing a variety of cellular and biochemical processes (Vallee and Ulmer, 1972). However, due the complexity and diversity of events associated with cell-Hg interactions, the wide-ranging effects induced in the cellular organelles and their involvement in cell death remain to be fully understood.

Hg treatment induced apoptosis (Achanzar *et al*., 1996; Shenker *et al*., 2000; Araragi *et al*., 2003; Rosales *et al*., 2005; Park *et al*., 2007) and necrosis in different cell types (Achanzar *et al*., 1996; Kuo and Shiau, 2004; Chen *et al*., 2010). Only recent reports demonstrated the occurrence of autophagy following exposure to low Hg concentration in rat hepatocytes (Chatterjee *et al*., 2012; Chatterjee *et al*., 2013). Mainly studies point the mitochondria as organelle target for Hg-induced cell death. In fact, the mitochondrial dysfunction is the main source of reactive oxygen species (ROS) that can trigger several adverse effects in cell machinery (Wang *et al*., 2004, Bertin and Averbeck, 2006; Gobe and Crane, 2010). However, the role of others cellular organelles in Hg toxicity process was neglected.

The present study aimed to investigate the structure and function of several cellular organelles as mitochondria, acidic organelles and vesicles, endoplasmic reticulum elements and microfilaments following Hg exposure in human hepatic cell line (HuH-7 cells). The evaluation of the metal damage in structure and functions of different cellular organelles was demonstrated to understand the sequence and cooperative events associated with Hg- induced cell death.

Material and Methods

Materials

Medium (DMEM -1152), mercury chloride ($HgCl_2$), MTT (3-(4,5-dimethylthiazol-2-yl)-2,5-diphenyltetrazolium bromide), rhodamine 123 (R123), acridine orange (AO), monodansylcadaverine (MDC), $DiOC_6$ (3,3′-dihexyloxacarbocyanine iodide) were purchased from Sigma-Aldrich (St. Louis, MO, USA). The foetal bovine serum (FBS) were from Gibco Laboratories (Grand Island, NY, USA). LysoTracker Red (LTR), Rhodamine phalloidin (RP) and YO-PRO-1 were obtained from Molecular Probes (Eugene, OR, USA).

Cell Culture

HuH-7 cells (human hepatic carcinoma cell line) were grown in Dulbecco's modified Eagle's medium (DMEM-1152) supplemented with 10% foetal bovine serum (FBS) in a humidified atmosphere containing 5% CO_2 at 37 °C. The cells plated at a density of 10^5 cells/mL were allowed to attach for 24 h before Hg treatments.

Hg treatments

For Hg toxicity assays stock solution (0.1M) were prepared using ultra-pure quality water. Dilutions with medium (DMEM) were made to 1 μM, 5 μM, 10 μM, 15 μM or 20 μM final concentrations. To observe of the progression of Hg damages, these concentrations were added to cell cultures for 2, 6, 12 and 24 h.

Cell viability assessment through MTT assay

Following each Hg treatment, the cells were incubated with an MTT (3-(4,5-dimethylthiazol-2-yl)-2,5-diphenyltetrazolium bromide) solution (6 mg/mL) in medium for 4 h at 37 °C (Mosmann, 1983). After the removal of MTT-containing medium, 200 μL of dimethyl sulfoxide (DMSO) was added, and the absorbance at 540 nm was measured after 5 min in a microplate reader (Thermoplate TP reader). The results were expressed as the mean ± standard deviation of triplicate experiments.

Morphological analysis of Hg effects

Control cells and Hg-exposed cells were fixed in Bouin's solution and stained with Giemsa (10%) for observation by light microscopy. All preparations were examined using a light microscope (Carl Zeiss, Axioplan, Goettingen, Germany) equipped with 20x and 40x objectives. The images were obtained using Olympus cellSens digital image software.

Apoptosis detection

YO-PRO-1 dye was used (Molecular Probes, Eugene, OR, USA) for detection of apoptosis, for only apoptotic cells take up YO-PRO-1, while viable cells exclude the dye (Idziorek *et al*., 1995; Plantin-Carrenard *et al*., 2003). YO-PRO-1 (1 µM) was added to HuH-7 cell cultures for 30 min for subsequent observation in fluorescence microscope (Carl Zeiss, Axioplan, Goettingen, Germany) using fluorescein excitation filter (485 nm). The incidence of apoptosis was analyzed by counting around 300 cells in each preparation and determined the percentage of YO-PRO-1 positive cells. The results were expressed as the mean ± standard deviation.

Observation of DNA fragmentation

DAPI (4',6-diamidino-2-phenylindole) staining was used for the observation of occurrence of DNA fragmentation following Hg treatment. Formaldehyde-fixed (4%) control and Hg treated cells (10 µM for 12 h) incubated with PBS containing 0.1% Triton-X were stained with DAPI solution (300 nM) for 3 min for subsequent observation in fluorescence microscope using UV excitation filter (350 nm) (Carl Zeiss, Axioplan, Goettingen, Germany).

Autophagy detection

For autophagic vacuole detection, a selective marker monodansylcadaverine (MDC) (Sigma- Aldrich, St. Louis, MO, USA) was used as described by Biederbick *et al*. (1995). The cell culture was incubated with 0.05 mM MDC in PBS at 37°C for 10 minutes for subsequent observation in a fluorescence microscope (Carl Zeiss, Axioplan, Goettingen, Germany) using UV excitation filter (350 nm). The incidence of autophagy was analyzed by counting around 300 cells in each preparation and determined the percentage of positive MDC autophagic vacuoles. The results were expressed as the mean ± standard deviation.

Mitochondria, acid compartments and lysosome staining

For assessment of mitochondrial function, control and Hg-exposed HuH-7 cells were incubated with rhodamine 123 (10 µg/mL) (Sigma- Aldrich, St. Louis, MO, USA) for 30 minutes in 5% CO_2 at 37 °C (Johnson *et al*., 1980). To observe acidic organelles and compartments, control and Hg-treated cultures were incubated with acridine orange (5 µg/mL) (Sigma- Aldrich, St. Louis, MO, USA) for 40 minutes in a 5% CO_2 incubator at 37 °C (Kielian and Cohn, 1980). Lysosomes were stained with LysoTracker Red (Molecular Probes, Eugene, OR) (50 nM) added to the HuH-7 cultures in cell medium without FBS for 30 minutes at 37°C. All the preparations were observed

under a fluorescence microscope (Carl Zeiss, Axioplan, Goettingen, Germany) using rhodamine excitation filter (546 nm).

Destabilization of lysosomal membrane

NR (neutral red) is a weak cationic dye that readily penetrates the cell membrane and accumulates intracellularly in lysosomes (Borenfreund and Puerner, 1984). Decrease in neutral red uptake indicates the destabilization in lysosomal membrane as proposed in protocol described by Borenfreund and Puerner (1984). Control and Hg treated cells (10 µM for 12 h) were incubated for 3 h with neutral red dye (50 µg/ml) in serum free medium (DMEM). After a rapid addition (1 min) of a fixative solution (0.1% $CaCl_2$ in 0.5% formaldehyde) for elimination of no incorporated dye, the incubation for 15 min with an elution solution (1% of acetic acid in ethanol 50%) allowed the solubilization of incorporated dye. Aliquots of the resulting solutions were transferred to 96-well plates and absorbance at 540 nm was recorded using the microplate spectrophotometer system. (Thermoplate TP reader). The results were expressed as the mean ± standard deviation of triplicate experiments.

PMA stimulation of phagolysosomes

Phorbol 12-myristate 13-acetate (Sigma Chemical Co., St. Louis, MO) (PMA) stimulates both the rate and extent of fusion of phagosomes with preexisting secondary lysosomes (Kielian and Cohn, 1981), then PMA pre-incubation can mimic the higher incidence of autophagic vacuoles in normal cells. PMA dissolved in DMSO (1 mM stock solution) was added to medium (DMEM) at a final concentration of 0.1 µM (Kielian and Cohn, 1981) and the cells were incubated 2 h. For the investigation of PMA and Hg synergistic effect the PMA pre-incubated cells (2 h) followed Hg exposure (10 µM for 12 h). After each treatment, the MTT viability test was performed as related before.

Endoplasmic reticulum and cytoskeleton microfilaments staining

$DiOC_6$ (Sigma- Aldrich, St. Louis, MO, USA) and Rhodamine phalloidin (Molecular Probes, Eugene, OR, USA) were used to observe the endoplasmic reticulum and F-actin (a major component of the cytoskeleton), respectively. Both staining and were added to formaldehyde-fixed control and Hg-treated cells. Rhodamine phalloidin (200 units/mL) was added to cell cultures for 40 minutes (Barak *et al*., 1980), and $DiOC_6$ (2.5 µg/mL) was incubated in cells for 10 minutes (Terasaki *et al*., 1984). All the preparations were observed under a fluorescence microscope (Carl Zeiss, Axioplan, Goettingen, Germany) using fluorescein (485 nm) or rhodamine excitation filters (546 nm) for $DiOC_6$ or rhodamine phalloidin staining, respectively.

Statistics

The statistical significance was determined using GraphPad Prism v.4 software (GraphPad Software, Inc. CA, USA). Two-way ANOVA followed by Bonferroni posttests was used to compare the difference of cell viability in relation control ($p<0.001$). T-test followed by Mann-Whitney posttest was used to compare difference among control and Hg treatment (10 µM for 12 h) ($p<0.05$) in incidence of Yopro-1 and MDC positive staining and neutral red assay. One-way ANOVA followed by Bonferroni posttests was used to compare the difference among the PMA treatments in relation to control ($p<0.05$).

Results

Hg exposure induced progressive effects in HuH-7 culture leading to cell death in a time and dose dependent process (Fig 1a). The cells lost their adhered and spread condition (Fig 1b) and several levels of cytoplasm shrinkage and nuclear condensation were observed following Hg treatments (Fig 1c, arrowheads). These gradual cell retractions evolved to subsequent cellular release from subtract. For the evaluation of the processes involved in Hg-induced cell death, the treatment with 10 µM for 12 h was chosen. This dose/time induced a considerable decrease (50 %) in cell viability and the cells showed severe damages, compromising the cell survival.

Yopro-1 nuclear staining was performed in order to investigate the occurrence of apoptotic cell death (Fig 2 a - d). No indicative probe was observed in the control adherent cells (Fig 2a, b). Whereas the Hg treated cells (10 µM for 12 h) showed indicative staining of apoptotic process (Fig 2 c, d). Both early apoptotic cells still adherent in the substrate (Fig 2c, d, arrowhead), as late apoptotic cells with cytoplasmic retraction (Fig 2c, d, arrow) showed positive yopro-1 staining. In fact, the incidence of yopro-1 positive cells increased 17% after Hg treatment (10 µM for 12 h) evidencing that severity of damages observed in culture (Fig 1c) are leading to cell death (Fig 2e). Another indicative of apoptotic process is the incidence of fragmented nucleus in treated cells (Fig 2f, arrowhead).

Apoptosis is not the unique process involved in Hg-induced cell death, since the occurrence of autophagy was also demonstrated after Hg exposure (Fig 3). While in control cells (Fig 3a) no indicative staining was seen (Fig 3b), the presence of autophagic MDC positive vacuoles (Fig 3c, d, arrowheads) was evident in the treated cells (Fig 3c, d). In fact, increased incidence (31%) of MDC positive vacuoles occurred after Hg treatment (10 µM for 12 h) (Fig 3c).

Cellular organelles and structures were investigated in order to understanding the overall damage induced by Hg exposure that is ultimately leading to cell death. Initially, the mitochondrial functionality was investigated through rhodamine 123 staining (Fig 4). While control cells (Fig 4a) showed intense and spread filaments indicative of functional mitochondria (Fig 4b, arrowheads), the Hg treated presented punctuate weak staining (Fig 4d, arrowheads), suggesting the loss of mitochondrial function. These results are in agreement with MTT assay (Fig 1a) that evidenced the decrease of cell viability as indicative in failure of mitochondrial function.

Together with mitochondrial dysfunction, the frequency of acidic compartments increased in treated cells (Fig 5a - d). The improvement of acidic vesicles correlated with higher presence of lysosomes in the cytoplasm (Fig 6 a - d). The regular punctuate pattern characteristic of acidic compartments (Fig 5a, b) and lysosomes (Fig 6a, b) changed after Hg treatment (10 µM for 12 h) to an intense fluorescence pattern corresponding to acid structures in the cytoplasm (Fig 5d, 6d arrowheads). Neutral red assay (Fig 6e) indicated a destabilization in lysosomal membrane, and then part of lysosomal content might be flowing to cytosol. NR is a weak cationic dye that readily penetrates the cell membrane and accumulates intracellularly in lysosomes (lysosomal pH < cytoplasmic pH), therefore the decreased in NR uptake (Fig 6e) is sign of fragility of lysosomal membrane (Babich and Borenfreund, 1991). Another demonstration of the importance of acidic compartments in induction of cell death came from PMA pre-incubation (Fig 6f). Since the PMA acts stimulating both the rate and extent of fusion of phagosomes with pre-existing secondary lysosomes (Kielian and Cohn, 1981), the PMA pre-incubation can mimic the higher incidence of autophagic vacuoles in normal cells. While the PMA incubation for 2 h induced a decrease of 17% in cell viability, the 2 h PMA pre-treatment together with Hg exposure (10 µM for 12 h) had synergistic effect in culture leading to a decrease of 75 % in cell viability (Fig 6f).

Hg treatment (10 µM for 12 h) also affected the structure and function of the endoplasmic reticulum, the main organelle involved in cellular detoxification (Fig 7 a - d). Spread aspect of reticular network observed in control cells (Fig 7a, b) changed to punctuate aspect after Hg treatment (Fig 7 b, d).

Cell retraction observed in treated cells indicates Hg effects over cytoskeleton elements. In fact, the extended cytoplasmic network of microfilaments (Fig 8b, arrowheads) and adhesion points (Fig 8b, arrow) changed after Hg treatment, given that the cells lost their microfilament projections in the cytoplasm (Fig 8d, arrowheads) and their adhesion points on the substrates (Fig 8d, arrow), leading to an alteration in cell morphology (Fig 8c, d, arrow).

Discussion

In the present study, the Hg treatment induced decrease in cell viability together with progressive damage to cell morphology leading to both apoptotic and autophagic cell death due to a multiple dysfunction in cellular organelles.

Apoptosis induction occurred in different cell lines as bronchial epithelial cells (BEAS-2B cell line) (Park *et al*., 2007), porcine renal cell line (LLC-PK1) (Achanzar *et al*., 1996), kidney OK cells (Rosales *et al*., 2005), human leukemia cell line (HL-60 cells) (Araragi *et al*., 2003), human lymphoid cells (Shenker *et al*., 2000) following Hg treatment. Apoptosis is an constitutive physiological involved in control of cell proliferation during the development (Tekpli, 2013). However, the exposure to a variety of chemicals, including many toxic metals might increase the apoptosis incidence (Rana, 2008). Typical morphological hallmarks of apoptotic cells include cell shrinkage, nuclear DNA fragmentation and membrane blebbing (Hengartner, 2000) were observed after Hg treatment in the present study. Moreover, the Hg treated cells also presented mitochondrial dysfunctions that are involved in induction of apoptotic cell death (Gobe and Crane, 2010).

Only few recent reports demonstrated the metal-induced autophagic cell death, as following arsenic (Kanzawa *et al*., 2003) and cadmium exposure (Dong *et al*., 2009; Chargui *et al*., 2011). Autophagy consists in selective elimination of dysfunctional organelles and/or proteins with resulting recirculation and reuse of their molecular constituents (Chatterjee *et al*., 2012; Templeton and Liu, 2010). However, when the cell damage is excessive, the autophagy becomes a cellular suicide pathway eliminating essential cellular proteins and structures, leading to cell death (Gozuacik and Kimchi, 2004). Alterations in mitochondria, endoplasmic reticulum function and cytoskeleton microfilaments architecture demonstrate the overall stress and collapse of cellular organelles after Hg treatment (10 µM for 12 h). During autophagy, the cytosolic material is involved in double-membrane autophagic vacuoles (autophagosomes). These double-membrane cytoplasmic vacuoles will further merge with lysosomes to form autolysosomes for degradation by lysosomal hydrolases (Tekpli, 2013; Chiarelli and Roccheri, 2012). Therefore, the increased acidic compartments and lysosomes following Hg treatment (10 µM for 12 h) correlate to the occurrence of autophagic process.

Following Hg exposure, the first autophagy report occurred after low concentration exposure (5 µM) in rat hepatocytes from 30 min to 4 h of incubation and no autophagic cell death was seen at 10 µM (Chatterjee *et al*., 2012; Chatterjee *et al*., 2013). According to Chatterjee *et al*.

(2012) the autophagy incidence occurs only after low concentration exposure since this type of cell death initiates before apoptosis during concentration-dependent metal exposures. In the present study, the incidence of MDC positive vacuoles observed were observed following the same Hg treatment (10 μM for 12 h) than the occurrence of YO-PRO-1 positive apoptotic cells. This suggests that autophagy not precede the apoptotic cell death, but the both pathways of cell death might occur together. However, the molecular mechanisms regulating this selectivity remain unclear.

Conclusion

The present study showed that Hg affect several multiple intra-cellular targets simultaneously including the mitochondria, cytoskeleton, endoplasmic reticulum and acidic compartments, leading to cell death through both apoptotic and autophagic pathways. These results reinforce the importance of investigations in cellular organelles to develop an overall understanding of Hg-induced toxicity.

Acknowledgments

This work was supported by Fundação Carlos Chagas Filho de Amparo à Pesquisa do Estado do Rio de Janeiro (E-26/171.315/2004) (E-26/ 100.470/2007) (E-26/110.921/2008).

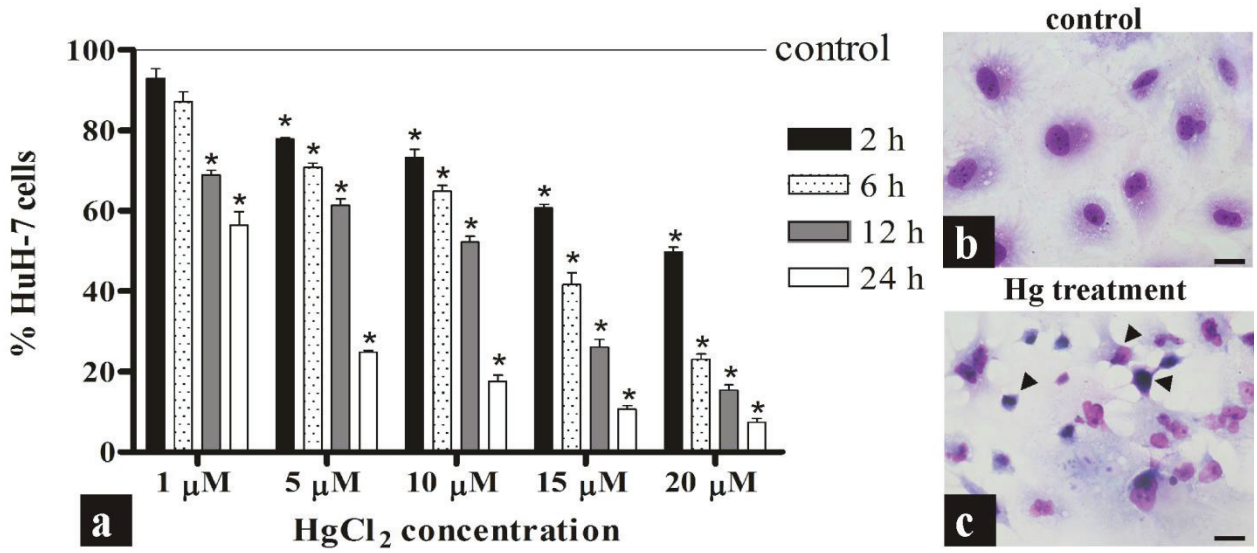

Fig 1. (a) Decrease in cell viability assessed by MTT assay following Hg treatments. The cells were submitted to progressive $HgCl_2$ concentrations (1 µM, 5 µM, 10 µM, 15 µM and 20 µM). The columns represents the different exposure times (2 h, 6 h, 12 h and 24 h). Data are means ± SD of triplicate experiments (n=3). * Significantly different from control (p<0.001). (b) Control adherent HuH-7 culture (c) Change of culture aspect following Hg treatment (10 µM for 12 h). The arrowheads evidenced cells with several levels of cytoplasm shrinkage and nuclear condensation. Scale bar= 20 µm.

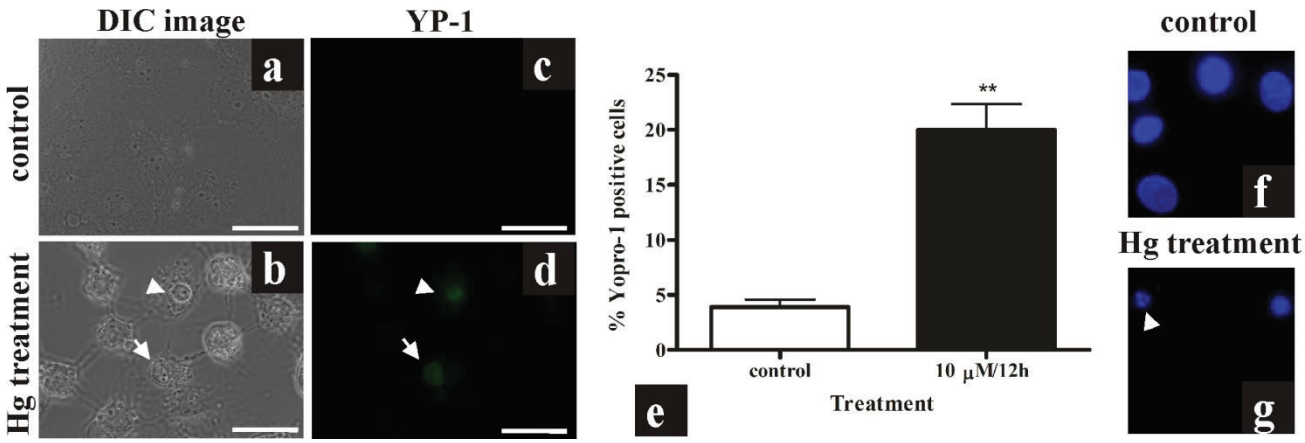

Fig 2. (a) Control adherent cells. (b) Hg treated cells (10 µM for 12 h) evidencing cell retractions and nuclear condensation. (c) Absence of YO-PRO-1 staining in control cells. (d) Positive YO-PRO-1 staining observed in both early apoptotic cells still adherent in the substrate (arrowhead), as in late apoptotic cells with cytoplasmic retraction (arrow) after Hg treatment (10 µM for 12 h). (e) Increase of incidence of YO-PRO-1 positive cells after Hg treatment (10 µM for 12 h). (f) Normal nuclear appearance evidenced through DAPI staining. (g) Incidence of fragmented nucleus in treated cells evidenced through DAPI staining (arrowhead). Data are means ± SD of triplicate experiments (n=3). DIC image= image employing differential interference contrast microscopy. YP-1= YO-PRO-1 staining. ** Significantly different from control ($p<0.05$). Scale bar= 10 µm.

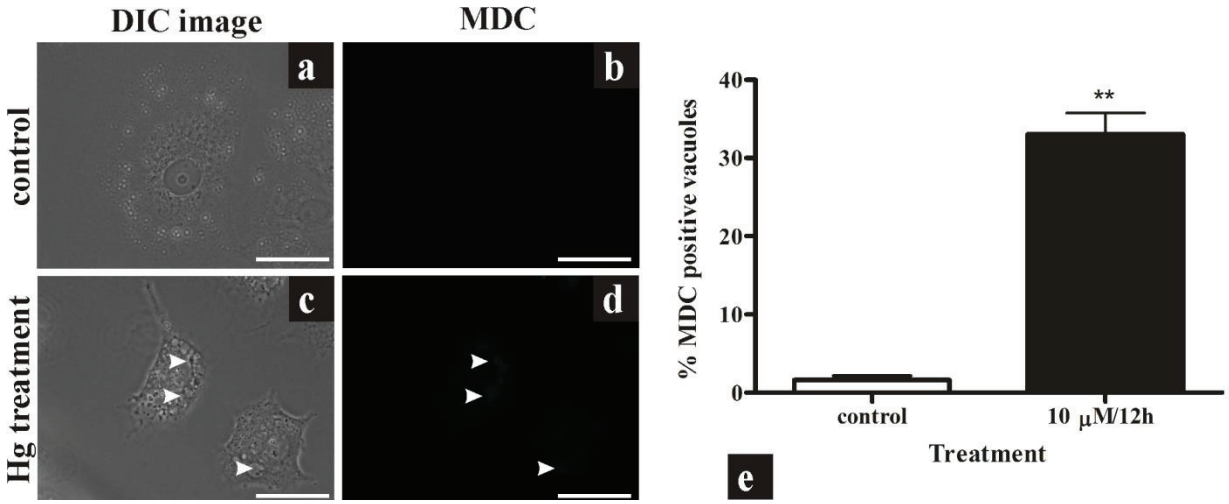

Fig 3. (a) Control adherent cell. (b) Absence of MDC staining in control cells. (c) Hg treated cells (10 μM for 12 h) evidencing cell retractions. (d) MDC positive staining evidencing the occurrence of the autophagic vacuoles in Hg treated cell (10 μM for 12 h) (arrowheads). (e) Increase of incidence of MDC positive autophagic vacuoles following Hg treatment (10 μM for 12 h). Data are means ± SD of triplicate experiments (n=3). DIC image= image employing differential interference contrast microscopy. MDC= Monodansylcadaverine staining. ** Significantly different from control (p<0.05). Scale bar= 10 μm.

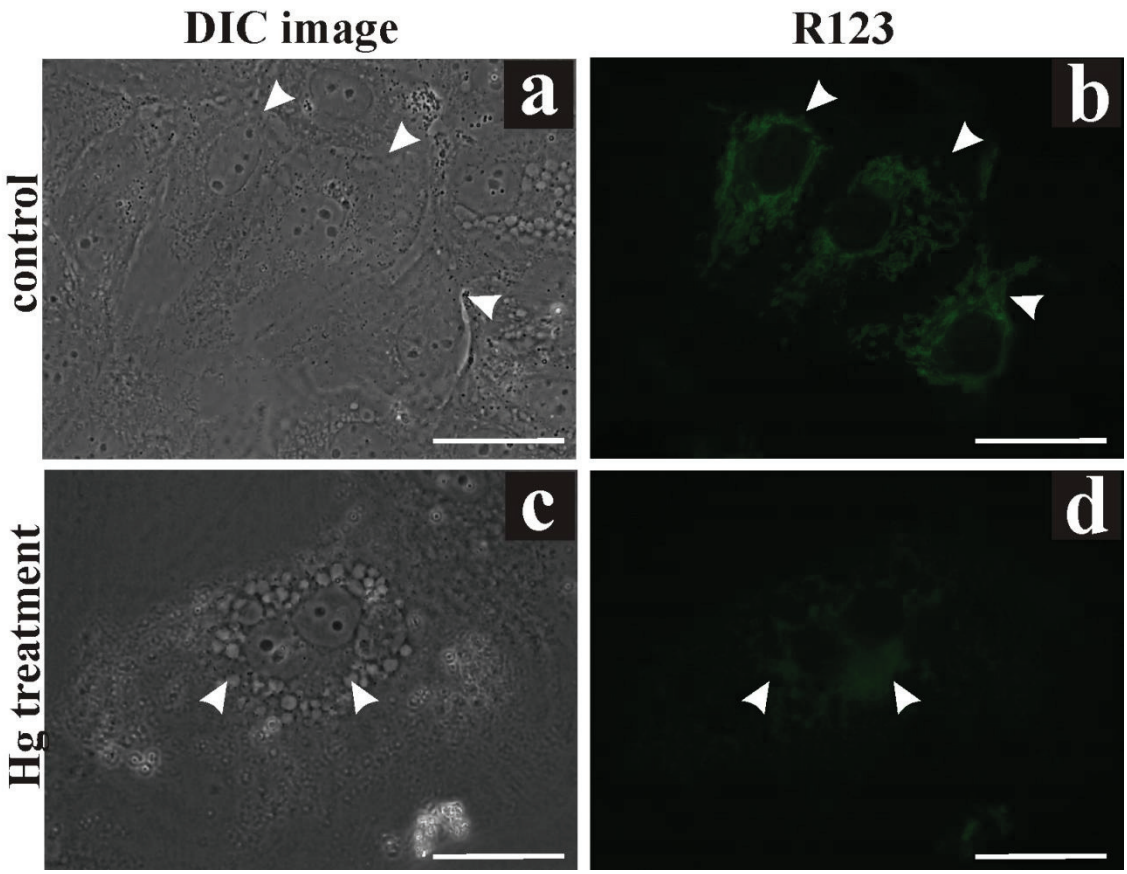

Fig 4. (a) Control adherent cells. (b) Intense and spread filaments evidenced by rhodamine 123 staining, indicative of functional mitochondria in control cells (arrowheads). (c) Hg treated cell (10 µM for 12 h) with cytoplasm vacuolization. (d) Punctuate and weak staining occurred in Hg treated cells (10 µM for 12 h) stained by rhodamine 123 cell suggesting loss of mitochondrial function (arrowheads). DIC image= image employing differential interference contrast microscopy. R123= Rhodamine 123 staining. Scale bar= 10 µm.

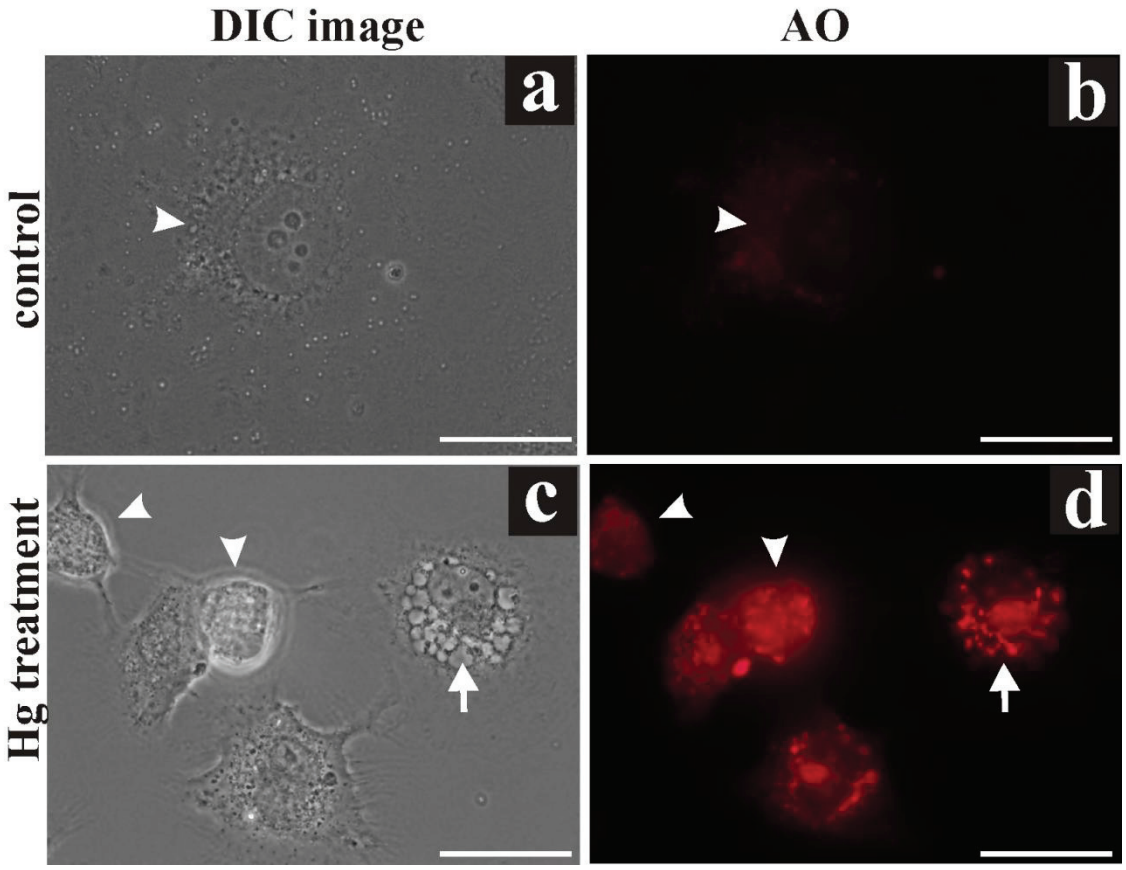

Fig 5. (a) Control adherent cell. (b) Control cell stained with acridine orange showing punctuate fluorescence staining in the cytoplasm of control cell corresponding to acidic organelles, such as endosome and lysosome (arrowheads) (c) Hg treated cells (10 μM for 12 h) evidencing cell retraction (arrowheads) and vacuolization (arrow). (d) Intense fluorescence pattern in the cytoplasm of treated cells (10 μM for 12 h) stained with acridine orange. DIC image= image employing differential interference contrast microscopy. AO= acridine orange staining. Scale bar= 10 μm.

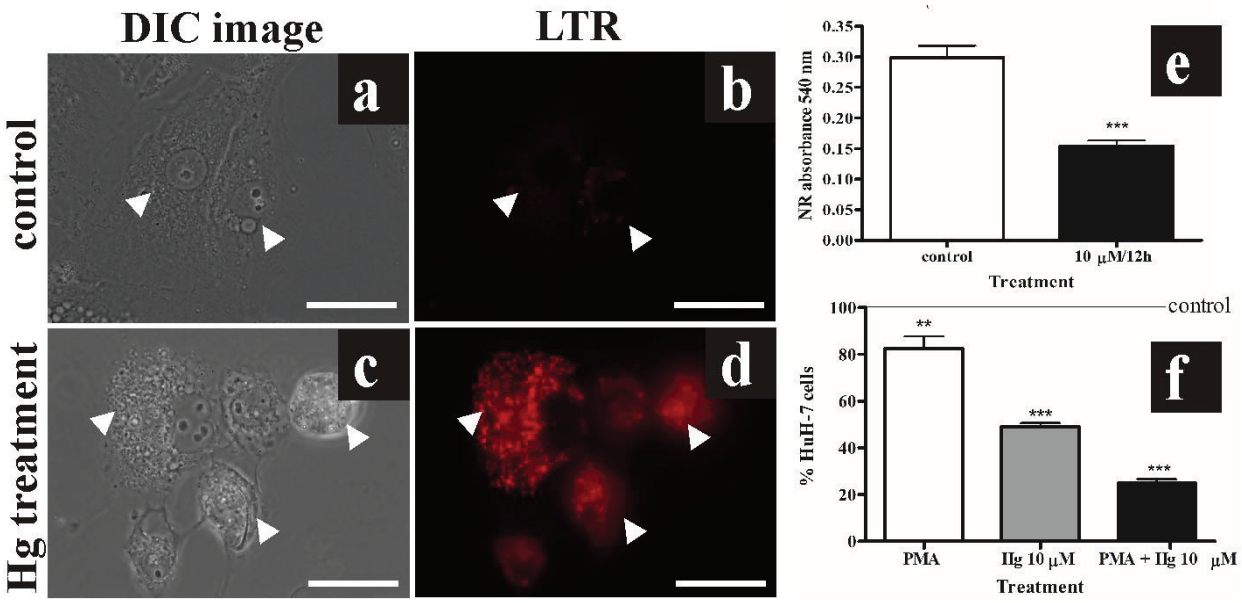

Fig 6. (a) Control adherent cells. (b) Punctuate staining observed in control cells stained with LysoTracker red (arrowheads). (c) Hg treated cells with retracted cytoplasm. (d) Intense fluorescence pattern indicate increased lysosomes throughout the cytoplasm (arrowheads). (e) NR is a weak cationic dye that readily penetrates the cell membrane and accumulates intracellularly in lysosomes. The decrease in neutral red uptake indicates the destabilization in lysosomal membrane after Hg treatment (10 µM for 12 h). ***Significantly different from control (p<0.01). (f) Importance of acidic compartments in induction of cell death evidenced by PMA pre-incubation. PMA acts stimulating both the rate and extent of fusion of phagosomes with pre-existing secondary lysosomes, the PMA pre-incubation can mimic the higher incidence of autophagic vacuoles in normal cells. While the PMA incubation for 2 h induced a decrease of 17% in cell viability, the PMA 2 h pre-treatment together with Hg exposure (10 µM for 12 h) had synergistic effect in culture leading to a decrease of 75 % in cell viability. **Significantly different from control (p<0.01) and *** (p<0.001). DIC image= image employing differential interference contrast microscopy. LTR= LysoTracker staining. Scale bar= 10 µm.

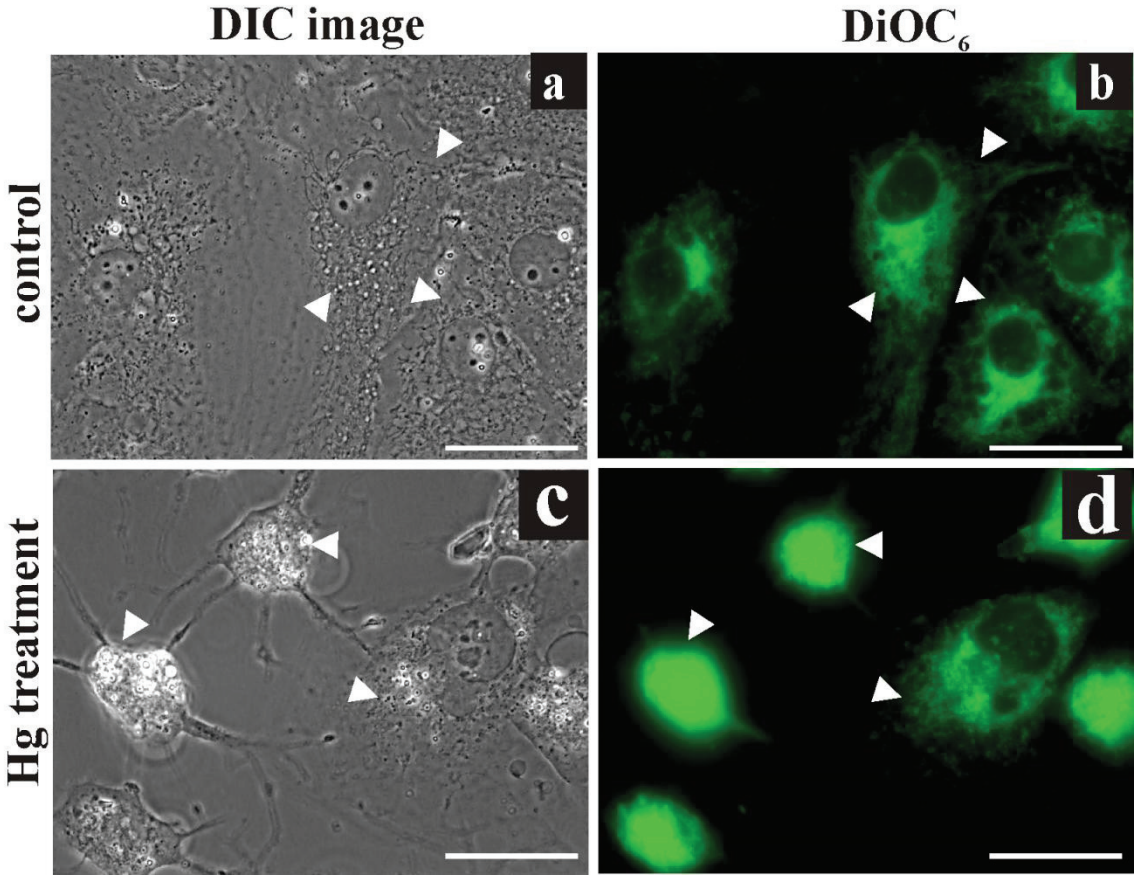

Fig 7. (a) Control adherent cells (b) Spread aspect of reticular network observed in control cells stained with $DiOC_6$ (arrowheads). (c) Hg treated culture with retracted cells. (d). Punctuate fluorescence pattern observed in Hg treated cells stained with $DiOC_6$ (arrowheads). DIC image= image employing differential interference contrast microscopy. $DiOC_6$= $DiOC_6$ staining. Scale bar= 10 μm.

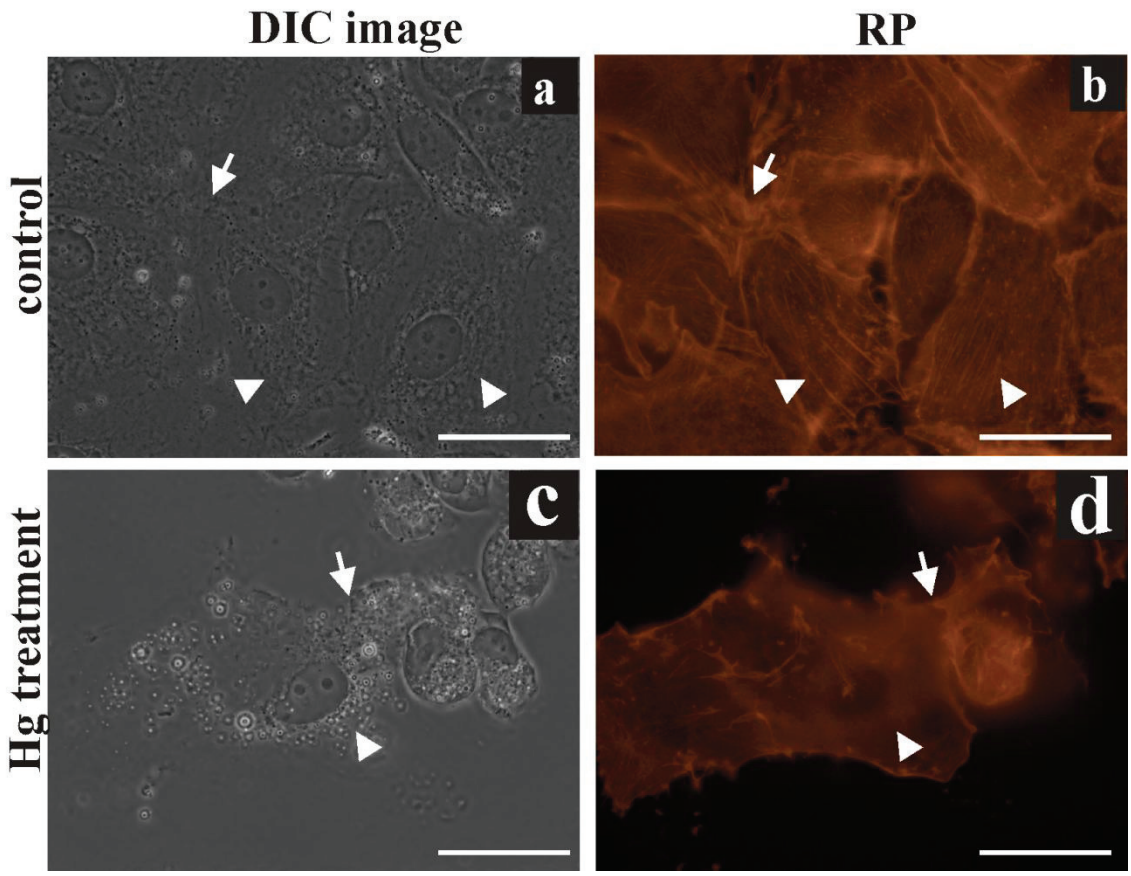

Fig 8. (a) Control adherent cell. (b) Extended cytoplasmic network of microfilaments (arrowheads) and adhesion points (arrow) in control cells stained with rhodamine phalloidin. (c) Hg treated cells (10 µM for 12 h) with cellular retraction. (d) Loss of microfilament projections in the cytoplasm (arrowhead) and of the adhesion points (arrow) in Hg treated cells (10 µM for 12 h). DIC image= image employing differential interference contrast microscopy. RP= Rhodamine Phalloidin staining. Scale bar= 10 µm.

References

Achanzar KBD, Jones JT, Burke MF, Carter DE, Laird HE. Inorganic mercury chloride-induced apoptosis in the cultured porcine renal cell line. J Pharmacol Exp Ther. 1996; 277: 1726-1732.

Araragi S, Kondoh M, Kawase M, Saito S, Higashimoto M, Sato M. Mercuric chloride induces apoptosis via a mitochondrial-dependent pathway in human leukemia cells. Toxicology. 2003; 184: 1-9.

Babich H, Borenfreund E. Cytotoxicity of T-2 toxin and its metabolites determined with the neutral red cell viability assay. Appl Environ Microbiol. 1991; 57: 2101-2103.

Barak LS, Yocum RR, Nothnagel EA, Webb WW. Fluorescence staining of the actin cytoskeleton in living cells with 7-nitrobenz-2-oxa-1,3-diazole-phallacidin. Proc Natl Acad Sci U S A. 1980; 77: 980-984.

Bertin G, Averbeck D. Cadmium: cellular effects, modifications of biomolecules, modulation of DNA repair and genotoxic consequences (a review). Biochimie. 2006; 88: 1549-1559.

Biederbick A, Kern HF, Elsasser HP. Monodansylcadaverine (MDC) is a specific in vivo marker for autophagic vacuoles. Eur J Cell Biol. 2006; 66: 3-14.

Borenfreund E, Puerner JA. A simple quantitative procedure using monolayer cultures for cytotoxicity assays. J Tissue Cult Meth. 1984; 9: 7-9.

Chargui A, Zerki S, Jacquillet G, Rubera I, Ilie M, Belaid A, Duranton C, Tauc M, Hofman P, Poujeol P, May MVE, Mograbi B. Cadmium-induced autophagy in rat kidney: an early biomarker of subtoxic exposure. Toxicol Sci. 2011; 121: 31-42.

Chatterjee S, Ray A, Mukherjee S, Agarwal S, Kundu R, Bhattachary S. Low concentration of mercury induces autophagic cell death in rat hepatocytes. Toxicol Ind Health. 2012; In press.

Chatterjee S, Nani P, Mukherjee S, Chattopadhyay A, Bhattachary S. Regulation of autophagy in rat hepatocytes treated in vitro with low concentration of mercury. Toxicol Environ Chem. 2013; 1-11. In press.

Chen YW, Huang CF, Yang CY, Yen CC, Tsai KS, Liu SH. Inorganic mercury causes pancreatic β-cell death via the oxidative stress-induced apoptotic and necrotic pathways. Toxicol Appl Pharmacol. 2010; 243: 323-331.

Chiarelli R, Roccheri MC. Heavy metals and metalloids as autophagy inducing agents: focus on cadmium and arsenic. Cells. 2012; 1: 597-616;

Dong Z, Wang L, Xu J, Li Y, Zhang Y, Zhang S, Miao J. Promotion of autophagy and inhibition of apoptosis by low concentrations of cadmium in vascular endothelial cells. Toxicol In Vitro. 2009; 23: 105-110.

Fabbri M, Urani C, Sacco MG, Procaccianti C, Gribaldo L. Whole genome analysis and microRNAs regulation in HepG2 cells exposed to cadmium. Altex. 2012; 29: 2-12.

Gobe G, Crane D. Mitochondria, reactive oxygen species and cadmium toxicity in the kidney. Toxicol Lett. 2010; 198: 49-55.

Gozuacik D, Kimchi A. Autophagy as a cell death and tumor suppressor mechanism. Oncogene. 2004; 23: 2891-2906.

Hengartner MO. The biochemistry of apoptosis. Nature. 2000; 407: 770-776.

Hinton DE, Segner H, Au DWT, Kullman SW, Hardman RC. Liver toxicity. In: Giulio RTD, Hinton DE. Eds. The toxicology of fishes. Florida: CRC Press, Taylor and Francis Group; 2008: 337-401.

Idziorek T, Estaquier J, De Bells F, Ameisen JC. YO-PRO-1 permits cytofluorometric analysis of programmed cell death (apoptosis) without interfering with cell viability. J Immunol Methods. 1995; 185: 249-258.

Johnson LV, Walsh ML, Chen LB. Localization of mitochondria in living cells with rhodamine 123. Proc Natl Acad Sci USA. 1980; 77: 990-994.

Kanzawa T, Kondo Y, Ito H, Kondo S and Germano I. Induction of autophagic cell death in malignant glioma cells by arsenic trioxide. Cancer Res. 2003; 63: 2103-2108.

Kielian MC, Cohn ZA. Phagosome-lysosome fusion. J Cell Biol. 1980; 85: 54-765.

Kielian MC, Cohn ZA. Phorbol myristate acetate stimulates phagosome-lysosome fusion in mouse macrophages. J Exp Med. 1981; 154: 101-111.

Kuo TC, Shiau SYL. Early acute necrosis and delayed apoptosis induced by methyl mercury in murine peritoneal neutrophils. Basic Clin Pharmacol Toxicol. 2004; 94: 274-281.

Liao C.Y., Fu J.J., Shi J.B., Zhou Q.F., Yuan C.G., Jiang G.B. Methylmercury accumulation, histopathology effects, and cholinesterase activity alterations in medaka (Oryzias latipes) following sublethal exposure to methylmercury chloride. Environ Toxicol Pharmacol. 2006; 22: 225-233.

Malhi H, Guicciardi ME, Gores GJ. Hepatocyte death: a clear and present danger. Physiol Rev. 2010; 90: 1165-1194.

Mosmann T. Rapid colorimetric assay for cellular growth and survival: application to proliferation and cytotoxicity assays. J Immunol Methods. 1983; 65: 55-63.

Park EJ, Kwangsik Park K. Induction of reactive oxygen species and apoptosis in BEAS-2B cells by mercuric chloride. Toxicol In Vitro. 2009; 21: 789-794.

Plantin-Carrenard E, Bringuier A, Derappe C, Pichon J, Guillot R, Bernard M, Foglietti MJ, Feldmann G, Aubery M, Braut-Boucher F. A fluorescence microplate assay using yopro-1 to measure apoptosis: application to HL60 cells subjected to oxidative stress. Cell Biol Toxicol. 2003; 19: 121-133.

Rana SVS. Metals and apoptosis: Recent developments. J Trace Elem Med Biol. 2008; 22: 262-284.

Rosales PC, Said-Fernández S, Sepúlveda-Saavedra J, Cruz-Veja DE, Jay Gandolfi A. Morphologic and functional alterations induced by low doses of mercuric chloride in the kidney OK cell line: ultrastructural evidence for an apoptotic mechanism of damage. Toxicology. 2005; 210: 111-121.

Shenker BJ, Guo TL, Shapiro IM. Mercury-induced apoptosis in human lymphoid cells: Evidence that the apoptotic pathway is mercurial species dependent. Environ Res. 2000; 84, 89-99.

Syversen T, Kaur P. The toxicology of mercury and its compounds. J Trace Elem Med Biol. 2012; 26: 215- 226.

Tekpli X, Holme JA, Sergenta O, Gossmann DL. Role for membrane remodeling in cell death: implication for health and disease. Toxicology. 2013; 304: 141-157.

Templeton DM, Liu Y. Multiple roles of cadmium in cell death and survival. Chem Biol Interact. 2010; 188: 267-275.

Terasaki M, Song J, Wong JR, Weiss MJ, Chen LB. Localization of endoplasmic reticulum in living and glutaraldehyde-fixed cells with fluorescent dyes. Cell. 1984; 38: 101-108.

Valee BL, Ulmer DD. Biochemical effects of mercury, cadmium, and lead. Annu Rev Biochem. 1972; 41: 91-128.

Wang Y, Fang J, Leonard SS, Rao KMK. Cadmium inhibits the electron transfer chain and induces reactive oxygen species. Free Radic Biol Med. 2004; 36(11): 1434-1443.

Differential Accumulation and Histopathological Effects of Cadmium Exposure in the Tropical Fish *Gymnotus carapo*

Cristiane dos S. Vergilio[1], R. V. Moreira[1], L. S. Gomes[2], C. E.V. Carvalho[2] and E. J. T. Melo[1]

1. Laboratório de Biologia Celular e Tecidual, Centro de Biociências e Biotecnologia, Universidade Estadual do Norte Fluminense, Campos dos Goytacazes, 28013-602, RJ, Brasil.

2. Laboratório de Ciências Ambientais, Centro de Biociências e Biotecnologia, Universidade Estadual do Norte Fluminense, Campos dos Goytacazes, 28013-602, RJ, Brasil.

Abstract

The present study investigated the progressive effects of $CdCl_2$ in the testis and sperm of the tropical fish tuvira *Gymnotus carapo* exposed to increasing Cd concentrations (5 µM - 40 µM) for 96 h. The exposure with increasing concentrations induced efficient accumulation of Cd in the testis; together with significantly decrease in the gonadosomatic index. Cd treatment induced disorganization of the cysts' arrangement with marked variations of cyst size, proliferation of interstitial tissue, infiltration of inflammatory cells, necrosis, reduction of germ cells and sperm aggregation. Exposed fishes (20 µM for 96 h) also showed reduction in sperm number and alteration in sperm morphology. These results are important for establish a direct correlation between the Cd accumulation and the incidence of damages, and help to characterize the mechanism of Cd-induced pathogenesis in the male reproductive system.

Key words: Cd, effect, histology, testis

Introduction

Cadmium (Cd) is a toxic metal that can accumulate in animals and induce adverse effects (Nordberg 2009). Fishes are good indicators of aquatic pollution that can express both human and ecological health, since the fishes have a high potential for Cd accumulation and consumption of contaminated fish and seafood is one of the main source of Cd exposure to human populations (Ju *et al*. 2012). The male reproductive system of fishes is highly vulnerable to toxicants, during the processes through which germ cells undergo a large number of cell divisions, before the release of mature spermatozoa (Bonde 2010). Alterations in testis and sperm may affect the fertilization success and alter fish populations (Crump and Trudeau 2009). Despite these known importance, little information is available concerning the mechanisms of metal-induced pathogenesis on male reproductive system of fishes (Boujbiha *et al.* 2009). In a overall way, studies describing histopathological damages in fish testis after Cd contamination events are still scarse and limited to a few species.

Therefore, the present study aimed in investigate the toxic effects of $CdCl_2$ in testes and sperm of a teleost fish, *G. carapo*, to elucidate the pathological processes during exposure to a range of Cd concentrations (5 µM - 40 µM) and different exposure times (24 h - 96 h).

Material and Methods

G. caparo specimens were obtained from Cima Lake, in northern Rio de Janeiro state (21º 46' S and 41º 31' W). All fishes used were sexually mature males with similar size (length: 36.8 ±6.0 cm/ weight: 205,8 ±59.9 g) to avoid differences in treatments. Fish exposure was performed by a single intra-peritoneal injection (0.1 mL) with $CdCl_2$ solution of 30 µM final concentration (equivalent to 0.6 $\mu g.g^{-1}$) for distinct exposure times (24 h, 48 h, 72 h and 96 h). For the control group, the fishes were injected with phosphate buffered saline solution (pH 7.2). The range of exposure times allowed the evaluation of the progression of toxic effects in different organs (gills, muscle, liver, testis and kidney), but with no induction of fish death. . The fishes (n=40) were separated in five groups containing six fishes in each (one group for each exposure time) and a control group with sixteen fishes. From the six fishes used for evaluation of effects in each exposure time, three were used for histological analysis and the other three for Cd chemical quantification. Following each

exposure period (24 h, 48 h, 72 h, 96 h), the fishes were measured, weighed and dissected to obtain the gills, muscle, liver, testis and kidney that were processed for histological preparations or frozen (-20°C) for subsequent analysis of Cd accumulation. The procedure for Cd extraction in nitric acidic followed the proposed by Páez-Osuna *et al*. (1995). The samples were analyzed by atomic emission spectrophotometry with induced coupled plasma (ICP-AES, Varian, model Liberty II). The method's limit of detection (0.02 $\mu g.Kg^{-1}$) was calculated according to Skoog and Leary (1992). The preparation of testis for morphological analysis included the fixation in 10% buffered formalin for 24 hours, dehydration in graded series of ethanol and embedding in paraffin. Tissue sections (5 µm) were stained with hematoxylin and eosin (H&E) for examination by light microscopy. Morphological damages were measured according to the injury index described by Bernet *et al*. (1999). The score ranking was based on the percentage of lesions in each organ, and the importance factor was determined for each lesion depending on the effects considered as minimal (1), moderate (2) and irreversible with marked pathological importance (3). The injury indexes were obtained after the application of a mathematical equation established for each group of lesions: (LI): LI= Σrp Σalt (a x w), where rp=reaction pattern, alt=alteration, a=score value of the alteration and w= importance factor. Muscle were sampled in order to investigate the activity of cholinesterase activity. Aliquots were thawed and homogenized at 4°C in 0.1M sodium phosphate buffer, pH 7.5. Homogenates were centrifuged at 10.000g for 10 min at 4 °C and enzyme activity was measured spectrophotometrically at 405 nm according to Ellman *et al*. (1961), with minor modifications for use in 96-well microplates by Silva de Assis (1998). Protein content of each sample was measured following Bradford (1976) using bovine serum albumin as a standard. All the concentrations presented in the graphics of the present study are averages and their standard deviations. Significant differences were determined with Graph-prism v.4 software (GraphPad Software, Inc. CA, USA). The data of Cd concentrations in organs were analyzed using two-way analysis of variance followed by the Bonferroni post-test. Differences were considered significant when $p < 0.05$.

Results and Discussion

Cd showed efficient accumulation in fish organs following the single exposure event. Cd accumulation was differential among the analyzed organs, following the order: liver > kidney > gills > testis > muscle. Despite the highest accumulation potential observed in liver, the gills showed the major improvement of Cd concentrations, with the levels enhanced almost 7 times in relation to control. While the liver and kidney concentrations were approximately 5 times higher than the observed in control. Muscle showed the lowest levels of Cd, presenting levels bellow or close to the limit of method detection (0.02 $\mu g.Kg^{-1}$).

In all organs, the Cd concentrations were lower in 24 h, followed by an increase in concentrations in 48 h and 72 h and reduced levels in 96 h. This occurs since the period of 24 h reflects the metal uptake in the organism, while the 48 h and 72 h increased levels indicate the metal circulation through blood circulation. The 96 h decreased levels indicate that the fishes are eliminating part of the introduced Cd. The muscle concentrations are an exception to this pattern presenting low levels, close to limit of method detection only after 96 h of exposure.

Changes in Cd concentrations during the time occurred due to redistribution processes during the metal residence in the body. The main factors involved in the distribution of chemical substances from blood to peripheral tissues are the (1) physicochemical characteristics of the compound (e.g., pKa, lipid solubility, molecular volume), (2) the concentration gradient between blood and tissues, (3) the ratio of blood flow to tissue mass, (4) the relative affinity of the chemical for blood and tissue constituents, and (5) the activity of specific membrane transport proteins (Kleinow *et al*., 2008). In the present study, the blood flow is the major determinant of the rate of Cd distribution to tissues. Kidney and liver that have the highest blood perfusion rate (Barron *et al*., 1987) showed the major Cd accumulation.

Gills levels can reflect current exposures for their permanent contact with water (Mieiro *et al*., 2011), however the fish gills are also able to accumulate chemicals absorbed from other exposure routes, due to their position between the venous and arterial circulation, thus receiving nearly all of the cardiac output (Pereira *et al*., 2010). Cd concentrations documented in gills might reflect the Cd distribution through blood circulation for elimination.

In the present study, the intra-peritoneal exposure offered great absorptive surface area in the peritoneal cavity allowing quickly absorption of Cd into the circulation (Vergilio *et al*., 2012). The route of administration also influences the chemical distribution of substances to tissues (Kleinow *et*

al., 2008). Therefore, the readily Cd accumulation in the testis, since 24 h might be occurred for their location in the peritoneal cavity.

Despite the differential accumulation, the treatment induced morphological damages even in the organs with lowest Cd levels (gills and testis) (Fig 2 and 3). Cd induced disorganization of proximal tubules arrangement, infiltration of inflammatory cells (arrows), increased incidence of melano-macrophages centres (MMC) and necrosis (arrowheads) in the kidney (Fig 2). In liver, Cd treatment induced loss of lipid reserves within the hepatocytes, congestion of blood vessels, incidence of pyknotic nuclei in the hepatocytes (inset) and necrosis, with incidence of the damages increasing in a time dependent matter (Fig 2). Cd treatment induced fusion of secondary lamellas and congestion of blood vessels in gills (Fig 3) and complete disorganization in testicular parenchyma together with proliferation of interstitial tissue and reduction of germ cells (Fig 3) occurred in testis after Cd single exposure (30 μM). These observed alteration can impair the normal organ functionality and can might decrease the fish performance in the natural environment. The severity of damages increased after 96 h of exposure as indicated by index of lesion (Fig 2 c, f and Fig 3e, f), with exception of the testis that showed high vales of the lesion index since 24 h, for exhibit overspread damage in the testicular parenchyma, with reduction of germ cells that might even lead to organ atrophy.

Despite these morphological effects, the Cd exposure did not alter the cholinesterasic activity in muscle (Fig 3g). Acetylcholinesterase (AChE) is an important enzyme responsible for rapid hydrolysis of acetylcholine (ACh) at the cholinergic synapses, a key enzyme of the nervous system (Liederer and Borchardt, 2006). Inhibition of cholinesterasic activity in muscle was doccumented after metal contamination events (Gill *et al*., 1990, Gill *et al*., 1991) indicating impairment of muscle normal function. The lowest and almost not detectable levels of Cd in muscle agree with not altered cholinesterasic activity.

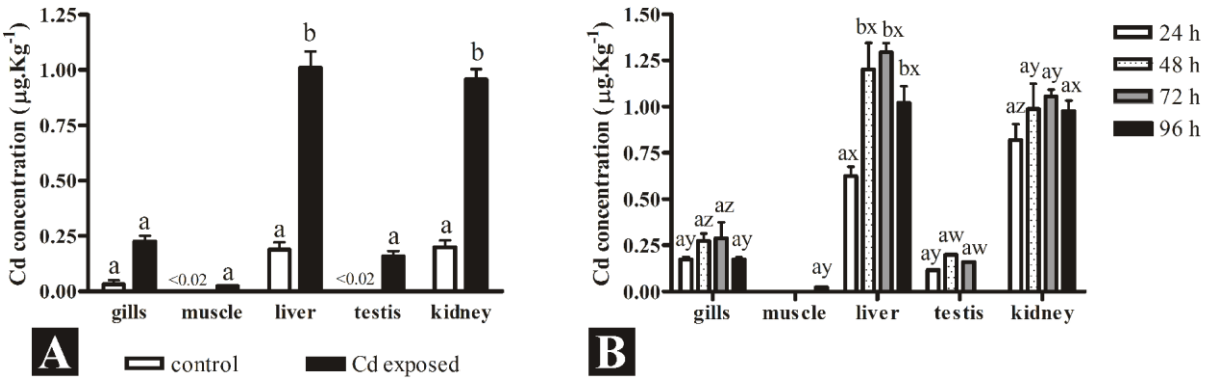

Fig 1. Cd differential accumulation in fish organs. The fishes exposed with a single contamination event (30 µM) and sacrificed after 24 h, 48 h, 72 h and 96 h. The graph (a) represents the bioaccumulation potential of the organs, and therefore not considered the different exposure times, representing the average of Cd concentrations (µg. Kg^{-1}) in gills, muscle, liver, testis and kidney of control and Cd exposed fishes (30 µM). The graph (b) represent the average of Cd concentrations in fish organs considering the distinct exposure times that the fishes were submitted (24 h, 48 h, 72 h and 96 h). The letters a and b in graph (a) represents statistical significance at p <0.05 among the Cd concentrations of control and Cd exposed fishes. In the graph (b) the letters indicate statistical significance at $p < 0.05$ among the exposure times (a, b, c) or different organs (x, y, w).

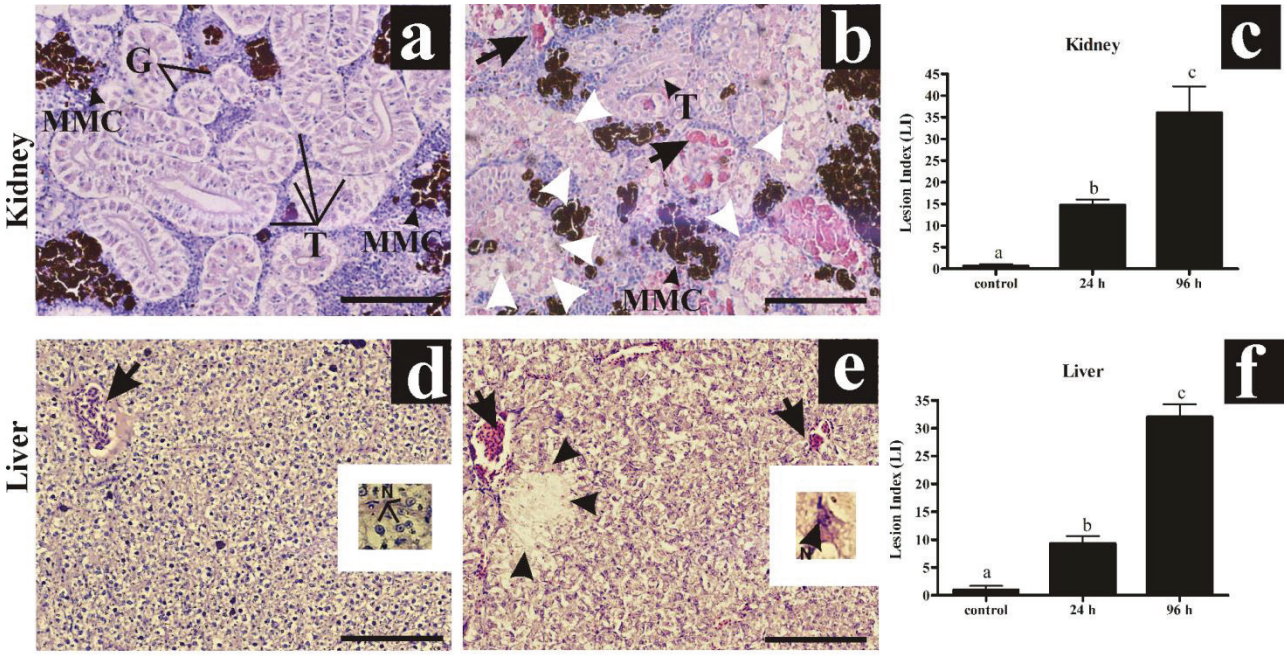

Fig 2. Cd induced alterations in *Gymnotus carapo* kidney and liver. (a) Morphological aspect of the kidney of control fishes with characteristic structure of the proximal tubules (T) and glomerulus (G) and the occurrence of melano-macrophages centres. (b) Disorganization of tubules arrangement and incidence of necrotic areas (arrowheads) after 96 h of Cd single exposure (30 μM). Infiltration of inflammatory cells and increased incidence of melano-macrophages centres occurred. (c) Increased lesion index score demonstrate the kidney effects become more severe after 96 h of exposure. (d) Morphological aspect of the liver of control fishes with characteristic structure of hepatic parenchyma with blood vessels (arrow) and hepatocytes presenting normal nuclei morphology (inset). (e) Alteration in the hepatic parenchyma aspect due to loss of lipid reserves within the hepatocytes, congestion of blood vessels, incidence of pyknotic nuclei in the hepatocytes (inset) and occurrence of necrosis after 96 h of Cd single exposure (30 μM). (f) Increased lesion index score demonstrate the liver effects become more severe after 96 h of exposure. The letters a, b and c indicate statistical significance at $p < 0.05$ among the exposure times. Scale bars= 100 μm.

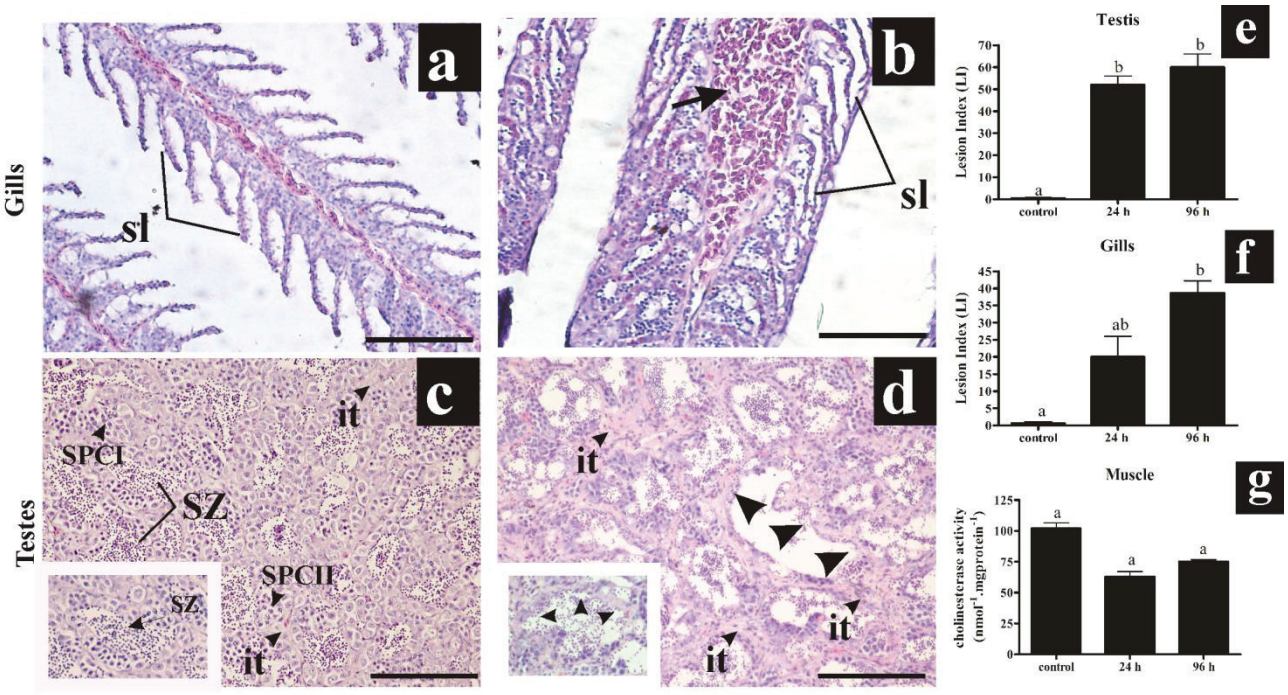

Fig 3. Cd induced alterations in *Gymnotus carapo* gills and testis. (a) Morphological aspect of the gills of control fishes with characteristic arrangement of primary and secondary lamellas (sl). (b) Complete fusion of secondary lamellas and congestion of blood vessels after 96 h of Cd single exposure (30 µM). (c) Morphological aspect of the testis of control fishes with characteristic organization in cysts surrounded by interstitial tissue (it). Germ cells (include the primary and secondary spermatocytes demonstrated in figure) in different stages of differentiation undergo a number of cell divisions until spermatozoa (SZ) formation inside the cysts. (d) Complete disorganization in testicular parenchyma together with proliferation of interstitial tissue and reduction of germ cells occurred after 96 h of Cd single exposure (30 µM). The incidence of damages in gills (e) and testis (f) demonstrated by the lesion index after 24 h and 96 h of the Cd single exposure (30 µM). (g) Cd accumulation lowest accumulation in muscle did not alter the cholinesterase activity. The letters a and b indicate statistical significance at $p < 0.05$ among the control and the 24 h and 96 h exposed fishes. Scale bars= 100 µm.

References

Barron, M. G., Tarr, B. D., & Hayton, W. L. (1987). Temperature-dependence of cardiac output and regional blood flow in rainbow trout, Salmo gairdneri Richardson. *Journal of Fish Biology, 31*(6), 735-744. doi: 10.1111/j.1095-8649.1987.tb05276.x

Gill, T. S., Tewari, H., & Pande, J. (1990). Use of the fish enzyme system in monitoring water quality: Effects of mercury on tissue enzymes. *Comparative Biochemistry and Physiology Part C: Comparative Pharmacology, 97*(2), 287-292. doi: http://dx.doi.org/10.1016/0742-8413(90)90143-W

Gill, T. S., Tewari, H., & Pande, J. (1991). In vivo and in vitro effects of cadmium on selected enzymes in different organs of the fish Barbus conchonius ham. (Rosy Barb). *Comparative Biochemistry and Physiology Part C: Comparative Pharmacology, 100*(3), 501-505. doi: http://dx.doi.org/10.1016/0742-8413(91)90030-W

Kleinow, K. M., Nichols, J. W., Hayton, W. L., McKim, J. M& Barron, M. G. (2008) Toxicokinetics in fishes. In: The toxicology of fishes. Eds. Giulio RTD, Hinton DE. CRC Press, Taylor and Francis Group, Boca Raton, FL.

Mieiro, C. L., Duarte, A. C., Pereira, M. E., & Pacheco, M. (2011). Mercury accumulation patterns and biochemical endpoints in wild fish (Liza aurata): A multi-organ approach. *Ecotoxicology and Environmental Safety, 74*(8), 2225-2232. doi: http://dx.doi.org/10.1016/j.ecoenv.2011.08.011

Pereira, P., Pablo, H. d., Vale, C., & Pacheco, M. (2010). Combined use of environmental data and biomarkers in fish (Liza aurata) inhabiting a eutrophic and metal-contaminated coastal system – Gills reflect environmental contamination. *Marine Environmental Research, 69*(2), 53-62. doi: http://dx.doi.org/10.1016/j.marenvres.2009.08.003

Vergilio CS, Carvalho CEV, Melo EJT (2012) Accumulation and histopathological effects of mercury chloride after acute exposure in tropical fish *Gymnotus carapo*. *Journal of Chemical Health Risks 2*(4): 01-08.

Journal of Chemical Health Risks 2(4): 01-08, 2012
ISSN:2251-6719

Accumulation and Histopathological Effects of Mercury Chloride after Acute Exposure in Tropical Fish *Gymnotus carapo*

C. S. Vergilio[1], C. E. V. Carvalho[2] and E. J. T. Melo[1]

[1] Laboratório de Biologia Celular e Tecidual, Centro de Biociências e Biotecnologia, Universidade Estadual do Norte Fluminense, Campos dos Goytacazes, 28013-602, RJ, Brasil.
[2] Laboratório de Ciências Ambientais, Centro de Biociências e Biotecnologia, Universidade Estadual do Norte Fluminense, 28013-602, Campos dos Goytacazes, RJ, Brasil.

Abstract: The present study evaluated potential Hg bioaccumulation and its morphological effects in different organs of the tropical fish, *Gymnotus carapo*, after a single acute intra-peritoneal exposure (0.6 $\mu g.g^{-1}$) and over progressively longer exposure times (24 h, 48 h, 72 h and 96 h). The Hg accumulation was differential and time dependent for most target organs (testis > liver > gills > muscle). Hg exposure leads the highest accumulation potential in testis since the initial examination point (24 h) until the last (96 h). The liver showed progressive Hg accumulation, presenting its highest levels only at the 96 h exposure point. Hg concentrations in the gills and muscle oscillated over the exposure times; however, the highest values of both organs also occurred in 96 h exposed fish. Histopathological alterations were observed in testis, liver and gills from 24 h of Hg exposure, and the extent of the alterations and their severity increased out to 96 h of exposure. These results shows a correlation between Hg accumulation and the induced morphological damages in different organs along the time in a tropical fish species *G. carapo*, being the histopathology a sensitive technique for the observation of the initial damage from Hg exposure.

Keywords: Hg, histopathology, intra-peritoneal, morphology, organs

INTRODUCTION

Mercury (Hg) is one of the most harmful pollutants due to its high toxicity and persistence in the environment [1]. Once Hg is in aquatic systems, different organisms can accumulate Hg, leading to its biomagnification through the food web [2]. Studies examining metal accumulation in fish tissues are important because these organisms represent the main human contamination pathway [3, 4, 5].

Studies of tissues and organs dealing with metal uptake, accumulation, biotransformation, and excretion are fundamental to increase the understanding of the effects of chemicals in fish [2].Information on the effects of Hg distribution and accumulation in temperate freshwater fish species have been intensely reported, but data on tropical fish and effects on different fish tissues are still scarce [6, 7]. Moreover, there are no studies dealing with the steps associated with metal toxicology including accumulation and damage in the different target organs. *Gymnotus carapo* (banded knife fish) is a widely distributed South American tropical freshwater fish with sedentary and omnivorous habits [8]. This species is a favorite prey of higher predator species and is easily maintained under experimental conditions. Accordingly, it is an interesting model for the evaluation of the toxic effects of pollutants in Brazilian ecosystems, especially because little is known about metal distribution in this species.

Bioassays have proven to be valuable tools to characterize the toxic action of chemicals in different target organs [9]. Under well-defined exposure levels, they allow the quantification of metals in organs together with an analysis of the effects in cells and tissues. This information gives an overall evaluation of the health status of fish and can help to predict comparative effects of metals, such as Hg, in natural aquatic systems [10]. Studies of Hg uptake in fish show relatively slow absorption and low bioavailability of this metal when exposure occurs through water or food; these effects result from a significant and variable elimination of Hg [11]. According to [10], approximately 60% of Hg in water is lost after 96 h. Consequently, an improved understanding of the relationship between dose and time in Hg accumulation and distribution could be more accurately evaluated using an intra-peritoneal exposure route. Intra-peritoneal exposure offers a bioavailability of 100% of the metal to the studied organs. This results from the great absorptive surface area of the peritoneal cavity from which substances are quickly absorbed into the circulation. These characteristics make possible a better portrayal of the distribution and persistence of metals in fish.

The objective of the present work was to evaluate Hg's potential for bioaccumulation and its effects on the morphology of different organs in the tropical fish

Corresponding Author: Edesio José Tenório de Melo. Adress: Universidade Estadual do Norte Fluminense, Laboratório de Biologia Celular e Tecidual, Centro de Biociências e Biotecnologia. Av. Alberto Lamego, 2000, Parque Califórnia, CEP 28013-600, Campos dos Goytacazes, R.J., Brasil. Tel: (+55) 22 2739-7175. E-mail: ejtm1202@gmail.com or ejtm@uenf.br

species, *Gymnotus carapo*. To achieve this objective, analyzes were conducted of Hg concentrations in testis, liver, gills, and muscle over progressive exposure periods, as well as the histological effects of higher bioaccumulation in certain organs. This study aimed to enhance the knowledge of Hg tissue damage after acute exposure in tropical fish.

MATERIAL AND METHODS

Fish contamination strategy

G. caparo specimens (n=48) were obtained from Cima Lake, in northern Rio de Janeiro state (21º 46' S and 41º 31' W). According to [12, 13], this region has low levels of metal pollution in sediments and biota. Fish exposure was performed by intra-peritoneal injection of a $HgCl_2$ solution (0.6 $\mu g.g^{-1}$), followed by progressive exposure times (24 h, 48 h, 72 h and 96 h). The fish control group received an injection with phosphate buffered saline solution (pH 7.2). Only a small volume (0.1 mL) of Hg solution was injected in the peritoneal cavity of the fishes. All fish used in this study were of similar size (length: 30.5 ± 1.2 cm and weight: 114.3 ±0.9 g) (Table 1) to avoid differences among the exposures.

Table 1. Number, average weight (g) and average length (cm) of *G. carapo* specimens used in each contamination experiment. The standard derivations follow the weight and length data.

Exposure time	Control	Hg exposed	Weight (g)	Lenght (cm)
24h	6	6	115.2 ± 4.9	29.8 ± 3.3
48h	6	6	114.4 ± 4.0	30.1 ± 2.6
72h	6	6	113.1 ± 3.9	32.3 ± 2.9
96h	6	6	114.6 ± 4.6	30.0 ± 3.6
total	24	24	114.3 ± 0.9	30.5 ± 1.2

From the eight specimens selected for each experiment, four fishes (one for each exposure time: 24 h, 48 h, 72 h and 96 h) were kept as a control group and the other four were exposed to $HgCl_2$. The above procedure was repeated six consecutive times. After each exposure, the specimens were measured, weighed and dissected to obtain the testis, liver, gills and muscle that were processed for histological analysis or were frozen (-20°C) for subsequent analysis of total Hg accumulation.

Chemical extraction method

The procedure for total Hg extraction followed the methodology described by [14]. Samples of testis, liver, gills and muscle from control and treated fishes were digested with an acid mixture (H_2SO_4:HNO_3, 1:1), followed by addition of $KMnO_4$ solution (5%). Excess $KMnO_4$ was then reduced by the addition of NH_2OHCl solution (12%). For analysis, $SnCl_2$ solution was added, allowing the Hg quantitation. Blanks were run after every 10 samples to ensure analytical control of the procedure. The accuracy of the methodology was confirmed by the use of certified reference material – DORM – 1 (muscle tissue of *Squalus acanthias*) - prepared by the "Marine Analytical Chemistry Standards Programs", Canada; 98.92% recovery was obtained. The method's detection limit, calculated according to [15] was 20 $\mu g.kg^{-1}$.

Instrumentation

The Hg concentrations were determined by CV-ICP (Varian, Liberty II model) with a cold vapor accessory (VGA-77).

Tissue Morphology

Samples of testis, liver and gills from the control and treated fishes were fixed by immersion in 10% buffered formalin for 24 hours. The samples were then dehydrated in a graded series of alcohol, cleared in xylene and embedded in paraffin. The samples were sectioned (5 µm) and stained with hematoxylin and eosin (H&E) for morphological examination by light microscopy. Digital images were obtained using an Axioplan microscope equipped with a Cannon Power Shot camera A610/620, employing 10x, 20x and 40x objectives.

Statistical analyses

All the concentrations presented in the graphics of the present study are averages and their standard deviations. Significant differences were determined with Graph-prism v.4 software (GraphPad Software, Inc. CA, USA). The data of Hg concentrations in organs were analyzed using two-way analysis of variance followed by the Bonferroni post-test. Differences were considered significant when $p < 0.05$.

RESULTS AND DISCUSSION

The total Hg concentrations were determined in each organ after 24 h, 48 h, 72 h and 96 h. For the Hg bioaccumulation potential, the organ concentrations of all fishes used in the present study (at all exposure times) were considered (Figs. 1 and 2). The Hg concentrations for all organs in exposed fishes (0.6 $\mu g.g^{-1}$ $HgCl_2$) were higher than observed for the control group. The Hg accumulation pattern was testis > liver > gills > muscle (Fig. 1).

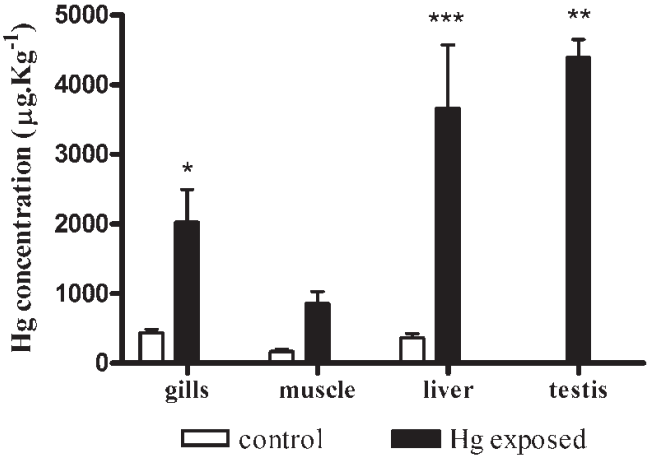

Fig 1. Hg total concentrations (µg.Kg^{-1}) in gills, muscle, liver, and testis of control and Hg-exposed (0.6 µg.g^{-1}) *G. carapo* fish. This graph presents the average of Hg concentrations in organs of fishes exposed to Hg for different exposure times (24 h, 48 h, 72 h and 96 h). The control bar for testis is not shown because it was below the limit of method detection. The statistical analyses used control testis assigned values of the detection limit (20 µg.Kg^{-1}) * $p<0.05$, ** $p<0.01$, *** $p<0.001$.

Therefore, the present study shows that even when the Hg is available over the same period for organ accumulation from the peritoneal cavity, the accumulation is differential (testis > liver > gills > muscle) and time dependent for each of the target organs. This is the result of the distinct metabolism and blood supplies of the examined organs (testis, liver, gills and muscle). It should also be noted that the blood is the main transport medium of metals in most organisms [16].

Testis and liver showed the highest Hg levels, with concentrations reaching up to 10 times higher than the values measured for the control group. The testis Hg concentrations of the control group were lower than the detection limit of the method (<20 µg.kg^{-1}). Gills and muscle of exposed fishes also showed increased Hg concentrations when compared to a control group, reaching up to four and five times the control specimen's concentrations, respectively (Fig. 1).

To evaluate Hg accumulation across the time range, Hg concentrations were analyzed in each organ after the distinct exposure times (Fig. 2). Hg accumulation in all the studied organs began with the first 24 h. The testis was the organ that showed the highest Hg accumulation over the first 24 hours and maintained the highest levels during all the following exposure times (Fig. 2). In contrast, liver showed a progressive increase in Hg concentration with exposure time, presenting the highest Hg levels after 96 h of exposure (Fig. 2). The Hg concentrations in gills and muscle showed some oscillation across the exposure times; however, the highest values for both organs also occurred in the fish exposed for 96 h (Fig. 2). These results suggest that even when the Hg was available over the same period, the Hg accumulation is differential and time dependent for all the target organs. The only exception was the testis, which did not show a clear accumulation trend (Fig.2).

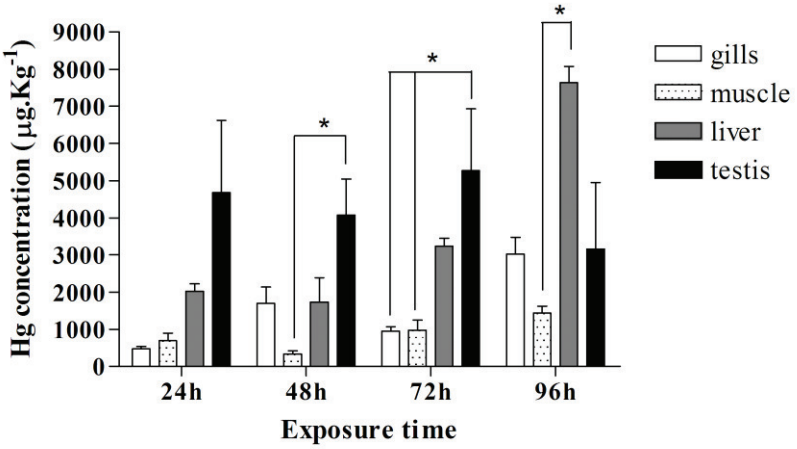

Fig 2. Hg total concentrations (µg.Kg^{-1}) in gills, muscle, and liver of *G. carapo* specimens exposed to Hg (0.6 µg.g^{-1}) for different times. Livers showed a progressive increase in Hg concentration; this pattern

was not clearly observed for the other organs. Despite having the highest bioaccumulation pattern, the testis had a slight decrease in Hg levels at 96 h. The gills did not show an increasing tendency due to a decrease in levels after 72 h of exposure. For muscle, the concentrations were similar for the different exposure times with a decrease in levels after 48 h. * $p<0.05$.

The first 24 h seems to reflect the beginning of Hg entrance. Because Hg introduction occurred via the intra-peritoneal cavity, the testis and liver, organs located in the visceral cavity, presented the highest Hg levels. The 48, 72 and 96 h exposure times most likely reflect Hg distribution by blood circulation through the organs. This is reflected in the gills and muscle, which presented a trend of increasing Hg levels with time. In gills, the higher levels, in longer exposure times, represent the Hg transport to gills, in order to be excreted. The muscle is not part of gastrointestinal absorption, therefore the muscle concentrations increased during the exposure time as due to Hg distribution through blood circulation.

To demonstrate the toxic effects of the Hg concentrations, histological observations were performed on the *G. carapo* organs. In this perspective, the morphology of testis, liver and gills were examined over the distinct exposure times (Figs. 3-5). The control and Hg-exposed fishes were healthy according to the external condition of their gills, eyes, scales, and organs. However, morphological analysis of the testis, liver and gills revealed alterations after 24 h of Hg exposure, which increased in severity over the 96 h of exposure.

The testis showed the highest Hg accumulation rate, presenting morphological alterations after 24 h of exposure onward. The untreated testicular tissue of *G. carapo* presented a characteristic organization with many spermatogenic cysts surrounded by interstitial tissue (Fig. 3A). Germ cells were present at different stages of differentiation, from undergoing cell division up to the formation of spermatozoa inside the cysts (SZ) (Fig. 3A). These observations agree with the features described in the literature by [17].

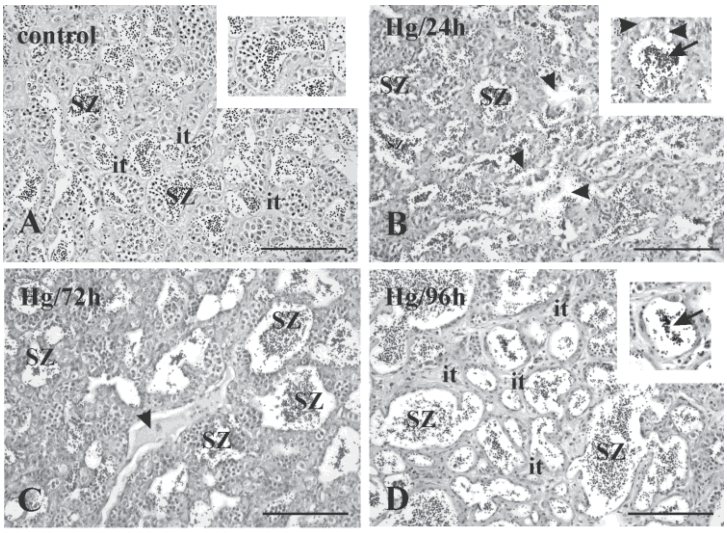

Fig 3. Light microscopy of hematoxylin and eosin (H&E) stained testis of control and Hg-exposed (0.6 $\mu g.g^{-1}$ for 24 h and 96 h) *G. carapo* fishes. (A) shows the characteristic organization of cysts surrounded by interstitial tissue (it). Germ cells typically undergo a number of cell divisions until spermatozoa (SZ) formation occurs inside the cysts. (B) shows disorganization of the cysts' arrangement (arrowheads), vacuolization of germ cells (inset, arrowheads) and sperm aggregation (inset, arrow), following 24 h of Hg exposure. (C) shows fibrosis in testicular tissue (arrowhead). (D) demonstrates the reduction of germ cells (inset), marked variations in cyst size and sperm aggregation (inset, arrow) after 96 h of Hg treatment. it= interstitial tissue, SZ= spermatozoa. Scale bar: 100 µm (x 200).

After 24 h of Hg exposure, there was a disorganization of the arrangement of the cysts (Fig. 3B, arrowheads), a vacuolization of germ cells (Fig. 3B, inset, arrowheads) and aggregation of the sperm (Fig. 3B, inset, arrow). More severe damage was observed after 72 h and 96 h of Hg treatment including fibrosis (Fig. 3C, arrowhead), a reduction in germ cells (Fig. 3C, inset), an increase in the cyst size (Fig. 3D) and sperm aggregation (Fig. 3D, inset, arrow).

The testis highest Hg accumulation potential occurred since this organ is located in the visceral cavity, where the Hg became immediately available after intra-peritoneal injection. The testis suffered progressive morphological alterations, which reflected the elevated Hg concentrations. This result is important because such damages can induce male reproductive dysfunction and impairment of both gonadal development and growth, thereby affecting fertilization success and offspring survival [18, 19]

The liver showed progressive accumulation of Hg over the exposure times and presented higher levels after 96 h of exposure. This observation is most likely related to the important role that liver has in the metabolism and excretion of toxic substances [20]; it is capable of transforming harmful compounds into

metabolites, which are excreted directly into bile for continued detoxification [21]. Accordingly, this organ is frequently used in monitoring studies [22]. Moreover, the blood that perfuses the liver comes from two sources: the major part comes from the portal vein that drains the gastrointestinal tract and the remainder comes from the hepatic artery. Therefore, as the exposure to Hg occurred from the peritoneal cavity rather than a contaminated diet, the liver showed a gradual increase in Hg concentration. This fact also explains the high accumulation in testis over the first 24 hours of exposure.

However, morphological alterations in liver were observed after 24 h, when the lowest Hg levels were measured. The untreated liver showed typical compact structure (Fig. 4A), where hepatocytes presented a characteristic cytoplasmic distribution and nuclear morphology (Fig. 4A, inset). The 24 h Hg treatment induced disorganization of hepatic tissue (Fig. 4B), with changes in hepatocyte cytoplasmic and nuclear morphology (Fig. 4B, inset). The 72 h and 96 h treatments displayed congestion of blood vessels (Fig. 4D, arrows). Areas with severe degradation of the liver parenchyma (Fig. 4C, 4D, arrowheads) were also observed, usually in close proximity to the blood circulation (Fig. 4C).

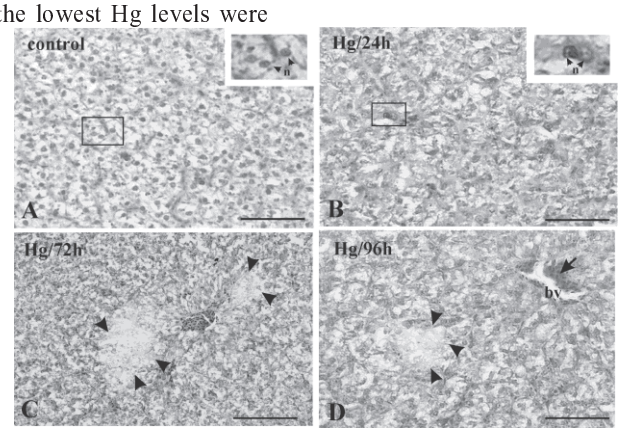

Fig 4. Light microscopy of hematoxylin and eosin (H&E) stained hepatic tissue of *G. carapo*. (A) demonstrates the compact hepatic parenchyma and the normal appe arance (inset) of hepatocytes in control fishes. (B) - (D) show the severe disorganization of hepatic tissue in $HgCl_2$ treated fishes (0.6 $\mu g.g^{-1}$). In (B), the inset shows the changes in the nuclear morphology of hepatocytes after a 24 h Hg-exposure. (C) and (D) demonstrate congestion of blood vessels (arrow) and an area with severe degradation of the liver parenchyma (arrowheads) after Hg exposure for 72 h and 96 h, respectively. n= nucleus. bv=blood vessel. Scale bar: 100 µm (x 200).

These Hg-induced alterations agree with other studies of Hg contamination in fishes [2, 6, 7]. Some of the observed changes seen in this study have also been reported after contamination with other metals [23, 24, 25, 26, 27, 28]. This trend likely indicates that the liver is a sensitive organ for the evaluation of damage after pollutant exposure [29]. However, the histological changes seen in the liver are not metal specific but are generally associated with the response of hepatocytes to toxicants [20].

In the present study, the gills showed increased levels of Hg after 96 h of exposure. Considering that Hg was provided directly to the peritoneal cavity, rather than through water contamination, gill levels reflected Hg distribution through blood circulation and Hg was likely transported to the gills in order to be excreted. However, alterations were observed in this organ at the 24 h exposure point, as observed in the testis and liver. The untreated gills showed a characteristic arrangement of primary and secondary lamellas (Fig. 5A). The gills of the 24 h and 96 h Hg-exposed fishes showed some areas with focal proliferation, occasionally resulting in fusion of adjacent secondary lamellas (arrowheads) (Figs. 5B-C). Epithelial cells also showed vacuolization after 96 h of exposure (Fig. 5C, *arrow*). Other studies examining Hg [2, 7] and others metal contaminants [28] also reported similar alterations to those described in the present study.

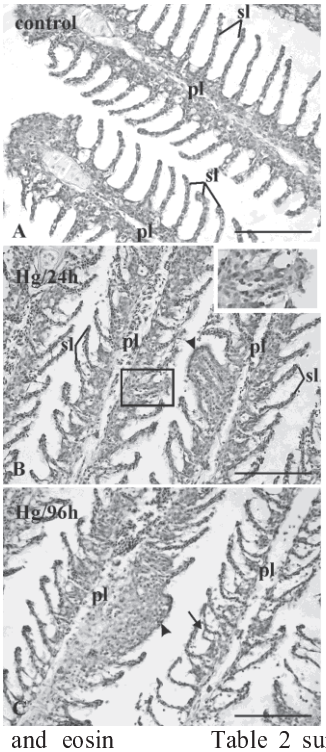

Fig 5. Light microscopy of hematoxylin and eosin (H&E) stained gills of *G. carapo*. In (A), the characteristic arrangement of primary and secondary lamellas in the gills of control fish is demonstrated. (B) and (C) show focal proliferation occasionally resulting in a fusion of adjacent secondary lamellae (arrowheads) in Hg-exposed fish (0.6 $\mu g.g^{-1}$) for 24 h and 96 h exposures, respectively. In (C), the arrow shows the vacuolization of epithelial cells in 96 h exposed fish. sl=secondary lamellae, pl=primary lamellae. Scale bar: 100 µm (x 200).

Table 2 summarizes the frequency of Hg alterations observed in testis, liver and gills of *G. caparo* in the different exposure times (24 and 96h). The histopathology was a sensitive technique for the observation of the initial damage from Hg exposure.

Table 2. Pathologies observed for each $HgCl_2$ treatment in testis, liver, and gills. A positive match means that the response was observed in all fishes submitted to each specific exposure time (n=3 fishes for each exposure time).

Alteration/ Exposure time	24h	96h
Testis		
Severe disorganization of the cysts' arrangement	+	+
Vacuolization of germ cells	+	
Reduction of germ cells		+
Sperm aggregation	+	+
Liver		
Disorganization of the hepatic tissue	+	+
Changes in hepatocytes nucleus	+	
Congestion of blood vessels		+
Areas of severe degradation of liver parenchyma		+
Gills		
Areas with focal proliferation	+	+
Fusion of adjacent secondary lamellas	+	+
Vacuolization of epithelial cells		+

Muscle showed the lowest Hg concentrations after Hg exposure, as was also observed by [2, 10]. According to [30], muscle is not in the passage route of Hg after gastrointestinal absorption; however, it seems to act as a site for Hg storage and generally shows the low Hg levels observed in the present study. Consequently, this tissue should be monitored because it is most closely associated with the risks of human Hg contamination by fish consumption [31].

CONCLUSION

The present study demonstrated the comparative Hg bioaccumulation potential of organs of tropical fish *G. caparo* after acute intra-peritoneal Hg exposure. The liver and testis showed high bioaccumulation potential followed by the gills and muscle. The differential of Hg concentration in organs was related to exposure time and the distribution of Hg through blood circulation. Histopathological analysis showed morphological alterations in testis, liver and gills of Hg-exposed fishes revealing differences in the types and severity of lesions according to increases in exposure time. These results are important in establishing a direct correlation between Hg accumulation and morphological damage, and therefore help to characterize the mechanism of Hg-induced pathogenesis. Moreover, these alterations can also be correlated with damages of target organs from fish exposed to natural Hg contamination.

ACKNOWLEDGMENTS

This work was supported by the Fundação Carlos Chagas Filho de Amparo à Pesquisa do Estado do Rio de Janeiro (FAPERJ – Proc. nº E-26/171.315/2004) (E-26/ 100.470/2007) (E-26/110.921/2008).

REFERENCES

1. Kehrig, H. A., Costa, M., Moreira, I., Malm, O., 2002. Total and methylmercury in a Brazilian estuary, Rio de Janeiro. Mar. Pollut. Bull., 44, 1018-1023.
2. Liao, C. Y., Fu, J. J., Shi, J. B., Zhou, Q. F., Yuan, C. G., Jiang, G. B., 2006. Methylmercury accumulation, histopathology effects, and cholinesterase activity alterations in medaka (*Oryzias latipes*) following sublethal exposure to methylmercury chloride. Environ. Toxicol. Pharmacol., 22, 225-233.
3. Dang, F., Wang, W. X., 2012. Why mercury concentration increases with fish size? Biokinetic explanation. Environ. Pollut., 163, 192-198.
4. Ceccatelli, S., Daréb, E., Moorsa, M., 2010. Methylmercury-induced neurotoxicity and apoptosis. Chem. Biol. Interact., 188, 301-308.
5. Malm, O., Branches, F. J. P., Akagi, H., Castro, M. B., Pfeiffer, W. C., Harada, M., Bastos, W. R., Kato, H., 1995. Mercury and methylmercury in fish and human hair from the Tapajós river basin, Brazil. Sci. Total Environ., 175, 141-150.
6. Mela, M., Randi, M. A. F., Ventura, D. F., Carvalho, C. E. V., Pelletier, E., Oliveira Ribeiro, C. A., 2007. Effects of dietary methylmercury on liver and kidney histology in the neotropical fish *Hoplias malabaricus*. Ecotoxicol. Environ. Saf., 68, 426-435.
7. Oliveira Ribeiro, C. A., Belger, L., Pelletier, E., Rouleau, C., 2002. Histopathological evidence of inorganic mercury and methyl-mercury toxicity in the arctic charr (*Salvelinus alpinus*). Environ. Res., 90, 217-225.
8. Albert, J. S., Crampton, W. G. R., Thorsen, D. H., Lovejoy, N. R., 2004. Phylogenetic systematics and historical biogeography of the Neotropical electric fish *Gymnotus* (Teleostei: Gymnotidae). Syst. Biodivers., 2, 375-417.
9. Fent, K., 2004. Ecotoxicological effects at contaminated sites. Toxicology, 205, 223-240.
10. Oliveira Ribeiro, C. A., Guimarães, D. R. J., Pfeiffer, C. W., 1996. Acumulation and distribution of inorganic mercury in a tropical fish (*Trichomycterus zonatus*). Ecotoxicol. Environ. Saf., 34, 190-195.
11. Schultz R. I., Peters L. E., Newman C. M., 1996. Toxicokinetics and disposition of inorganic mercury and cadmium in channel catfish after intravascular administration. Toxicol. Appl. Pharmacol., 140, 39-50.
12. Ferreira, A. G., Melo, E. J. T., Carvalho, C. E. V., 2003. Histological aspects of mercury contamination in muscular and hepatic tissues of *Hoplias malabaricus* (Pisces, Erytrinidae) from lakes in the north of Rio de Janeiro State, Brazil. Acta Microsc., 12, 49-54.
13. Sousa, W. P., Carvalho, C. E. V., Carvalho, C. C. V., Suzuki, M. S., 2004. Mercury and organic carbon distribution in six lakes from the north of Rio de Janeiro state. Braz. Arch. Biol. Technol., 47, 139-145.
14. Bastos, W. R., Malm, O., Pfeiffer, W. C., Cleary, D., 1998. Establishment and analytical quality control of laboratories for Hg determination in biological and geological samples in the Amazon, Brazil. Cien. Cult., 50 (4), 255-260.
15. Skoog, D. A., Leary, J. J., 1992. Principles of Instrumental Analysis. Fourth edition, Philadelphia, Saunders College Publishing, 700p.
16. Beckett, W.S., Nordberg, G.F., Clarkson, T.W., 2007. Routes of exposure, dose, and metabolism of metals. Pp. 50. In: Nordberg, G.F., Fowler, B.A., Nordberg, M., Friberg, L.T. (Eds.), Handbook on the Toxicology of Metals. Elsevier Publishing.
17. Vergilio, C.S., Moreira, R.V., Carvalho, C.E.V. and Melo, E.J.T., 2012. Characterization of mature testis and sperm morphology of *Gymnotus carapo* (Gymnotidae, Teleostei) from the southeast of Brazil. Acta Zoologica (Stockholm). In press.
18. Crump, K. L., Trudeau, V. L., 2009. Mercury-induced reproductive impairment in fish. Environ. Toxicol. Chem., 28, 895-907.
19. Friedmann AS, Watzin MC, Johnsen TB, Leiter JC., 1996. Low levels of dietary methylmercury inhibit growth and gonadal development in juvenile walleye *(Stizostedion vitreum)*. Aquat. Toxicol., 35, 265-278.

20. Hinton, D. E., Laurén, D. J., 1990. Integrative histopathological effects of environmental stressors on fishes. Am. Fish. Soc. Symp., 8, 51-66.
21. Boening, D. W., 2000. Ecological effects, transport, and fate of mercury: A general review. Chemosphere, 40, 1335-1351.
22. Mieiro, C. L., Duarte, A. C., Pereira, M. E., Pacheco, M., 2011. Mercury accumulation patterns and biochemical endpoints in wildfish (*Liza aurata*): A multi-organ approach. Ecotoxicology and Environmental Safety. Ecotoxicol. Environ. Saf., 74, 2225-2232.
23. Teh, S. J., Adams, S. M., Hinton, D. E., 1997. Histopathologic biomarkers in feral freshwater fish populations exposed different types of contaminant stress. Aquat. Toxicol., 37, 51-70.
24. Schwaiger, J., Wanke, R., Adam, S., Pawert, M., Honnen, W., Triebskorn, R., 1997. The use of histopathological indicators to evaluate contaminant-related stress in fish. J. Aquat. Ecosyst. Stress Recovery 6, 75-86.
25. Paris-Palacios, S., Biagianti-Risbourg, S., Vernet, G., 2000. Biochemical and (ultra)structural hepatic pertubations of *Brachydanio rerio* (teleostei, Cyprinidae) exposed to two sublethal concentrations of cooper sulfate. Aquat. Toxicol., 50, 109-124.
26. Ortiz, J. B., Gonzalez de Canales, M. L., Sarasquete, C., 1999. Quantification and histopathological alterations produced by sublethal copper concentrations in *Fundulus heteroclitus*. Cienc. Mar., 25, 119-143.
27. Dyk, J. C., Pieterse, G. M., Vuren, J. H. J., 2007. Histological changes in the liver of *Oreochromis mossambicus* (Cichlidae) after exposure to cadmium and zinc. . Ecotoxicol. Environ. Saf., 66, 432-440.
28. Giari, L., Manera, M., Simoni, E., Dezfuli, B. S., 2007. Cellular alterations in different organs of European sea bass *Dicentrarchus labrax* (L.) exposed to cadmium. Chemosphere, 67, 1171-1181.
29. Benett, D., Schmidt, H., Meier, W., Holm, P. B., Wahli, T., 1999. Histopathology in fish: Proposal for a protocol to assess aquatic pollution. J. Fish Dis., 22, 25-34.
30. Foster, E. P., Drake, D. L., Didomenico, G., 2000. Seasonal changes and tissue distribution of mercury in largemouth bass (*Micropterus salmoides)* from Dorena Reservour. Arch. Environ. Contam. Toxicol., 38, 78-82.
31. Régine, M. B., Gilles, D., Yannick, D., Alain, B., 2006. Mercury distribution in fish organs and food regimes: Significant relationships from twelve species collected in French Guiana (Amazonian basin). Sci. Total Environ., 368, 262-270.

Acta Zoologica

Published for The Royal Swedish Academy of Sciences and The Royal Danish Academy of Sciences and Letters

Acta Zoologica (Stockholm) **94**: 364–370 (July 2013) doi: 10.1111/j.1463-6395.2012.00569.x

Characterization of mature testis and sperm morphology of *Gymnotus carapo* (Gymnotidae, Teleostei) from the southeast of Brazil

Cristiane dos S. Vergílio,[1] Renata V. Moreira,[1] Carlos E.V. de Carvalho[2] and Edésio J. T. de Melo[1]

[1]Laboratório de Biologia Celular e Tecidual, Centro de Biociências e Biotecnologia, Universidade Estadual do Norte Fluminense, Campos dos Goytacazes, RJ, 28013-602, Brazil; [2]Laboratório de Ciências Ambientais, Centro de Biociências e Biotecnologia, Universidade Estadual do Norte Fluminense, Campos dos Goytacazes, RJ, 28013-602, Brazil

Keywords:
Banded knifefish, gymnotidae, spermatogenesis, spermatozoa, testis structure

Accepted for publication:
23 April 2012

Abstract

Vergilio, C.S., Moreira, R.V., Carvalho, C.E.V. and Melo, E.J.T. 2013. Characterization of mature testis and sperm morphology of *Gymnotus carapo* (Gymnotidae, Teleostei) from the southeast of Brazil. —*Acta Zoologica* (Stockholm) **94**: 364–370.

The present study examined the testicular structure and sperm morphology of freshwater fish *Gymnotus carapo*. Testicular structure and sperm morphology were analyzed using light, transmission and scanning electron microscopy. Anatomically, the testes weighed 0.070 ± 0.01 g and were oval with a yellow-white color. The *G. caparo* testis is organized in interstitial and tubular compartments. Spermatogenesis occurs in seminiferous tubules where the germinal epithelium is organized in spermatogenic cystis. Germ cells are seen in different stages of differentiation: type A (SPGA) and type B (SPGB) spermatogonia, primary (SPCI) and secondary (SPCII) spermatocytes, and spermatids (SPD). Differentiated spermatozoa (SZ) are seen within the cysts, characterized by a round head, a short midpiece, and a single flagellum with absence of acrosome. Spermatids were seen in the lumen of the testicular tubules together with spermatozoa, suggesting that spermatogenesis is of the semicystic type. The present study shows that *G. carapo* has an anastomosing tubular type of testis with an unrestricted distribution of the spermatogonia and semicystic type of spermatogenesis. Sperm structure follows the general pattern described for other teleostei species. These descriptions are important for a better understanding of reproductive biology and phylogeny, particularly of tropical fishes, for which data remain scarce in the literature.

Edesio J. T. Melo. Laboratório de Biologia Celular e Tecidual, Centro de Biociências e Biotecnologia, Universidade Estadual do Norte Fluminense, Av. Alberto Lamego 2000, Parque Califórnia, CEP 28013-602, Campos dos Goytacazes, RJ, Brasil. E-mails: ejtm1202@gmail.com or ejtm@uenf.br

Introduction

Characterization of mature testis and sperm morphology of fish species might not only be important in systematics and phylogeny, but also have practical applications related to artificial fertilization and sperm preservation (Furbock *et al.* 2010). Owing to the large diversity of the fish fauna, data on spermatogenic ultrastructure in teleosts are scarce and restricted to a few species (Magalhães *et al.* 2011).

Gymnotus carapo (banded knifefish) is a tropical freshwater fish, belonging to the family Gymnotidae, widely distributed in South and Central America (Albert *et al.* 2004; Lovejoy *et al.* 2010). *Gymnotus carapo* are nocturnal predators of fishes and other small aquatic animals, and most are territorial (Crampton 1998). This species is largely used in professional and sportive fishery, as live bait it is preferred by higher predator fish species. Therefore, information about its reproductive biology is important for aquaculture programs.

Although aspects of reproductive dynamics and gonadal histology of *Gymnotus* sp. has already been described in the literature (Barbieri and Barbieri 1984; Cognato and Fialho 2006; França *et al.* 2007), a detailed characterization of testis structure and sperm morphology is still needed. Therefore, the present study examined the testicular structure and sperm morphology of the freshwater fish *Gymnotus carapo*.

Materials and Methods

Fish samples

Gymnotus carapo specimens (n = 36) used in the present study were all males in same sexual maturity stage, obtained from Cima Lake, northern part of Rio de Janeiro state (21° 46′ S and 41° 31′ W). The samples were collected from October 2009 to January 2010. This sampling season was during the peak of spermatogenic activity of *G. carapo* (Barbieri and Barbieri 1984; Cognato and Fialho 2006). These animals were measured, weighed, and dissected to take testis samples that were subsequently used for the morphological studies. The gonadosomatic index was determined using the following formula (De Vlaming *et al.* 1982): GSI = (gonadal weight/total body weight) ×100.

Analysis of testis morphology

Samples of testis of sexually mature males were fixed by immersion technique in 10% neutrally buffered formalin for 24 h, dehydrated in alcohol, cleared in xylene and embedded in paraffin. Sections (5 μm) were obtained using Leica RM 2125RT microtome and stained with hematoxylin and eosin (H&E) for examination by light microscopy. Digital images were obtained using an Axioplan microscope equipped with a Cannon PowerShot camera A610/620.

Small fragments of testis were also fixed by immersion technique for 24 h in 4% formaldehyde, 2.5% glutaraldehyde, 5% sucrose in 0.1 M cacodylate buffer, pH 7.2. The material was then post-fixed in (1 : 1) 1% osmium tetroxide and 0.8% potassium ferricyanide, dehydrated with acetone, and embedded in Epon®. Semithin (0.4 μm) and ultrathin (70 nm) sections were obtained with a Reichercuts Leica ultramicrotome. Semithin sections were stained with toluidine blue (1%) and examined by light microscope described previously. Ultrathin sections were contrasted with uranyl acetate and lead citrate for a Zeiss TEM 900 transmission electron microscope.

Sperm morphology

Testes (n = 4) were minced with anatomic scissors in 2 mL of 0.1 M cacodylate buffer (pH 7.2) for 5 min at room temperature. Seminal fluid was fixed in fixative solution (4% formaldehyde, 2.5% glutaraldehyde, 5% sucrose in 0.1 M cacodylate buffer, pH 7.2), attached onto a coverslip with poly-L-lysine, post-fixed in 1% osmium tetroxide, dehydrated in ethanol, critical-point dried in CO_2 (BAL-TEC CPD 030 Critical Point Dryer), and sputtered with gold (BAL-TEC SCD 050 Sputter Coater) for observation in a Zeiss Evo 40 microscope scanning electron at 15 kV, employing secondary electrons.

Results

Gymnotus carapo testes are paired, consistent, and oval organs with a yellow-white color (Fig. 1A,B) and weighted 0.070 ± 0.01 g (n = 36). They are located in the caudal extremity of viscera (Fig. 1A) during all maturation stages. The testis is connected by spermatic ducts to the cranial region, ending in the genital papilla (Fig. 1A), under the head immediately posterior to the anus. The mean gonadosomatic index (GSI) was 0.070 ± 0.002%.

Male gonads are surrounded by tunica albuginea (Fig. 2A), which is composed of connective fibers that enter the organ interior where it forms the interstitial tissue that subdivide the testis in irregular seminiferous tubules (Fig. 2B, *inset*; Fig. 3A–C). In the interstitial compartment (it, Fig. 2B–E; Fig. 3B), blood cells (Fig. 2D, *arrowhead*), neural connections, conjunctive tissue fibers, and Leydig cells are

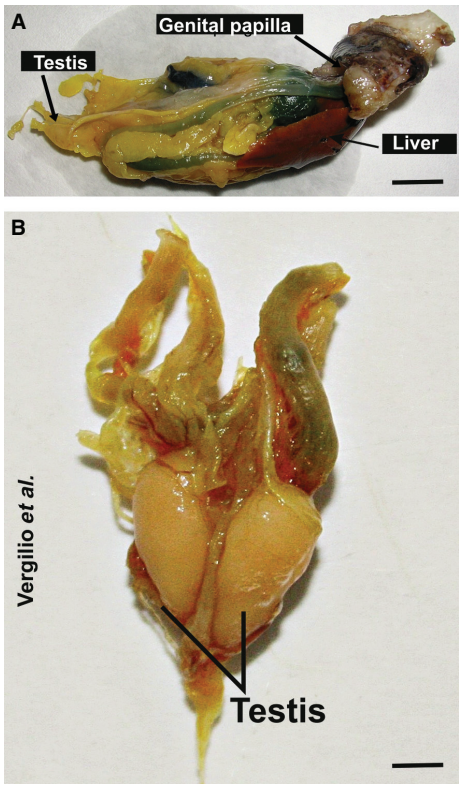

Fig. 1—General aspect of *Gymnotus carapo* testis (**A**) Testicular localization in relation to other organs (**B**) shows the paired testis with ovoid aspect. Scale bars: 1 cm.

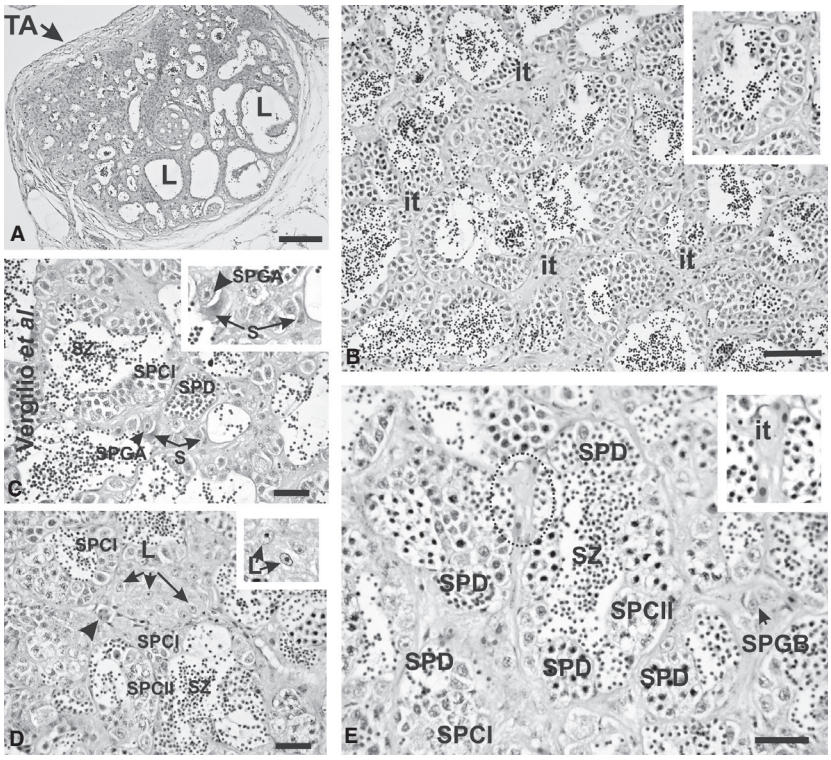

Fig. 2—Light microscopy of hematoxylin and eosin (**H&E**) stained *Gymnotus carapo* testis (**A**) Cross-section of testes surrounded by tunica albuginea (TA) (*arrow*) and lumen lobes (L) are also seen. —(**B**) Testicular organization with seminiferous lobes (*inset*) and interstitial tissue (it). —(**C**) Seminiferous lobes containing germ cells: primary spermatogonia (SGA), primary spermatocytes (SCI) and spermatids (SD). Spermatozoids (SZ) are also seen within the lobes lumen. Sertoli cells (S) are also present, supporting germ cells (*inset*). —(**D**) Interstitial tissue containing Leydig cells (L) (*inset*) also occurs between lobes and blood vessels (*arrowhead*). —(**E**) shows the arrangement of lobes surrounded by interstitial tissue (it) (*inset*). Scale bars: A: 200μm, B: 50μm (200×), **C–E**: 20μm (400×).

present. Leydig cells are large ovoid cells and usually appear in groups (Fig. 2D).

These cysts are lined by germinal epithelium containing germ cells (Fig. 2C–E, Fig. 3A,B) surrounded by Sertoli cells (Fig. 2C–E). Germ cells undergo different stages of differentiation as: type A (SPGA) and type B (SPGB) spermatogonia, spermatocytes (SPC), and spermatids (SPD) (Fig. 2C–E, Fig. 3A,B). In this cystic arrangement, the germ cells develop synchronously until sperm formation. Mature spermatozoa (SZ) can be found in the lumen of cysts (Fig. 2D,E).

For internal structure, the *G. carapo* testis has lobular type, in which the seminiferous tubules are grouped in many cysts, where spermatogenesis occurs. The tubules are anastomosing at different areas and mostly in the region of the spermatic duct. The lobular testis may also be divided into restricted and unrestricted types according to the distribution of spermatogonia (Parenti and Grier 2004). In *G. carapo* testis, the spermatogonia are unrestricted, being dispersed along the length of the lobule.

Type A spermatogonia (SPGA) are the largest cells of germ line, located in the base of germ epithelium, usually associated with Sertoli cells (Fig. 2C). SPGA have hyaline cytoplasm, a prominent nucleus, and one well-developed nucleolus that is centrally located (Fig. 2C, *inset*). Type B spermatogonia (SPGB) are characterized by a decrease in cell size compared to SPGA (Figs 3A, 2E), and differences in chromatin aggregation are also evident.

Spermatogonia divisions lead to spermatocyte formation. Spermatocytes are usually observed in different stages of the first meiotic division, being characterized as primary (SPCI) and secondary (SPCII) spermatocytes (Fig. 2C–E, Fig. 3A, B). These cells can present different degrees of nuclear material compaction (Fig. 2C–E, Fig. 3A,B). Spermatids (SPD) result from the second meiotic division and have a heterogeneous population in appearance (Fig. 2C–E, Fig. 3A,B; Fig. 4A). Owing to the spermatogenic process, there is size reduction as the nuclei become smaller, when the chromatin condenses (Fig. 4A,B). These cells were seen in the cyst (Fig. 2C–E, Fig. 3A,B) and also in the lumen (L) (Fig. 4A, B) next to the cyst periphery, in different stages of spermiation, and are recognizable by their large, darkly stained nucleus (Fig. 4A,B).

The presence of spermatids in the lumen of the testicular tubules together with spermatozoa suggests that spermatogenesis is of the semicystic type. Therefore, these cells are being released from the cysts for completion of the spermatogenic

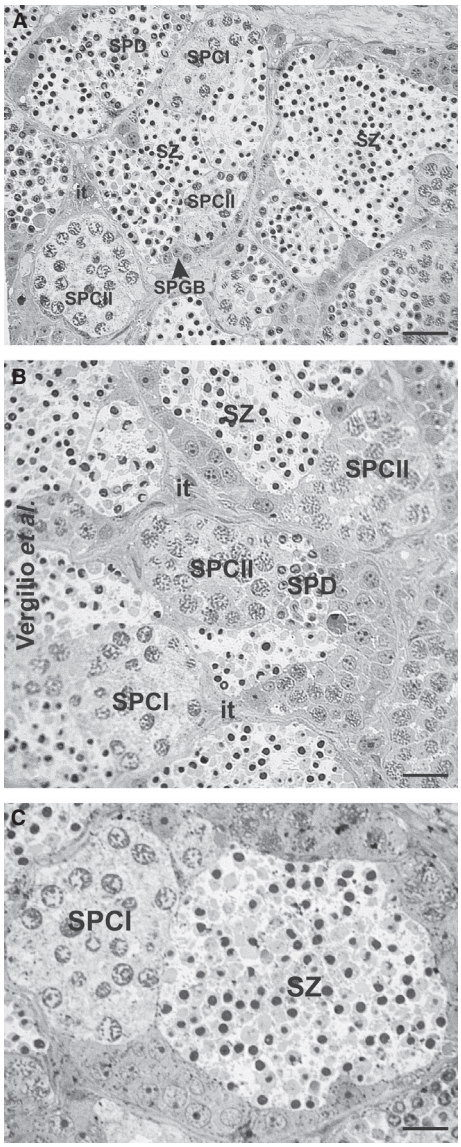

Fig. 3—Light microscopy of semithin sections of *Gymnotus carapo* testis stained with toluidine blue (**A**) shows organization of cysts connected by interstitial tissue (it) with germ cells in different stages of differentiation: Secondary spermatogonia (SGB), primary spermatocytes (SCI), secondary spermatocytes (SPCII) and spermatids (SD). Spermatozoa (SZ) are also seen within the lobes lumen. (**B**) and (**C**) also shows details of cyst arrangement. Scale bars: A–B: 20 μm (200×), C: 20 μm (400×).

process in the lumen of the seminiferous lobules. Subsequently, spermatozoa (SZ) are characterized by extraordinary nuclear compaction and cytoplasmatic reduction (Fig. 2C–E, Fig. 3A–C, Fig. 4C–F, Fig. 5).

The *G. carapo*-differentiated spermatozoa are characterized by a head, a short midpiece, single flagellum, and absence of acrosome (Fig. 4C–F, Fig. 5). The head measured about 2.3 μm in diameter and was occupied almost totally by the nucleus (Fig. 4B–F). It has an ovoid shape (Fig. 5) and contains highly electron dense chromatin, homogeneously dispersed (Fig. 4C–F). At the base of the nucleus, the nuclear envelope invaginated, forming a depression called the nuclear fossa (Fig. 4E,F *arrows*).

The midpiece is short, with ovoid mitochondria and some vesicles clustered in regions close to the plasma membrane (Fig. 4C). Inserted in the midpiece, close to the nucleus is also the centriolar complex, which is formed by proximal and distal centrioles (Fig. 4C). The flagellum is lateral and parallel to the nucleus, measuring about 26 μm in length, and has the classical 9 + 2 microtubular pattern (Fig. 4D, *inset*). It has a cylindrical shape through its length, and the flagellar membrane does not have lateral projections (Fig. 4C–E, Fig. 5).

Discussion

The determination of mature reproductive stage based in germ cells and alterations of germinal epithelium is an important tool for characterization of reproductive biology in teleosts (Grier 1981). As *G. carapo* males do not show alterations in testis external morphology, accurate identification of distinct maturation stage, knowledge of the reproductive cycle, and microscopic analysis are necessary.

In the present study, the male fish were in a mature stage as indicated by advanced spermatogenic process. According to Barbieri and Barbieri (1984), the *G. carapo* spermatogenic activity occurs throughout the year but with intensity changes, being higher from November to January and reaching a peak between October and December. *Gymnotus carapo* spring–summer reproductive cycle was also observed by Cognato and Fialho (2006) as occurring between November and March.

The testis size and GSI of mature *G. carapo* were very small throughout spermatogenic development. This feature, also observed in *Solea senegalensis* (García-López *et al.* 2005), is rare in other teleosts, which shows higher percentage of testis relative to overall body.

The ovoid external morphology of the *G. carapo* testis with two long spermatic ducts differs from the description of an elongated testis extensive through all abdominal cavity of most teleost fishes (Barbieri and Barbieri 1984). Testis organization in two compartments, the interstitial and tubular compartments, is observed in all vertebrates, from fish to mammals (Schulz *et al.* 2010). The interstitial compartment is composed of Leydig cells, blood/lymphatic vessels, macrophages and mast cells, neural and connective tissue cells (Koulish *et al.* 2002) and is continuous with the tunica albuginea, composed of fibrous tissue that surrounds the organ (Rupik *et al.* 2011).

Seminiferous tubules contain spermatogenic cysts formed by Sertoli cells that sustain synchronously developing germ cells. This cystic spermatogenesis occurs in fish and amphibians (Santos and Oliveira 2008). The morphology of different germ cell types observed for *G. carapo* is similar to those

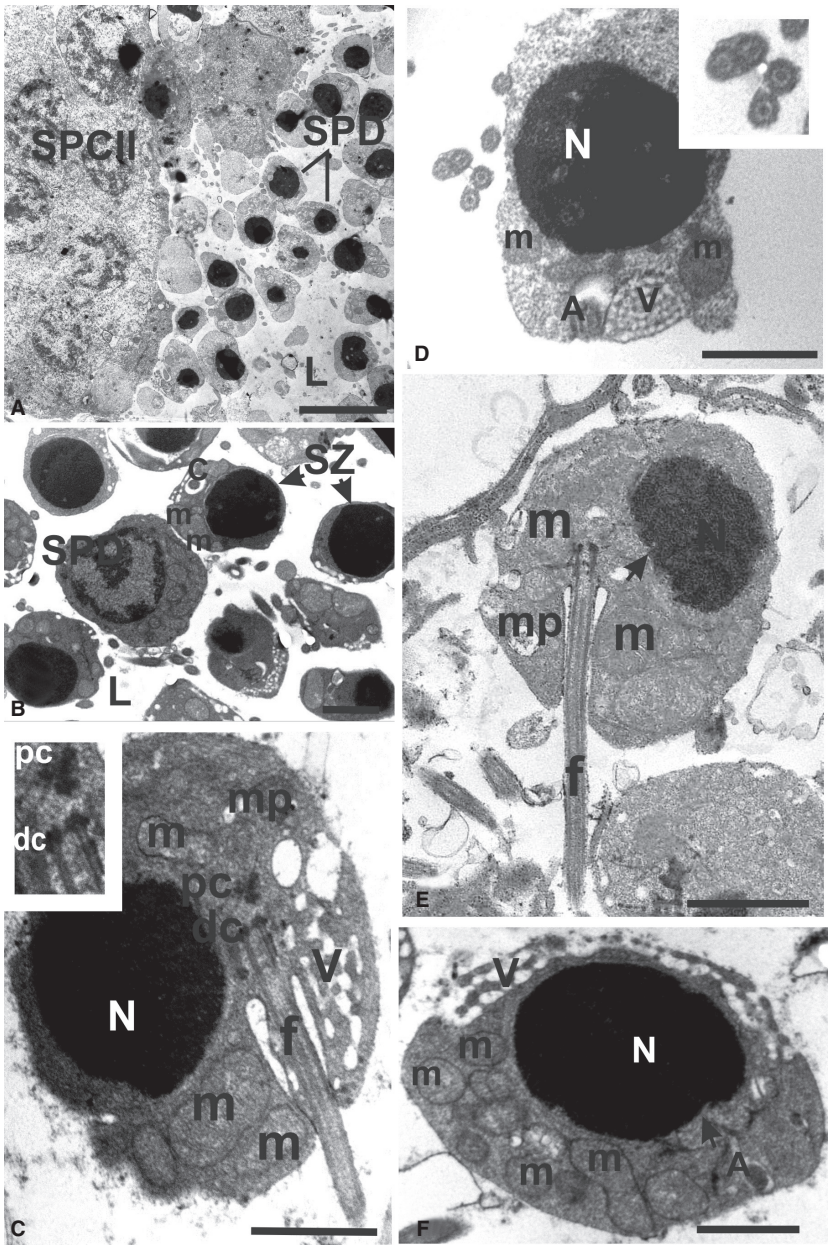

Fig. 4—Transmission electron microscopy of *Gymnotus carapo* testis. —(**A**) shows a cyst with secondary spermatocytes (SPCII) and spermatids (SPD) released in the cyst lumen (L). The presence of spermatids (SPD) together with spermatozoa (SZ) is demonstrated in (**B**). —(**C**) shows details of spermatozoa structure as the short midpiece (mp), ovoid mitochondria (m), the lateral and parallel position of the flagellum (f), the centriolar complex which is formed by proximal (pc) and distal centrioles (pd) and some vesicles (V) clustered in regions close to the plasma membrane. —(**D**) shows the axoneme (**A**) of flagellum with the classical 9 + 2 microtubular pattern (*inset*). —(**E**) shows the nuclear fossa (*arrows*) at the base of the nucleus as an invagination of the nuclear envelope forming a depression. In (**F**) is demonstrated nucleus with highly electron dense chromatin, homogeneously dispersed. N= nucleus, A= axoneme. Scale bars: A and E: 1 μm, B–D and F: 500 nm.

described for most species of teleost fish (Leal *et al.* 2009; Muñoz *et al.* 2011; Rupik *et al.* 2011).

For *G. carapo*, the presence of both spermatids and spermatozoa in the lumen of the testicular lobules suggests that spermatogenesis is of the semicystic type. Semicystic spermatogenesis is also found in different taxonomic groups, such as Characidae (*Hemigrammus marginatus*) (Magalhães *et al.* 2011), Scorpaenidae (*Scorpaena notata*) (Muñoz *et al.* 2002; Sàbat *et al.* 2009), Opheliidae (Mattei 1993; Hernández *et al.* 2005), Siluriformes (*Malapterurus electricus*) (Shahin 2006), Soleidae (*Solea senegalensis*) (García-López *et al.* 2005), Corydoradinae *(Corydoras flaveolus, Corydoras aeneus, Sclero-*

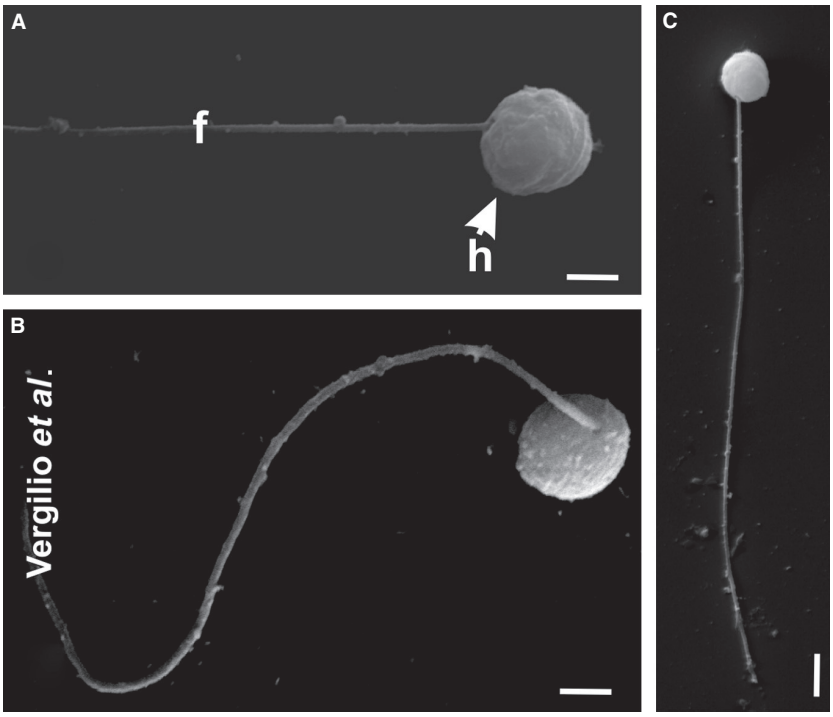

Fig. 5—Morphology of *Gymnotus carapo* spermatozoa. —(**A**–**C**) show scanning electron microscopy of sperm. Round head (H) and flagellum (F) can be seen. Scale bars: 1μm.

mystax lacerdai, Aspidoras poecilus) (Spadella *et al.* 2007), and Bleniidae (Lahnsteiner and Patzner 1990). The fact that individual spermatids from different germ cell clones proceed through spermiogenesis in the tubular lumen seems but a variation of the timing of germ cell individualization (Schulz *et al.* 2010).

The patterns of spermatozoa structure are highly conserved within taxonomic groups, thus being a powerful tool for phylogenetic analyses in fish (Jamieson 1991). Fish spermatozoa can be classified according to the external or internal mode of fertilization into two forms, aquasperm and introsperm, respectively (Jamieson 1991). *Gymnotus carapo* spermatozoa show the typical organization of externally fertilizing teleosts (Matos *et al.* 1998; Mansour *et al.* 2002; Furbock *et al.* 2010), as they have an ovoid nucleus, a small midpiece, and no acrosome. This differs from sperm of internally fertilizing fishes, which have an elongated head and a more complicated midpiece structure (Lahnsteiner *et al.* 1997).

Based on flagellum orientation and the occurrence of nuclear rotation, three types of spermiogenesis (type I, II, and III) have been described (Mattei 1970, Jamieson 1991; Schulz *et al.* 2010). In *G. caparo*, type II spermatogenesis occurs as the flagellum develops parallel to the nucleus without nuclear rotation. This type of spermatogenesis is characteristic of more derived teleosts like Perciformes, but also occurs in Characiformes (Silveira *et al.* 2006). The type II aquasperm has also been described for other gymnotiform species (França *et al.* 2007).

Conclusion

The present study shows that *G. carapo* testis and sperm structure follow the general pattern described for other teleost species. These descriptions are very important for a better understanding of reproductive biology, particularly of tropical fishes, for which data remain scarce in the literature. Moreover, it can also be helpful for this species' aquaculture programs.

Acknowledgements

This work was supported by Fundação Carlos Chagas Filho de Amparo à Pesquisa do Estado do Rio de Janeiro (E-26/171.315/2004) (E-26/100.470/2007) (E-26/110.921/2008).

References

Albert, J. S., Crampton, W. G. R., Thorsen, D. H. and Lovejoy, N. R. 2004. Phylogenetic systematics and historical biogeography of the Neotropical electric fish *Gymnotus* (Teleostei: Gymnotidae). – *Systematics and Biodiversity* **2:** 375–417.

Barbieri, C. B. and Barbieri, G. 1984. Reprodução de *Gymnotus carapo* (Linnaeus, 1758) na represa do Lobo (SP). Morfologia e histo-

logia de testículo. Variação sazonal. (Pisces, Gymnotidae). – *Revista Brasileira de Biologia* **44:** 141–148.

Cognato, D. P. and Fialho, C. B. 2006. Reproductive biology of a population of *Gymnotus* aff. *carapo* (Teleostei: Gymnotidae) from southern Brazil. – *Neotropical Ictiology* **4:** 339–348.

Crampton, W. G. R. 1998. Electric signal design and habitat preferences in a species rich assemblage of gymnotiform fishes from the upper Amazon Basin. – *Anais da Academia Brasileira de Ciência* **70:** 805–847.

De Vlaming, V. L., Grossman, G. and Chapman, F. 1982. On the use of gonadosomatic index. – *Comparative Biochemistry and Physiology* **73:** 31–39.

França, G. F., Oliveira, C. and Grassioto, I. Q. 2007. Ultrastructure of spermiogenesis and spermatozoa of *Gymnotus cf. anguillaris* and *Brachyhypopomus cf. pinnicaudatus* (Teleostei: Gymnotiformes). – *Tissue and Cell* **39:** 131–139.

Furbock, S., Patzner, R. A. and Lahnsteiner, F. 2010. Fine structure of spermatozoa of *Chondrostoma nasus* and *Rutilus meidingerii* (Teleostei, Cyprinidae), as revealed by scanning and transmission electron microscopy. – *Acta Zoologica* **91:** 88–95.

García-López, Á., Martínez-Rodríguez, G. and Sarasquete, C. 2005. Male reproductive system in Senegalese sole *Solea senegalensis* (Kaup): Anatomy, histology and histochemistry. – *Histology and Histopathology* **20:** 1179–1189.

Grier, H. J. 1981. Cellular organization of the testis and spermatogenesis in fishes. – *American Zoologist* **21:** 345–357.

Hernández, M. R., Sàbat, M., Muñoz, M. and Casadevall, M. 2005. Semicystic spermatogenesis and reproductive strategy in *Ophidion barbatum* (Pisces, Ophidiidae). – *Acta Zoologica (Stockholm)* **86:** 295–300.

Jamieson, B. G. M., 1991. Fish Evolution and Systematics: Evidence from Spermatozoa. Cambridge University Press, Cambridge.

Koulish, S., Kramer, C. R. and Grier, H. J. 2002. Organization of the male gonad in a protogynous fish, *Thalassoma bifasciatum* (Teleostei: Labridae). – *Journal of Morphology* **254:** 292–311.

Lahnsteiner, F. and Patzner, R. A. 1990. Spermiogenesis and structure of mature spermatozoa in bleniid fishes (Pisces, Bleniidae). – *Journal of Submicroscopic Cytology and Pathology* **22:** 565–576.

Lahnsteiner, F., Berger, B., Weismann, T. and Patzner, R. A. 1997. Sperm structure and motility of the freshwater teleost *Cottus gobio*. – *Journal of Fish Biology* **50:** 564–574.

Leal, M. C., Waal, P. P., López, A. G., Chen, S. X., Bogerd, J. and Schulz, R. W. 2009. Zebrafish primary testis tissue culture: An approach to study testis function *ex vivo*. – *General and Comparative Endocrinology* **162:** 134–138.

Lovejoy, N. R., Lester, K., Crampton, W. G. R., Marques, F. P. L. and Albert, J. S. 2010. Phylogeny, biogeography, and electric signal evolution of Neotropical knifefishes of the genus *Gymnotus* (Osteichthyes: Gymnotidae). – *Molecular Phylogenetics and Evolution* **54:** 278–290.

Magalhães, A. L. B., Andrade, R. F., Gomes, B. V. C., Perini, V. R., Rizzo, E. and Bazzoli, N. 2011. Ultrastructure of the semicystic spermatogenesis in the South American freshwater characid *Hemigrammus marginatus* (Teleostei, Characiformes). – *Journal of Applied Ichthyology* **27:** 1041–1046.

Mansour, N., Lahnsteiner, F. and Patzner, R. A. 2002. The spermatozoon of the African catfish: Fine structure, motility, viability and its behavior in seminal vesicle secretion. – *Journal of Fish Biology* **60:** 545–560.

Matos, E., Matos, P., Santos, M. N. S. and Azevedo, C. 1998. Aspectos morfológicos do espermatozóide de *Curimata inornata* Vari, 1989 (Pisces, Teleostei) do rio Amazonas. – *Acta Amazonica* **28:** 449–453.

Mattei, X. 1970. Spermiogenése comparé des poisson. In: Baccetti, B. (Ed.): *Comparative Spermatology*, pp. 57–72, Academic Press, New York.

Mattei, X. 1993. Peculiarities in the organization of testis of *Ophidion* sp. (Pisces: Teleostei). Evidence for two types of spermatogenesis in teleost fish. – *Journal of Fish Biology* **43:** 931–937.

Muñoz, M., Casadevall, M. and Bonet, S. 2002. Testicular structure and semicystic spermatogenesis in a specialized ovuliparous species: *Scorpaena notata* (Pisces, Scorpaenidae). – *Acta Zoologica* **83:** 213–219.

Muñoz, M. E., Batlounia, S. R., Vicentini, I. B. F. and Vicentini, C. A. 2011. Testicular structure and description of the seminal pathway in *Leporinus macrocephalus* (Anostomidae, Teleostei). – *Micron* **42:** 892–897.

Parenti, L. R. and Grier, H. J. 2004. Evolution and phylogeny of gonad morphology in bony fishes. – *Integrative and Comparative Biology* **44:** 333–348.

Rupik, W., Huszno, J. and Klag, J. 2011. Cellular organisation of the mature testes and stages of spermiogenesis in *Danio rerio* (Cyprinidae; Teleostei) – Structural and ultrastructural studies. – *Micron* **42:** 833–839.

Sàbat, M., Lo Nostro, F., Casadevall, M. and Munõz, M. 2009. A light and electron microscopic study on the organization of the testis and the semicystic spermatogenesis of the genus *Scorpaena* (Teleostei, Scorpaenidae). – *Journal of Morphology* **270:** 662–672.

Santos, L. R. S. and Oliveira, C. 2008. Histological aspects and structural characteristics of the testes of *Dendropsophus minutus* (Anura, Hylidae). – *Micron* **39:** 1266–1270.

Schulz, R. W., França, L. R., Lareyre, J. J., LeGac, F., Garcia, H. C., Nobrega, R. H. and Miura, T. 2010. Spermatogenesis in fish. – *General and Comparative Endocrinology* **165:** 390–411.

Shahin, A. A. B. 2006. Semicystic spermatogenesis and biflagellate spermatozoon ultrastructure in the Nile eletric catfish *Malapterurus electricus* (Teleostei: Siluriformes: Malapteruridae). – *Acta Zoologica* **87:** 215–227.

Spadella, M. A., Oliveira, C. and Quagio-Grassiotto, I. 2007. Comparative analyses of spermiogenesis and sperm ultrastructure in Callichthyidae (Teleostei: Ostariophysi: Siluriformes). – *Neotropical Ichthyology* **5:** 337–350.

Effects of Cadmium Exposure in Male Gonads and Sperm Structure of the Tropical Fish *Gymnotus carapo*

C. dos S. Vergilio[1], R. V. Moreira[1], L. S. Gomes[2], C. E.V. Carvalho[2] and E. J. T. Melo[1]

1. Laboratório de Biologia Celular e Tecidual, Centro de Biociências e Biotecnologia, Universidade Estadual do Norte Fluminense, Campos dos Goytacazes, 28013-602, RJ, Brasil.

2. Laboratório de Ciências Ambientais, Centro de Biociências e Biotecnologia, Universidade Estadual do Norte Fluminense, Campos dos Goytacazes, 28013-602, RJ, Brasil.

Abstract

The present study investigated the progressive effects of $CdCl_2$ in the testis and sperm of the tropical fish tuvira *Gymnotus carapo* exposed to Cd increasing concentrations (5 µM - 40 µM) for 96 h. The exposure with the increasing concentrations induced efficient accumulation of Cd in the testis; together with significantly decrease in the gonadosomatic index. Cd treatment induced disorganization of the cysts' arrangement with marked variations of the cyst size, proliferation of the interstitial tissue, infiltration of inflammatory cells, necrosis, reduction of germ cells and sperm aggregation. Exposed fishes (20 µM for 96 h) also showed reduction in sperm number and alteration in sperm morphology. These results are important for establish a direct correlation between the Cd accumulation and the incidence of damages, and help to characterize the mechanism of Cd-induced pathogenesis in the male reproductive system.

Key words: Cd, Effect, Histology, Spermatozoa, Testis

Introduction

Cadmium (Cd) is a toxic metal that can accumulate in animals and induce adverse effects (Nordberg 2009). Fishes are good indicators of aquatic pollution that can express both human and ecological health, since the fishes have a high potential for Cd accumulation and consumption of contaminated fish and seafood is one of the main source of Cd exposure to the human populations (Ju *et al*. 2012). The male reproductive system of fishes is highly vulnerable to toxicants, during the processes through which germ cells undergo a large number of cell divisions, before the release of mature spermatozoa (Bonde 2010). Alterations in testis and sperm may affect the fertilization success and alter fish populations (Crump and Trudeau 2009). Despite this known importance, little information is available concerning the mechanisms of metal-induced pathogenesis on male reproductive system of fishes (Boujbiha *et al.* 2009). In a overall way, studies describing histopathological damages in fish testis after Cd contamination events are still scarce and limited to a few species.

Therefore, the present study aimed to investigate the toxic effects of $CdCl_2$ in testes and sperm of a teleost fish *G. carapo* for elucidation of the pathological processes during exposure to a range of Cd concentrations (5 µM - 40 µM) and different exposure times (24 h - 96 h).

Materials and Methods

Gymnotus carapo specimens (n=48) used in the present study were all sexually mature males with similar sizes (length: 36.8 ±6.0 cm/ weight: 205.8 ±59.9 g) to avoid differences in treatments. The fishes were obtained from Cima Lake, in the northern region of Rio de Janeiro state (21º 46' S and 41º 31' W). Fish contamination was performed by intra-peritoneal injection (0.1 mL) with progressive $CdCl_2$ concentrations (5 µM, 10 µM, 20 µM, 30 µM, 40 µM) for 96 h. For the control group, the fishes were injected with phosphate buffered saline solution (pH 7.2). This range of doses allowed the evaluation of damages in testis, from the observation of none apparent effect until the occurrence of severe alterations, but with no induction of fish death. The fishes (n=40) were separated in five groups containing six fishes in each (one group for each concentration tested), and a control group with ten fishes. From the six fishes used for evaluation of effects in each concentration, three were used for histological analysis and the other three for Cd chemical

determination. Following the period of 96 h of exposure, the fishes were measured, weighed and dissected to obtain testis that were processed for histological preparations or frozen (-20°C) for subsequent analysis of Cd accumulation. The procedure for Cd extraction in nitric acid followed the proposed by Páez-Osuna *et al*. (1995). The samples were analyzed by atomic emission spectrophotometry with induced coupled plasma (ICP-AES, Varian, Liberty II model). The method's limit of detection (0.02 $\mu g.Kg^{-1}$) was calculated according to Skoog and Leary (1992). The gonadosomatic index was determined using the following formula (De Vlaming *et al*. 1982): GSI= (gonadal weight/total body weight) x100. The preparation of testis for the morphological analysis included the fixation in 10% buffered formalin for 24 hours, dehydration in graded series of ethanol and embedding in paraffin. Tissue sections (5 µm) were stained with hematoxylin and eosin (H&E) for examination by light microscopy. Morphological damages were measured according to the injury index described by Bernet *et al*. (1999), where testis observations were classified in three severity factors (minimal, moderate and marked pathological importance). The injury indexes were obtained after the application of a mathematical equation established for each group of lesions: (LI): LI= Σrp Σalt (a x w), where rp=reaction pattern, alt=alteration, a=score value of the alteration and w= importance factor. For evaluation of Cd effects in sperm, the testis from control fish (n=4) and those exposed to Cd (20 µM for 96 h) (n=4) were minced with anatomic scissors in 2 mL of 0.1 M cacodylate buffer (pH 7.2) for 5 minutes. After dilution, the sperm count was determined with a hemocytometer using phase contrast microscopy at x400 magnification. Sperm morphology was evaluated through scanning electron microscopy. The seminal fluid from control and contaminated fishes were fixed in fixative solution (4% formaldehyde, 2.5% glutaraldehyde, 5% sucrose in 0.1 M cacodylate buffer, pH 7.2), attached to a coverslip with poly-L-lysine, post-fixed in osmium tetroxide (1%), dehydrated in ethanol, critical-point dried, and sputtered with gold. The samples were observed in Zeiss Evo 40 scanning electron microscope at 15 kV, employing secondary electrons. Quantitative data expressed as the means and standard errors represent experimental replicates. Statistical significance was determined using GraphPad Prism v.4 software (GraphPad Software, Inc. CA, USA). One-way ANOVA followed by Tukey test was performed for comparison the results of Cd accumulation, gonadosomatic index, lesion index and sperm count between control and Cd treatments. Differences were considered with significance level of 95% ($p < 0.05$).

Results and Discussion

Treatments with increasing concentrations induced efficient accumulation of Cd in the testis (Fig. 1a). However, in the lowest dose treatments (5 µM and 10 µM), the Cd concentrations in testes were below the limit of method detection (Fig. 1a). This accumulation induced a significantly decrease in the gonadosomatic index from exposure to 10 µM concentration (Fig. 1b), accompanied by increased incidence of morphological alterations assessed through lesion index (Fig. 1c).

GSI reduction may be associated with decreases in formation or storage of testis fluids leading to reduction in organ weight and length. In the present study, the decrease in GSI index occurred together with the increase in the incidence of the morphological alterations; and both agreed in express the initial Cd toxicity in the testis of treated fishes from 10 µM exposure. However, since the histology allows the visualization of damages, expressing the severity and extension of alterations, the morphological evaluations provide a more sensitive indicator than GSI for assessing the effects of metal exposure on gonadal development (Crump and Trudeau 2009).

Testicular organization from control fishes was correlated with the already described for this species (Vergilio *et al.* 2012). The testis showed the typical cystic organization where germ cells (Fig. 2a) in different stages of differentiation are distributed as: primary (SPGI) and secondary (SPGII) spermatogonia, primary (SPCI) and secondary (SPCI) spermatocytes and spermatids (SPD). These cells undergo a number of cell divisions until the formation of spermatozoa (SZ) in the lumen of the cysts (Fig. 2a, arrows). Between the cysts is present the interstitial tissue (it), composed of Leydig cells, blood and lymphatic vessels and connective tissue (Fig. 2a).

No apparent damage occurred in the testis of fishes exposed to 5 µM concentration (Fig. 2b). However, the following doses induced progressive alterations in testicular morphology (Fig. 2 c-f) as already indicated by lesion index (Fig. 1c). Areas of proliferation of interstitial tissue (it) occurred (Fig. 2c) together with incidence of necrosis and infiltration of inflammatory cells after 10 µM treatment (Fig. 2c, square marked). The extension and severity of damage increased with the exposure to the following concentrations. Complete disorganization of the cysts' arrangement (Fig. 2d, e) with evident proliferation of the interstitial tissue (Fig. 2e), reduction of germ cells (Fig. 2e, arrows), infiltration of inflammatory cells (Fig. 2d, arrows), marked variations of cyst size (Fig. 2d) and sperm aggregation (Fig. 2d) were observed after treatments with 20 µM and 30 µM. The treatment with 40 µM concentration induced almost a complete absence of germ cells (Fig. 2e,

inset, arrow). Only a few cysts contained sperm (SZ) but they appeared in aggregates in the cyst lumen (Fig. 2e, arrowheads). The cellular alterations observed in testis of fishes exposed to this concentration (40 µM) might lead to complete organ atrophy.

Increased Cd concentrations induced higher incidence and severity of morphological damages observed in the testis of treated fishes. The index application enabled an objective assessment of the integrity of fish organs through histological investigation, expressing the alterations between normal histology of the testis and the pathological conditions, being an important tool to link the degree of pollution with the severity of induced alterations (Bernet *et al*. 1999). Few studies described alterations in fish testicular morphology following Cd treatment. The occurrence of disruption of the testicular normal architecture (Das 1988, Kumari and Dutt 1991), lobular degeneration (Kumari and Dutt 1991, Sangalang and O'Halloran 1972), reduction of germ cells (Kumari and Dutt 1991) and disappearance of spermatozoa inside the cysts (Kumari and Dutt 1991) agree with observed in the *Gymnotus carapo* fishes exposed to Cd concentrations. Moreover, the use of increasing doses in the present study allowed the documentation of the progression of Cd-induced damage in testis.

Cd also decreased (51%) the sperm number in the testis of the fishes treated with 20 µM for 96 h. Reduction in sperm number occurred together with the induction in alterations in sperm morphology. *G. carapo* sperm have an ovoid-shaped head, midpiece and flagellum as observed in the control fishes (Fig. 3b). The treatment with 20 µM induced changes in the sperm heads (Fig. 3c). There is still little information about the sperm normal morphology and the description of alterations in fish sperm parameters following metal contamination are still scarce and restricted to a few species, arising the need of further studies. However, the decrease in sperm motility documented following the Cd exposure (Chy *et al*. 2001, Dietrich *et al*. 2010) indicates the sperm vulnerability to metal exposure.

The present study showed that Cd exposure induced severe damages to the testis morphology, reduced the sperm number, and altered the sperm morphology in a tropical fish species, *Gymnotus carapo.* Cd exposure with progressive doses allowed the complete evaluation of Cd effects, since the observations were performed from the occurrence of no apparent effects, until the induction of severe damages in the testis that might lead to atrophy. These results are important for establish a direct correlation between the Cd accumulation and the incidence of damages, and help to characterize the mechanism of Cd-induced pathogenesis in the male reproductive system.

Acknowledgments

This work was supported by Fundação Carlos Chagas Filho de Amparo à Pesquisa do Estado do Rio de Janeiro (E-26/171.315/2004) (E-26/ 100.470/2007) (E-26/110.921/2008).

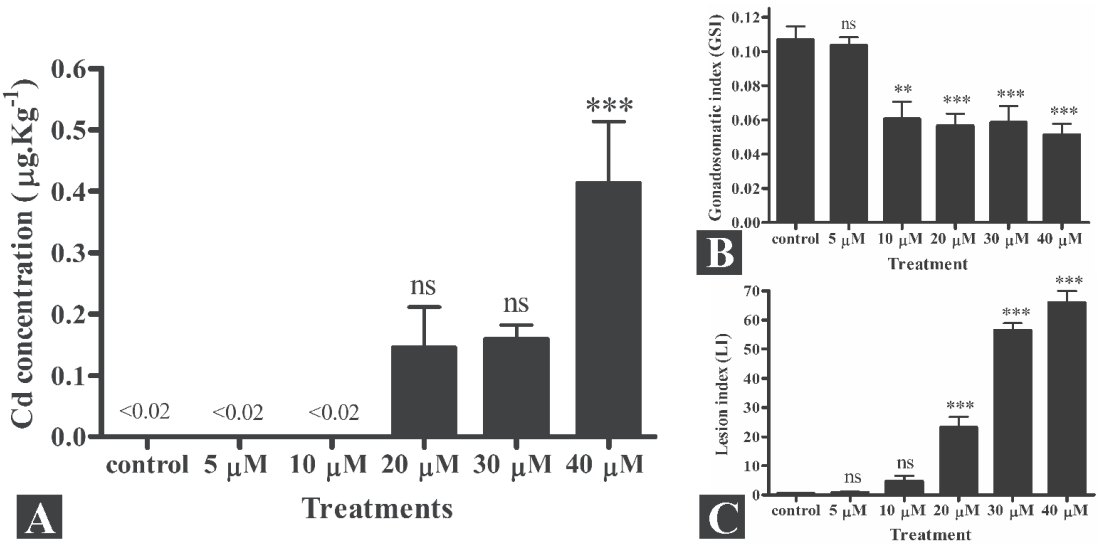

Fig 1. (a) Cd accumulation in testis of fishes exposed to progressive concentrations. In the treatments with the lower doses (5 µM and 10 M) the concentrations were bellow the limit of method detection. (b) Gonadosomatic index of fishes exposed to progressive Cd concentrations. A reduction in gonadosomatic index was observed from fishes exposed to 10 µM concentration. (c) Increased incidence of morphological alterations assessed through lesion index. ** and *** means that significance level was $p<0.01$ and $p<0.001$, respectively. ns means that difference was not significant in comparison with control.

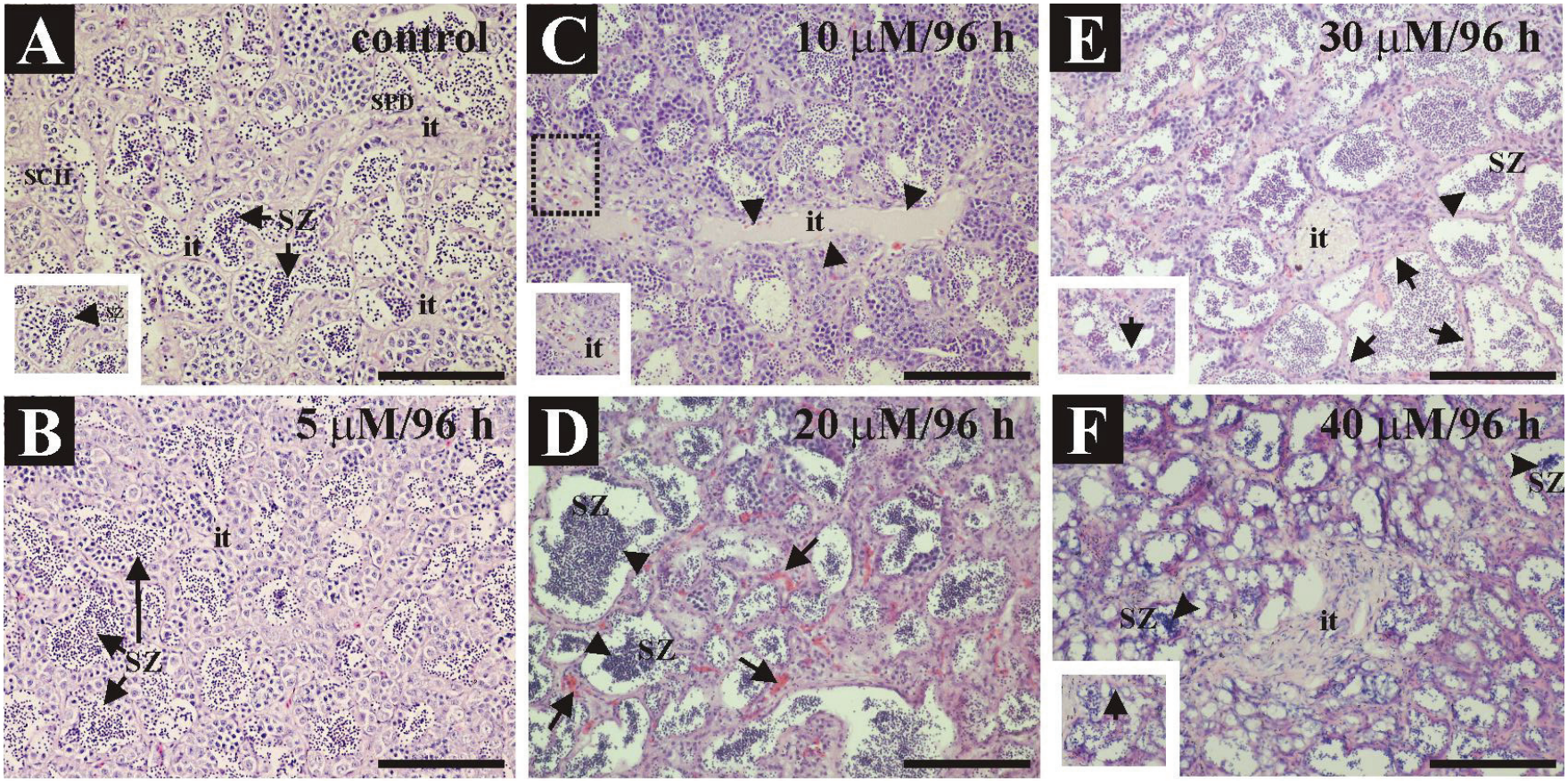
A
control
SPD
it
SCIT
SZ
it
it
SZ
C
10 µM/96 h
it
it
E
30 µM/96 h
SZ
it
B
5 µM/96 h
it
SZ
D
20 µM/96 h
SZ
SZ
F
40 µM/96 h
SZ
SZ
it

Fig 2. Testicular aspect of *Gymnotus carapo* fishes submitted to progressive Cd treatments. (a) Normal appearance of testis observed in control fishes. Germ cells in different stages are arranged in cysts where spermatogenesis occurs. Germ cells as primary spermatogonia (SGI), primary (SPCI) and secondary (SPCII) spermatocytes and spermatids (SD) occurred in cysts but only the SPCII and SPD are marked in figure. Germ cells undergo a number of cell divisions until spermatozoa (SZ) formation in the lumen of the cysts (arrows, inset). Interstitial tissue (it) is present between the cysts. (b) Typical appearance of testis observed in fishes exposed to 5 µM concentration. This treatment did not induce alteration treated fishes. (c) Areas of proliferation of interstitial tissue (it) (arrowheads, inset) occurred after 10 µM treatment. The square marked also demonstrates the incidence of necrosis and infiltration of inflammatory cells. (d) Disorganization of the cysts' arrangement together with marked variations of cyst size, infiltration of inflammatory cells (arrows) and sperm aggregation (arrowheads) occurred after 20 µM treatments. (e) Reduction of germ cells (arrows, inset), disorganization of testicular parenchyma, and proliferation of the interstitial tissue occurred following 30 µM treatment. (f) The treatment with 40 µM concentration induced almost a complete absence of germ cells (inset, arrow). Only a few cysts contained spermatozoa (SZ) but they appeared in aggregates in the cyst lumen (arrowheads). The cellular alterations observed in testis of fishes exposed to this concentration (40 µM) might lead to complete organ atrophy. Scale bars: 100 µm.

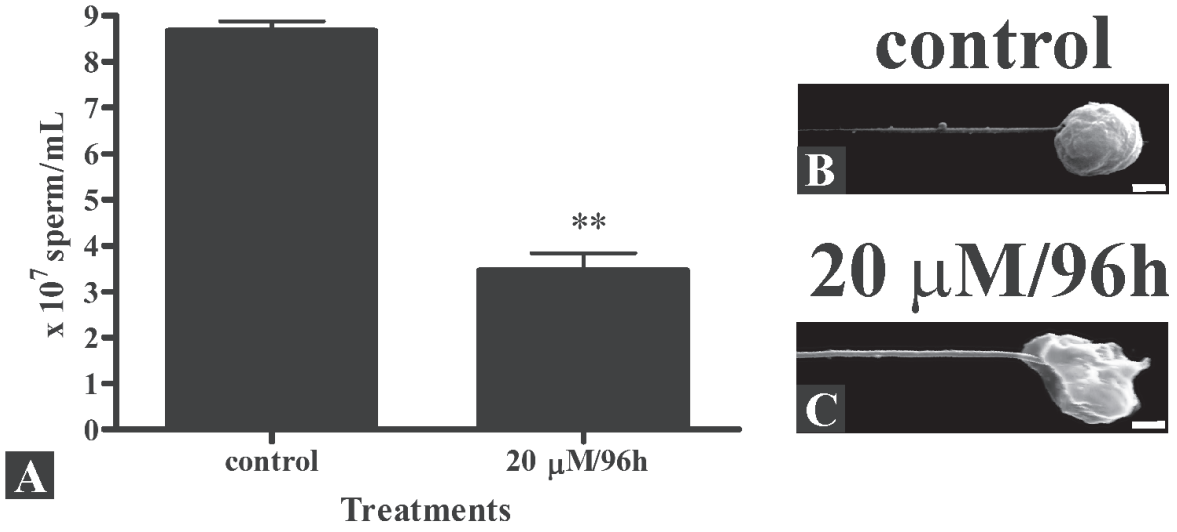

Fig 3. Effect of Cd exposure (20 μM for 96 h) observed in sperm count and morphology. (a) Cd-induced reduction in sperm count (51%). (b) Characteristic ovoid-shape aspect of spermatozoa head observed in control fishes. (c) Alteration in ovoid aspect of spermatozoa head occurred after Cd treatment. Scale bars: 1 μm. ** means that significance level was $p<0.01$.

References

Bernet D, Schmidt H, Meier W, Holm PB, Wahli T (1999) Histopathology in fish: proposal for a protocol to assess aquatic pollution. J Fish Dis 22: 25-34.

Bonde JP (2010) Male reproductive organs are at risk from environmental hazards. Asian J Androl 12: 152-156.

Boujbiha MA, Hamden K, Guermazi F, Bouslama A, Omezzine A, Kammoun A, Feki AE (2009) Testicular toxicity in mercuric chloride treated rats: Association with oxidative stress. Reprod Toxicol 28: 81-89.

Chyb J, Kime DE, Szczerbik P, Mikołajczyk T, Epler P (2001) Computer-assisted analysis (casa) of common carp *Cyprinus carpio* L. spermatozoa motility in the presence of cadmium. Arch Pol Fish 9 (2): 173-181.

Crump KL, Trudeau VL (2009) Mercury-induced reproductive impairment in fish. Environ Toxicol Chem 28: 895-907.

Das RC (1988) Cadmium toxicity to gonads in freshwater fish, *Labeo bata* (Hamilton). Arch Hydrobiol 112: 467-474.

De Vlaming VL, Grossman G, Chapman F (1983) On the use of gonadosomatic index. Comp Biochem Physiol 73: 31-39.

Dietrich GJ, Dietrich M, Kowalski RK, Doboszb S, Karol H, Demianowicz W, Glogowski J (2010) Exposure of rainbow trout milt to mercury and cadmium alters sperm motility parameters and reproductive success. Aquat Toxicol 97: 277-284

Ju YR, Chen WY, Liao CM (2012) Assessing human exposure risk to cadmium through inhalation and seafood consumption. J Hazard Mater 227-228(0): 353-361.

Kumari M., Dutt, N.H.G. (1991). Cadmium-induced histomorphological changes in the testis and pituitary gonadotrophic hormone secreting cells of the cyprinid *Puntius sarana*. B Zool 58(1): 71-76.

Nordberg GF (2009) Historical perspectives on cadmium toxicology. Toxicol Appl Pharmacol 238: 192-200.

Paez-Osuna P, Frias-Espericueta MG, Osuna-Lopez JI (1995) Trace metal concentrations in relation to season and gonadal maturation in the oyster *Crassostrea iridescens*. Mar Environ Res 40: 19-31.

Sangalang, G. B., O'Halloran, M. J. (1972). Cadmium-induced testicular injury and alterations of androgen synthesis in brook trout. Biol Reprod 240: 470-471.

Skoog DA, Leary JJ (1992) Principles of Instrumental Analysis. Saunders College Publishing, Philadelphia.

Effects of *in vitro* exposure to mercury on male gonads and sperm structure of the tropical fish tuvira *Gymnotus carapo* (L.)

C S Vergílio[1], R V Moreira[1], C E V Carvalho[2] and E J T Melo[1]

1 Laboratório de Biologia Celular e Tecidual, Centro de Biociências e Biotecnologia, Universidade Estadual do Norte Fluminense, Campos dos Goytacazes, RJ, Brasil

2 Laboratório de Ciências Ambientais, Centro de Biociências e Biotecnologia, Universidade Estadual do Norte Fluminense, Campos dos Goytacazes, RJ, Brasil

Abstract

This study investigated the progressive effects of $HgCl_2$ in the testis and sperm of the tropical fish tuvira *Gymnotus carapo* L. exposed to increasing Hg concentrations (5–30 μM) and increasing exposure times (24–96 h). Histopathology and metal concentrations in the testis were observed. Hg concentrations in the testis reached 5.1 and 5.2 μg g^{-1} in fish exposed to 20 and 30 μM of Hg, respectively. Hg effects on testicular tissue were observed even at low Hg concentrations, with no alterations in gonadosomatic index. However, the quantitative analysis of the induced alterations (lesion index) demonstrated that the Hg effects in testis became more severe after exposure to higher concentrations (20 and 30 μM) and during longer exposure (72 and 96 h), probably leading to partial or total loss of the organ function. Hg exposure (20 μM) also affected sperm count and altered sperm morphology. This study showed that $HgCl_2$ caused progressive damage to testicular tissue, reduced sperm count and altered sperm morphology. These results are important in establishing a direct correlation between Hg accumulation and severity of lesions.

Keywords: Hg effects, metal, morphology, spermatozoa, testis, tropical fish.

Correspondence *E J T de Melo, Universidade Estadual do Norte Fluminense, Centro de Biociências e Biotecnologia, Laboratório de Biologia Celular e Tecidual, Av. Alberto Lamego, 2000, Parque Califórnia, CEP 28013-602, Campos dos Goytacazes, R.J., Brasil*
(e-mail: ejtm1202@gmail.com or ejtm@uenf.br)

Introduction

Mercury (Hg) is recognized as a toxic metal with adverse effects that can even lead to the death of exposed organisms. Hg-induced toxic effects in fish have already been described in the nervous system (Baatrup 1991; Berntssen, Aatland & Handy 2003; Farina, Rocha & Aschner 2011), kidneys, liver (Mela *et al.* 2007) and gills (Oliveira Ribeiro *et al.* 2000; Rabitto *et al.* 2011). Although it is widely recognized that Hg toxicity can lead to severe deleterious health effects, little is known about the sequence of toxic effects in tissue structures during progressive metal exposure.

Fish are considered sensitive indicators of aquatic pollution and have a high potential for accumulation of both organic and inorganic forms of Hg (Gochefeld 2003). Therefore, the consumption of contaminated fish and seafood is one of the main sources of Hg exposure for human populations (Malm *et al.* 1995; Ceccatelli, Daréb & Moorsa 2010). Information regarding Hg distribution, accumulation and effects is primarily

J F D 1 2 1 4 8 B
Journal Name Manuscript No.
Dispatch: 13.6.13 Journal: JFD CE: Maheshwari B.
Author Received: No. of pages: 9 PE: Murugavel

based on temperate freshwater fish species; there still are little data on Hg exposure in tropical fish and its toxic effects in different tissues and organs (Oliveira Ribeiro, Guimarães & Pfeiffer 1996; Mela *et al.* 2007) and this is generally restricted to a small number of species. However, the Hg uptake and effects on fish physiology can change due to complex interactions with environmental factors between the ecosystems (Oliveira Ribeiro *et al.* 2000). Therefore, there is a need for studies to examine the direct toxicological effects of Hg on tissues and organs of tropical fish species.

The male reproductive system is highly vulnerable to toxicants during the processes through which germ cells undergo a large number of cell divisions before the release of mature spermatozoa (Bonde 2010). In fish, the Hg exposure can inhibit gametogenesis (Wester & Canton 1992) and change tissue morphology (Friedmann *et al.* 1996), leading to testicular atrophy (Wester & Canton 1992; Friedmann *et al.* 1996; Liao *et al.* 2006). These effects can impair both gonadal development and growth, in turn affecting offspring survival (Friedmann *et al.* 1996). Such induced alterations, when quantified, might allow an objective assessment of the degree of damages in exposed organisms (Bennet *et al.* 1999). However, a direct correlation between the levels of Hg accumulation and the severity of lesions has not been established (Falnoga *et al.* 1993; Boujbiha *et al.* 2009), and little information is available concerning the underlying mechanisms in the pathogenesis of Hg-induced male reproductive dysfunction (Boujbiha *et al.* 2009).

Sperm are useful for assessing the Hg effects on male reproductive system (Crump & Trudeau 2009). Reduction in sperm motility (Khan & Weis 1987; Rurangwa *et al.* 1998; Van Look & Kime 2003) and alterations in flagellum morphology and length (Van Look & Kime 2003; Hatef *et al.* 2011) were already demonstrated after Hg exposure. However, further investigations into sperm count and morphology are needed for different fish species, as these effects may dramatically decrease sperm performance in an aquatic environment, thereby affecting fertilization success and altering fish populations (Crump & Trudeau 2009).

The tuvira *Gymnotus carapo* (Linnaeus, 1758) is a tropical electric freshwater fish with typical carnivorous and sedentary habits, preferred by higher predator fish species (Vergilio *et al.* 2012). This species is widely distributed in South American basins (Albert *et al.* 2004) and is easily maintained under experimental conditions. These characteristics make this organism a useful model with which to evaluate toxic effects of pollutants in Brazilian ecosystems.

In this study, the toxic effects of $HgCl_2$ were investigated in the testis and sperm of *G. carapo* to elucidate the pathological processes during exposure to a range of $HgCl_2$ concentrations (5–30 μM) and different exposure times (24–96 h).

Material and methods

Fish contamination

This study was conducted in accordance with the ethics committee of the university. *Gymnotus carapo* specimens ($n = 116$) used in this study were all males at the same sexual maturity stage, defined by correlation between the total length and body weight as described by Barbieri & Barbieri (1984). The fish were obtained from Cima Lake, in the northern region of Rio de Janeiro State (21° 46′ S and 41° 31′ W). Distribution of heavy metals in the sediments and biota of Cima Lake indicated low levels of metal pollution (Ferreira, Melo & Carvalho 2003; Sousa *et al.* 2004; Jesus *et al.* 2012).

Fish were contaminated by intraperitoneal injections of $HgCl_2$ of increasing concentrations (5, 10, 20 and 30 μM). The treatment was performed with exposure to each concentration for different exposure times (24, 48, 72 and 96 h). Only a small volume (0.1 mL) of Hg solution was injected into the peritoneal cavity of fish. Phosphate-buffered saline solution (pH 7.2) was injected in fish in the control group. All fish used in this study were of similar size (length: 32 ± 1 cm/ weight: 125.8 ± 17.8 g) to avoid differences in treatments. These doses were chosen considering results from preliminary toxicity tests to induce toxic effects (dose-dependent) but to avoid fish death. Moreover, it was considered that intraperitoneal exposure offers 100% of Hg bioavailability, being important for direct dose-and-effect correlation.

Fish ($n = 108$) were divided into four groups containing 24 fish in each (one group for each concentration tested: 5, 10, 20 and 30 μM), and a control group with 12 fish. The fish exposed to each Hg concentration ($n = 24$) were dissected at

each exposure time (24, 48, 72 and 96 h), resulting in six fish for evaluation of effects in each exposure time, being three fish used for histological analysis and three for quantification of Hg. Control fish ($n = 12$) were dissected after 24 and 96 h of exposure, being six for histological evaluations and six for analysis of Hg (three fish in each exposure time). The fish were killed by reducing temperature to induce gradual decrease in swimming movements of fish (approximately 30 s, depending on the animal size) followed by decapitation. The specimens were then measured, weighed and dissected to obtain testes that were processed for morphological analysis or frozen (−20 °C) for subsequent analysis of Hg accumulation.

Gonadosomatic index (GSI)

The gonadosomatic index was determined using the following formula (De Vlaming, Grossman & Chapman 1983): GSI = (gonadal weight/total body weight) × 100.

Light microscopy

Samples of testis from control and treated fish were fixed by immersion in 10% buffered formalin for 24 h. The samples were then dehydrated in a graded series of alcohol, cleared in xylene and embedded in paraffin. The samples were sectioned at 5 μm and stained with haematoxylin and eosin (H&E) for examination by light microscopy. Additional samples of testis (approximately 1 mm^3) were also fixed in 4% formaldehyde, 2.5% glutaraldehyde, 0.1 M cacodylate buffer, 5% sucrose and 5 mM calcium chloride. These samples were then post-fixed in 1% osmium tetroxide and 0.8% potassium ferricyanide (1:1), dehydrated with acetone and embedded in Epon®. Semi-thin slices (0.4 μm) were sectioned with an ultramicrotome (Reichercuts Leica) and stained with toluidine blue (1%). For evaluation of the testis, histological analyses triplicate of each concentration and time were performed. Therefore, the results show the alterations observed in the three fish submitted to the same treatment.

Lesion Index

A lesion index proposed by Bennet *et al.* (1999) was applied to objectively estimate the histological changes or lesions in the testis of exposed fish specimens. This grading system considers the degree of damage to an organ and the importance factor of the lesions. Every alteration was assessed using a score depending on the degree and extension of the alteration as follows: 0 – unchanged; 2 – mild occurrence; 4 – moderate occurrence; 6 – severe occurrence (diffuse lesion). The lesions were also classified into three importance factors as follows: (1) minimal pathological importance, the lesion is easily reversible; (2) moderate pathological importance, the lesion is reversible in most of the cases; and (3) marked pathological importance, the lesion is generally irreversible, leading to partial or total loss of the organ function. Organ alteration was calculated according to the following lesion index (LI): $LI = \Sigma rp\ \Sigma alt\ (a \times w)$, where rp = reaction pattern, alt = alteration, a = score value of the alteration and w = importance factor. For the analysis of lesion index, the histology data from all the 54 fish used for morphological evaluation were assessed individually (six control fish + 12 fish per each concentration = 48 fish, a total of 54 fish). Therefore, the results represent an average of the histological characteristics assigned by the lesion index identified in each treatment group.

Hg quantification in the testis

Total Hg extraction from the testis was performed according to the methodology described by Bastos *et al.* (1998). Samples of control and treated testis tissue were digested with an acid mixture (H_2SO_4: HNO_3, 1:1). $KMnO_4$ solution (5%) was then added for pre-oxidation of the sample Hg^{+2}. Excess $KMnO_4$ was then reduced by the addition of NH_2OHCl (12%). For analysis, $SnCl_2$ solution was added to reduce the Hg^{+2} to Hg^0 form, allowing the quantification using ICP-AES (Varian, Liberty II model) with a cold vapour accessory (VGA-77). Analytical control blanks were prepared for each group of 10 samples. The limit of detection of the method was calculated according to Skoog & Leary (1992) and was determined to be 0.23 μg g^{-1}.

Sperm sampling

Hg effects on sperm were evaluated after 24 and 96 h of exposure to observe time-dependent effects after administration of the 20 μM concentration.

The 20 μM concentration was chosen according to previous observations of damage to the testicular tissue. Testes from control fish ($n = 4$) and those exposed to Hg at 20 μM for 24 h ($n = 2$) and 20 μM for 96 h ($n = 2$) were minced with anatomical scissors in 2 mL of 0.1 M cacodylate buffer (pH 7.2) for 5 min at room temperature. After dilution, the sperm count was determined with a haemocytometer using phase contrast microscopy at ×400 magnification.

Scanning electron microscopy

Seminal fluid from control and contaminated fishes was fixed in a fixative solution (4% formaldehyde, 2.5% glutaraldehyde, 5% sucrose in 0.1 M cacodylate buffer, pH 7.2). The samples were adhered to a coverslip with poly-L-lysine, post-fixed in osmium tetroxide (1%), dehydrated in ethanol, critical-point-dried in CO_2 (BAL-TEC CPD 030 critical point dryer) and sputtered with gold (BAL-TEC SCD 050 sputter coater) for observation in Zeiss Evo 40 scanning electron microscope at 15 kV, employing secondary electrons.

Statistical analysis

All data are expressed as means and standard errors. Statistical significance was determined using GraphPad Prism, version 4 (GraphPad Software, Inc). Data on Hg concentration were analysed using two-way analysis of variance followed by Bonferroni's test, and data on gonadosomatic index and sperm were analysed using one-way analysis of variance followed by Tukey's test. Differences were considered with significance level of 95% ($P < 0.05$).

Results

The control and Hg-exposed fishes showed gills, eyes and scales of normal external conditions. Moreover, no anatomical alterations of the gills, eyes, scales, liver, kidney and especially the testis were found before and after the experiments.

No significant difference was observed in gonadosomatic index (GSI) between control and Hg-treated fishes (Table 1), and then, further analysis of Hg effects was performed using histological observations (Figs. 1–3). The testicular tissue showed the characteristic organization of cysts in which spermatogenesis occurs (Fig. 1a). Inside the cysts, germ cells (Figs 1c,d & 2a,b) in different stages of differentiation are distributed as follows: primary (SPGI) and secondary (SPGII) spermatogonia, primary (SPCI) and secondary (SPCI) spermatocytes and spermatids (SPD). These cells undergo a number of cell divisions until sperm formation is completed inside the cysts (arrowheads) (Figs 1c,d & 2a,b). Interstitial tissue (IT), composed of Leydig cells, blood and lymphatic vessels and connective tissue, is present between the cysts (Fig. 1b). This testicular organization agrees with that already described for this species (Vergilio *et al.* 2012).

Hg treatment induced the complete disorganization of the arrangement of cysts (Figs 2c–e & 3a–f), with evident proliferation of the interstitial tissue (Figs 2c–e &3a,c) and congestion of the blood vessels (Fig. 3b). Other severe damages, including reduction in germ cells (Fig. 3d), marked variations in cyst size (Fig. 3e), interstitial and lobular disintegration (Fig. 3f), sperm aggregation (Fig. 3e) and vacuolization of germ cells (Fig. 2d), were also observed.

Importance factors were assigned for each of these alterations (Table 2), and the lesion index

Table 1 Morphology and GSI of fish used in $HgCl_2$ contamination experiments. Weight and length data are expressed in standard derivations.

	Length (cm)	Body weight (g)	Testes weight (g)	Gonadosomatic index (GSI)
Control ($n = 32$)	31	115	0.070	0.07[a]
5 μM ($n = 20$)	31	110	0.081	0.07[a]
10 μM ($n = 20$)	33	110	0.080	0.07[a]
20 μM ($n = 24$)	32	113	0.080	0.07[a]
30 μM ($n = 20$)	32	131	0.080	0.06[a]
Average	32 ± 1	115.8 ± 8.8	0.080 ± 0.005	–

Letter a indicates that there was no statistical difference in gonadosomatic index between treatments

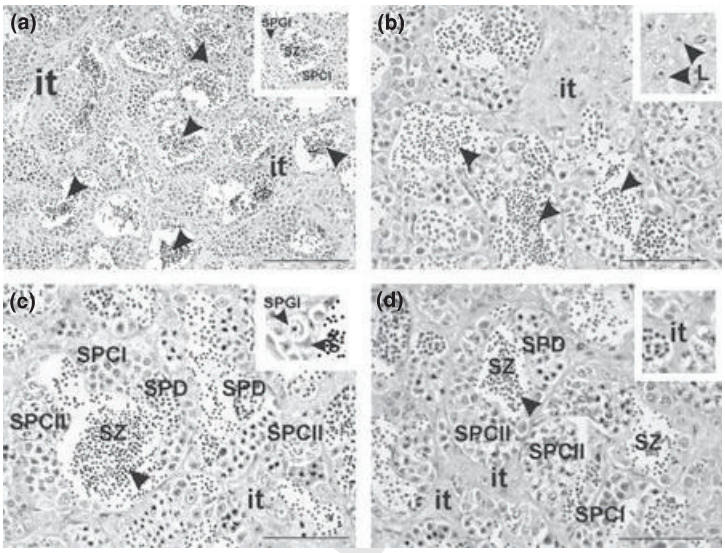

Figure 1 Light microscopy of thin (5 μm) paraffin sections of *Gymnotus carapo* testis of control fish stained with hematoxylin and eosin (H&E). (a) Cyst arrangement of germ cells (inset) and interstitial tissue (it). (b) Interstitial tissue (it) containing Leydig cells (L) (inset) occurs between cysts. (c, d) Cysts containing germ cells: primary spermatogonia (SGI), primary (SPCI) and secondary (SPCII) spermatocytes and spermatids (SD). Spermatozoids (SZ) are also observed within the lobes lumen (arrowheads). Sertoli cells (S) are also demonstrated in (c) supporting the germ cells (inset). (a–d) show Scale bars: (a) 200 μm, (b–d) 100 μm.

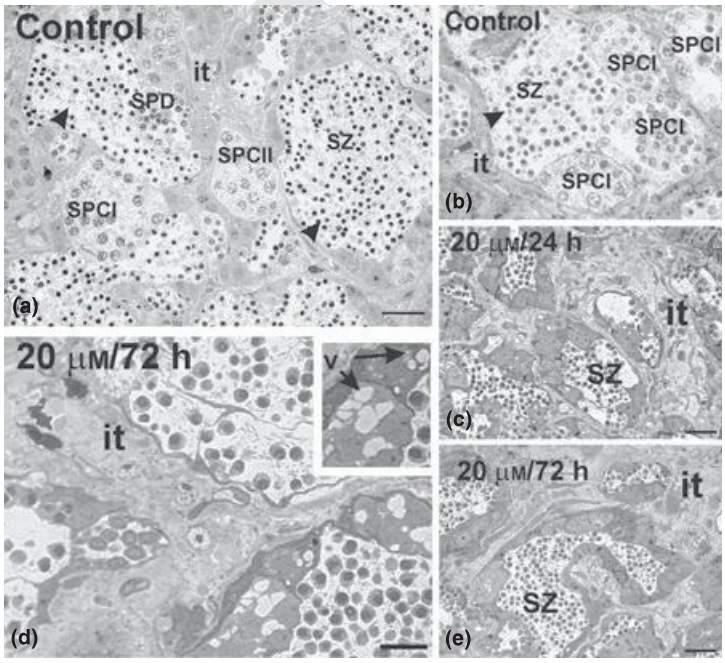

Figure 2 Light microscopy of semi-thin slices (0.4 μm) of *Gymnotus carapo* testis of control (a, b) and Hg- treated fishes (c–e) stained with toluidine blue. (a, b) Cysts containing germ cells: primary (SPCI) and secondary (SPCII) spermatocytes and spermatids (SD). Surrounding the cysts the interstitial tissue is present (it). Spermatozoids (SZ) are also observed within the lobes lumen (arrowheads). (d–e) Proliferation of interstitial tissue (it) and disorganization after Hg 20 μM treatment for 24 h (d) and 72 h (c, e). (d) Also shows vacuolization (v) of germ cells (inset). Scale bars: 20 μm.

was evaluated for each concentration tested (Fig. 4). The lesion index demonstrated the increase in the testicular damage with Hg concentration, indicating that the effects became more severe with 20 and 30 μM, probably leading to partial or total loss of the organ function. The time that fish were exposed to the Hg was also a preponderant factor for the increase in the lesion index, because higher scores were observed after longer exposure (72 h and 96 h) for almost all concentrations tested (Table 3).

Differences observed in severity of testicular damage between the concentrations tested were not so evident in the analysis of Hg content, because the fish treated with 20 and 30 μM reached the highest testicular concentrations of 5.1 and 5.2 μg g^{-1}, respectively (Table 4). On the other hand, Hg concentrations in control fish and those treated with 5 and 10 μM, although below the detection limit of the analysis method, were still able to induce morphological effect (Table 4).

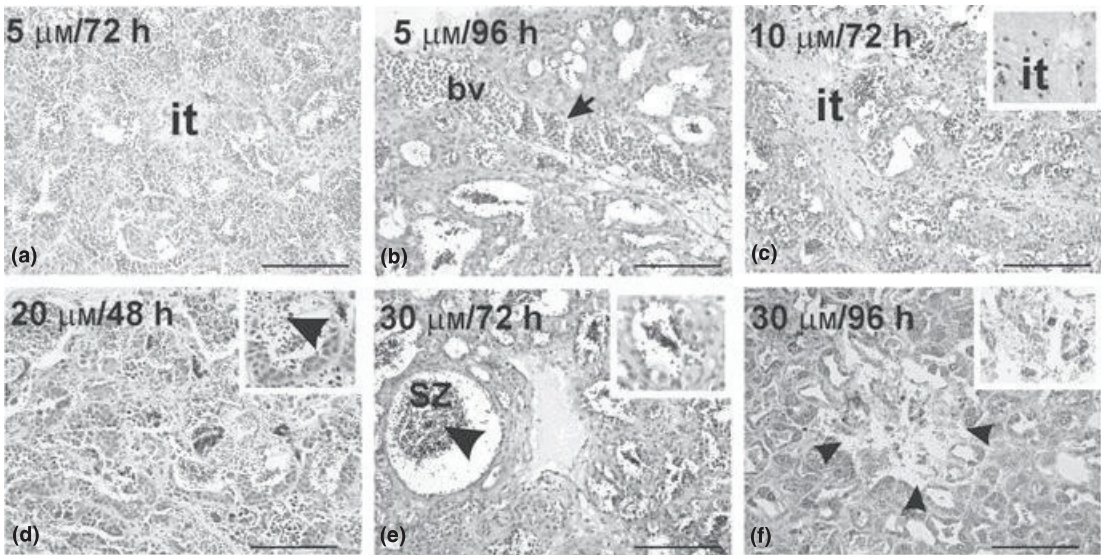

Figure 3 Light microscopy of the *Gymnotus carapo* testis from Hg – exposed fishes. The treatment with $HgCl_2$ caused dose-dependent increase in the extent and severity of the damage (a–i). (a) Disorganization of testicular arrangement is observed after treatment with 5 µM for 72 h. (b) Congestion of blood cells is evident after 5 µM for 96 h. (c) Shows the proliferation of interstitial tissue (it) (inset) after 10 µM for 72 h. (d) Treatment with 20 µM for 48 h induced tissue disorganization and reduction of germ cells (inset). (e) Marked variation in the size of the seminiferous lobules and sperm aggregation are observed after treatment with 30 µM for 72 h. (f) Severe damage to interstitial and lobular tissue is evident after treatment with 30 µM for 96 h. Scale bars: (a) 200 µm, (b–f) 100 µm.

Table 2 Histological alterations observed in different functional units of *Gymnotus carapo* testis after Hg treatments and respective importance factors (adapted from Bennet *et al.* 1999)

Functional unit	Alteration	Importance factor
Lobules	Lobular disorganization	1
Blood vessels	Congestion of blood vessels	1
Germ cells	Vacuolization of germ cells	1
Interstitial tissue	Proliferation of interstitial tissue	2
Lobules	Reduction in germ cells (lobular atrophy)	2
Lobules	Marked variation in seminiferous lobules size (lobular hypertrophy)	3
Lobules and interstitial tissue	Severe damage to interstitial and lobular tissue (necrosis)	3
Spermatozoa	Sperm aggregation	3

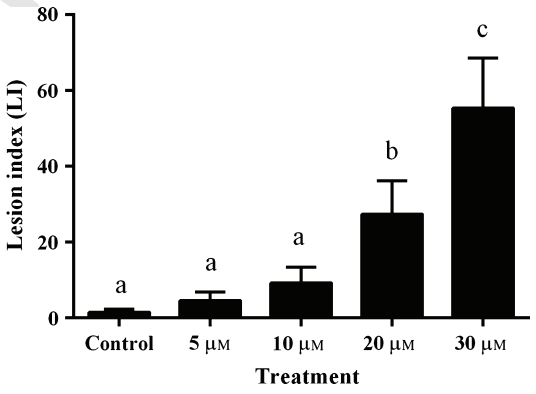

Figure 4 Differences in the lesions index (LI) among the treatments. The graph demonstrates the increase of incidence and severity of the alterations in fishes exposed to higher Hg concentrations. The letters a, b and c indicates the groups that are significantly different at $P < 0.001$.

Hg induced severe damage to testis structure and affected the germ cells that are involved in spermatogenesis. Therefore, investigations into sperm were also necessary for an overall evaluation of Hg effects in male gonads. Hg affected the sperm count (Fig. 5) in a time-dependent manner. A significant reduction (36.8%) in the sperm number was observed after treatment with 20 µM for 24 h (Fig. 5). A further reduction (48.7%) was observed in fish treated with the same concentration (20 µM) for 96 h (Fig. 5). Sperm morphology was also altered after Hg exposure (Fig. 6). *Gymnotus carapo* sperm have an ovoid-shaped head, midpiece and flagellum (Fig. 6a), as

Table 3 Differences in lesion index (LI) in fish exposed to progressive Hg concentrations and exposure times. The table demonstrates higher index scores in the testis of fish exposed for longer times

Exposure time/ Treatment	Control	5 μM	10 μM	20 μM	30 μM
24 h	0.7	2.7	7.3	20	49.3
48 h	1.3	6	12.7	24	46.7
72 h	0	4	6	32.7	53.3
96 h	0	5.3	10.7	32.7	72

Table 4 Total mercury (HgT) concentrations (μg g^{-1}) in the testis at different doses and exposure times

Treatment \concentration	5 μM	10 μM	20 μM	30 μM
Control	nd[a]	nd[a]	nd[a]	nd[a]
24 h	nd[a]	nd[a]	nd[a]	4.6 ± 3.3[b]
48 h	nd[a]	nd[a]	4.7 ± 1.7[b]	4.1 ± 1.7[b]
72 h	nd[a]	nd[a]	5.1 ± 2.5[b]	5.2 ± 2.8[b]
96 h	nd[a]	nd[a]	3.6 ± 0.7[a]	3.2 ± 1.1[a]

nd: not detected by equipment because concentrations were below the method's limit of detection. Letters a and b indicate the groups that are significantly different at 5% significance level. For statistical comparison, in the treatments that were not detected (nd) for being below limit of method detection were considered as 0.23 μg g^{-1}.

observed in control fish. The 20 μM treatments for 24 and 96 h induced changes in the sperm heads (Fig. 6b–d, *arrows*).

Discussion

The present study enhances the knowledge of the adverse effects induced by progressive concentrations of $HgCl_2$ on testicular structure, sperm count and sperm morphology in fish. The results of treatment with screening doses are important in establishing a direct correlation between Hg accumulation and the severity of lesions and in

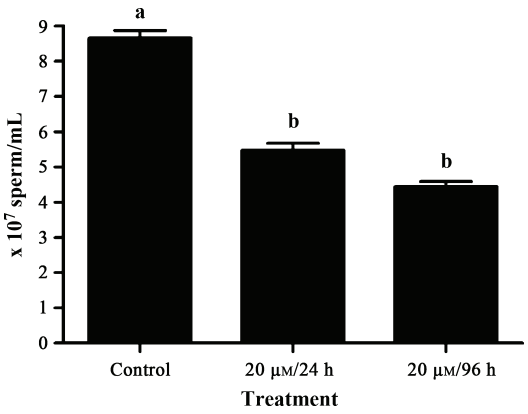

Figure 5 Effect of 20 μM Hg on sperm count after different exposure times (24 and 96 h). A reduction in sperm count was observed after 24 h (36.8%) and a subsequent reduction occurred after 96 h (48.7%). The letters a, b indicate the groups that are significantly different at $P < 0.05$.

helping to characterize the mechanism of Hg-induced pathogenesis in the male reproductive system.

During the spermatogenesis cycle, stem cells undergo many divisions until mature spermatozoa are formed. During this process, the testes increase in size, which can be measured by an increase in the gonadosomatic index (Crump & Trudeau 2009). GSI reduction was observed in catfish *Clarias batrachus* L. after exposure to organic and inorganic Hg (Kirubagaran & Joy 1992) and in walleye *Stizostedion vitreum* (Mitchill) exposed to environmentally relevant levels of organic mercury (Friedmann *et al.* 1996). In both studies, the fish were exposed over a long term (at least 45 days for *C. batrachus* and 180 days to *S. vitreum*). In the present study, the fish were exposed to maximum for 4 days, revealing severe testicular alterations even without significant changes in GSI. This demonstrates that histology may be a more

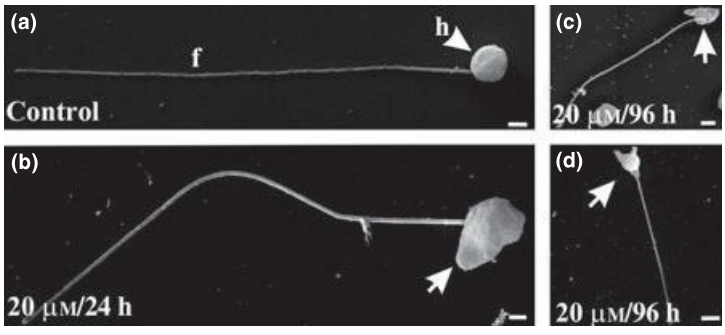

Figure 6 Ultrastructural changes of *Gymnotus carapo* spermatozoa after $HgCl_2$ treatment. (a) Spermatozoa from control fish with characteristic morphology: rounded head (h) and a long flagellum (f). (b–d) show abnormalities in the head morphology of sperm from Hg-exposed fish after treatment with 20 μM for 24 h (b) and 20 μM for 96 h (c, d). Scale bars: (a, c) 2 μm; (b, d) 1 μm.

sensitive indicator than GSI for assessing the effects of Hg on gonadal development (Crump & Trudeau 2009).

Treatment with $HgCl_2$ caused concentration-dependent increases in the extent and severity of damage observed in male reproductive system. Such severe alterations are important for understanding the biological effects of Hg on male reproductive function and the associated reproductive performance of exposed fish. Using an index enabled an objective assessment of integrity of fish organs through histological investigation, as it was clearly possible to distinguish between normal testis histology and the pathological conditions. Therefore, the present study encourages the use of histopathological indexes as a tool to link the degree of pollution with the severity of induced alterations (Bennet *et al.* 1999).

Complete disorganization of the seminiferous lobules and hyperplasia of the fibrous tissue in the tubule walls were also observed after three months of exposure to organic Hg in guppies *Poecilia reticulate* (Peters) (Wester & Canton 1992) and in medaka *Oryzias latipes* (Temminck & Schlegel) exposed for 8 days (Liao *et al.* 2006). In the present study, such changes were observed after only 96 h in treatment with highest concentrations (20 and 30 μM) of inorganic Hg.

Hg also reduced the sperm count in a time-dependent manner. A similar decrease in sperm count was observed in rodents treated with inorganic Hg (Rao & Sharma 2001; Boujbiha *et al.* 2009). These results revealed an inhibitory effect of $HgCl_2$ on spermatogenesis (Rao & Sharma 2001) and agree with severe effects observed in germ cells in the histological analyses of the testis.

Abnormalities in sperm morphology of the Hg-treated fish were documented in the present study. Organic Hg exposure also caused changes in the head of rat sperm (Silva *et al.* 2011). In perch *Perca fluviatilis L.*, agglomerated spermatozoa with a curling shape indicative of flagellar injuries (due to damage to the plasma membrane) were observed following $HgCl_2$ treatment (Hatef *et al.* 2011). Such structural effects may be the result of Hg interference with cell membrane structure. Hg also immobilizes sperm by inhibition of microtubule assembly (Rao & Sharma 2001; Crump & Trudeau 2009).

The present study showed that $HgCl_2$ caused dose- and time-dependent testicular pathology, reduced the sperm count and altered the sperm morphology in a tropical fish species *Gymnotus carapo.* Importantly, these results establish a direct correlation between the Hg accumulation and the severity of lesions. Even the treatment with low Hg doses induced morphological alterations in the testis, and the extension and severity of damage increased with higher doses.

Acknowledgements

This work was supported by Fundação Carlos Chagas Filho de Amparo à Pesquisa do Estado do Rio de Janeiro (E-26/171.315/2004) (E-26/100.470/2007) (E-26/110.921/2008).

References

Albert J.S., Crampton W.G.R., Thorsen D.H. & Lovejoy N.R. (2004) Phylogenetic systematics and historical biogeography of the Neotropical electric fish *Gymnotus* (Teleostei: Gymnotidae). *Systematics and Biodiversity* **2**, 375–417.

Baatrup E. (1991) Structural and functional effects of heavy metals on the nervous system, including sense organs, of fish. *Comparative Biochemistry and Physiology Part C Toxicology and Pharmacology* **100**, 253–257.

Barbieri C.B. & Barbieri G. (1984) Reprodução de *Gymnotus carapo* (Linnaeus, 1758) na represa do Lobo (SP). Morfologia e histologia de testículo. Variação sazonal. (Pisces, Gymnotidae). *Brazilian Journal of Biology* **44**, 141–148.

Bastos W.R., Malm O., Pfeiffer W.C. & Cleary D. (1998) Establishment and analytical quality control of laboratories for Hg determination in biological and geological samples in the Amazon, Brazil. *Ciência e Cultura* **50**, 255–260.

Bennet D., Schmidt H., Meier W., Burkhardt-Holm P. & Wahli T. (1999) Histopathology in fish: proposal for a protocol to assess aquatic pollution. *Journal of Fish Diseases* **22**, 25–34.

Berntssen M.H.G., Aatland A. & Handy R.D. (2003) Chronic dietary mercury exposure causes oxidative stress, brain lesions, and altered behavior in Atlantic salmon (*Salmo salar*) parr. *Aquatic Toxicology* **65**, 55–72.

Bonde J.P. (2010) Male reproductive organs are at risk from environmental hazards. *Asian Journal of Andrology* **12**, 152–156.

Boujbiha M.A., Hamden K., Guermazi F., Bouslama A., Omezzine A., Kammoun A. & Feki A.E. (2009) Testicular toxicity in mercuric chloride treated rats: association with oxidative stress. *Reproductive Toxicology* **28**, 81–89.

Ceccatelli S., Daréb E. & Moorsa M. (2010) Methylmercury-induced neurotoxicity and apoptosis. *Chemical Biological Interactions* **188**, 301–308.

Crump K.L. & Trudeau V.L. (2009) Mercury-induced reproductive impairment in fish. *Environmental Toxicology and Chemistry* **28**, 895–907.

De Vlaming V.L., Grossman G. & Chapman F. (1983) On the use of gonadosomatic index. *Comparative Biochemistry and Physiology* **73**, 31–39.

Falnoga I., Kregar I., Skreblin M., Tusek-Znidaric M. & Stegnar P. (1993) Interactions of mercury in rat brain. *Biological of Trace Elements Research* **37**, 71–83.

Farina M., Rocha J.B.T. & Aschner M. (2011) Mechanisms of methylmercury-induced neurotoxicity: evidence from experimental studies. *Life sciences* **89**, 555–563.

Ferreira A.G., Melo E.J.T. & Carvalho C.E.V. (2003) Histological aspects of mercury contamination in muscular and hepatic tissues of *Hoplias malabaricus* (Pisces, Erythrinidae) from lakes in the north of Rio de Janeiro State, Brazil. *Acta Microscopica* **12**, 49–54.

Friedmann A.S., Watzin M.C., Johnsen T.B. & Leiter J.C. (1996) Low levels of dietary methylmercury inhibit growth and gonadal development in juvenile walleye *(Stizostedion vitreum). Aquatic Toxicolgy* **35**, 265–278.

Gochefeld M. (2003) Cases of mercury exposure, bioavailability, and absorption. *Ecotoxicology and Environmental Safety* **56**, 174–179.

Hatef A., Alavi S.M.H., Butts I.A.E., Policar T. & Linhart O. (2011) Mechanism of action of mercury on sperm morphology, adenosine triphosphate content, and motility in *Perca fluviatilis* (Percidae; Teleostei). *Environmental Toxicology and Chemistry* **30**, 905–914.

Jesus T.B., Carvalho C.E.V., Ferreira A.G., Siqueira E.M. & Machado A.M. (2012) Mercury distribution in muscular tissues of a tropical carnivorous fish (*Hoplias malabaricus*) from four lakes in the north of Rio de Janeiro state, SE Brazil. *Journal of Brazilian Society of Ecotoxicology* **7**, 37–42.

Khan A.T. & Weis J.S. (1987) Effects of methylmercury on sperm and egg viability of two populations of killifish (*Fundulus heteroclitus*). *Archives of Environmental Contamination and Toxicology* **16**, 499–505.

Kirubagaran R. & Joy K.P. (1992) Toxic effects of mercury on testicular activity in the freshwater teleost, *Clarias batrachus. Journal of Fish Biology* **41**, 305–315.

Liao C.Y., Fu J.J., Shi J.B., Zhou Q.F., Yuan C.G. & Jiang G.B. (2006) Methylmercury accumulation, histopathology effects, and cholinesterase activity alterations in medaka (*Oryzias latipes*) following sublethal exposure to methylmercury chloride. *Environmental Toxicology and Pharmacology* **22**, 225–233.

Malm O., Branches F.J.P., Akagi H., Castro M.B., Pfeiffer W.C., Harada M., Bastos W.R. & Kato H. (1995) Mercury and methylmercury in fish and human hair from the Tapajós river basin, Brazil. *Science of Total Environment* **175**, 141–150.

Mela M., Randi M.A., Ventura D.F., Carvalho C.E., Pelletier E. & Oliveira Ribeiro C.A. (2007) Effects of dietary methylmercury on liver and kidney histology in the neotropical fish *Hoplias malabaricus. Ecotoxicology and Environmental Safety* **68**, 426–435.

Oliveira Ribeiro C.A., Guimarães J.R.D. & Pfeiffer W.C. (1996) Accumulation and distribution of inorganic mercury in a tropical fish (*Trichomycterus zonatus*). *Ecotoxicology and Environmental Safety* **34**, 190–195.

Oliveira Ribeiro C.A., Pelletier E., Pfeiffer W.C. & Rouleau C. (2000) Comparative uptake, bioaccumulation, and gill damages of inorganic mercury in tropical and nordic freshwater fish. *Environmental Research* **83**, 286–292.

Rabitto I.S., Bastos W.R., Almeida R., Anjos A., Holanda I.B.B., Galvão R.C.F., Neto F.F., Menezes M.L., Santos C.A.M. & Ribeiro C.A.O. (2011) Mercury and DDT exposure risk to fish-eating human populations in Amazon. *Environmental International* **37**, 56–65.

Rao M.V. & Sharma P.S.N. (2001) Protective effect of vitamin E against mercuric chloride reproductive toxicity in male mice. *Reproductive Toxicology* **15**, 705–712.

Rurangwa E., Roelants I., Huyskens G., Ebrahimi M., Kime D.E. & Ollevier F. (1998) The minimum effective spermatozoa: egg ratio for artificial insemination and the effects of mercury on sperm motility and fertilization ability in *Clarias gariepinus. Journal of Fish Biology* **53**, 402–413.

Silva D.A.F., Teixeira C.T., Scarano R., Favareto A.P., Fernandez C.D.B., Grotto D., Barbosa F. Jr & Kempinas W.G. (2011) Effects of methylmercury on male reproductive functions in Wistar rats. *Reproductive Toxicology* **31**, 431–439.

Skoog D.A. & Leary J.J. (1992) *Principles of Instrumental Analysis*, 4th edn. Saunders College Publishing, Philadelphia, PA.

Sousa W.P., Carvalho C.E.V., Carvalho C.C.V. & Suzuki M.S. (2004) Mercury and organic carbon distribution in six lakes from the north of Rio de Janeiro state. *Brazilian Archives of Biology and Technology* **47**, 139–145.

Van Look K.J.W. & Kime D.E. (2003) Automated sperm morphology analysis in fishes: the effect of mercury on goldfish sperm. *Journal of Fish Biology* **63**, 1020–1033.

Vergilio C.S., Moreira R.V., Carvalho C.E.V. & Melo E.J.T. (2012). Characterization of mature testis and sperm morphology of *Gymnotus carapo* (Gymnotidae, Teleostei) from the southeast of Brazil. *Acta Zoologica (Stockholm)* **????**, ????–????. In press. 8

Wester P.W. & Canton J.H. (1992) Histopathological effects in *Poecilia reticulate* (guppy) exposed to methyl mercury chloride. *Toxicology Pathology* **20**, 81–92.

Received: 18 January 2013
Revision received: 19 May 2013
Accepted: 28 May 2013

DISCUSSÃO

Os metais cádmio e mercúrio foram capazes de induzir efeitos nos exemplares de *Gymnotus carapo*, modificando a estrutura de diversos órgãos dos peixes, como o rim, fígado, brânquias e testículo, através de ação em diversos alvos intracelulares, como a mitocôndria, núcleo, lisossomos, retículo endoplasmático e citoesqueleto. Muitas das alterações observadas no presente estudo podem comprometer a saúde e a sobrevivência dos organismos expostos, se tal exposição ocorrer no ambiente natural.

A realização dos experimentos em laboratório foi importante para a observação dos efeitos nocivos do cádmio e mercúrio, na ausência de ações sinérgicas ou antagônicas que podem ocorrer com outros elementos do ambiente. Os bioensaios de contaminação em laboratório oferecem ainda a vantagem da avaliação da toxicidade dos metais pesados em concentrações específicas, facilitando a observação das relações dose/resposta dos organismos expostos **(Nodberg & Fowler, 2007).**

A utilização de ampla faixa de concentrações e tempos de exposição crescentes auxiliaram no entendimento da progressão tóxica dos efeitos do cádmio e mercúrio. Desde níveis sem efeitos adversos aparentes, até severas alterações capazes de induzir morte celular e atrofia testicular. Além disso, a aplicação de índices histopatológicos permitiu uma avaliação objetiva da integridade dos órgãos dos peixes, expressando as alterações entre a morfologia normal e as condições patológicas de forma quantitativa e uma correlação entre as concentrações utilizadas e a gravidade das alterações observadas **(Bernet *et al.*, 1999).**

A utilização de ambos os metais na forma de cloreto, possibilitou comparações toxicológicas dos seus efeitos, uma vez que a forma química pode afetar diretamente a solubilidade, absorção e toxicidade dos compostos metálicos **(Bjerregaard & Andersen, 2007)**. A presença do radical metil ao metilmercúrio confere uma maior reatividade e toxicidade ao composto. Com isso, os efeitos da exposição ao mercúrio orgânico podem ser observados em concentrações pelo menos 10 vezes inferior comparado ao inorgânico **(Boening, 2000).** No entanto, é relevante o estudo dos efeitos dos compostos inorgânicos, já que esses podem ser diretamente absorvidos pelos organismos aquáticos **(Morel *et al.*, 1998)**, e além disso, as formas do mercúrio podem interconverter no

ambiente aquático **(Bisinoti & Jardim, 2004),** com todas elas apresentando sua toxicidade intrínseca **(Berlin *et al*., 2007).**

- Efeitos comparativos do cádmio e mercúrio em cultura de células HuH-7

O tratamento com cádmio e mercúrio induziu efeitos similares em cultura de células HuH-7, ocasionando decréscimo na viabilidade celular e severos danos a morfologia celular que culminaram na morte celular por apoptose e autofagia. As progressivas concentrações e tempos de exposição auxiliaram no entendimento do processo de toxicidade desses metais nas células HuH-7.

O cádmio e mercúrio atuaram simultaneamente em múltiplos alvos intracelulares, sendo observadas disfunções na mitocôndria, retículo endoplasmático, lisossomos, compartimentos ácidos e componentes do citoesqueleto. Alguns estudos já descreveram a participação das organelas celulares individualmente na indução de morte celular **(Cannino *et al*., 2009; Fotakis *et al*., 2005; Faverney *et al*., 2004; Marchi *et al*., 2004; L'Azou *et al*., 2002)**, no entanto, o presente estudo reforça que esses alvos estão sendo afetados ao mesmo tempo e assim contribuem para uma disfunção generalizada da maquinaria celular.

Poucos estudos demonstraram a indução de autofagia após a exposição ao cádmio **(Gioacchino *et al*., 2008; Dong *et al*., 2009; Yang *et al*., 2009; Wang *et al*., 2008; Wang *et al*., 2009; Chargui *et al*., 2011; Lim *et al*., 2010; Son *et al*., 2011)** e mercúrio **(Chatterjee *et al*., 2012**; **Chatterjee *et al*., 2013).** A autofagia estaria ocorrendo como um processo inicial de reparo para remoção das organelas defeituosas **(Gioacchino *et al*., 2008)**, no entanto como diversos sítios intracelulares são afetados após a exposição ao cádmio e mercúrio, a capacidade de reparo celular é ultrapassada, levando a um processo de morte celular por autofagia **(Templeton & Liu, 2010).**

- Acumulação de cádmio e mercúrio nos diferentes órgãos do peixe Gymnotus carapo

Os metais cádmio e mercúrio foram eficientemente acumulados nos diferentes órgãos dos peixes *Gymnotus carapo* submetidos à exposição intraperitoneal. O padrão de acumulação dos peixes tratados com cádmio (fígado > rim > brânquias > testículo >

músculo) foi distinto do observado nos peixes tratados com mercúrio (testículo > fígado > brânquias > músculo).

O elevado potencial de acumulação observados no rim e fígado após o tratamento com cádmio, e no fígado após a exposição ao mercúrio é reflexo do elevado aporte sanguíneo desses órgãos, necessário para a execução das suas funções no metabolismo dos peixes **(Barron *et al*., 1987)**. No presente estudo, como a via de exposição intraperitoneal foi utilizada, as concentrações observadas nas brânquias são um reflexo da redistribuição dos íons de cádmio e mercúrio pela circulação sanguínea para sua excreção. O músculo recebe um menor aporte sanguíneo, não sendo um órgão indicado para avaliação de contaminações recentes **(Foster *et al*., 2000; Vergilio *et al*., 2012a)**. No entanto, as concentrações do músculo devem ser avaliadas por ser uma das principais vias de exposição humana **(Régine *et al*., 2003)**. Os altos níveis de cádmio e principalmente de mercúrio observados no testículo, desde 24 h de exposição, são um reflexo da via de exposição (intraperitoneal) que foi empregada, uma vez que esse órgão se encontra localizado nessa cavidade. O diferente padrão de acumulação observado no testículo após exposição ao cádmio e mercúrio é um indicativo da existência de mecanismos distintos de absorção desses metais nesse órgão.

O fígado apresentou um potencial de acumulação mais elevado para o mercúrio, sendo observado um incremento das concentrações desse metal cerca de 10 vezes em relação ao controle. No caso do cádmio, uma acumulação um pouco inferior (7 vezes) foi observada no fígado. Após a exposição dos peixes com a mesma dose (30 µM) dos diferentes metais, o mercúrio foi mais eficientemente acumulado no fígado do que o cádmio, permanecendo retido nesse órgão, mesmo após 96 h de exposição. Esse padrão crescente das concentrações de mercúrio não ocorreu após o tratamento com cádmio, uma vez que foi observada uma tendência de redução das concentrações no fígado e nos outros órgãos analisados. Em relação as brânquias, o mercúrio induziu um incremento de 4 vezes as concentrações em relação ao controle. No caso do cádmio, um aumento superior, de 7 vezes os níveis do controle foi observado. Esses resultados demonstram que o cádmio e mercúrio possuem uma toxicocinética distinta no organismo (envolve os processos de absorção, a distribuição, o armazenamento, a biotransformação e a excreção das substâncias químicas). Isso pode ocorrer em função de diferenças nas interações desses íons com moléculas endógenas, que estaria afetando a sua permanência no organismo.

A alta afinidade com grupamentos sulfidrila reduz a possibilidade desses metais existirem na forma livre no organismo **(Bridges & Zalups, 2005; Berlin *et al*., 2007).** Íons de cádmio e mercúrio se ligam a moléculas de baixo peso molecular que possuem o grupamento sulfidrila, como a metalotioneína (MT) e glutationa (GSH). Esses íons também podem se ligar a albumina e alguns aminoácidos como a cisteína, formando compostos miméticos a fim de serem transportados **(Zalups, 2000)**. O cádmio pode ainda ser um mimético iônico do cálcio, em função da similaridade dos seus raios iônicos, com isso, processos responsáveis pelo efluxo de cálcio também podem estar facilitando a saída dos íons de cádmio dos diferentes órgãos **(Zalups and Ahmad, 2003)**. A presença e atividade de proteínas transportadoras de membrana específicas também podem influenciar diretamente a taxa de eliminação de mercúrio e cádmio nos diferentes órgãos **(Kleinow *et al*., 2008)**.

- *Efeito comparativo da exposição ao cádmio e mercúrio no testículo de Gymnotus carapo*

A exposição com progressivas doses e tempos de exposição ao cádmio e mercúrio possibilitou uma avaliação da evolução dos danos no testículo do peixe *Gymnotus carapo*. Os danos morfológicos observados no parênquima testicular, juntamente com redução do número e alteração estrutural dos espermatozóides podem afetar diretamente a reprodução e a sobrevivência da prole dos peixes se submetidos a tal contaminação.

Danos testiculares mais severos foram observados após a exposição ao mercúrio, desde o tratamento com a concentração de 5 μM, mesmo apresentando concentrações inferiores ao limite do equipamento (<0,23 $\mu g.g^{-1}$). Em relação ao tratamento com cádmio, essa concentração não induziu alterações aparentes na estrutura testicular. Esse efeito diferencial também é um indicativo da existência de mecanismos distintos de absorção e retenção no testículo.

O tratamento com cádmio induziu um decréscimo significativo do índice gonadossomático, o que não foi observado após o tratamento com mercúrio. Com isso, o cádmio poderia estar afetando a formação ou o armazenamento de fluidos do testículo, levando a uma redução no peso e comprimento desse órgão **(Friedmann *et al*., 1996)**. Porém, a observação de alterações morfológicas após o tratamento com mercúrio, mesmo na ausência de mudanças no índice gonadossomático indicam que a

histopatologia é uma ferramenta mais sensível na avaliação dos efeitos da exposição aos metais no desenvolvimento das gônadas **(Crump and Trudeau, 2009)**.

A elucidação dos danos progressivos nos testículos possibilita uma avaliação do processo de toxicidade induzido pelo cádmio e mercúrio nesse órgão. Esse conhecimento traz a perspectiva da avaliação dos órgãos reprodutores nos programas de monitoramento das condições ambientais, pois além de se apresentarem sensíveis à exposição aos metais, podem ser um indicativo do sucesso reprodutivo das espécies.

CONCLUSÕES

No presente estudo foi possível avaliar os efeitos progressivos a exposição ao cádmio e mercúrio em linhagem hepatoma humano (células HuH-7) e nos diferentes tecidos do peixe tropical *Gymnotus carapo*.

O cádmio e mercúrio são capazes de induzir danos estruturais e funcionais em diversas organelas celulares, sendo a diminuição da funcionalidade mitocondrial, acidificação citoplasmática, disfunções do microfilamento e do reticulo endoplasmático os principais processos envolvidos na indução da morte celular por apoptose e autofagia.

Os metais cádmio e mercúrio foram eficientemente acumulados nos órgãos dos peixes *Gymnotus carapo* submetidos à exposição intraperitoneal, sendo o padrão de acumulação dos peixes tratados com cádmio (fígado > rim > brânquias > testículo > músculo) distinto do observado nos peixes tratados com mercúrio (testículo > fígado > brânquias > músculo). O padrão de acumulação entre os órgãos expressa o diferente aporte sanguíneo e funções exercidas por esses órgãos no metabolismo dos peixes. Além disso, a maior tendência de retenção do mercúrio nos órgãos mesmo após 96 h de exposição em comparação ao cádmio indica que existem diferenças na toxicocinética desses metais.

A exposição dos peixes com progressivas doses e tempos de exposição possibilitou uma avaliação da evolução dos danos no testículo do peixe *Gymnotus carapo,* desde níveis sem efeitos adversos aparentes, até a indução de severas alterações capazes de induzir morte celular e atrofia testicular. Os danos morfológicos observados no parênquima testicular, juntamente com redução do número e alteração estrutural dos espermatozóides podem afetar diretamente a reprodução e a sobrevivência da prole dos peixes se submetidos a tal contaminação.

O presente estudo auxilia no entendimento da progressão dos efeitos tóxicos do cádmio e mercúrio à nível celular e tecidual, possibilitando a identificação dos principais alvos intracelulares e danos nos distintos órgãos dos peixes expostos. As alterações observadas nos exemplares tratados de *Gymnotus carapo* aumenta o conhecimento da histopatologia dos peixes tropicais e traz a perspectiva dessas alterações morfológicas serem empregadas como um indicador adicional de contaminação de peixes no ambiente natural, sendo uma ferramenta sensível a presença de agentes estressores.

REFERÊNCIAS

Albert, J. S., Crampton, W. G. R., Thorsen, D. H., & Lovejoy, N. R. (2004). Phylogenetic systematics and historical biogeography of the Neotropical electric fish Gymnotus (Teleostei: Gymnotidae). *Systematics and Biodiversity, 2*(04), 375-417. doi: doi:10.1017/S1477200004001574

Amuro, Y., Kudo, K., Aoki, E., Ueki, N., Hada, T., Uchida, K., & Higashino, K. (1994). Bile acid synthesis by the HuH-7 cell line derived from a human hepatocellular carcinoma. *International Hepatology Communications, 2*(1), 21-28. doi: http://dx.doi.org/10.1016/0928-4346(94)90005-1

Baatrup, E. (1991). Structural and functional effects of heavy metals on the nervous system, including sense organs, of fish. *Comparative Biochemistry and Physiology Part C: Comparative Pharmacology, 100*(1–2), 253-257. doi: http://dx.doi.org/10.1016/0742-8413(91)90163-N

Barbieri, G., & Barbieri, M. C. (1984). Note on nutritional dynamics of Gymnotus carapo (L.) from the Lobo Reservoir, São Paulo State, Brazil. *Journal of Fish Biology, 24*(4), 351-355. doi: 10.1111/j.1095-8649.1984.tb04807.x

Barron, M. G., Tarr, B. D., & Hayton, W. L. (1987). Temperature-dependence of cardiac output and regional blood flow in rainbow trout, Salmo gairdneri Richardson. *Journal of Fish Biology, 31*(6), 735-744. doi: 10.1111/j.1095-8649.1987.tb05276.x

Berlin, M., Zalups, R. K., & Fowler, B. A. (2007). Chapter 33 - Mercury. In F. N. Gunnar, A. F. Bruce, N. Monica, B. A. F. M. N. Lars T. FribergA2 - Gunnar F. Nordberg & T. F. Lars (Eds.), *Handbook on the Toxicology of Metals (Third Edition)* (pp. 675-729). Burlington: Academic Press.

Bernet, D., Schmidt, H., Meier, W., Burkhardt-Holm, P., & Wahli, T. (1999). Histopathology in fish: proposal for a protocol to assess aquatic pollution. *Journal of Fish Diseases, 22*(1), 25-34. doi: 10.1046/j.1365-2761.1999.00134.x

Bertin, G., & Averbeck, D. (2006). Cadmium: cellular effects, modifications of biomolecules, modulation of DNA repair and genotoxic consequences (a review). *Biochimie, 88*(11), 1549-1559. doi: http://dx.doi.org/10.1016/j.biochi.2006.10.001

Beyenbach, K. W. (1995). Secretory Electrolyte Transport in Renal Proximal Tubules of Fish. In M. W. Chris & J. S. Trevor (Eds.), *Fish Physiology* (Vol. Volume 14, pp. 85-105): Academic Press.

Bisinoti, M. C., & Jardim, W. F. (2004). O comportamento do metilmercúrio (metilHg) no ambiente. *Química Nova, 27*, 593-600.

Bjerregaard, P., & Andersen, O. (2007). Chapter 13 - Ecotoxicology of Metals—Sources, Transport, and Effects in the Ecosystem. In F. N. Gunnar, A. F. Bruce, N. Monica, B. A. F. M. N. Lars T. FribergA2 - Gunnar F. Nordberg & T. F. Lars (Eds.), *Handbook on the Toxicology of Metals (Third Edition)* (pp. 251-280). Burlington: Academic Press.

Blazka, M. E., & Shaikh, Z. A. (1991). Differences in cadmium and mercury uptakes by hepatocytes: role of calcium channels. *Toxicology and Applied Pharmacology, 110*(2), 355-363.

Boening, D. W. (2000). Ecological effects, transport, and fate of mercury: a general review. *Chemosphere, 40*(12), 1335-1351. doi: http://dx.doi.org/10.1016/S0045-6535(99)00283-0

Bonde, J. P. (2010). Male reproductive organs are at risk from environmental hazards. *Asian Journal of Andrology, 12*(2), 152-156.

Bonga, S. E. W. &. Lock, R. A. C. (2008). The Osmoregulatory System. In: *The Toxicology of Fishes* (pp. 401-415): CRC Press.

Bose, S., Ghosh, P., Ghosh, S., & Bhattacharya, S. (1993). Distribution kinetics of inorganic mercury in the subcellular fractions of fish liver. *Science of The Total Environment, 134, Supplement 1*(0), 533-538. doi: http://dx.doi.org/10.1016/S0048-9697(05)80055-5

Boudou, A., & Ribeyre, F. (1997). Aquatic ecotoxicology: from the ecosystem to the cellular and molecular levels. *Environmental Health Perspectives, 105 Suppl 1*, 21-35.

Boujbiha, M. A., Hamden, K., Guermazi, F., Bouslama, A., Omezzine, A., Kammoun, A., & Feki, A. E. (2009). Testicular toxicity in mercuric chloride treated rats: Association with oxidative stress. *Reproductive Toxicology, 28*(1), 81-89. doi: http://dx.doi.org/10.1016/j.reprotox.2009.03.011

Bridges, C. C., Bauch, C., Verrey, F., & Zalups, R. K. (2004). Mercuric conjugates of cysteine are transported by the amino acid transporter system b(0,+): implications of molecular mimicry. *J Am Soc Nephrol, 15*(3), 663-673.

Bridges, C. C., & Zalups, R. K. (2005). Molecular and ionic mimicry and the transport of toxic metals. *Toxicology and Applied Pharmacology, 204*(3), 274-308. doi: http://dx.doi.org/10.1016/j.taap.2004.09.007

Bridges, C. & Zalups, R. (2010). Ionic and Molecular Mimicry and the Transport of Metals. In: *Cellular and Molecular Biology of Metals* (pp. 241-294): CRC Press.

Brown, J.R. & Shockley, P. (1982). Serum albumin: structure and characterization of its ligand binding sites. In: Jost, P.C., Griffith, O.H. (Eds.), *Lipid-Protein Interactions* (pp. 25–68.): Wiley Inc.

Bucio, L., Souza, V., Albores, A., Sierra, A., Chávez, E., Cárabez, A., & Gutiérrez-Ruiz, M. C. (1995). Cadmium and mercury toxicity in a human fetal hepatic cell line (WRL-68 cells). *Toxicology, 102*(3), 285-299. doi: http://dx.doi.org/10.1016/0300-483X(95)03095-W

Bucio, L., García, C., Souza, V., Hernández, E., González, C., Betancourt, M., & Gutiérrez-Ruiz, M. C. (1999). Uptake, cellular distribution and DNA damage produced by mercuric chloride in a human fetal hepatic cell line. *Mutation Research/Fundamental and Molecular Mechanisms of Mutagenesis, 423*(1–2), 65-72. doi: http://dx.doi.org/10.1016/S0027-5107(98)00226-7

Burger, J. (2008). Assessment and management of risk to wildlife from cadmium. *Science of The Total Environment, 389*(1), 37-45. doi: http://dx.doi.org/10.1016/j.scitotenv.2007.08.037

Cannino, G., Ferruggia, E., Luparello, C., & Rinaldi, A. M. (2009). Cadmium and mitochondria. *Mitochondrion, 9*(6), 377-384. doi: http://dx.doi.org/10.1016/j.mito.2009.08.009

Capurro, A., Reyes-Parada, M., Olazabal, D., Perrone, R., Silveira, R., & Macadar, O. (1997). Aggressive behavior and jamming avoidance response in the weakly electric fish Gymnotus carapo: Effects of 3,4-methylenedioxymethamphetamine (MDMA). *Comparative Biochemistry and Physiology Part A: Physiology, 118*(3), 831-840. doi: http://dx.doi.org/10.1016/S0300-9629(97)00132-1

Cardoso, L. M. N. & Chasin, A. A. M. (2001). Ecotoxicologia do cádmio e seus compostos. In: *Cadernos de referência ambiental* (Volume 6, pp. 122): CRA.

Carranza-Rosales, P., Said-Fernández, S., Sepúlveda-Saavedra, J., Cruz-Vega, D. E., & Gandolfi, A. J. (2005). Morphologic and functional alterations induced by low doses of mercuric chloride in the kidney OK cell line: ultrastructural evidence for an apoptotic mechanism of damage. *Toxicology, 210*(2–3), 111-121. doi: http://dx.doi.org/10.1016/j.tox.2005.01.006

Ceccatelli, S., Daré, E., & Moors, M. (2010). Methylmercury-induced neurotoxicity and apoptosis. *Chemico-Biological Interactions, 188*(2), 301-308. doi: http://dx.doi.org/10.1016/j.cbi.2010.04.007

Celino, F. T., Yamaguchi, S., Miura, C., Ohta, T., Tozawa, Y., Iwai, T., & Miura, T. (2011). Tolerance of spermatogonia to oxidative stress is due to high levels of Zn and Cu/Zn superoxide dismutase. *PLoS One, 6*(2), e16938-e16938. doi: 10.1371/journal.pone.0016938

Chargui, A., Zekri, S., Jacquillet, G., Rubera, I., Ilie, M., Belaid, A., Duranton, C., Tauc, M., Hofman, P., Poujeol P., El May, M. V. & Mograbi, B. (2011). Cadmium-induced autophagy in rat kidney: an early biomarker of subtoxic exposure. *Toxicol Sci, 121*(1), 31-42. doi: 10.1093/toxsci/kfr031

Chatterjee, S., Ray, A., Mukherjee, S., Agarwal, S., Kundu, R., & Bhattacharya, S. (2012). Low concentration of mercury induces autophagic cell death in rat hepatocytes. *Toxicology and Industrial Health*. doi: 10.1177/0748233712462442

Chatterjee, S., Nandi, P., Mukherjee, S., Chattopadhyay, A., & Bhattacharya, S. (2013). Regulation of autophagy in rat hepatocytes treated in vitro with low concentration of mercury. *Toxicological & Environmental Chemistry*, 1-11. doi: 10.1080/02772248.2013.786941

Chyb, J., Kime, D. E., Szczerbik, P., Mikołajczyk, T. & Epler, P. (2001). Computer-assisted analysis (casa) of 4 common carp *Cyprinus carpio* L. spermatozoa motility in the presence of cadmium. Archives *of* 5 *Polish Fisheries, 9* (2): 173-181.

Cognato, D. d. P., & Fialho, C. B. (2006). Reproductive biology of a population of Gymnotus aff.carapo (Teleostei: Gymnotidae) from southern Brazil. *Neotropical Ichthyology, 4*, 339-348.

Cornelis, R., & Nordberg, M. (2007). General Chemistry, Sampling, Analytical Methods, and Speciation. In F. N. Gunnar, A. F. Bruce, N. Monica, B. A. F. M. N. Lars T. FribergA2 - Gunnar F. Nordberg & T. F. Lars (Eds.), *Handbook on the Toxicology of Metals (Third Edition)* (pp. 11-38). Burlington: Academic Press.

Corrêa, S. A. L., & Hoffmann, A. (1999). Reciprocal connections between the preglomerular complex and the dorsolateral telencephalon in the weakly electric fish, Gymnotus carapo. *Neuroscience Letters, 261*(3), 131-134. doi: http://dx.doi.org/10.1016/S0304-3940(98)01004-0

Costa, P. M., Chicano-Gálvez, E., López Barea, J., DelValls, T. À., & Costa, M. H. (2010). Alterations to proteome and tissue recovery responses in fish liver caused by a short-term combination treatment with cadmium and benzo[a]pyrene. *Environmental Pollution, 158*(10), 3338-3346. doi: http://dx.doi.org/10.1016/j.envpol.2010.07.030

Costa, P. M., Carreira, S., Costa, M. H., & Caeiro, S. (2013). Development of histopathological indices in a commercial marine bivalve (Ruditapes decussatus) to determine environmental quality. *Aquatic Toxicology, 126*(0), 442-454. doi: http://dx.doi.org/10.1016/j.aquatox.2012.08.013

Crampton, W. G. R. (1996). Gymnotiform fish: an important component of Amazonian fioodplain fish communities. *Journal of Fish Biology, 48*(2), 298-301. doi: 10.1111/j.1095-8649.1996.tb01122.x

Crump, K. L., & Trudeau, V. L. (2009). Mercury-induced reproductive impairment in fish. *Environmental Toxicoogy and Chemistry, 28*(5), 895-907. doi: 10.1897/08-151.1

Cuello, S., Goya, L., Madrid, Y., Campuzano, S., Pedrero, M., Bravo, L., Cámara, C., Ramos, S. (2010). Molecular mechanisms of methylmercury-induced cell death in human HepG2 cells. *Food and Chemical Toxicology, 48*(5), 1405-1411. doi: http://dx.doi.org/10.1016/j.fct.2010.03.009

Dang, F., & Wang, W.-X. (2012). Why mercury concentration increases with fish size? Biokinetic explanation. *Environmental Pollution, 163*(0), 192-198. doi: http://dx.doi.org/10.1016/j.envpol.2011.12.026

Dong, Z., Wang, L., Xu, J., Li, Y., Zhang, Y., Zhang, S., & Miao, J. (2009). Promotion of autophagy and inhibition of apoptosis by low concentrations of cadmium in vascular

endothelial cells. *Toxicology in Vitro, 23*(1), 105-110. doi: http://dx.doi.org/10.1016/j.tiv.2008.11.003

Douhri, H., & Sayah, F. (2009). The use of enzymatic biomarkers in two marine invertebrates Nereis diversicolor and Patella vulgata for the biomonitoring of Tangier's bay (Morocco). *Ecotoxicology and Environmental Safety, 72*(2), 394-399. doi: http://dx.doi.org/10.1016/j.ecoenv.2008.07.016

Duncan-Achanzar, K. B., Jones, J. T., Burke, M. F., Carter, D. E., & Laird, H. E., 2nd. (1996). Inorganic mercury chloride-induced apoptosis in the cultured porcine renal cell line LLC-PK1. *Journal Pharmacology and Experimental Therapeutics, 277*(3), 1726-1732.

Evans, D. H., Piermarini, P. M., & Choe, K. P. (2005). The Multifunctional Fish Gill: Dominant Site of Gas Exchange, Osmoregulation, Acid-Base Regulation, and Excretion of Nitrogenous Waste. *Physiological Reviews, 85*(1), 97-177. doi: 10.1152/physrev.00050.2003

Faverney, C. R., Orsini, N., de Sousa, G., & Rahmani, R. (2004). Cadmium-induced apoptosis through the mitochondrial pathway in rainbow trout hepatocytes: involvement of oxidative stress. *Aquatic Toxicology, 69*(3), 247-258. doi: http://dx.doi.org/10.1016/j.aquatox.2004.05.011

Ferreira, A. G.; Melo, E. J. T.; Carvalho, C. E. V. (2003) Histological aspects of mercury contamination in muscular and hepatic tissues of *Hoplias malabaricus* (Pisces, Erytrinidae) from lakes in the north of Rio de Janeiro State, Brazil. Acta Microscopica; 12: 49-54.

Filipak Neto, F., Zanata, S. M., Randi, M. A. F., Pelletier, É., & Oliveira Ribeiro, C. A. (2006). Hepatocytes primary culture from the Neotropical fish, trahira Hoplias malabaricus (Bloch). *Journal of Fish Biology, 69*(5), 1524-1532. doi: 10.1111/j.1095-8649.2006.01217.x

FISHBASE. (2013). Disponível em: http://www.fishbase.gr/summary/Gymnotus-carapo.html. Data de acess: 30/04/2013.

Foster, E. P., Drake, D. L., & DiDomenico, G. (2000). Seasonal changes and tissue distribution of mercury in largemouth bass (Micropterus salmoides) from Dorena Reservoir, Oregon. *Archives of Environmental Contamination and Toxicology, 38*(1), 78-82.

Fotakis, G., Cemeli, E., Anderson, D., & Timbrell, J. A. (2005). Cadmium chloride-induced DNA and lysosomal damage in a hepatoma cell line. *Toxicology in Vitro, 19*(4), 481-489. doi: http://dx.doi.org/10.1016/j.tiv.2005.02.001

Friedmann, A. S., Watzin, M. C., Brinck-Johnsen, T., & Leiter, J. C. (1996). Low levels of dietary methylmercury inhibit growth and gonadal development in juvenile walleye (Stizostedion vitreum). *Aquatic Toxicology, 35*(3–4), 265-278. doi: http://dx.doi.org/10.1016/0166-445X(96)00796-5

Giari, L., Manera, M., Simoni, E., & Dezfuli, B. S. (2007). Cellular alterations in different organs of European sea bass Dicentrarchus labrax (L.) exposed to cadmium. *Chemosphere, 67*(6), 1171-1181. doi: http://dx.doi.org/10.1016/j.chemosphere.2006.10.061

Giari, L., Simoni, E., Manera, M., & Dezfuli, B. S. (2008). Histo-cytological responses of Dicentrarchus labrax (L.) following mercury exposure. *Ecotoxicology and Environmental Safety, 70*(3), 400-410. doi: http://dx.doi.org/10.1016/j.ecoenv.2007.08.013

Gioacchino, M. D., Petrarca, C., Perrone, A., Farina, M., Sabbioni, E., Hartung, T., Martino, S., Esposito, D. L., Lotti, L. V. & Mariani-Costantini, R. (2008). Autophagy as an ultrastructural marker of heavy metal toxicity in human cord blood hematopoietic stem cells. *Science of The Total Environment, 392*(1), 50-58. doi: http://dx.doi.org/10.1016/j.scitotenv.2007.11.009

Global Environmental Information Facility (GEIF). (2013). Free and open diversity data. Disponível em: http://data.gbif.org/species/5212798?extent=-88%2B-63%2B-68%2B-53&minMapLat=-63&maxMapLat=-53&minMapLong=-88&maxMapLong=68&zoom=5&c[0].s=20&c[0]. p=0&c[0].o=5212798. Data de acesso: 30/04/2013.

Gobe, G., & Crane, D. (2010). Mitochondria, reactive oxygen species and cadmium toxicity in the kidney. *Toxicology Letters, 198*(1), 49-55. doi: http://dx.doi.org/10.1016/j.toxlet.2010.04.013

Gomes, S. R. (2004). Contaminação ambiental de *Hoplias malabaricus* – Traíra (Pisces, Erythrinidae) por mercúrio no Norte do Estado do Rio de Janeiro. Caracterização histológica e ultraestrutural de hepatócitos. Monografia. Universidade Estadual do Norte Fluminense, 57 p.

Guillouzo, A., Morel, F., Langouët, S., Maheo, K., & Rissel, M. (1997). Use of hepatocyte cultures for the study of hepatotoxic compounds. *Journal of Hepatology, 26, Supplement 2*(0), 73-80. doi: http://dx.doi.org/10.1016/S0168-8278(97)80499-0

Hartwig, A. (2010). Mechanisms in cadmium-induced carcinogenicity: recent insights. *BioMetals, 23*(5), 951-960. doi: 10.1007/s10534-010-9330-4

Hinton, D. E., Segner, H., Au, D. W. T. Kullman, S. W., & Hardman, R. C. (2008). Liver Toxicity *The Toxicology of Fishes* (pp. 327-400): CRC Press.

Holmes, P., James, K. A. F., & Levy, L. S. (2009). Is low-level environmental mercury exposure of concern to human health? *Science of The Total Environment, 408*(2), 171-182. doi: http://dx.doi.org/10.1016/j.scitotenv.2009.09.043

International Agency for Research on Cancer (IARC). (1993). Beryllium, cadmium, mercury and exposures in the glass manufacturing industry. IARC Monographs on the Evaluation of Carcinogenic Risk of Chemicals to Humans, vol. 58. International Agency for Research on Cancer, Lyon, France. 444 pp. Disponível em: http:// monographs.iarc.fr/ENG/Monographs/vol58/volume58.pdf

Jagoe, C. H., Faivre, A., & Newman, M. C. (1996). Morphological and morphometric changes in the gills of mosquitofish (Gambusia holbrooki) after exposure to mercury (II). *Aquatic Toxicology, 34*(2), 163-183. doi: http://dx.doi.org/10.1016/0166-445X(95)00033-Z

Järup, L., Berglund, M., Elinder, C. G., Nordberg, G., & Vahter, M. (1998). Health effects of cadmium exposure--a review of the literature and a risk estimate. *Scandinavian Journal of Work and Environmental Health, 24 Suppl 1*, 1-51.

Järup, L. (2003). Hazards of heavy metal contamination. *British Medical Bulletin, 68*(1), 167-182. doi: 10.1093/bmb/ldg03

Järup, L., & Åkesson, A. (2009). Current status of cadmium as an environmental health problem. *Toxicology and Applied Pharmacology, 238*(3), 201-208. doi: http://dx.doi.org/10.1016/j.taap.2009.04.020

Jozefczak, M., Remans, T., Vangronsveld, J., & Cuypers, A. (2012). Glutathione Is a Key Player in Metal-Induced Oxidative Stress Defenses. *International Journal of Molecular Sciences, 13*(3), 3145-3175.

Ju, Y.-R., Chen, W.-Y., & Liao, C.-M. (2012). Assessing human exposure risk to cadmium through inhalation and seafood consumption. *Journal of Hazardous Materials, 227–228*(0), 353-361. doi: http://dx.doi.org/10.1016/j.jhazmat.2012.05.060

Klaassen, C. D., Liu, J., & Choudhuri, S. (1999). Metallothionein: an intracellular protein to protect against cadmium toxicity. *Annu Rev Pharmacol Toxicol, 39*, 267-294. doi: 10.1146/annurev.pharmtox.39.1.267

Klaassen, C. D., Liu, J., & Diwan, B. A. (2009). Metallothionein protection of cadmium toxicity. *Toxicology and Applied Pharmacology, 238*(3), 215-220. doi: http://dx.doi.org/10.1016/j.taap.2009.03.026

Kleinow, K., Nichols, J., Hayton, W. L., McKim, J. M., Barron, M. G. (2008). Toxicokinetics in Fishes *The Toxicology of Fishes* (pp. 55-152): CRC Press.

Kumari, M., & Dutt, N. H. G. (1991). Cadmium-induced histomorphological changes in the testis and pituitary gonadotrophic hormone secreting cells of the cyprinid Puntius sarana. *Bolletino di zoologia, 58*(1), 71-76. doi: 10.1080/11250009109355730

Lasfer, M., Vadrot, N., Aoudjehane, L., Conti, F., Bringuier, A. F., Feldmann, G., & Reyl-Desmars, F. (2008). Cadmium induces mitochondria-dependent apoptosis of normal human hepatocytes. *Cell Biology and Toxicology, 24*(1), 55-62. doi: 10.1007/s10565-007-9015-0

Laurent, P. & Perry, S.F. (1991). Environmental effects on fish gill morphology. *Physiological Zoology, 64* (1), 4-25.

L'Azou, B., Dubus, I., Ohayon-Courtès, C., Labouyrie, J.-P., Perez, L., Pouvreau, C., Juvet, L. & Cambar, J. (2002). Cadmium induces direct morphological changes in mesangial cell culture. *Toxicology, 179*(3), 233-245. doi: http://dx.doi.org/10.1016/S0300-483X(02)00374-8

Li, P., Feng, X. B., Qiu, G. L., Shang, L. H., & Li, Z. G. (2009). Mercury pollution in Asia: A review of the contaminated sites. *Journal of Hazardous Materials, 168*(2–3), 591-601. doi: http://dx.doi.org/10.1016/j.jhazmat.2009.03.031

Liao, C.-Y., Fu, J.-J., Shi, J.-B., Zhou, Q.-F., Yuan, C.-G., & Jiang, G.-B. (2006). Methylmercury accumulation, histopathology effects, and cholinesterase activity alterations in medaka (Oryzias latipes) following sublethal exposure to methylmercury chloride.

Environmental Toxicology and Pharmacology, 22(2), 225-233. doi: http://dx.doi.org/10.1016/j.etap.2006.03.009

Lim, S.-C., Hahm, K.-S., Lee, S.-H., & Oh, S.-H. (2010). Autophagy involvement in cadmium resistance through induction of multidrug resistance-associated protein and counterbalance of endoplasmic reticulum stress WI38 lung epithelial fibroblast cells. *Toxicology, 276*(1), 18-26. doi: http://dx.doi.org/10.1016/j.tox.2010.06.010

Linnaeus, C. (1758). Systema naturae per regna tria naturae: secundum classes, ordines, genera, species, cum characteribus, differentiis, synonymis, locis (Vol. 1). Holmiae:: Impensis Direct. Laurentii Salvii.

Liu, X. J., Luo, Z., Li, C. H., Xiong, B. X., Zhao, Y. H., & Li, X. D. (2011). Antioxidant responses, hepatic intermediary metabolism, histology and ultrastructure in Synechogobius hasta exposed to waterborne cadmium. *Ecotoxicology and Environmental Safety, 74*(5), 1156-1163. doi: http://dx.doi.org/10.1016/j.ecoenv.2011.02.015

Lovejoy, N. R., Lester, K., Crampton, W. G. R., Marques, F. P. L., & Albert, J. S. (2010). Phylogeny, biogeography, and electric signal evolution of Neotropical knifefishes of the genus Gymnotus (Osteichthyes: Gymnotidae). *Molecular Phylogenetics and Evolution, 54*(1), 278-290. doi: http://dx.doi.org/10.1016/j.ympev.2009.09.017

Malm, O., Branches, F. J. P., Akagi, H., Castro, M. B., Pfeiffer, W. C., Harada, M., . . . Kato, H. (1995). Mercury and methylmercury in fish and human hair from the Tapajós river basin, Brazil. *Science of The Total Environment, 175*(2), 141-150. doi: http://dx.doi.org/10.1016/0048-9697(95)04910-X

Marano, K. M., Naufal, Z. S., Kathman, S. J., Bodnar, J. A., Borgerding, M. F., Garner, C. D., & Wilson, C. L. (2012). Cadmium exposure and tobacco consumption: Biomarkers and risk assessment. *Regulatory Toxicology and Pharmacology, 64*(2), 243-252. doi: http://dx.doi.org/10.1016/j.yrtph.2012.07.008

Marchi, B., Burlando, B., Moore, M. N., & Viarengo, A. (2004). Mercury- and copper-induced lysosomal membrane destabilisation depends on [Ca2+]i dependent phospholipase A2 activation. *Aquatic Toxicology, 66*(2), 197-204. doi: http://dx.doi.org/10.1016/j.aquatox.2003.09.003

Mela, M., Randi, M. A. F., Ventura, D. F., Carvalho, C. E. V., Pelletier, E., & Oliveira Ribeiro, C. A. (2007). Effects of dietary methylmercury on liver and kidney histology in the

neotropical fish Hoplias malabaricus. *Ecotoxicology and Environmental Safety, 68*(3), 426-435. doi: http://dx.doi.org/10.1016/j.ecoenv.2006.11.013

Menin, E. (1989). Anatomia funcional do tubo digestivo de *Gymnotus carapo* Linnaeus, 1758 (Siluriformes, Gymnotoidei, Gymnotidae). *Revista Ceres*, *36*(207), 435-457.

Messner, B., Ploner, C., Laufer, G., & Bernhard, D. (2012). Cadmium activates a programmed, lysosomal membrane permeabilization-dependent necrosis pathway. *Toxicology Letters, 212*(3), 268-275. doi: http://dx.doi.org/10.1016/j.toxlet.2012.05.026

Mieiro, C. L., Duarte, A. C., Pereira, M. E., & Pacheco, M. (2011). Mercury accumulation patterns and biochemical endpoints in wild fish (Liza aurata): A multi-organ approach. *Ecotoxicology and Environmental Safety, 74*(8), 2225-2232. doi: http://dx.doi.org/10.1016/j.ecoenv.2011.08.011

Migliarini, B., Campisi, A. M., Maradonna, F., Truzzi, C., Annibaldi, A., Scarponi, G., & Carnevali, O. (2005). Effects of cadmium exposure on testis apoptosis in the marine teleost Gobius niger. *General Comparative Endocrinology, 142*(1–2), 241-247. doi: http://dx.doi.org/10.1016/j.ygcen.2004.12.012

Moore, M. N. (2002). Biocomplexity: the post-genome challenge in ecotoxicology. *Aquatic Toxicology, 59*(1–2), 1-15. doi: http://dx.doi.org/10.1016/S0166-445X(01)00225-9

Moore, M. N., Icarus Allen, J., & McVeigh, A. (2006). Environmental prognostics: An integrated model supporting lysosomal stress responses as predictive biomarkers of animal health status. *Marine Environmental Research, 61*(3), 278-304. doi: http://dx.doi.org/10.1016/j.marenvres.2005.10.005

Moraes, G., Avilez, I. M., Altran, A. E., & Barbosa, C. C. (2002). Biochemical and hematological responses of the banded knife fish Gymnotus carapo (Linnaeus, 1758) exposed to environmental hypoxia. *Brazilian Journal of Biology, 62*, 633-640.

Morel, F. M. M., Kraepiel, A. M. L., & Amyot, M. (1998). The chemical cycle and bioaccumulation of mercury. *Annual Review of Ecology and Systematics, 29*(1), 543-566. doi: doi:10.1146/annurev.ecolsys.29.1.543

Mumford, S., Heidel, J., Smith, C., Morrison, J., MacConnell, B., Blazer, V. (2007). Fish Histology and Histopathology. Disponível em: training.fws.gov/EC/Resources/Fish_Histology/histology.html

Nakabayashi, H., Taketa, K., Miyano, K., Yamane, T., & Sato, J. (1982). Growth of human hepatoma cells lines with differentiated functions in chemically defined medium. *Cancer Research, 42*(9), 3858-3863.

Nordberg, G. F., & Fowler, B. A. (2007). Chapter 14 - Risk Assessment. In F. N. Gunnar, A. F. Bruce, N. Monica, B. A. F. M. N. Lars T. FribergA2 - Gunnar F. Nordberg & T. F. Lars (Eds.), *Handbook on the Toxicology of Metals (Third Edition)* (pp. 281-301). Burlington: Academic Press.

Nordberg, M., & Nordberg, G. F. (2000). Toxicological aspects of metallothionein. *Cellular and Molecular Biology (Noisy-le-grand), 46*(2), 451-463.

Nordberg, G. F., Fowler, B. A., Nordberg, M., & Friberg, L. T. (2007a). Chapter 1 - Introduction—General Considerations and International Perspectives. In F. N. Gunnar, A. F. Bruce, N. Monica, B. A. F. M. N. Lars T. FribergA2 - Gunnar F. Nordberg & T. F. Lars (Eds.), *Handbook on the Toxicology of Metals (Third Edition)* (pp. 1-9). Burlington: Academic Press.

Nordberg, G. F., Nogawa, K., Nordberg, M., & Friberg, L. T. (2007b). Chapter 23 - Cadmium. In F. N. Gunnar, A. F. Bruce, N. Monica, Lars T. Friberg - Gunnar F. Nordberg & T. F. Lars (Eds.), *Handbook on the Toxicology of Metals (Third Edition)* (pp. 445-486). Burlington: Academic Press.

Nriagu, J. O. (1988). A silent epidemic of environmental metal poisoning? *Environmental Pollution, 50*(1–2), 139-161. doi: http://dx.doi.org/10.1016/0269-7491(88)90189-3

Oliveira Ribeiro, C. A., Guimarães, J. R. D., & Pfeiffer, W. C. (1996). Accumulation and Distribution of Inorganic Mercury in a Tropical Fish (Trichomycterus zonatus). *Ecotoxicology and Environmental Safety, 34*(2), 190-195. doi: http://dx.doi.org/10.1006/eesa.1996.0063

Oliveira Ribeiro, C. A., Pelletier, E., Pfeiffer, W. C., & Rouleau, C. (2000). Comparative Uptake, Bioaccumulation, and Gill Damages of Inorganic Mercury in Tropical and Nordic Freshwater Fish. *Environmental Research, 83*(3), 286-292. doi: http://dx.doi.org/10.1006/enrs.2000.4056

Oliveira Ribeiro, C. A., Belger, L., Pelletier, É., & Rouleau, C. (2002). Histopathological evidence of inorganic mercury and methyl mercury toxicity in the arctic charr (Salvelinus

alpinus). *Environmental Research, 90*(3), 217-225. doi: http://dx.doi.org/10.1016/S0013-9351(02)00025-7

Palacin, M., Fernandez, E., Chillaron, J., & Zorzano, A. (2001). The amino acid transport system b(o,+) and cystinuria. *Mol Membr Biol, 18*(1), 21-26.

Pastore, A., Federici, G., Bertini, E., & Piemonte, F. (2003). Analysis of glutathione: implication in redox and detoxification. *Clinica Chimica Acta, 333*(1), 19-39. doi: http://dx.doi.org/10.1016/S0009-8981(03)00200-6

Pastorelli, A. A., Baldini, M., Stacchini, P., Baldini, G., Morelli, S., Sagratella, E., . . . Ciardullo, S. (2012). Human exposure to lead, cadmium and mercury through fish and seafood product consumption in Italy: a pilot evaluation. *Food Additives & Contaminants: Part A, 29*(12), 1913-1921. doi: 10.1080/19440049.2012.719644

Pereira, P., Pablo, H. d., Vale, C., & Pacheco, M. (2010). Combined use of environmental data and biomarkers in fish (Liza aurata) inhabiting a eutrophic and metal-contaminated coastal system – Gills reflect environmental contamination. *Marine Environmental Research, 69*(2), 53-62. doi: http://dx.doi.org/10.1016/j.marenvres.2009.08.003

Pratap, H. B., & Wendelaar Bonga, S. E. (1993). Effect of ambient and dietary cadmium on pavement cells, chloride cells, and Na+/K+-ATPase activity in the gills of the freshwater teleost Oreochromis mossambicus at normal and high calcium levels in the ambient water. *Aquatic Toxicology, 26*(1–2), 133-149. doi: http://dx.doi.org/10.1016/0166-445X(93)90010-X

Rabitto, I. d. S., Bastos, W. R., Almeida, R., Anjos, A., de Holanda, Í. B. B., Galvão, R. C. F., Neto, F. F., Menezes, M. L., Santos, C. A. M. & Oliveira Ribeiro, C. A. (2011). Mercury and DDT exposure risk to fish-eating human populations in Amazon. *Environment International, 37*(1), 56-65. doi: http://dx.doi.org/10.1016/j.envint.2010.07.001

Ram, R. N., & Sathyanesan, A. G. (1987). Histopathological and biochemical changes in the liver of a teleost fish, Channa punctatus (Bloch) induced by a mercurial fungicide. *Environmental Pollution, 47*(2), 135-145. doi: http://dx.doi.org/10.1016/0269-7491(87)90043-1

Régine, M.-B., Gilles, D., Yannick, D., & Alain, B. (2006). Mercury distribution in fish organs and food regimes: Significant relationships from twelve species collected in French

Guiana (Amazonian basin). *Science of The Total Environment, 368*(1), 262-270. doi: http://dx.doi.org/10.1016/j.scitotenv.2005.09.077

Resende, E. K. de & Pereira, R. A. C. (2000). Dieta alimentar de *Gymnotus* cf. *carapo*, (Ostariophysi, Gymnotiformes), na planície inundável do Rio Negro, Mato Grosso do Sul, Brasil. In: *Simpósio sobre recursos naturais e socioeconômicos do pantanal*, Corumbá. Os desafios do novo milênio. **Resumos...** Corumbá: Embrapa Pantanal, 285p.

Romero, D., Gómez-Zapata, M., Luna, A., & García-Fernández, A. J. (2004). Comparison of cytopathological changes induced by mercury chloride exposure in renal cell lines (VERO and BGM). *Environmental Toxicology and Pharmacology, 17*(3), 129-141. doi: http://dx.doi.org/10.1016/j.etap.2004.03.007

Rupik, W., Huszno, J., & Klag, J. (2011). Cellular organisation of the mature testes and stages of spermiogenesis in Danio rerio (Cyprinidae; Teleostei)—Structural and ultrastructural studies. *Micron, 42*(8), 833-839. doi: http://dx.doi.org/10.1016/j.micron.2011.05.006

Sangalang, G. B., & O'halloran, M. J. (1973). Adverse Effects of Cadmium on Brook Trout Testis and on in Vitro Testicular Androgen Synthesis. *Biology of Reproduction, 9*(4), 394-403.

Schulz, R. W., de França, L. R., Lareyre, J.-J., LeGac, F., Chiarini-Garcia, H., Nobrega, R. H., & Miura, T. (2010). Spermatogenesis in fish. *General and Comparative Endocrinology, 165*(3), 390-411. doi: http://dx.doi.org/10.1016/j.ygcen.2009.02.013

Schwaiger, J., Wanke, R., Adam, S., Pawert, M., Honnen, W., & Triebskorn, R. (1997). The use of histopathological indicators to evaluate contaminant-related stress in fish. *Journal of Aquatic Ecosystem Stress and Recovery, 6*(1), 75-86. doi: 10.1023/A:1008212000208

Shea, J., Moran, T., & Dehn, P. F. (2008). A bioassay for metals utilizing a human cell line. *Toxicology in Vitro, 22*(4), 1025-1031. doi: http://dx.doi.org/10.1016/j.tiv.2008.02.014

Silva, J. M.; Oliveira, J.I.J. (1997). Morfologia do intestino do "tuvira" *Gymnotus carapo* L., 1758 (Pices – Gymnotidae). *Revista Científica, UFMS, Campo Grande, 4*(1), 18-22.

Sirot, V., Samieri, C., Volatier, J.-l., & Leblanc, J.-c. (2007). Cadmium dietary intake and biomarker data in French high seafood consumers. *Journal of Exposure Science and Environmental Epidemiology, 18*(4), 400-409.

Son, Y.-O., Wang, X., Hitron, J. A., Zhang, Z., Cheng, S., Budhraja, A., . . . Shi, X. (2011). Cadmium induces autophagy through ROS-dependent activation of the LKB1–AMPK signaling in skin epidermal cells. *Toxicology and Applied Pharmacology, 255*(3), 287-296. doi: http://dx.doi.org/10.1016/j.taap.2011.06.024

Soriano, A., Pallarés, S., Pardo, F., Vicente, A. B., Sanfeliu, T., & Bech, J. (2012). Deposition of heavy metals from particulate settleable matter in soils of an industrialised area. *Journal of Geochemical Exploration, 113*(0), 36-44. doi: http://dx.doi.org/10.1016/j.gexplo.2011.03.006

Sousa, W.P. (2000) Determinação de mercúrio e carbono orgânico em solos e sedimentos da região norte do estado do Rio de Janeiro. Dissertação de Mestrado. Universidade Estadual do Norte Fluminense. Centro de Biociências e Biotecnologia. 75p.

Souza, V., Bucio, L., & Gutiérrez-Ruiz, M. C. (1997). Cadmium uptake by a human hepatic cell line (WRL-68 cells). *Toxicology, 120*(3), 215-220. doi: http://dx.doi.org/10.1016/S0300-483X(97)00057-7

Syversen, T., & Kaur, P. (2012). The toxicology of mercury and its compounds. *Journal of Trace Elements in Medicine and Biology, 26*(4), 215-226. doi: http://dx.doi.org/10.1016/j.jtemb.2012.02.004

Tan, F., Wang, M., Wang, W., & Lu, Y. (2008). Comparative evaluation of the cytotoxicity sensitivity of six fish cell lines to four heavy metals in vitro. *Toxicology in Vitro, 22*(1), 164-170. doi: http://dx.doi.org/10.1016/j.tiv.2007.08.020

Teh, S. J., Adams, S. M., & Hinton, D. E. (1997). Histopathologic biomarkers in feral freshwater fish populations exposed to different types of contaminant stress. *Aquatic Toxicology, 37*(1), 51-70. doi: 10.1016/S0166-445X(96)00808-9

Templeton, D. M., & Liu, Y. (2010). Multiple roles of cadmium in cell death and survival. *Chemico-Biological Interactions, 188*(2), 267-275. doi: http://dx.doi.org/10.1016/j.cbi.2010.03.040

Thévenod, F. (2009). Cadmium and cellular signaling cascades: To be or not to be? *Toxicology and Applied Pharmacology, 238*(3), 221-239. doi: http://dx.doi.org/10.1016/j.taap.2009.01.013

Tsuda, T., Yorifuji, T., Takao, S., Miyai, M., & Babazono, A. (2009). Minamata disease: catastrophic poisoning due to a failed public health response. *J Public Health Policy, 30*(1), 54-67. doi: 10.1057/jphp.2008.30

van der Oost, R., Beyer, J., & Vermeulen, N. P. E. (2003). Fish bioaccumulation and biomarkers in environmental risk assessment: a review. *Environmental Toxicology and Pharmacology, 13*(2), 57-149. doi: http://dx.doi.org/10.1016/S1382-6689(02)00126-6

van Dyk, J. C., Pieterse, G. M., & van Vuren, J. H. J. (2007). Histological changes in the liver of Oreochromis mossambicus (Cichlidae) after exposure to cadmium and zinc. *Ecotoxicology and Environmental Safety, 66*(3), 432-440. doi: http://dx.doi.org/10.1016/j.ecoenv.2005.10.012

Vergilio, C. S., Carvalho, C. E. V., Melo, E. J. T. (2012a). Accumulation and histopathological effects of mercury chloride after acute exposure in tropical fish *Gymnotus carapo*. *Journal of Chemical Health Risks 2*(4): 01-08.

Vergílio, C. d. S., Moreira, R. V., de Carvalho, C. E. V., & de Melo, E. J. T. (2012b). Characterization of mature testis and sperm morphology of Gymnotus carapo (Gymnotidae, Teleostei) from the southeast of Brazil. *Acta Zoologica*, n/a-n/a. doi: 10.1111/j.1463-6395.2012.00569.

Voeltz, G. K., Rolls, M. M., & Rapoport, T. A. (2002). Structural organization of the endoplasmic reticulum. *EMBO Rep, 3*(10), 944-950. doi: 10.1093/embo-reports/kvf202

Wang, Y., Fang, J., Leonard, S. S., & Krishna Rao, K. M. (2004). Cadmium inhibits the electron transfer chain and induces Reactive Oxygen Species. *Free Radical Biology and Medicine, 36*(11), 1434-1443. doi: http://dx.doi.org/10.1016/j.freeradbiomed.2004.03.010

Wang, S. H., Shih, Y. L., Ko, W. C., Wei, Y. H., & Shih, C. M. (2008). Cadmium-induced autophagy and apoptosis are mediated by a calcium signaling pathway. *Cellular and Molecular Life Sciences, 65*(22), 3640-3652. doi: 10.1007/s00018-008-8383-9

Wang, S.-H., Shih, Y.-L., Kuo, T.-C., Ko, W.-C., & Shih, C.-M. (2009). Cadmium Toxicity toward Autophagy through ROS-Activated GSK-3β in Mesangial Cells. *Toxicological Sciences, 108*(1), 124-131. doi: 10.1093/toxsci/kfn266

Wang, Y., Zalups, R. K., & Barfuss, D. W. (2010). Potential mechanisms involved in the absorptive transport of cadmium in isolated perfused rabbit renal proximal tubules. *Toxicology Letters, 193*(1), 61-68. doi: http://dx.doi.org/10.1016/j.toxlet.2009.12.007

Wang, M., Wang, Y., Wang, J., Lin, L., Hong, H., & Wang, D. (2011). Proteome profiles in medaka (Oryzias melastigma) liver and brain experimentally exposed to acute inorganic mercury. *Aquatic Toxicology, 103*(3–4), 129-139. doi: http://dx.doi.org/10.1016/j.aquatox.2011.02.020

Wang, M., Wang, Y., Zhang, L., Wang, J., Hong, H., & Wang, D. (2013). Quantitative proteomic analysis reveals the mode-of-action for chronic mercury hepatotoxicity to marine medaka (Oryzias melastigma). *Aquatic Toxicology, 130–131*(0), 123-131. doi: http://dx.doi.org/10.1016/j.aquatox.2013.01.012

Wangsongsak, A., Utarnpongsa, S., Kruatrachue, M., Ponglikitmongkol, M., Pokethitiyook, P., & Sumranwanich, T. (2007). Alterations of organ histopathology and metallolhionein mRNA expression in silver barb, Puntius gonionotus during subchronic cadmium exposure. *Journal of Environmental Sciences, 19*(11), 1341-1348. doi: http://dx.doi.org/10.1016/S1001-0742(07)60219-8

Westby, G. W. M. (1975). Comparative studies of the aggressive behaviour of two gymnotid electric fish (Gymnotus carapo and Hypopomus artedi). *Animal Behaviour, 23, Part 1*(0), 192-213. doi: http://dx.doi.org/10.1016/0003-3472(75)90065-2

Wester, P. W., & Canton, H. H. (1992). Histopathological Effects in Poecilia reticulata (Guppy) Exposed to Methyl Mercury Chloride. *Toxicologic Pathology, 20*(1), 81-92. doi: 10.1177/019262339202000110

Wilson, J. M., & Laurent, P. (2002). Fish gill morphology: inside out. *Journal of Experimental Zoology, 293*(3), 192-213. doi: 10.1002/jez.10124

World Health Organisation (WHO). (1991). International Programme on Chemical Safety. Inorganic Mercury. Disponível em: http://www.inchem.org/documents/ehc/ehc/ehc118.htm

World Health Organization (WHO). (1992). Environmental Health Criteria 134 - Cadmium International Programme on Chemical Safety (IPCS) Monograph.

World Health Organization (WHO). (2004). International Programme on Chemical Safety. Methylmercury. Disponível em: http://www.inchem.org/documents/jecfa/jecmono/v52je23.htm

World Health Organization (WHO). (2007). Exposure to mercury: a major public health concern. Disponível em: http://www.who.int/phe/news/Mercury-flyer.pdf

World Health Organization (WHO). (2013). Ten chemicals of major public health concern. http://www.who.int/ipcs/assessment/public_health/chemicals_phc/en/index.html. Data de acesso: 28/04/2013.

Yang, L.-Y., Wu, K.-H., Chiu, W.-T., Wang, S.-H., & Shih, C.-M. (2009). The cadmium-induced death of mesangial cells results in nephrotoxicity. *Autophagy, 5*(4), 571-572.

Ye, J.-L., Mao, W.-P., Wu, A.-L., Zhang, N.-N., Zhang, C., Yu, Y.-J., Zou, L. & Wei, C.-J. (2007). Cadmium-induced apoptosis in human normal liver L-02 cells by acting on mitochondria and regulating Ca2+ signals. *Environmental Toxicology and Pharmacology, 24*(1), 45-54. doi: http://dx.doi.org/10.1016/j.etap.2007.01.007

Zagatto, P. A. & Bertoletti, E. (2006) Ecotoxicologia aquática princípios e aplicações. Ed Rima, pp. 463.

Zalups, R. K. (2000). Molecular interactions with mercury in the kidney. *Pharmacology Reviews, 52*(1), 113-143.

Zalups, R. K., & Ahmad, S. (2003). Molecular handling of cadmium in transporting epithelia. *Toxicology and Applied Pharmacology, 186*(3), 163-188. doi: http://dx.doi.org/10.1016/S0041-008X(02)00021-2

Zalups, R. K., & Barfuss, D. W. (1998). Small Aliphatic Dicarboxylic Acids Inhibit Renal Uptake of Administered Mercury. *Toxicology and Applied Pharmacology, 148*(1), 183-193. doi: http://dx.doi.org/10.1006/taap.1997.8320